USGS
science for a changing world

Prepared in cooperation with the
NEW MEXICO ENVIRONMENT DEPARTMENT

Questa Baseline and Pre-Mining Ground-Water Quality Investigation. 25. Summary of Results and Baseline and Pre-Mining Ground-Water Geochemistry, Red River Valley, Taos County, New Mexico, 2001–2005

Professional Paper 1728

U.S. Department of the Interior
U.S. Geological Survey

Cover: Satellite-based relief image, Red River Valley
Courtesy of Jonathan Caine

Questa Baseline and Pre-Mining Ground-Water Quality Investigation. 25. Summary of Results and Baseline and Pre-Mining Ground-Water Geochemistry, Red River Valley, Taos County, New Mexico, 2001–2005

By D. Kirk Nordstrom

Prepared in cooperation with the New Mexico Environment Department

Professional Paper 1728

U.S. Department of the Interior
U.S. Geological Survey

U.S. Department of the Interior
DIRK KEMPTHORNE, Secretary

U.S. Geological Survey
Mark D. Myers, Director

U.S. Geological Survey, Reston, Virginia: 2008

For product and ordering information:
World Wide Web: http://www.usgs.gov/pubprod
Telephone: 1-888-ASK-USGS

For more information on the USGS—the Federal source for science about the Earth, its natural and living resources, natural hazards, and the environment:
World Wide Web: http://www.usgs.gov
Telephone: 1-888-ASK-USGS

Suggested citation:
Nordstrom, D.K, 2008, Questa baseline and pre-mining ground-water quality investigation. 25. Summary of results and baseline and pre-mining ground-water geochemistry, Red River Valley, Taos County, New Mexico, 2001–2005: U.S. Geological Survey Professional Paper 1728, 111 p.

Contents

Abstract....1
Introduction....2
Purpose and Scope....3
Questa Baseline and Pre-Mining Ground-Water Quality Investigation....4
Meaning of Natural Background and Baseline....4
New Mexico Ground-Water Quality Standards....4
The Questa Molycorp Molybdenum Mine....5
Acknowledgments....5
Study Site....7
Physical Features....7
Geology....7
Climate and Vegetation....9
Hydrology....9
Surface Water....9
Ground Water....10
Database for Speciation and Mineral Saturation Calculations....10
Summary Conclusions from Previous Reports....10
Historical Review of Water Quality....11
Ground Water....11
Red River Surface Water....11
Seeps, Springs, and Tributaries....14
Geologic Investigations....14
Airborne Visible-Infrared Imaging Spectrometry....14
Geologic Characterization of Weathering Processes....14
Mineralogical Characterization....16
Leaching Studies....16
Bedrock Structure and Ground-Water Flow....17
Lake-Sediment Chemistry....17
Seismic Profiles....17
Geomorphology....18
Hydrologic Investigations....19
Quality Control and Quality Assurance (QA/QC) of Water Analyses....19
Synoptic and Tracer Studies of Red River....19
Reactive-Transport Modeling in the Red River....21
Diel, Storm Event, and Long-Term Trends in Red River....22
Ground Water....24
Water Balances....24
Straight Creek....24
Red River Valley....25
Integrating Water-Flow and Sulfate Mass-Load Balances for the Hottentot–La Bobita Reach....25
Interpretation of Ground-Water Geochemistry....29
Median Concentrations from Monitoring Data....30

Chemistry of Water Developed from Scar Weathering....30
Water-Chemistry Classification for the Red River Valley Ground Water....30
Geochemical Mass Balance on Straight Creek Drainage....40
Geochemical Controls on Solute Concentrations....41
Trends in Specific Conductance....41
Geochemical Controls on Dissolved Sulfate Concentrations....45
Geochemical Controls on Dissolved Iron Concentrations....47
Ferric Iron Concentrations....48
Ferrous Iron Concentrations....48
Geochemical Controls on Dissolved Manganese Concentrations....48
Geochemical Controls on Dissolved Aluminum and Silica Concentrations....54
Aluminum....54
Silica....57
Geochemical Controls on Dissolved Fluoride Concentrations....57
Geochemical Controls on Dissolved Calcium Concentrations....59
Geochemical Controls on Dissolved Magnesium Concentrations....65
Geochemical Controls on Dissolved Strontium Concentrations....65
Geochemical Controls on Dissolved Barium Concentrations....67
Geochemical Controls on Dissolved Zinc Concentrations....70
Geochemical Controls on Dissolved Cadmium Concentrations....70
Geochemical Controls on Dissolved Copper Concentrations....73
Geochemical Controls on Dissolved Nickel and Cobalt Concentrations....73
Geochemical Controls on Dissolved Chromium Concentrations....76
Geochemical Controls on Dissolved Lithium, Sodium, and Potassium Concentrations....76
Geochemical Controls on Dissolved Beryllium Concentrations....79
Pre-Mining Ground-Water Chemistry at Molycorp's Questa Mine Site....79
Pre-Mining Ground Water at Molycorp's Questa Mine....79
Capulin Canyon....79
Goat Hill Gulch....87
Sulphur Gulch....90
Sugar Shack Catchments....91
Bedrock Ground Water....95
Summary....96
References Cited....98
Appendix 1....105
Table 1–1. Thermodynamic data used by WATEQ4F for modeling aqueous speciation and mineral solubility....106
Table 1–2. List of analytic equations for linear best fits of correlated data in the form of y = mx + b....110
Appendix 2. Mathematical derivation of curves for mixing lines shown in figures 8 and 9....111

Plate

(View this plate by following the link at http://pubs.usgs.gov/pp/1728)

1. Surficial geologic map showing late Quaternary sediments, waste-rock piles, wells, catchments, and tributary streams, in the middle Red River Valley, New Mexico. Modified from Vincent (in press)

Figures

1. Maps showing the Red River Valley and the study reach between the town of Red River and the U.S. Geological Survey gage near Questa, New Mexico 6
2. Satellite image of the Red River showing scar areas, Molycorp mine site, and the town of Red River with photographs of scar areas superimposed on the satellite image....8
3. Diagram showing study components and their relationships for inferring pre-mining ground-water chemistry 13
4. Schematic geologic cross section of alteration zones with overlying dashed lines depicting the relative position of the erosional surface for five catchments along the Red River....15
5. Example of a cross section for seismic line 3 showing bedrock, water, and ground surface and unsaturated zone from seismic refraction tomography....18
6. Longitudinal cross section of the Red River along the reach of the mine site projected onto a two-dimensional plane with bedrock surface, water tables, projections of the debris-fan surface, and Red River streambed surface 19

7–10. Graphs showing:

7. Longitudinal profiles of discharge, pH, alkalinity, dissolved sulfate, manganese, zinc, total recoverable aluminum, and dissolved aluminum with distance from the synoptic/tracer study of 2001....20
8. Mixing line constructed between Red River upstream from ground-water emergence (7,200 meters) and well water from SC–1A, using calcium/sulfate molar ratios relative to sulfate concentrations 22
9. Mixing line constructed between Red River upstream from ground-water emergence (7,200 meters) and well water from SC–1A using magnesium/sulfate mass ratios relative to sulfate concentrations....23
10. Changes in discharge, pH, and sulfate and manganese concentrations at the U.S. Geological Survey Questa gage during the storm of September 17–18, 2002....24

11–14. Diagrams showing:

11. Water-flow balance for the Red River alluvial aquifer shown schematically for synoptic/tracer studies of 2001 and 2002 for the reach from Hottentot debris fan to La Bobita 26
12. Sulfate mass-load balance for the Red River alluvium shown schematically for the synoptic/tracer studies of 2001 and 2002 for the reach from Hottentot debris fan to La Bobita 27

13. Sulfate mass loads for Model II in which the sulfate mass loads of the catchments are back-calculated from the ground-water emergence mass loads 28
14. Sulfate mass loads for Model III in which the sulfate mass load of the alluvial ground-water inflow is back-calculated from the ground-water emergence mass loads and the catchment inflows are kept constant 29
15. Map showing location of observation wells in Straight Creek catchment and Advanced Waste-Water Treatment facilities....31
16. Graphs of (A) frequency distribution plot of pH for scar-drainage water in the Red River Valley and (B) frequency distribution plot of sulfate concentrations for scar-drainage water in the Red River Valley (excluding Goat Hill water) 40
17. Plot of pH against median sulfate concentration for all ground waters and Straight Creek surface water....41
18. Graph showing decrease in pH with the incremental oxidation of pyrite to (a) an acid ferrous sulfate solution with no dissolved iron oxidation, (b) oxidation of the dissolved iron sulfate solution but no precipitation of hydrous ferric oxides, and (c) oxidation with precipitation of ferrihydrite 42
19. Diagram showing evolutionary flow paths based on changes in ground-water chemistry with downstream gradient....43
20. Plot of specific conductance against sulfate concentrations for (A) Straight Creek surface and alluvial ground waters and (B) median values for all ground waters and Straight Creek surface water 44
21–40. Graphs showing:
21. Correlation between specific conductance and sulfate concentration for Red River surface-water samples from this study....45
22. Relation between sulfate concentrations of Straight Creek well waters and elevation of the bottom of the screened interval for each well....46
23. (A) Iron concentrations plotted against sulfate concentrations for all ground waters and Straight Creek surface water. (B) Ferrous iron: total dissolved iron molar ratio plotted against sulfate concentrations for all ground waters and Straight Creek surface water 47
24. (A) Ferric iron concentrations plotted against pH for all ground waters and Straight Creek surface water. Ferrihydrite saturation index plotted against (B) pH and (C) iron for all ground waters and Straight Creek surface water fulfilling the Eh measurement requirements described in Naus and others (2005) and in Nordstrom and others (2005)....49
25. Saturation indices for potassium jarosite plotted relative to pH....50
26. (A) Ferrous iron plotted against alkalinity. Siderite saturation index plotted against (B) pH, (C) calcium concentrations, and (D) dissolved inorganic carbon concentrations for all ground waters and Straight Creek surface water 51
27. Manganese concentrations plotted against sulfate concentrations for (A) Straight Creek surface and alluvial ground waters and (B) median manganese and sulfate concentrations for all ground waters and Straight Creek surface water....52
28. (A) Dissolved manganese concentrations plotted against alkalinity. Rhodochrosite saturation index plotted against (B) dissolved inorganic carbon concentrations and against (C) pH for all ground waters and Straight Creek surface water 53

29. Dissolved aluminum concentrations plotted against sulfate concentrations for (A) Straight Creek surface and alluvial ground waters, (B) median aluminum and sulfate concentrations for all ground waters and Straight Creek surface water, and (C) dissolved aluminum concentrations plotted against pH 55
30. (A) The log of the activity of free Al^{3+} plotted against pH for all ground waters and Straight Creek surface water, (B) amorphous aluminum hydroxide saturation index plotted against pH for all ground waters and Straight Creek surface water. Alunite saturation index normalized to the total stoichiometric coefficient plotted against (C) pH, and (D) aluminum concentration 56
31. (A) Silica concentrations plotted against pH for all ground waters. (B) Silica concentrations plotted against aluminum concentrations for all ground waters. For samples having a pH value less than 4, silica concentrations plotted against sulfate concentrations for (C) Straight Creek alluvial ground water; and (D) median silica and sulfate concentrations for all ground waters and Straight Creek surface water 58
32. (A) Silica saturation index plotted against pH, and (B) kaolinite saturation index plotted against pH 59
33. Fluoride concentrations plotted against sulfate concentrations for (A) Straight Creek alluvial ground waters and (B) median fluoride and sulfate concentrations for all ground waters and Straight Creek surface water. Fluoride concentrations plotted against calcium concentrations for (C) Straight Creek and alluvial ground water and (D) median concentrations for all ground waters and Straight Creek surface water 60
34. (A) Fluoride concentrations plotted against calcium concentrations. Fluorite saturation index plotted against (B) pH, (C) aluminum concentrations, and (D) aluminum concentrations less than 10 milligrams per liter for all ground waters and Straight Creek surface water 61
35. Fluoride concentrations plotted in relation to aluminum concentrations for all ground waters and Straight Creek surface water 62
36. Calcium concentrations plotted against sulfate concentrations for (A) Straight Creek surface and alluvial ground waters and (B) for median ground-water concentrations and Straight Creek surface water. (C) Ground waters and Straight Creek surface water, all data. (D) Calcium:sulfate molar ratio plotted against pH for all ground waters and Straight Creek surface water 63
37. Gypsum saturation index plotted against (A) calcium concentrations, (B) sulfate concentrations, (C) the calcium:sulfate molar ratio for Straight Creek ground water and surface water. (D) Gypsum saturation index plotted against calcite saturation index 64
38. Calcite saturation index plotted against pH for all ground waters and Straight Creek surface water 65
39. Magnesium concentrations plotted against calcium concentrations for (A) Straight Creek surface and alluvial ground waters and (B) median concentrations for all ground waters and Straight Creek surface water. Magnesium concentrations plotted against sulfate concentrations for (C) Straight Creek surface and alluvial ground waters and (D) all ground waters and Straight Creek surface water 66

40. Dolomite saturation index plotted against calcium concentrations....67
41. (A) Plot of strontium concentrations against sulfate concentrations for all ground waters and Straight Creek surface water. (B) Plot of strontium concentrations against calcium concentrations for all ground waters and Straight Creek surface water. (C) Strontianite saturation index relative to calcium concentrations for ground water and Straight Creek surface water. (D) Celestine saturation index relative to calcium concentrations for all ground waters and Straight Creek surface water....68
42–50. Graphs showing:
42. (A) Barium concentrations plotted against sulfate concentrations for all ground waters and Straight Creek surface water. Barite saturation index plotted against (B) barium concentration and (C) pH for all ground waters and Straight Creek surface water. (D) Dissolved (0.45-micrometer filtration) barium concentrations plotted against total recoverable barium concentrations for all ground waters and Straight Creek surface water....69
43. Zinc concentrations plotted against sulfate concentrations for (A) Straight Creek surface and alluvial ground waters and (B) median values for all ground and surface waters. Zinc concentrations plotted against manganese concentrations for (C) Straight Creek surface and alluvial ground waters and (D) median values for all ground and surface waters....71
44. Cadmium concentrations plotted against sulfate concentrations for (A) Straight Creek surface and alluvial ground waters and (B) all ground and surface waters. Cadmium concentrations plotted against zinc concentrations for (C) Straight Creek surface and alluvial ground waters and (D) all ground waters and Straight Creek surface water....72
45. Copper concentrations plotted against sulfate concentrations for A) Straight Creek surface and alluvial ground waters and (B) all ground and surface waters. Copper concentrations plotted against zinc concentrations for (C) Straight Creek surface and alluvial ground waters and (D) all ground waters and Straight Creek surface water....74
46. Nickel concentrations plotted against sulfate concentrations for (A) Straight Creek surface and alluvial ground waters and (B) all ground and surface waters. Cobalt concentrations plotted against nickel concentrations for (C) Straight Creek surface and alluvial ground waters and (D) all ground waters and Straight Creek surface water....75
47. Chromium concentrations plotted against sulfate concentrations for (A) Straight Creek surface and alluvial ground waters and (B) all ground and surface waters. Chromium concentrations plotted against nickel concentrations for (C) Straight Creek surface and alluvial ground waters and for (D) all ground waters and Straight Creek surface water....77
48. Lithium concentrations plotted against sulfate concentrations for (A) Straight Creek surface and alluvial ground waters and (B) all ground and surface waters. Potassium concentrations plotted against sodium concentrations for (C) Straight Creek surface and alluvial ground waters and for (D) all ground waters and Straight Creek surface water....78
49. Beryllium concentrations plotted against sulfate concentrations for (A) Straight Creek surface and alluvial ground waters and (B) all ground and surface waters....80

50. Beryllium concentrations plotted against fluoride concentrations for (A) Straight Creek alluvial ground waters and (B) all ground and surface waters. Beryllium concentrations plotted against lithium concentrations for (C) Straight Creek alluvial ground waters and for (D) all ground waters and Straight Creek surface water 81
51. Topographic map of mine site with watershed boundaries, scar areas, debris fans, and Red River alluvium 82
52. Plot of pH against sulfate concentration for (A) seeps and ground waters in Capulin Canyon with less than 3,000 milligrams per liter sulfate concentration and (B) same waters including those surface-water impoundment waters with greater than 3,000 milligrams per liter sulfate concentration....83
53. (A) Plot of fluoride concentrations against calcium concentrations for Capulin Canyon waters. (B) Plot of fluoride concentrations against sulfate concentrations. (C) Same plot as figure 53A but showing the entire range of concentrations. (D) Same plot as figure 53B but showing the entire range of concentrations 84
54. (A) Plot of zinc against manganese concentrations for Capulin Canyon waters. (B) Plot of zinc against sulfate concentrations for Capulin Canyon waters. (C) Same plot as figure 54A but showing the entire range of concentrations. (D) Same plot as figure 54B but showing the entire range of concentrations 85
55. (A) Plot of nickel against sulfate concentrations for Capulin Canyon waters. (B) Plot of cobalt against nickel concentrations for Capulin Canyon waters. (C) Same plot as figure 55A but showing the entire range of concentrations. (D) Same plot as figure 55B but showing the entire range of concentrations....86
56. Topographic map of the three subcatchments that constitute Sulphur Gulch–upper Sulfur Gulch, Blind Gulch, and Spring Gulch....91
57. Geologic map of the three subcatchments that constitute Sulphur Gulch–upper Sulfur Gulch, Blind Gulch, and Spring Gulch....92

Tables

1. New Mexico ground-water quality standards....5
2. Compilation of reports published within this project....12
3. Catchments that contribute ground water and sulfate loads to the Red River alluvium near natural scar drainages (Hottentot to La Bobita) for August 2001....27
4. Catchment yields, sulfate concentrations, and sulfate mass loads using Model II for 2001 28
5. Median values for pH, temperature, specific conductance, redox potential, dissolved oxygen (DO), dissolved solute concentrations, dissolved organic carbon (DOC), cation- and anion-equivalent sum, and speciated charge imbalance for Straight Creek drainage water and ground water analyzed in this study....32
6. Weathering mass balances of minerals that can account for the median chemistry of Straight Creek scar-drainage water....42
7. Range of values for water-quality constituents of concern for Capulin Canyon alluvial ground waters unaffected by scar drainage....88

8. Range of values for water-quality constituents of concern for Capulin Canyon alluvial ground waters affected by scar drainage....88
9. Range of values for water-quality constituents of concern for Capulin Canyon bedrock ground waters....88
10. Preliminary values for water-quality constituents of concern for alluvial ground waters in Goat Hill....89
11. Estimated preliminary values for pre-mining ground-water quality constituents for Goat Hill Gulch debris fan compared to the range of values from water in wells MMW–42A and MMW–44A....89
12. Estimated final values for water-quality constituents of concern for alluvial ground waters in Goat Hill....90
13. Compositions of water used for the reactive mixing calculations....93
14. pH, aluminum, and iron concentrations calculated by assuming different aluminous minerals precipitate upon mixing in the Sulphur Gulch catchment....94
15. Water-quality constituents of concern for lower Sulphur Gulch drainage and debris fan....94
16. Water-quality constituents of concern for two Sugar Shack catchments (8 and 10 on plate 1)....95
17. Water-quality constituents of concern for middle Sugar Shack catchment (area 9 on plate 1)....95
18. Water-quality constituents of concern for the range of pre-mining bedrock ground waters exclusive of those in Capulin Canyon....96

Conversion Factors

SI to Inch/Pound

Multiply	By	To obtain
	Length	
kilometer (km)	0.6214	mile (mi)
meter (m)	3.281	foot (ft)
centimeter (cm)	0.3937	inch (in.)
millimeter (mm)	0.03937	inch (in.)
	Area	
square kilometer (km^2)	247.1	acre
square kilometer (km^2)	0.3861	square mile (mi^2)
square meter (m^2)	10.76	square foot (ft^2)
square centimeter (cm^2)	0.1550	square inch (ft^2)
	Volume	
cubic meter (m^3)	35.31	cubic foot (ft^3)
cubic meter (m^3)	264.2	gallon (gal)
liter (L)	0.2642	gallon (gal)
liter (L)	1.057	quart (qt)
liter (L)	33.82	ounce, fluid (fl. oz)
cubic centimeter (cm^3)	0.06102	cubic inch (in^3)
	Flow rate	
cubic meter per second (m^3/s)	35.31	cubic foot per second (ft^3/s)
cubic meter per second (m^3/s)	22.83	million gallons per day (Mgal/d)
liter per second (L/s)	15.85	gallon per minute (gal/min)
liter per second (L/s)	0.03532	cubic foot per second (ft^3/s)
	Mass	
ton, short (2,000 lb)	0.9072	metric ton
kilogram (kg)	2.205	pound avoirdupois (lb)
gram (g)	0.03527	ounce, avoirdupois (oz)

Temperature in degrees Celsius (°C) may be converted to degrees Fahrenheit (°F) as follows:

$$°F=(1.8×°C)+32.$$

Vertical coordinate information is referenced to the National Geodetic Vertical Datum of 1929 (NGVD 29).

Horizontal coordinate information is referenced to North American Datum of 1927 (NAD 27).

Altitude, as used in this report, refers to distance above the vertical datum.

Specific conductance is given in microsiemens per centimeter at 25 degrees Celsius (µS/cm at 25°C).

Abbreviations used in this report

°C	degree Celsius
AVIRIS	Airborne Visible-Infrared Imaging Spectrometry
AWWT	Advanced Waste-Water Treatment
cm	centimeters
DIC	dissolved inorganic carbon
DOC	dissolved organic carbon
Eh	redox potential relative to the Standard Hydrogen Electrode
ft^3/s	cubic feet per second
HFO	hydrous ferric oxides
IAP	ion-activity product
kg/day	kilograms per day
km	kilograms
km^2	kilograms squared
K_{sp}	solubility-product constant
m	meters
MAD	mean absolute deviation
MCL	maximum contaminant level
meq/L	milliequivalents per liter
mg/L	milligrams per liter
mm	millimeter
mmol/L	millimoles per liter
m/m	meters per meter
NMAC	New Mexico Administration Code
NMED	New Mexico Environment Department
NMSA	New Mexico Statutory Authority
QA/QC	quality assurance/quality control
QSP	quartz-sericite-pyrite
SI	saturation index
TDS	total dissolved solids
USEPA	U.S. Environmental Protection Agency
USGS	U.S. Geological Survey
µg/L	micrograms per liter
µm	micrometer
µS/cm	microsiemens per centimeter
WQCC	Water Quality Control Commission

Questa Baseline and Pre-Mining Ground-Water Quality Investigation. 25. Summary of Results and Baseline and Pre-Mining Ground-Water Geochemistry, Red River Valley, Taos County, New Mexico, 2001–2005

By D. Kirk Nordstrom

Abstract

Active and inactive mine sites are challenging to remediate because of their complexity and scale. Regulations meant to achieve environmental restoration at mine sites are equally challenging to apply for the same reasons. The goal of environmental restoration should be to restore contaminated mine sites, as closely as possible, to pre-mining conditions. Metalliferous mine sites in the Western United States are commonly located in hydrothermally altered and mineralized terrain in which pre-mining concentrations of metals were already anomalously high. Typically, those pre-mining concentrations were not measured, but sometimes they can be reconstructed using scientific inference.

Molycorp's Questa molybdenum mine in the Red River Valley, northern New Mexico, is located near the margin of the Questa caldera in a highly mineralized region. The State of New Mexico requires that ground-water quality standards be met on closure unless it can be shown that potential contaminant concentrations were higher than the standards before mining. No ground water at the mine site had been chemically analyzed before mining. The aim of this investigation, in cooperation with the New Mexico Environment Department (NMED), is to infer the pre-mining ground-water quality by an examination of the geologic, hydrologic, and geochemical controls on ground-water quality in a nearby, or proximal, analog site in the Straight Creek drainage basin. Twenty-seven reports contain details of investigations on the geological, hydrological, and geochemical characteristics of the Red River Valley that are summarized in this report. These studies include mapping of surface mineralogy by Airborne Visible-Infrared Imaging Spectrometry (AVIRIS); compilations of historical surface- and ground- water quality data; synoptic/tracer studies with mass loading and temporal water-quality trends of the Red River; reaction-transport modeling of the Red River; environmental geology of the Red River Valley; lake-sediment chemistry; geomorphology and its effect on ground-water flow; geophysical studies on depth to ground-water table and depth to bedrock; bedrock fractures and their potential influence on ground-water flow; leaching studies of scars and waste-rock piles; mineralogy and mineral chemistry and their effect on ground-water quality; debris-flow hazards; hydrology and water balance for the Red River Valley; ground-water geochemistry of selected wells undisturbed by mining in the Red River Valley; and quality assurance and quality control of water analyses. Studies aimed specifically at the Straight Creek natural-analog site include electrical surveys; high-resolution seismic survey; age-dating with tritium/helium; water budget; ground-water hydrology and geochemistry; and comparison of mineralogy and lithology to that of the mine site.

The highly mineralized and hydrothermally altered volcanic rocks of the Red River Valley contain several percent pyrite in the quartz-sericite-pyrite (QSP) alteration zone, which weather naturally to acid-sulfate surface and ground waters that discharge to the Red River. Weathering of waste-rock piles containing pyrite also contributes acid water that eventually discharges into the Red River. These acid discharges are neutralized by circumneutral-pH, carbonate-buffered surface and ground waters of the Red River. The buffering capacity of the Red River, however, decreases from the town of Red River to the U.S. Geological Survey (USGS) gaging station near Questa. During short, but intense, storm events, the buffering capacity is exceeded and the river becomes acid from the rapid flushing of acidic materials from natural scar areas.

The lithology, mineralogy, elevation, and hydrology of the Straight Creek proximal analog site were found to closely approximate those of the mine site with the exception of the mine site's Sulphur Gulch catchment. Sulphur Gulch contains three subcatchments—upper Sulphur Gulch, Blind Gulch, and Spring Gulch. Blind and Spring Gulches are largely propylitic zones with negligible pyrite mineralization, and although this lithology is not found at Straight Creek, it is found to the west of the Hansen Creek area where the geology extends to the Spring Gulch catchment. In lower Sulphur Gulch the erosion surface has cut deeper into the hydrothermal-alteration sequence than that found at Straight Creek, exposing the

carbonate-fluorite alteration zone. Nevertheless, concentration limits from mineral solubilities and from the highest measured concentrations in ground water undisturbed by mining in the Red River Valley provide a basis for constraining the most likely concentrations for pre-mining conditions at the mine site.

The Straight Creek natural-analog site consists of acid surface drainage derived from the weathering of QSP altered rocks at the headwaters. The surface drainage of pH 2.5–3 disappears into a debris fan and becomes acid alluvial ground water of pH 3–4. Most dissolved constituents behave conservatively during downgradient ground-water transport and are diluted by side-canyon seepage waters and by Red River alluvial ground water at the toe of the debris fan. The main change in chemistry is a transition from strongly oxidizing conditions in the surface drainage (dissolved iron is in the Fe[III] oxidation state) to moderately reducing conditions (dissolved iron is in the Fe[II] oxidation state, without sulfate reduction) in the alluvial ground water. As a result of reduction, substantial amounts of copper are removed from solution and some chromium is removed. A substantial increase in silica concentration is observed between Straight Creek surface drainage and the alluvial ground water. Aluminum and silica appear to coprecipitate once the alluvial ground waters have reached a pH of 4. Bedrock ground waters are circumneutral pH (6–7.8) but also high in iron, manganese, and sulfate. Ferrous iron concentrations in bedrock are limited by siderite saturation, manganese by rhodochrosite saturation, calcium by calcite and gypsum saturation, barium by barite saturation, and fluoride by fluorite saturation.

A water-flow and sulfate-load balance was developed for the reach of the Red River from the Hottentot debris fan to the La Bobita campground. In spite of uncertainties in the data, these estimates indicate that ground waters in the Red River alluvium leaving the La Bobita area are 8 to 9 cubic feet per second and the sulfate flux is approximately 3,000 to 5,000 kilograms per day. Further fluxes of sulfate-laden waters enter the Red River alluvium between La Bobita and the Columbine Park area, but more field work and calculations would be needed to define the ground-water flow and sulfate fluxes in this area.

The origin and geochemical behavior of individual solutes in Straight Creek surface drainage, acid alluvial ground water, and neutral-pH bedrock ground water are compared to solute concentrations and their geochemical behavior in other catchments undisturbed by mining. The same trends apply generally with a few exceptions that can be explained by local mineralized zones that may be suboxic without substantial pyrite oxidation; that is, pyrite (if present) has not been exposed at the ground surface to intense weathering. The results show that acid ground waters derived from scar areas follow regular solute trends demonstrated by linear correlations of elements with sulfate based on the Straight Creek analog trend. The only mineral solubility controls that apply to oxidized acid ground water are hydrous ferric oxide saturation for ferric iron, gypsum for calcium, barite for barium, and aluminum and silica solubility control by an as-yet-unidentified phase when pH values reach 4. Circumneutral-pH anoxic ground water achieves mineral saturation for siderite, rhodochrosite, calcite, fluorite, $Al(OH)_3$, gypsum, and barite. The results also show that a wide range of ground-water chemistry is possible over rather short distances. This wide range of solute concentration greatly complicates the objective of obtaining the pre-mining ground-water quality.

The geochemical behavior of solutes that were interpreted for Straight Creek, then applied to other undisturbed catchments, were then applied to catchments on the mine site for pre-mining conditions. The wide range of water chemistry that depends on changes in lithology and alteration, the presence or absence of scar, whether alluvial or bedrock ground water along with the uncertainty that accompanies the data led to the conclusion that a range of concentration for each solute of regulatory concern had to be applied, and that different solute concentrations had to be applied to bedrock than to alluvial ground waters, and that different concentrations had to be used for different parts of the same catchment if the lithology changed markedly. Different ranges of solute concentrations had to be estimated for each different watershed on the mine site because the geology changed markedly from one catchment to another. In spite of these complications, there is little doubt that under natural, pre-mining conditions, several elements of regulatory concern must have exceeded New Mexico ground-water quality standards by as much as tenfold in several locations both at the mine site and along the Red River Valley between the towns of Red River and Questa. The most common exceedances were for iron, manganese, sulfate, and fluoride. Manganese exceeded New Mexico ground-water standards by as much as 250 times. This exceedance is caused by the dissolution of rhodochrosite, $MnCO_3$, and manganiferous calcite, $(Ca,Mn)CO_3$, that are common accessory minerals from hydrothermal alteration.

Introduction

Ore deposits are defined as mineral deposits that contain economic concentrations of minerals. In the Western United States, metalliferous ore deposits are found commonly in mountainous regions where rapid weathering has exposed them, making them visible to prospectors and more easily mapped and evaluated by economic geologists. Mining of metal-sulfide deposits exposes more minerals to oxidation and solubilization, which leads to deleterious contamination of receiving streams if unabated (Blowes and others, 2004). Water quality commonly is degraded by acid mine waters containing high concentrations of metals such as iron, aluminum, copper, zinc, cadmium, arsenic, and mercury. Precipitation and transport of iron and aluminum colloids as well as naturally occurring clay minerals can cause high turbidity during storm-runoff events at mine sites. Numerous fishkills and elimination of benthic invertebrates have been documented for many of

these mine sites. Today, these sites are subject to regulations that require remediation and restoration of mined lands and affected waters.

Important questions that often arise are: How clean do these waters have to be? If natural waters unaffected by mining exceeded water-quality goals or criteria because of highly mineralized rock, shouldn't different standards apply? What criteria can provide a basis for water-quality goals at any particular mine site? The answers to these questions have a direct bearing on the costs of remediation. It seems reasonable to assume that improvements to water quality need not proceed beyond those conditions that existed before mining took place. But what was the quality of water prior to mining? Before the 1950s, ground-water quality (regardless of whether before, during, or after mining) was rarely, if ever, sampled and analyzed at mine sites. The same situation was still common until the last decade or two. Most mine sites have no direct or reliable information regarding ground-water quality, although many surface-water samples have been analyzed for acid and metal contaminants. Documented ground-water chemistry (not just the water chemistry of mine water discharged to the surface) affected by mining operations include midwestern lead-zinc mines of the United States (Playton and others, 1980; Parkhurst, 1987; Toran, 1987), coal mines in Illinois and Appalachia (Booth, 2002; Brady and others, 1998), mines in Europe, South America, Russia, and South Africa (Goleva, 1977; Vartanyan, 1988; Fernández-Rubio, 1999; Younger and Robins, 2002; Younger and others, 2002).

Before the 1970s, routine analytical techniques were not available to determine low concentrations of many trace elements in water samples. Concentrations and detection limits at the level of today's water-quality standards could not have been determined reliably, if at all, by routine analytical techniques at that time. Therefore, any attempt to determine pre-mining ground-water quality at older mine sites must rely on indirect methods and scientific inference. Inference of ground-water quality constituents in a complex mineralized terrain of poorly known hydrology will always carry larger uncertainties than any direct methods of measuring ground-water quality, and the degree of uncertainty depends on the approach used.

Mineralized areas undisturbed by mining are known to contain acid-sulfate water with toxic concentrations of metals (Runnells and others, 1992; Posey and others, 2000; Mast and others, 2000; Yager and others, 2000). These conditions occur because the same geochemical and microbiological processes that produce acid mine water also produce natural acidic water. Important differences between acid mine drainage and natural acidic drainage are that (a) mining greatly increases the surface area of pyrite and other sulfides exposed to air and water, thereby increasing substantially the rate of acidity produced, (b) mining increases the total mass amount of pyrite and other sulfides exposed to air and water, thereby increasing substantially the amount of metal-rich acid waters produced, and (c) the increased quantities of acidic production from mining increases the mobility of heavy metals to waterways. Hence, the risks to aquatic, terrestrial, and human health increase substantially from mining and mineral-processing activities compared to pre-mining conditions in the same areas, unless remedial measures offering environmental protection are incorporated into the mining plans.

The key to understanding pre-mining water-quality conditions depends directly on understanding the processes that produce acid rock drainage and high concentrations of soluble constituents for a given hydrogeological setting. Our understanding of rock weathering, pyrite oxidation, the inorganic and microbial processes that lead to the development of acidity, and processes affecting the mobility of metals in surface and ground waters has improved considerably over the last 2 decades (Alpers and Blowes, 1994; Plumlee and Logsdon, 1999; Nordstrom, 2000, 2004; Jambor and others, 2003; Nordstrom and others, 2007). A prudent choice of empirical relationships interpreted by geologic and hydrologic context and geochemical models can provide the necessary constraints to estimate pre-mining water-quality conditions for Molycorp's Questa molybdenum mine. To address this need, the U.S. Geological Survey (USGS), in cooperation with New Mexico Environment Department (NMED), conducted a multidiscipline investigation to infer pre-mining ground-water chemistry at the mine site.

Purpose and Scope

This report is a summary of a 5-year investigation (2001–2005) on geological and hydrological conditions that affect ground water and surface water in the mineralized area of the Red River Valley from the town of Red River to the USGS gaging station (08265000, Red River near Questa) at the Questa District Ranger Station of the USDA Forest Service. The size and complexity of the field site necessitated a multidisciplinary approach gathering field data and utilizing expertise in surface-water hydrology, ground-water hydrology, geology (environmental, economic, and structural geology), mineralogy, geochemistry, geomorphology, and geophysics. Information gained from all of these fields of study is integrated in this report for the purpose of inferring the pre-mining ground-water quality at the Questa mine. This report does not attempt to determine how much of Molycorp's current or past mining activities have contributed contaminants to the Red River or other aspects of the Red River Valley ecosystem. Those assessments are proceeding independently under an agreement between the U.S. Environmental Protection Agency (USEPA) and Molycorp. Results from the USGS study may be helpful in the ongoing site characterization and risk assessments, but they are not part of the USGS purpose or scope of work.

Among several useful approaches that could be used to estimate pre-mining water quality (Runnells and others, 1992; Alpers and Nordstrom, 2000), the most direct one is the proximal analog. Other approaches are a distal or remote analog site (examples are found in Runnells and others, 1992; unnecessary if a proximal analog site is available); sediment sampling

(provides no information on water chemistry); stable isotopes of water and dissolved sulfate (can be used in conjunction with analog site studies; the composition of oxygen isotopes in dissolved sulfate can be complicated to interpret); geochemical modeling with or without kinetics (numerous assumptions are usually necessary; strongly dependent on practical experience of the modeler); statistical analysis (sites having more than two sources may not be interpretable; interpretations still dependent on geochemical experience); mass balance on oxygen flux (requires considerable site-specific knowledge); and mass balance based on age of weathered sulfides (can give long-term metal and sulfate fluxes, but geologic reconstruction over long periods is needed). Several of these approaches were used in the present investigation.

The most useful proximal analog should be similar to the mine site in lithology, geologic structure, topography, hydrology, climate, and ground-water characteristics. This study is likely the first comprehensive study to use a proximal analog site to estimate pre-mining ground-water quality at a mine site by a third party (a party independent of those who have a vested interest in the outcome). The site chosen for the natural analog is the Straight Creek catchment, located approximately 3 miles to the east of the eastern boundary of the mine site.

Questa Baseline and Pre-Mining Ground-Water Quality Investigation

Meaning of Natural Background and Baseline

There is a tendency to think of "natural background" as unpolluted or pristine preindustrial conditions. Unfortunately, such concepts are not helpful because water-quality data for such conditions are nonexistent; natural variations around the world can be large and do not permit a simple, single analytical result for a given element or compound; and there is often a value judgment or anticipated "use" judgment associated with natural substances (rocks, soils, air, and water) that precludes a simple, unambiguous result. Bates and Jackson (1980) state that a natural area is "An area of land or water that has retained its wilderness character, although not necessarily completely natural and undisturbed… ." John Hem (1985) stated that "Natural waters need not be pristine—unaffected by the works of man. Indeed, probably few are completely free from such influences." The USGS, therefore, has avoided use of the word in the course of this study. Instead, the term "baseline" is preferred to refer to current conditions of water quality and "pre-mining" to describe those conditions that likely existed during the few hundred to few thousand years before mining took place. The time period must be constrained to the recent Holocene (the last 4,000 years). Early Holocene or earlier would have had markedly different climatic conditions with different weathering rates. Furthermore, the ground surface would have been higher with respect to the depth of mineralized zones (that is, pyrite-rich rock currently exposed would have been deeper and less exposed to weathering in several areas).

Baseline conditions refer to current conditions either affected by mining or not affected by mining. Those areas not affected by mining could have been affected by anthropogenic activities such as exploration drilling, clearings for roads and power lines, and other structures, but not by the large-scale excavation of rock or the dumping of waste rock or tailings typical of metals extraction and concentration. Baseline conditions unaffected by the responsible person's facility refer to the same background conditions stated in Section 20.6.2.7.E of the New Mexico Administration Code (NMAC), though other anthropogenic activities or natural sources might have affected the analytical results.

"Background" is primarily used in this study to refer to the conditions defined by the State of New Mexico and their regulatory framework. The regulatory enforcement agency for the State is the New Mexico Environment Department (NMED).

The Water Quality Control Commission (WQCC) Regulations were adopted in 1977 pursuant to the New Mexico Water Quality Act, New Mexico Statutory Authority (NMSA) Sections 74–6–1 through 74–6–17. The purpose of these regulations is to protect ground- and surface-water quality. The ground-water discharge permit requirements of the WQCC Regulations are the State's primary tool for protecting ground-water quality. These regulations limit certain discharges to ground water at current mining operations and closure of those discharge sites. In addition to the permit program, the regulations specify requirements for certain reclamation activities, including ground-water cleanup standards. Section 20.6.2.4103.F NMAC also allows an operator to petition the WQCC for approval of alternative abatement standards, which are a type of variance from the numerical WQCC ground-water quality standards. It is within this regulation that the term "background" is defined. Background is defined by Section 20.6.2.7.1101.E NMAC and means "…the amount of ground contaminants naturally occurring from undisturbed geologic sources or water contaminants which the responsible person establishes are occurring from a source other than the responsible person's facility… ."

New Mexico Ground-Water Quality Standards

According to WQCC regulations on September 15, 2002, and pursuant to discussions with NMED (§20.6.2.3103; *www.nmenv.state.nm.us./NMED_Regs/gwb/20_6_2_NMAC.pdf*), the list of constituents in table 1 were considered potential contaminants of concern for the purposes of characterizing pre-mining ground-water quality in the study area. However, this list does not preclude the possibility of other dissolved inorganic constituents of concern in the study area, especially mercury, molybdenum, uranium, and vanadium. These additional constituents were considered and analytically determined in the present study, but no instances of anomalous concentrations were observed. There is no New Mexico

Table 1. New Mexico ground-water quality standards.

[mg/L, milligrams per liter; MCL, maximum contaminant level]

Constituent or property	Concentration (mg/L)
[1]Aluminum (Al)	5.0
[2]Beryllium (Be)	.004
[3]Cadmium (Cd)	.01
[3]Chromium (Cr)	.05
[1]Cobalt (Co)	.05
[4]Copper (Cu)	1.0
[3]Fluoride (F)	1.6
[4]Iron (Fe)	1.0
[3]Lead (Pb)	.05
[4]Manganese (Mn)	.2
[1]Nickel (Ni)	.2
[4]Sulfate (SO_4)	600.0
[4]Total dissolved solids (TDS)	1,000.0
[4]Zinc (Zn)	10.0
[4]pH	Between 6 and 9

[1] Standards for irrigation use.

[2] National Drinking Water MCL (U.S. Environmental Protection Agency).

[3] Human-health standard.

[4] Other standards for domestic water supply.

ground-water quality standard for beryllium, but it is considered a potential element of concern for this site for which the drinking-water maximum contaminant level (MCL) is used (U.S. Environmental Protection Agency, *http://www.epa.gov/safewater/mcl.html*).

The Questa Molycorp Molybdenum Mine

Molycorp, Inc., operates a molybdenum mine east of the town of Questa, northern New Mexico, in the Red River Valley (fig. 1 and front cover image). The Red River approximates the southern boundary of the mine site and flows to the west where it joins the Rio Grande. Molycorp is subject to New Mexico's mine closure regulations and operates in a highly mineralized area likely to have solute concentrations greater than New Mexico ground-water quality standards. There are no known ground-water chemistry data prior to 1982 when the utility Advanced Waste-Water Treatment (AWWT) near the town of Red River drilled an observation well in the Straight Creek alluvium and analyzed their first sample collected in November of that year. Although wells were installed in the mid-1960s in conjunction with the milling operations, no water-chemistry data were reported until 1992. Consequently, there are no pre-mining ground-water analyses; they must be inferred based on best available scientific methods. That inference is the main objective of this investigation.

Prior to 1916, prospectors discovered outcrops of bright yellow, weathered rock that looked like sulfur (hence the name, Sulphur Gulch) and a greasy mineral that looked like graphite. The graphitic mineral was identified as molybdenite (MoS_2) in 1916, and the yellow mineral was ferrimolybdite, the oxidized product derived from the weathering of molybdenite (Schilling, 1956). By 1920 the Molybdenum Corporation of America had acquired the property to mine the deposit, and the company subsequently shortened its name to Molycorp, Inc. Mill and flotation plants were set up by 1923 for production, and small-scale underground mining of high-grade veins (averaging 4 percent with a maximum of 35 percent molybdenum) continued until 1958. During the 1950s exploration had identified a large, low-grade deposit (about 0.3 percent) below the high-grade deposit, and the decision was made to extract this ore by open-pit methods (Carpenter, 1968). Extraction of ore from the open pit began in 1965. Mill tailings were transported 9 miles by pipeline to a tailings facility in the Rio Grande Valley just west of Questa. Peak molybdenum production occurred in 1976 with 11.5 million pounds per year. In 1977 Molycorp, Inc., became a wholly owned subsidiary of Union Oil Company of California. In 2005 Molycorp became a wholly owned subsidiary of Chevron Corporation.

Open-pit mining ceased in 1983 and underground mining restarted. Waste rock was no longer dumped onto piles at the mine site, but the amount of tailings continued to increase. Low market values for molybdenum have periodically caused the mine to shut down (1986–89 and 1992–95). Active mining continues at Molycorp's Questa Mine in response to market demand. Further history and related information are available from Molycorp, Inc. (*www.molycorp.com*) and from the USEPA (*www.epa.gov/superfund/sites/npl/narl1599.htm*).

Acknowledgments

I am indebted to Blaine McCleskey, who artfully provided graphs and tables for this report; to Jim Ball, who also provided graphs, tables, and PHREEQC and WATEQ4F calculations; to Geoff Plumlee, Kirk Vincent, Jonathan Caine, Jim Ball, and Doug McAda, who graciously provided figures from other reports; and to the reviewers who carefully read and commented on the report: Roger Lee, Charles Alpers, Geoff Plumlee, Phil Verplanck, Christoph Wels, Bruce Walker, Anne Wagner, Mike Reed, and Kevin Myers. My appreciation is extended to NMED for clarifying the regulatory statutes. I am grateful to Nathan Myers and Doug McAda for assistance with the sulfate flux calculations, figures, and additional hydrologic data. I am deeply grateful to the 30+ USGS personnel who made this investigation possible. This investigation could not have been accomplished without the support and cooperation of Molycorp, Inc., NMED, and the USDA Forest Service, and the helpful comments of Amigos Bravos. The encouragement of Mark Purcell of the USEPA is also appreciated. This project was truly collaborative and was only successful insofar as all parties gave generously and openly of their time and expertise to see its completion.

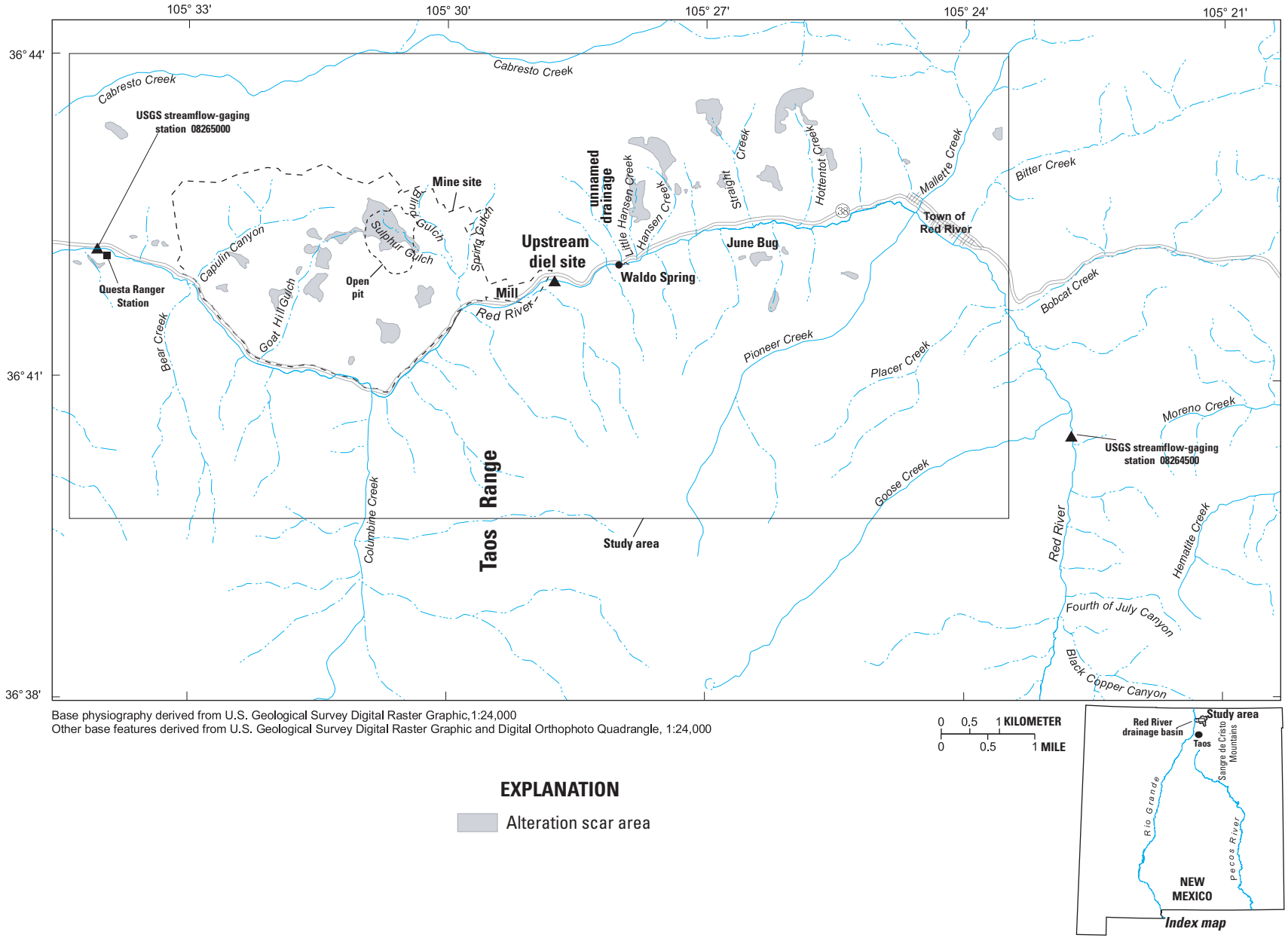

Figure 1. The Red River Valley and the study reach between the town of Red River and the U.S. Geological Survey gage near Questa, New Mexico.

Study Site

Physical Features

The study area is located in Taos County in the Taos Range of the Sangre de Cristo Mountains of north-central New Mexico (fig. 1; a detailed map with well locations at a scale of 1:50,000 is provided on plate 1, from Vincent, in press). The Red River drainage basin is a tributary to the Rio Grande within the Carson National Forest. The area has a rugged terrain with steep slopes and V-shaped valleys. The study area is the Red River Valley between the Questa ranger station at 2,280 m (7,480 ft) elevation at the west end and the town of Red River at 2,646 m (8,680 ft) elevation at the east end (fig. 1). The canyon walls of the Red River basin rise rapidly from about 2,400 m to over 3,000 m at the ridgecrest on both the north and south sides of the river. Some peaks reach nearly 3,500 m. The 600-m difference in elevation between the Red River and the adjacent ridgecrest can occur over a horizontal distance of less than 2,000 m.

The Questa Molycorp molybdenum mine, referred to as the mine site, is located on the north side of State Highway No. 38 and the Red River 13 km east of the ranger station. The mine site is approximately 16 km^2 (6 mi^2) and encompasses three main tributary valleys to the Red River—Capulin Canyon, Goat Hill Gulch, and Sulphur Gulch, from west to east, respectively (pl. 1 and fig. 1).

Mining activities produced extensive underground workings and an open pit of approximately 0.65 km^2 (162 acres) near or in Sulphur Gulch. Waste-rock piles cover steep slopes on the north side of the Red River between Capulin Canyon and Spring Gulch (a tributary valley of Sulphur Gulch). Hydrothermally altered bedrock is present in Capulin, Goat Hill, Sulphur, Hansen, Straight, June Bug, Hottentot, and Bitter Creek drainages (fig. 1). The latter five drainages are examples of unmined drainages with the exception of minor prospects in Bitter Creek. Weathering of extensively altered rock has resulted in steep, highly erosive, sparsely vegetated "scars" that are clearly visible from the ground and in aerial photographs (fig. 2).

Geology

The geochemical interaction of water with soil, colluvium, alluvium, and fractured bedrock produces the composition of surface and ground waters that are the focus of this study. Hence, the geology is a fundamental component to understanding the ground-water chemistry. This section briefly summarizes the general geologic framework from Schilling (1956), Rehrig (1969), Lipman (1981), and Meyer and Leonardson (1990, 1997) in addition to observations made by the USGS scientists working at the site. More detailed geologic results related to ground-water geochemistry appear in later sections of this report.

The Taos Range is composed of Precambrian metamorphic assemblages and granitic intrusive rocks overlain by Tertiary volcanics. The volcanic rocks are primarily intermediate to felsic composition (andesites to rhyolites), and they have been intruded by late Oligocene and early Miocene quartz monzonites and granites that provided the source of the hydrothermal fluids and molybdenite mineralization. The hydrothermally altered volcanics often contain pyrite mineralization (generally 1–3 percent). The Red River Valley is located along the southern edge of the Questa volcanic caldera and contains complex structural features and extensive hydrothermal alteration. The mineral deposits in the Red River Valley are considered Climax-type deposits that are associated with silica- and fluorine-rich rhyolite porphyry and granitic intrusives. The three principal alteration zones include a highly altered quartz-sericite-pyrite (QSP) zone, less-altered argillic (dominantly kaolinite) zones, and mildly altered propylitic zones (containing calcite mineralization). QSP alteration, as the name implies, produces a mixture of quartz, pyrite (as much as 10 percent), and fine-grained mica (sericite) or illite. Chlorite, epidote, albite, and calcite typically are found in the propylitic assemblages. Ore deposits contain quartz, molybdenite, pyrite, fluorite, calcite, manganiferous calcite, dolomite, and rhodochrosite. Lesser amounts of galena, sphalerite, chalcopyrite, magnetite, and hematite also are present. The hydrothermal alteration related to mineralization overprints an older, regional propylitic alteration. In these areas, rocks can contain a mixture of quartz, pyrite, and illite clays replacing feldspars, chlorite, carbonates, and epidote. Abundant minerals in waste rock produced by mining activities include chlorite, gypsum, illite, illite-smectite, jarosite, kaolinite, and muscovite (Gale and Thompson, 2001).

Andesite volcanic and volcaniclastic rocks are present in most scar-area bedrock outcrops and are the dominant bedrock units in the Straight Creek, South and Southeast Straight Creek, South Goat Hill, Sulphur Gulch, and Southwest Hansen scars. Amalia Tuff, a mildly alkaline, rhyolitic tuff, is the dominant rock type in the Goat Hill and Hansen scars, and quartz latite porphyry is the main rock type in the June Bug and Southeast Hottentot scars. Rhyolite porphyry is the main rock type in the Hottentot scar, and quartz latite and rhyolite porphyries form the hillslopes of several scars. Rhyolite porphyry and tuff do not seem to have been substantially affected by propylitization. Advanced argillic alteration was identified in the Hansen and Hottentot scars and in areas southwest of the Molycorp open pit. Propylitized andesite bedrock is present in the La Bobita drainage, an area that does not contain alteration scars.

Samples collected from a weathering profile in the Straight Creek scar were studied in detail to characterize the mineralogic variations. Unweathered bedrock exposed in the creek bottom is propylitized andesite with a QSP overprint. Depending on location within the weathering profile, altered rocks contain variable amounts of quartz, illite, chlorite, and plagioclase feldspar, with smaller amounts of pyrite, gypsum, rutile, jarosite, and goethite (Livo and Clark, 2002; Ludington

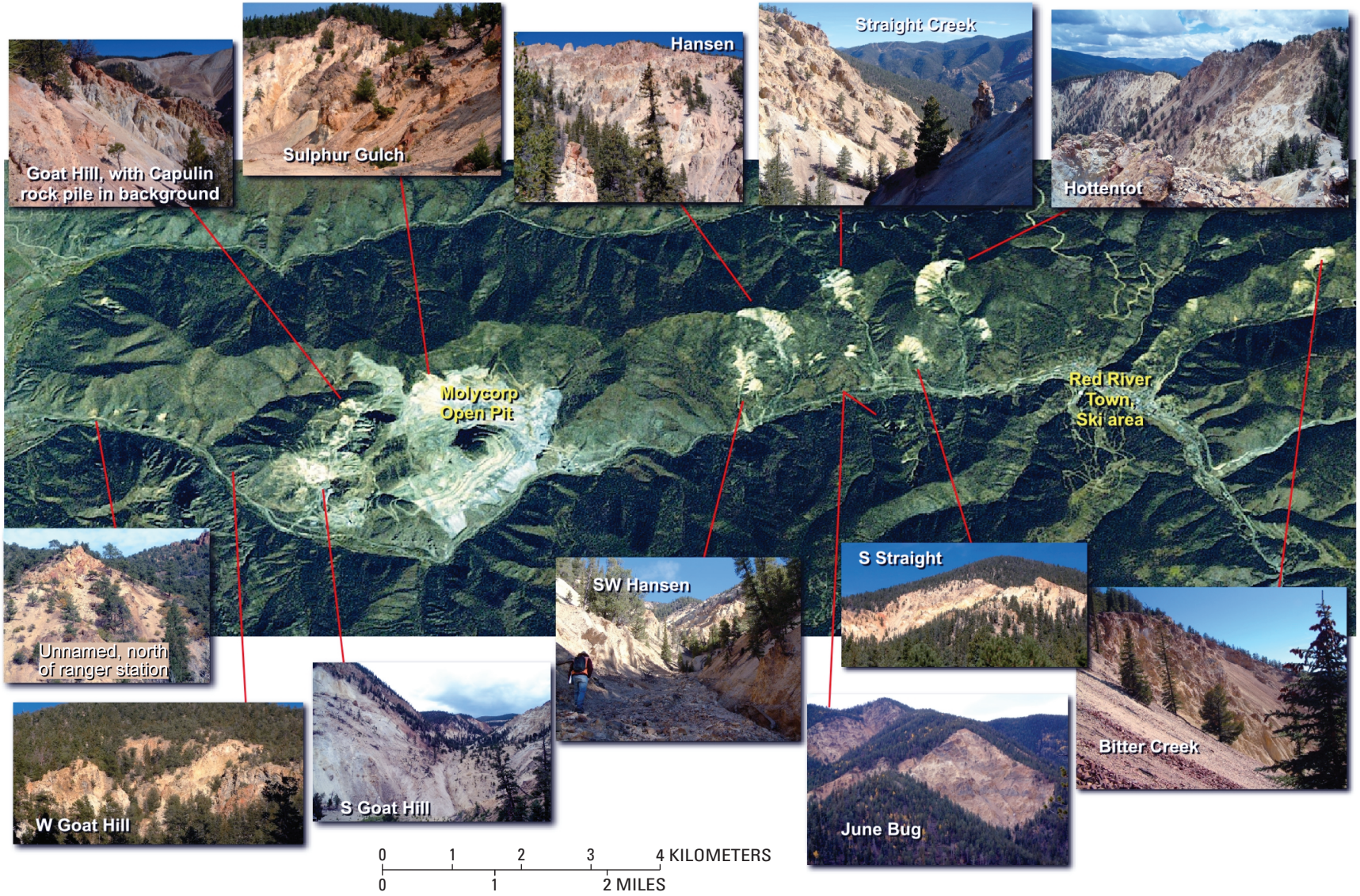

Figure 2. Satellite image of the Red River showing scar areas, Molycorp mine site, and the town of Red River with photographs of scar areas superimposed on the satellite image (from Ludington and others, 2004).

and others, 2005). Calcite, goethite, and sericite are widely distributed in the Red River Valley rocks and soils as revealed by Airborne Visible/InfraRed Imaging Spectrometry (AVIRIS; Livo and Clark, 2002). Calcite is an important mineral in the Red River Valley because its dissolution effectively neutralizes the acid inflows so that pH values in the Red River tend to be slightly alkaline (pH 7–8). Gypsum is common throughout the Red River Valley and forms as a secondary product of acid-sulfate weathering when pyrite oxidizes and reacts with calcite. Because gypsum is readily soluble in water, calcium and sulfate are the dominant ions for most surface and ground waters in the Red River Valley.

The major minerals in rock samples collected during mineral exploration and mining are biotite, calcite, chalcopyrite, fluorite, galena, molybdenite, pyrite, quartz, rhodochrosite, and sphalerite. Mining activities produced roughly 328 million tons of rock overburden deposited in Capulin Canyon, along the north slope of the Red River, and in Goat Hill, Sulphur, and Spring Gulches (Robertson Geoconsultants, Inc., 2000b). The abundant minerals in waste-rock samples include chlorite, gypsum, illite, illite-smectite, jarosite, kaolinite, and muscovite (Gale and Thompson, 2001). Recently, magnesite has been found in carbonate-altered rock at the mine site (Molycorp, Inc., oral commun., 2006).

Climate and Vegetation

The Red River Valley is located within a semiarid desert that receives precipitation throughout the year and sustains moderate biodiversity. Between 1915 and 2002, the annual average temperature was 4°C, and the precipitation and snowfall were 52 and 370 cm, respectively, with average daily temperatures fluctuating by 18°C (Western Regional Climate Center, 2003).

Climate and vegetation vary greatly within short distances because of differences in topography, weather, and soil composition. The altitude in the study area ranges from 2,280 m at the ranger station to 2,704 m at the Zwergle gage (USGS station number 08264500, upstream from the town of Red River) and 3,000 m at the ridge crest (fig. 1). Orographic effects of mountainous topography lead to precipitation on the windward slopes and localized storms within tributary valleys. Major precipitation events include summer thunderstorms and winter/spring snowstorms. Thunderstorms and monsoon rains are responsible for mass wasting in hydrothermally altered areas, producing debris flows that potentially affect vegetation, alluvial aquifers, and the Red River. Winter snowpack contributes to ground-water recharge through snowmelt infiltration and runoff.

Prevalent vegetation in the Red River Valley is representative of the following altitude zones: piñon-juniper woodland (1,800–2,300 m), mixed conifer woodland (2,300–2,740 m), and spruce-fir woodland (2,740–3,660 m; Knight, 1990). Willows, cottonwoods, shrubs, perennial grasses, and flowering vegetation are common near the banks of the Red River. Extending from the river are widely spaced piñon pines and junipers. This mountainous valley has an abundance of ponderosa pines and limber pines except at higher altitudes where Douglas fir and white fir grow. This typical mountain community, although diverse, is dominated by ponderosa pines (Larry Gough, U.S. Geological Survey, oral commun., 2003).

Hydrology

Surface Water

The Red River originates at an altitude of approximately 3,658 m (12,000 ft) near Wheeler Peak, the highest peak in New Mexico (4,011 m or 13,161 ft), and flows roughly 55 km (35 mi) to its confluence with the Rio Grande at an altitude of 2,012 m (6,600 ft). The USGS maintains a streamflow-gaging station at the USDA Forest Service ranger station at an elevation of 2,271 m (7,452 ft) about 1 mi downstream from the western boundary of the mine site. Total basin drainage area is 492 km^2 (190 mi^2); the drainage area upstream from the Questa ranger station gaging station is 293 km^2 (113 mi^2). Peak streamflow usually occurs from late May to mid-June, with snowmelt-related flows typically beginning in late March and increasing through mid-April. Summer thunderstorms are prevalent in July and August. Between 1930 and 2001, the mean annual discharge of the Red River at the Questa ranger station gage has ranged from 12.8 to 103 cubic feet per second (ft^3/s), while the average daily discharge ranged from 2.5 to 750 ft^3/s with an average of 46.8 ft^3/s (U.S. Geological Survey, 2004).

The main drainages in the vicinity of the mine site are Capulin Canyon, Goat Hill Gulch, and Sulphur Gulch on the north side of the Red River (fig. 1). Upstream from the mine site, Little Hansen, Hansen, Straight, Hottentot, and Bitter Creeks drain scar areas, whereas Mallette Creek drains a nonscar area on the north side of the Red River. Bear Canyon, Columbine, Pioneer, and Placer Creeks drain largely unmineralized land on the south side of the river. Bear Canyon and upper Pioneer Creeks contain some mineralization. Downstream from the mine site, the Red River joins with Cabresto Creek, entering from the north side of the Red River before it discharges to the Rio Grande.

Springs and shallow alluvial ground-water discharge to the Red River, rendering it a gaining stream over much of its length (Smolka and Tague, 1989). Between the town of Red River and the gaging station near Questa, there are about 25 ephemeral seeps and springs along the banks of the Red River and approximately 20 intermittent seeps and springs in tributary drainages on the north side of the river (South Pass Resources, Inc., 1995; Steffen, Robertson, & Kirsten, 1995; Robertson GeoConsultants, Inc., 2001b). Aluminum hydroxide often precipitates from springs downgradient from scar and mined areas on the north side of the Red River, affecting the color and turbidity of the river (Vail Engineering, Inc., 1989).

Ground Water

There are four main types of water-bearing units present in the Red River Valley—fractured bedrock, waste-rock piles, debris fans, and Red River alluvium. Bedrock constitutes the largest volume of aquifer in the study area but probably contains only small amounts of ground water because of low porosity. Low hydraulic conductivity is controlled by fractures. Waste-rock piles and scars with associated debris fans are geochemically reactive, have high porosities, and have fast infiltration rates. Alluvium consists of alluvial aquifers that are restricted in areal extent, compared to bedrock aquifers, and have variable composition.

Streamflow and hillslope processes have been eroding the mountainous study area throughout the late Cenozoic because of uplift. Deposits of unconsolidated sediments are present in only specific locations and are relatively small in volume. Hillslope soils are thin and composed of materials eroded from adjacent upgradient slopes. Debris fans are composed of sediments rapidly shed from their respective catchments. Where the tributary catchments contain "erosion scars" the debris fans are large and active and contain both coarse- and fine-grained, largely unsorted, debris-flow sediments. The chemistry of these sediments reflects the chemistry of their rapidly eroding and altered erosion scars. Sediments deposited by the Red River, in contrast, generally consist of well-washed, rounded sands, gravels, and cobbles and are composed of a mix of lithologies present in the entire Red River basin. The largest debris fans caused the Red River alluvium to aggrade behind the fans during the Quaternary. Thus, water flowing in the shallow alluvial aquifers likely passes alternately through Red River alluvium and debris-fan alluvium. Both the Red River alluvium and debris-fan alluvium are less than several hundred meters wide and less than 100 m thick.

Alluvial ground water is a calcium-sulfate type with magnesium commonly the second most abundant cation. Ground water downgradient from the waste-rock dumps and scars has acidic pH values and elevated metal concentrations compared to ground water upgradient from these altered areas. Bedrock ground waters are also calcium-sulfate type, but commonly of neutral pH. Most wells developed in the Red River Valley were installed to monitor water quality downgradient from mining operations (waste-rock dumps and tailings piles) and(or) scar areas. Wells installed during this study were located and developed for the purpose of measuring water levels and collecting water-chemistry data for a range of environments in the Red River Valley, similar to the mine environment, and to interpret the water/rock interactions under nonmining baseline conditions as a reference for pre-mining water quality for the mine site.

Hydrothermal alteration has produced substantial changes in mineralogy in the study area over relatively short distances, a common feature of hydrothermally altered terrains. Hence, both the mineralogy and the resultant water chemistry can change substantially over short distances. Such hydrogeochemical environments are highly heterogeneous, making the estimation of pre-mining ground-water chemistry a function of highly variable lithologies over an area the size of the mine site, rather than single fixed concentrations of various constituents.

Database for Speciation and Mineral Saturation Calculations

Computer software used for model applications continually undergoes modification with respect to both the primary coding and the databases. The two geochemical models used for speciation and mineral saturation calculations in this study were the WATEQ4F code (Ball and Nordstrom, 1991, which has been regularly updated since then) and the PHREEQC code (Parkhurst, 1995; Parkhurst and Appelo, 1999, which has also been regularly updated and enhanced). Both codes use the same thermodynamic database that is occasionally updated through critical evaluations (Nordstrom and others, 1990; Nordstrom and May, 1996; Ball and Nordstrom, 1998; Nordstrom and Archer, 2003; notes to recent versions of WATEQ4F, James Ball, written commun., 1995–present). To document the database used for the computations in this report, a compilation of the thermodynamic data has been tabulated in table 1–1 of Appendix 1.

Mineral saturation indices are defined as the logarithm of the ratio of the ion-activity product, IAP, to the solubility-product constant, K_{sp}, for a given mineral:

$$\log\left(\frac{IAP}{K_{sp}}\right)$$

The IAP is calculated from the speciation using the ion-association model (see Nordstrom and Munoz, 1994), and the K_{sp} is calculated from data given in Appendix 1. Both the speciation and the K_{sp} values are temperature-dependent and are calculated for the temperature at which the sample was collected.

Mass-balance calculations were done with the BALANCE code (Parkhurst and others, 1982), which does not use any thermodynamic data.

Summary Conclusions from Previous Reports

The basic data, computations, and interpretations for this investigation are based on a series of studies on the relevant geology, hydrology, and geochemistry of the Red River Valley that ultimately led to the elucidation of processes governing water/rock interactions and the evolution of ground-water chemistry. This section summarizes the main results from these studies, which are tabulated in table 2. The diagram in figure 3 shows the main components of the investigation and

their relationships to each other. It also shows how the individual reports on diverse tasks are grouped into major subject categories to lead to the final objective—pre-mining groundwater chemistry.

Historical Review of Water Quality

Numerous surface-water and ground-water quality studies were completed in the Red River Valley before the present investigation began. No compilation of these studies or evaluation of the quality of the data had been performed. It was unclear what some of the data sets indicated and how reliable they were. Consequently, one of the first tasks was to compile and evaluate these data and determine if it was possible to interpret the data sets.

Ground Water

Some 608 ground-water analyses were available for the time period 1992–2002. Ground waters were not analyzed prior to 1992 because monitoring ground-water quality for regulatory purposes was not required before that time. These analyses were compiled, evaluated, and reported by LoVetere and others (2004). They found that many of the analyses were incomplete in that not all the major ions were always reported, charge imbalances were occasionally too large, and fluoride concentrations were highly biased until there was a change in method (and laboratory) in 1997. Nevertheless, ion-ion plots were prepared for several constituents to see if there were any recognizable trends in the data. Sulfate concentrations covered a broad range from 100 to 8,000 mg/L. The highest concentrations were associated with waste-rock piles, and the highest concentrations of most other constituents tended to correlate with high sulfate concentrations. The strong positive correlation of calcium with sulfate reflects the influence of gypsum dissolution and calcite plus pyrite oxidation. The common occurrence of acidic waters with sulfate enrichment relative to the $Ca:SO_4$ molar ratio of gypsum (1:1) reflects the influence of pyrite oxidation on many of these ground waters.

Some concentrations were among the highest ever reported for those elements worldwide. For example, the highest beryllium concentration in ground water that Veselý and others (2002) reported was 160 µg/L, whereas the concentration was as high as 280 µg/L in ground water from the mine site. Some seeps had even higher concentrations. The highest concentration of cobalt reported by a National Academy of Sciences (1977) survey was 99 µg/L, whereas concentrations as high as 5 mg/L were reported from ground water likely associated with waste-rock piles.

Out of all these ground-water analyses, 328 were found to have acceptable charge imbalances (less than ±20 percent). Acceptable charge imbalances were a requirement for speciation and saturation index computations for calcite, gypsum, fluorite, rhodochrosite, manganite, and aluminum hydroxide. Saturation was reached for gypsum, calcite, fluorite, and aluminum hydroxide in many of the samples. These results provided the first indication of concentration limits on constituents from mineral-solubility limits. Further, the positive correlation of calcium with sulfate, and zinc with cadmium, especially for acid-sulfate waters, reflects the effect of acid dissolution on mobilization of metals and simple mineralogical sources for some constituents.

Red River Surface Water

Nearly 300 surface-water analyses were compiled for the time period 1965–2001 by Maest and others (2004). Most of these analyses were incomplete because the objective was to determine if concentrations of copper, zinc, cadmium, arsenic, and lead were found unacceptable for the Red River; the incomplete analyses resulted in unacceptable charge balances. Nevertheless, the analyses were evaluated for quality assurance/quality control (QA/QC) and usually met reasonable standards considered acceptable at the time of each study. An exception is the Melancon and others (1982) study, which reported high concentrations of arsenic that were never observed before or since and were considered unreliable. The most commonly sampled site for surface water was the Red River at the USGS Questa gage (site 08265000), next to the USDA Forest Service ranger station (fig. 1). Samples had been collected and analyzed from here since 1965, and trends in sulfate concentration were examined for the period 1965–2002. The variability in sulfate concentration overwhelmed any temporal trend until the data were discriminated on the basis of flow conditions. Three general flow conditions are recognizable—snowmelt, late summer (often monsoonal) rainstorms, and dry periods. Furthermore, solute concentrations varied differently for rising limb of snowmelt or rainstorm relative to falling limb of snowmelt or rainstorm conditions and varied differently for snowmelt and rainstorm. Hence, the hydrologic conditions were discriminated on the basis of rising limb of snowmelt, peak snowmelt, falling limb of snowmelt, rising limb of rainstorm, peak rainstorm, falling limb of rainstorm, and low flow (little or no change in flow). When samples were collected nearly simultaneously on the Red River at the Questa USGS gage and a site just upstream from the mine site from 1965 to 2002 and only low-flow sulfate concentrations used, there appears to be an upward trend to about 1993 that would indicate some influence from the mine site. The trend is only indicative because insufficient data were collected in the late 1960s and the early to mid-1970s to demonstrate this trend clearly. Furthermore, the observation that the increase in concentration occurs in the reach of the river that flows past the mine site does not necessarily mean that it is related to mining activities. The data do show very clearly the large variations in concentration that result from dynamic changes in the hydrologic conditions of the Red River Valley. The most striking change in water quality occurred on September 7, 1986, when a sudden drop in pH (from 7.4 to 3.8) occurred due to a storm.

Further trends in the water quality of the Red River were discussed by Verplanck and others (2006) with another

Table 2. Compilation of reports published within this project.

[n/a, not applicable]

Series report no.	Title: Questa Baseline and Pre-Mining Ground-Water Quality Investigation	Reference
n/a	Results of electrical surveys near Red River, New Mexico	Lucius and others (2001)
n/a	Mapped minerals at Questa, New Mexico, using Airborne Visible-Infrared Imaging Spectrometer (AVIRIS)	Livo and Clark (2002)
1.	Depth to bedrock determinations using shallow seismic data acquired in the Straight Creek drainage near Red River, New Mexico	Powers and Burton (2004)
2.	Low-flow (2001) and snowmelt (2002) synoptic/tracer water chemistry for the Red River, New Mexico	McCleskey and others (2003)
3.	Historical ground-water quality for the Red River Valley, New Mexico	LoVetere and others (2004)
4.	Historical surface-water quality for the Red River Valley, New Mexico, 1965–2001	Maest and others (2004)
5.	Well installation, water-level data, and surface- and ground-water geochemistry in the Straight Creek drainage basin, Red River Valley, New Mexico, 2001–2003	Naus and others (2005)
6.	Preliminary brittle structural geologic data, Questa mining district, southern Sangre de Cristo Mountains, New Mexico	Caine (2003)
7.	A pictorial record of chemical weathering, erosional processes, and potential debris-flow hazards in scar areas developed on hydrothermally altered rocks	Plumlee and others (in press)
8.	Lake-sediment geochemical record from 1960–2002, Eagle Rock and Fawn Lakes, Taos County, New Mexico	Church and others (2005)
9.	Historical seep, spring, underground, and tributary water quality for the Red River Valley, New Mexico	LoVetere and Nordstrom (written commun., 2006)
10.	Geologic influences on ground and surface waters in the Red River watershed, New Mexico	Ludington and others (2004)
11.	Geochemistry of alteration scars and waste piles	Briggs and others (2003)
12.	Geochemical and reaction-transport modeling based on tracer injection-synoptic sampling studies for the Red River, New Mexico, 2001–2002	Ball and others (2005)
13.	Mineral microscopy and chemistry of mined and unmined porphyry molybdenum mineralization along the Red River, New Mexico—Implications for ground- and surface-water quality	Plumlee and others (2005)
14.	Interpretation of ground-water geochemistry in catchments other than the Straight Creek catchment, Red River Valley, Taos County, New Mexico, 2002–2003	Nordstrom and others (2005)
15.	Methods and results of Phase II and III well installation and development and results of well logging, hydraulic testing, and water-level measurements in the Red River Valley, New Mexico, 2002–04	Blanchard and others (2007)
16.	Quality assurance and quality control for water analyses	McCleskey and others (2004)
17.	Geomorphology of the shallow alluvial aquifer of the Red River Valley, New Mexico	Vincent (in press)
18.	Characterization of brittle structures in the Questa caldera and speculation on their potential impacts on the bedrock ground-water flow system, Red River watershed, New Mexico	Caine (2007)
19.	Leaching characteristics of composited materials from mine waste-rock piles and naturally altered areas near Questa, New Mexico	Smith and others (2007)
20.	Water-chemistry trends of the Red River, Taos County, New Mexico, with data from selected seeps, tributaries, and snow, 2000–2004	Verplanck and others (2006)
21.	Hydrology and water balance of the Red River Valley, New Mexico	Naus and others (2006)
22.	Ground-water budget for the Straight Creek drainage basin, Red River Valley, New Mexico	McAda and Naus (in press)
23.	Quantification of mass loading from mined and unmined areas along the Red River, New Mexico	Kimball and others (2006)
24.	Seismic refraction tomography for volume analysis of saturated alluvium in the Straight Creek drainage and its confluence with the Red River, Taos County, New Mexico	Powers and Burton (2007)
25.	Summary of results and baseline and pre-mining ground-water geochemistry, Red River Valley, Taos County, New Mexico, 2001–2005	Nordstrom, this volume.

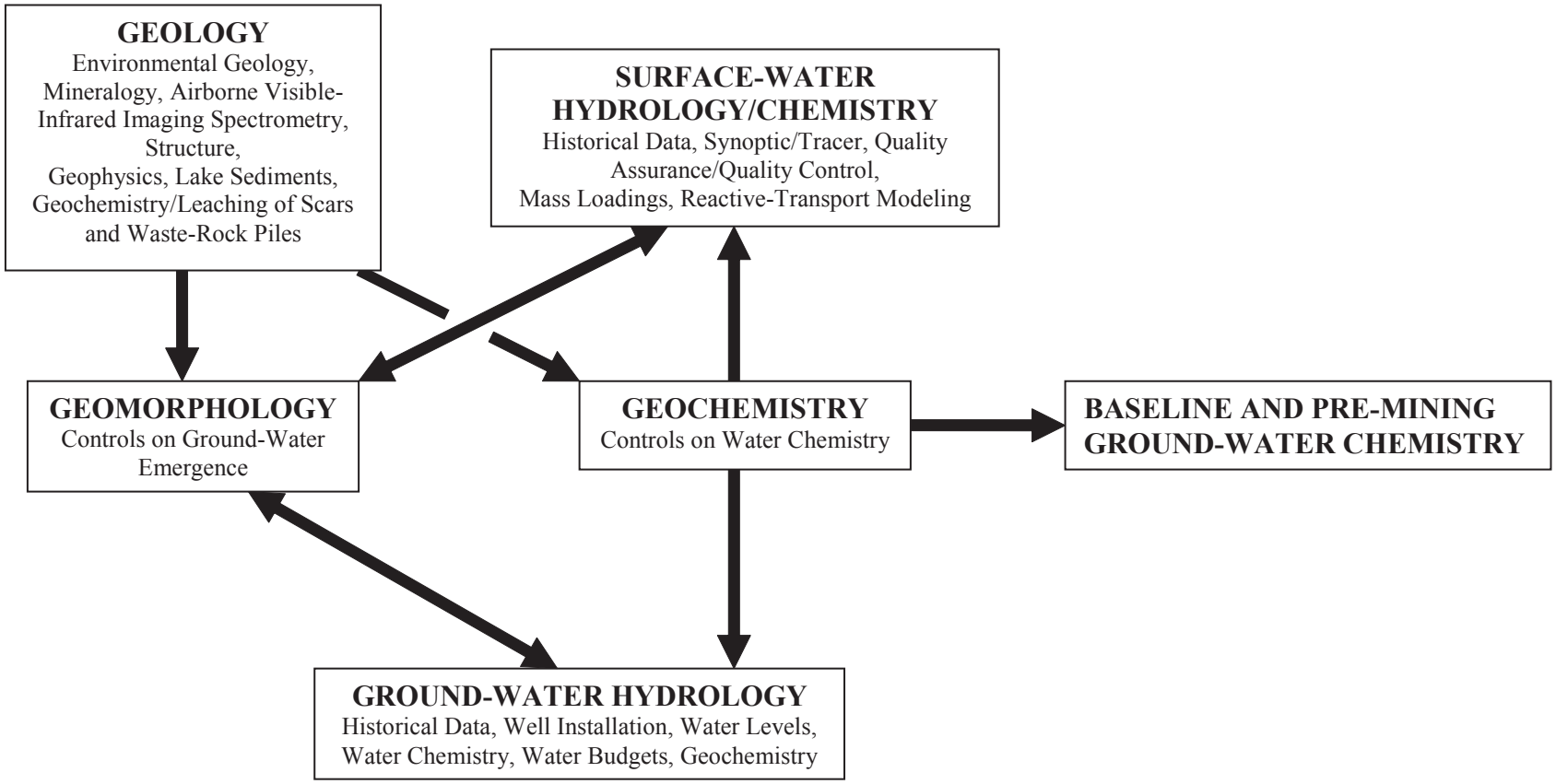

Figure 3. Study components and their relationships for inferring pre-mining ground-water chemistry.

example of the effect of a storm on the water quality of the Red River during September 2002. The pH at the USGS gage decreased from 7.8 to 4.8, and large increases in iron, aluminum, and manganese concentrations were evident. More recent effects of storms have been documented by Molycorp's consultants. These storm-related changes and degradation of water quality in the Red River are caused by sudden flushing of acidity from the scars and debris fans, such as those at Hansen, Hottentot, and Straight Creek, by heavy rainstorms. During monsoonal rains, these scar-containing catchments mobilize large amounts of debris, dissolve soluble salts, and discharge subsurface waters containing high solute concentrations into the Red River.

Seeps, Springs, and Tributaries

Five hundred and thirty-six samples of seeps, springs, and tributaries were collected from 1992 to 2002 (LoVetere and Nordstrom, in press). The general range of solute concentrations is similar to those for historical ground-water analyses, but solutes achieve higher concentrations for seeps from waste-rock piles than those for ground water in waste-rock piles. For example, waste-rock seeps from Capulin Canyon and Goat Hill Gulch have sulfate concentrations in the range of 10,000 to 20,000 mg/L, whereas concentrations from well water in waste rock are usually less than 10,000 mg/L. These historical data, when combined with seeps sampled and analyzed for this investigation, provide a chemical profile of scar-drainage seep chemistry. Values of pH for scar-drainage water were well constrained to 2.9 (±0.4), and sulfate concentrations were well constrained to 2,000 (±860) mg/L. These data are shown in histograms in the section on the chemistry of waters developed from scar weathering. The one exception to this scar-water chemistry trend is Bitter Creek, where seep samples were collected six times during 2000 by Robertson Geoconsultants, Inc. (2001a), and the sulfate concentrations ranged from 9,000 to 15,000 mg/L (values corrected from original report to comply with reasonable charge balances). The cause for the exceptionally high sulfate and other solute concentrations at Bitter Creek is not known and was not considered in this investigation.

The same general trends in solute concentrations found for the ground water at the Molycorp site apply to the seeps, springs, and tributaries. Mineral solubility controls by $Al(OH)_3$, gypsum, rhodochrosite, and fluorite provide upper limits to concentrations of Al, Ca, Mn, and F.

Geologic Investigations

Airborne Visible-Infrared Imaging Spectrometry

Airborne visible and infrared imaging spectrometry (AVIRIS) had been flown shortly before this investigation began so that data reduction and interpretation of the data were possible within the time constraints of this project. Livo and Clark (2002) completed AVIRIS maps for major minerals occurring at the surface for the study reach of the Red River Valley. These results provided a clear picture of the overall areal extent and composition of the hydrothermal mineralization for the valley and guidance for what minerals to seek during later investigations of mineralization in outcrops and surficial deposits. One of the distinguishing features of the AVIRIS study was the widespread extent of QSP and acid alteration in the valley. The QSP alteration has been largely weathered at the surface to an assemblage dominated by jarosite, gypsum, and kaolinite. Jarosite is indicative of acid-sulfate weathering with pH values in the range of 1–3.

Geologic Characterization of Weathering Processes

The development of surface- and ground-water composition begins with the geologic framework. The geology is both the physical and chemical medium through which the water flows and reacts. The overall perspective on the geology for the context of this investigation was reported by Ludington and others (2005). The most important aspect of this study was the geologic comparison of the chosen analog site with the mine site to answer the question of how satisfactory the Straight Creek catchment is as an analog. Descriptions of the mineralogy also provide the framework for the water/rock interactions that produce the observed ground-water chemistry.

Generally, the geologic analogy holds well. The scar at Straight Creek has similar topography, size, lithology, alteration and mineralogy, intensity and type of fracturing, geochemical abundance of elements, slope aspect and direction, and processes of physical erosion as the scars at the mine site, especially the larger scars in upper Sulphur Gulch and Goat Hill Gulch. An important difference between the Straight Creek analog site and the mine site is the Sulphur Gulch catchment. Sulphur Gulch eroded to deeper levels within the mineralized and altered zones than did Straight Creek (or Hansen or Hottentot Creeks). The depth that the erosional surface reached relative to the alteration zones is depicted schematically in figure 4. The erosion of Sulphur Gulch penetrates and intersects not only areas of extensive carbonate, fluorite, and molybdenite mineralization but exposes the intrusive stock. However, the mineralogy of this zone is well documented, which makes possible an estimation of the effect of mineral

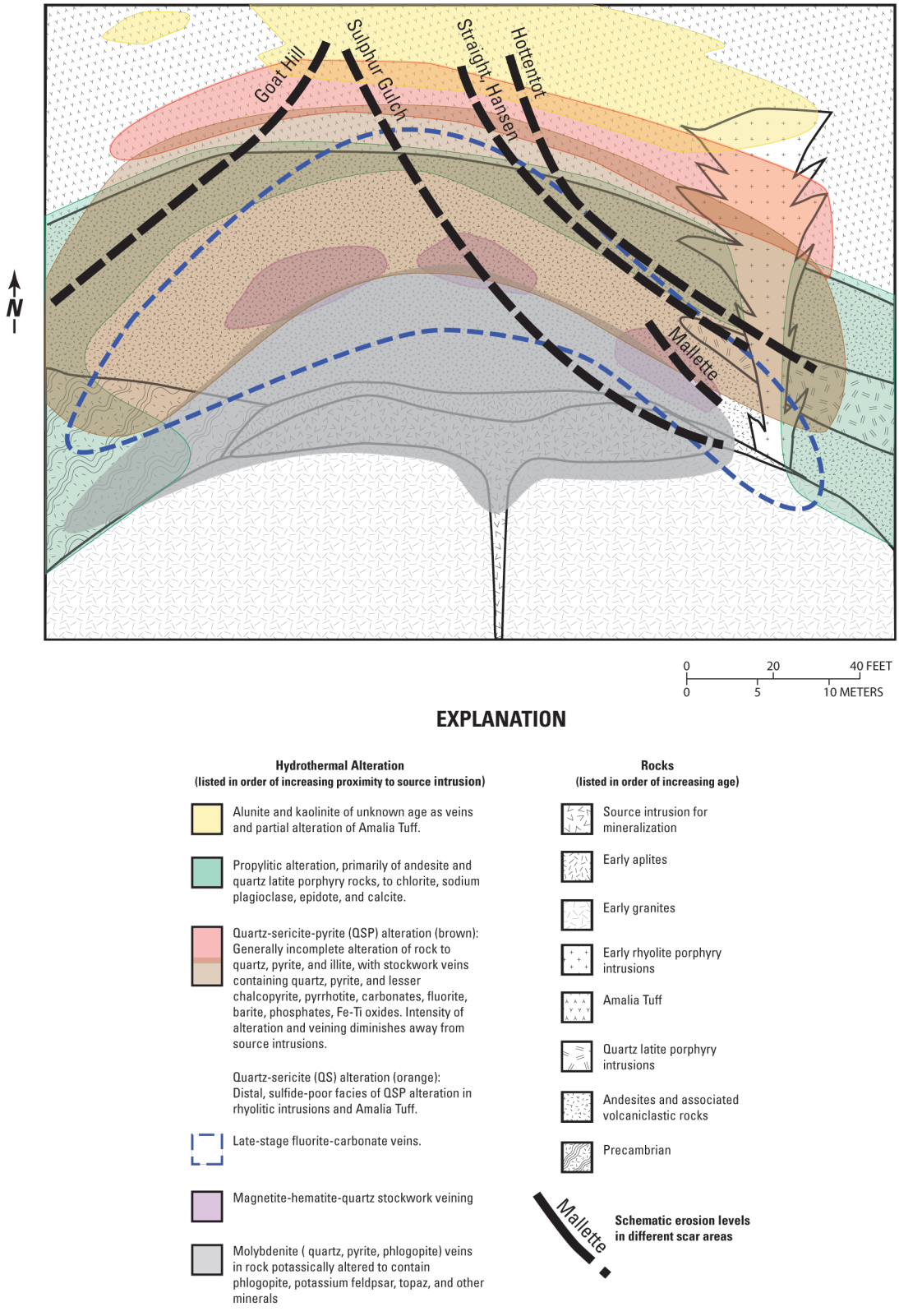

Figure 4. Schematic geologic cross section of alteration zones with overlying dashed lines depicting the relative position of the erosional surface for five catchments along the Red River (from Ludington and others, 2005).

dissolution on water chemistry. The exposure of carbonates and fluorite, the low pyrite content, and the exposure of granitic stock and aplites will produce circumneutral-pH water with low iron and magnesium concentrations, but with high concentrations of manganese and fluoride. Geochemical maps from Robertson Geoconsultants, Inc. (2001b), indicate some metals could be more abundant in Sulphur and Goat Hill Gulches than in Straight Creek, Hansen Creek, or Hottentot Creek catchments. Also the Sulphur Gulch debris fan is much smaller than the Straight Creek debris fan because of its location on a bend in the stream channel where it likely has been washed downstream by high flows of the Red River.

Another important observation documented in Ludington and others (2005) is the coexistence of calcite and pyrite in veins within altered volcanic rocks. As the calcite and pyrite weather, they react in place to form crystals of gypsum which then dissolve into the infiltrating water. Gypsum crystals are abundant in the Red River Valley, and they are predominantly secondary in origin (formed from original "primary" minerals by weathering).

Mineralogical Characterization

General features of the mineralization, hydrothermal alteration, and host rock geology were reported in Ludington and others (2005). More detailed aspects of the mineralogy and mineral chemistry, especially the trace-element content of individual minerals, were reported in Plumlee and others (2005). The results of the mineral chemistry study identified the source minerals for trace elements of environmental concern, chiefly Mn, Pb, Zn, Cd, Co, Cr, Ni, Li, Be, and Cu. Optical microscopy, scanning electron microscopy with energy-dispersive X-ray analysis, electron probe microanalysis, and laser-ablation inductively coupled plasma mass spectrometry were used to identify individual mineral phases and their trace-element content. Trace-element determinations in bulk rock samples (Amalia Tuff, Tertiary andesite, quartz latite porphyry, and rhyolite) were also reported.

Most of the dissolved constituents have identifiable sources in specific minerals. Calcium is derived primarily from calcite and gypsum dissolution. Some calcium may be derived from plagioclase where it is locally abundant. Strontium and yttrium are predominantly associated with calcite. High-magnesium calcite and dolomite can be important sources of magnesium, but the widespread occurrence of chlorite and its fine-grain size indicate that it also could contribute magnesium to water bodies. The chlorites are also rich in iron and may contribute some iron to ground water. Pyrite is the dominant source for iron, cobalt, nickel, and, in combination with gypsum dissolution, sulfate. The most abundant source of copper is chalcopyrite, of lead is galena, and of zinc is sphalerite. The dominant source of cadmium is also sphalerite. The dominant source of fluorine is fluorite because of its widespread occurrence and rapid dissolution rate in acid water. Fluoride-rich biotites, chlorites, and illites do occur but likely contribute only minor amounts to ground water because of their slower dissolution rates and lower fluorine content. Rhodochrosite and manganese-rich calcites are the dominant source of manganese. There are multiple sources of aluminum and silica that include chlorite, kaolinite, smectite, feldspars, and to a lesser extent, illite. Lithium and beryllium do not seem to be identified with a distinct Li or Be mineral but rather are dispersed in lattices of several silicate minerals. Illites tend to carry high concentrations of lithium and beryllium in some samples. Chromium tends to be more concentrated in chlorites than any other phase although it is also somewhat dispersed. The elements cobalt, nickel, and chromium all tend to associate together, which is characteristic of a mafic source rock. Mafic rocks such as andesites are typically enriched in these elements, and ultramafic rocks are even more enriched in these same elements. Hence, the andesite is the likely original source for cobalt, nickel, and chromium, but hydrothermal alteration would likely have changed the initial mineralogical distribution of these elements in the andesite so that pyrite contains most of the cobalt and nickel, and chlorites contain most of the chromium.

Leaching Studies

Less than 2-mm-size composite samples from five mine waste-rock piles, nine erosional-scar areas, a less-altered site, and a tailings slurry pipe were analyzed for bulk chemistry and mineralogy and then subjected to two back-to-back leaching procedures. A 5-minute leach for easily soluble constituents (Hageman and Briggs, 2000) was followed by an 18-hour, end-over-end, rotating leach using deionized water. The purpose was to compare and contrast the leachability of acidity, metals, and sulfate from unmined scar areas with mine waste rock. The results showed that scar leachates have low pH values (less than 4.1). Under these low-pH conditions, many metals can be mobilized and remain in solution; however, anionic species (such as molybdenum) tend to be less mobile under acidic conditions. Waste-rock leachates generally have the same or higher pH values but still are acidic. Some increases in pH occurred with leaching time, which indicates there is some buffering capacity left in waste rock.

An important difference appeared in leachate composition for some of the waste-rock samples. Both Capulin and Sugar Shack West samples had lower pH, independent of leaching time, than the other waste-rock samples. Generally, metal concentrations in the waste-rock leachates do not exceed the upper range of those metal concentrations in the erosional-scar leachates. One notable exception is molybdenum, which is significantly higher in the waste-rock leachates compared with the scar leachates. The pH values in the waste-rock leachates span the range for some pH-dependent solubility and metal-attenuation reactions. Hence, as pH increased in the waste-rock leachates, concentrations of several metals decreased with increasing time and agitation. Beryllium was consistently higher as the pH of the leachate decreased, but most other constituents were not consistent except for calcium and sulfate. Capulin and Sugar Shack West samples had

consistently lower calcium and sulfate concentrations than the other waste-rock samples. This difference reflects the higher gypsum and calcite content of the Old Sulphur Gulch, Sugar Shack Middle, and Sugar Shack South rock piles compared to the Capulin and Sugar Shack West piles. The consistently higher sulfur stable isotope composition for the three rock piles (Old Sulphur Gulch, Sugar Shack Middle, and Sugar Shack South) also suggests the presence of some primary (or hypogene) gypsum. Indeed, the difference in calcium concentration is greater (in moles per liter) than the difference in sulfate concentration. That is, the three rock piles have about five times as much calcium as the other two (Capulin and Sugar Shack West) but only 3.5 times as much sulfate concentration. Hence, there is likely some calcite dissolution in addition to gypsum dissolution to account for this difference. Further, these interpretations would indicate that the wastes dumped at Capulin and Sugar Shack West are inherently depleted in calcite and gypsum relative to the other three waste piles, a situation that could be caused by (1) longer residence time and exposure to weathering after extraction or (2) the material had weathered more before extraction because it was closer to the surface. The data available on mine rock-pile production (Robertson Geoconsultants, Inc., 2000a) show that the development of Capulin and Sugar Shack West was nearly the same time period, at the beginning of open-pit operations (about 1965), whereas the other three began development about 1969 (Old Sulphur Gulch) or 1971 (Sugar Shack Middle and South). Therefore, the difference in leachate properties likely reflects the difference in the natural weathering profile of the area now occupied by the open pit. Capulin and Sugar Shack West rock piles contain a preponderance of shallow earth material containing more pyrite and less calcite and gypsum, whereas the other three sampled waste piles contain deeper, less oxidized rock with less pyrite and more carbonates.

Bedrock Structure and Ground-Water Flow

Fault zones, joints, and other fractures that might be permeable to ground-water flow were mapped in the vicinity of the southern Questa caldera boundary (Caine, 2003). Information on mapped fractures was then used to estimate the potential for bedrock to transmit ground water to the Red River by Caine (2007). Prior to this investigation, the bedrock through which the ground water flowed was thought to be impermeable and had not been considered a likely source of ground-water discharge to the Red River. Of particular importance was to determine whether bedrock discharge of ground water to the Red River on the north side and in the vicinity of the Columbine Park area adjacent to the mine site could explain some of the substantial solute-loading increase.

Pervasive, high-intensity fracturing was found along the southern portion of the Questa caldera. North-south-trending permeable fault zones run parallel to the presumed hydraulic gradient which, along with the joint network, makes bedrock transmission of ground water likely. The range of reasonable ground-water flow rates was constrained by a series of calculations that assumed hydraulic gradients consistent with the topography, permeabilities consistent with hydraulic aquifer tests in bedrock, and cross-sectional areas. The conclusion was that it was possible for ground-water flow to be conveyed by bedrock in this area. The concept that bedrock is impermeable in the vicinity of the caldera margin is not tenable. Bedrock in other areas away from the caldera margin is not likely to carry much ground water (unless other hydrothermal activity or tectonic activity produced similarly intensive jointing and faulting).

Lake-Sediment Chemistry

Sediments from two lakes in the study reach, Fawn Lakes and Eagle Rock Lake, were cored, dated with ^{137}Cs, and analyzed for 34 elements. The lakes are manmade, having been dug as borrow pits for highway construction in about 1960. An abrupt change in the sediment element concentrations for Eagle Rock Lake occurred at the time of a major flood in 1979 and caused significant changes in concentrations after 1979 that suggest a new source of sediment. Comparisons of the post-1979 sediment-core chemistry with both mine wastes and pre-mining sediments from the vicinity of the mine site indicate that both are possible sources.

Seismic Profiles

Boundary conditions for ground-water flow in the Straight Creek analog site must include the bedrock/alluvium contact as it defines the lower boundary of the alluvial aquifer and it defines a permeability discontinuity between the alluvial and bedrock aquifers. Furthermore, definition of the bedrock contact would permit an estimate of the volume of alluvial material in the debris fan. Electrical geophysical methods did not detect a material property contrast between the bedrock and the alluvium (Lucius and others, 2001). Four geophysical seismic lines were run in 2002 (Powers and Burton, 2004), but bedrock reflection was still uncertain. Five more seismic lines were established, and seismic refraction tomography was employed, encompassing the Red River alluvium to complete the definition of the debris fan. Two different software packages were used for the tomography, and the results were compared for optimal definition of subsurface features. Powers and Burton (2007) reported on the refined seismic tomography for the Straight Creek debris fan and defined both the bedrock contact and the ground-water table. The results from these additional lines and refinements gave a much clearer picture of the cause of discontinuities in the ground-water table between wells SC–4A, SC–3A, and SC–6A. It revealed a drainage channel in bedrock that is located to the east of the surficial drainage channel. Well SC–6A is located in the bedrock channel, but SC–4A and SC–3A are not. For example, the water level in SC–6A was approximately 60 ft lower in elevation than SC–3A during the period of observation. Wells SC–3A and SC–4A are on an elevated bedrock surface that gives rise

to perched water tables and explains the apparent water-table discontinuity. The bedrock surface also reveals a rough, tortuous outline of local heterogeneities that probably indicate large boulders incorporated into the debris fan. An example of the roughness of the bedrock surface is shown in figure 5 in which the contact between alluvium and bedrock is estimated by the contact between velocity contrast represented by the blue and red zones in the figure. The morphology of these heterogeneities makes it easier to understand how the Straight Creek alluvial ground water can remain separate from the Red River alluvial ground water. There could have been a small natural berm or boulder-packed divide that built up between the mouth of Straight Creek and the Red River to keep them spatially separate. Hardpan surfaces commonly form at contacts between acidic iron-rich water (such as Straight Creek) and circumneutral-pH water such as the ground water in the Red River (Blowes and others, 2003). A hardpan, possibly a fericrete, could have formed at the contact or interface between Straight Creek alluvial water and Red River alluvial water to sustain separation of these waters.

Geomorphology

The geochemical and hydrologic processes in the Red River Valley occur within a complex terrain of evolving landforms. These landforms, lithologies, and associated hydraulic conductivities control surface-water and ground-water movement, ground-water discharge to surface water, and the spatial distribution of ground-water emergence. A geomorphological analysis by Vincent (in press) provided the necessary link between landforms and the spatial distribution of ground-water emergence into the Red River as found in the mass-loading profiles reported by Kimball and others (2006; following section). It also put the erosional processes of the Red River Valley into geologic context. Rates of scar erosion and debris-fan formation in the Red River Valley are among the fastest rates measured.

Ground-water emergence increases the solute mass loadings to the Red River and is not easily recognized as input from proximal catchments. The complexity of the link between ground-water flow and Red River flow was recognized by Vail Engineering, Inc. (1993, 2000) and shown quantitatively for the first time. Vincent (in press) demonstrated that debris fans, having lower hydraulic conductivity than the Red River alluvial sediments, but faster sediment-transport and deposition rates, would retard Red River alluvial ground-water flow and force Red River alluvial ground water to emerge into the water column in the debris fans. Debris fans can act as confining units, and the emerging ground water can change the chemistry of the water column intermittently and cause the ground-water table to drop well beneath the level of the riverbed on the downstream side of the fan. A substantial fraction of the ground water can emerge to become streamflow, the amount depending upon the overall properties of the debris fan. Narrowing of the canyon by bedrock can also restrict alluvial sediment transport and ground-water flow, forcing emergence of alluvial ground water. These geomorphic influences were in effect long before the onset of mining. Figure 6 shows the Red River in longitudinal profile with the ground-water table between Sulphur Gulch and Bear Creek.

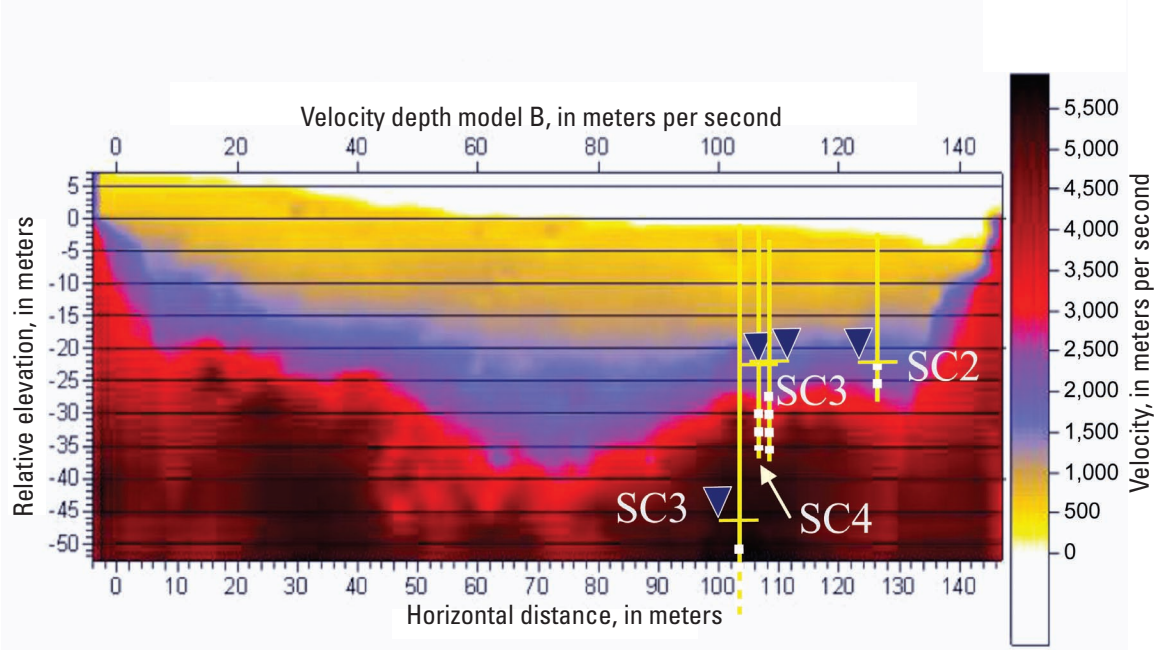

Figure 5. Example of a cross section for seismic line 3 showing bedrock (red), water (blue), and ground surface and unsaturated zone (yellow to beige) from seismic refraction tomography (from Powers and Burton, 2007).

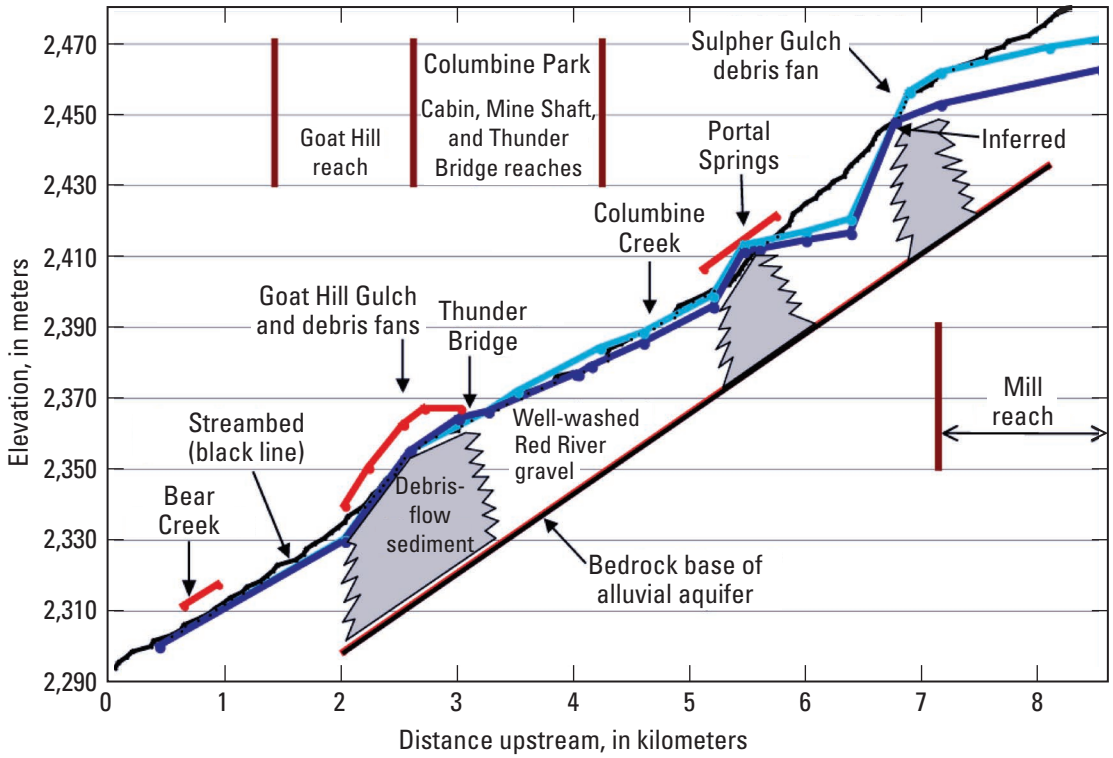

Figure 6. Longitudinal cross section of the Red River along the reach of the mine site projected onto a two-dimensional plane with bedrock surface, water tables (light blue for August 21, 2001, and dark blue for January–February 2002), projections of the debris-fan surface (red), and Red River streambed surface (from Vincent, in press).

Hydrologic Investigations

Quality Control and Quality Assurance (QA/QC) of Water Analyses

Reliable water analyses are crucial to the objective of this investigation. Particular emphasis was placed on the QA/QC of all the analytical data. McCleskey and others (2004) reported on the QA/QC and found that for 72 blanks there was minimal to no contamination from processing, handling, and analyzing the samples. Occasionally different analytical methods were used to determine the same constituents in the same samples. These comparisons showed that for constituents more than 10 times the detection limit, the percent error was less than 8.5 for 95 percent of the samples. Charge imbalance was less than 12 percent for 98 percent of the samples. The range in all charge imbalances was ±16 percent. Spiked recoveries, standard reference water samples, and an interlaboratory comparison all performed well. Timing of filtration after sample collection for surface-water samples, effect of pore size on trace-element concentration, effect of sequential filtration on trace-element concentration, effect of filtration method (diameter of filter, and plate, capsule, syringe, or ultrafilter types), and ultrafiltration were compared as part of the QA/QC. The results showed that for concentrations greater than 0.05 mg/L, the various filtration procedures did not affect the determinations except for iron and aluminum. Below 0.05 mg/L, the metals mostly affected by filtration methods were iron, aluminum, and copper.

Synoptic and Tracer Studies of Red River

Ground-water flow travels from recharge to discharge along some flow path. The discharge endpoint for ground waters of the study reach is the Red River. Hence, it was necessary to obtain synoptic solute concentrations along the Red River with constant-flow tracer injection to quantify the discharge and determine portions of the reach receiving ground-water influx and the chemistry of that influx. Previous studies by Vail Engineering, Inc. (1993, 2000) and Robertson Geoconsultants, Inc. (2001b) of the water balance and sulfate load balance for the Red River showed that a substantial amount of ground water was discharged to the streamflow of the Red River just upstream from the Goat Hill debris fan. At least one-half of the solute load of this influx was thought to be derived from natural acidic scar drainage several miles

upstream (from Hansen Creek, Straight Creek, Hottentot Creek, and Bitter Creek scars).

Two synoptic/tracer studies were performed, one in August 2001 and the other in March–April 2002. The basic chemical data were published by McCleskey and others (2003), and the mass-loading curves for sulfate and other constituents and their interpretation were reported by Kimball and others (2006). In 2002 a study was planned for measuring the effect of snowmelt; however, there was no snowmelt peak recorded in the hydrograph for that year because of prolonged drought. The winter was warmer and drier than usual. It was the first year in 75 years of record that no snowmelt peak appeared.

The results revealed several step increases in discharge, concentrations, and mass loadings—(a) through the town of Red River, (b) near the boundary between the lower end of the Straight Creek debris fan and the upper end of the Hansen Creek debris fan, (c) near La Bobita, (d) just upstream from Sulphur Gulch debris fan, (e) Columbine Park–Cabin Springs area, (f) Thunder Bridge area (just upstream from the Goat Hill Gulch debris fan), and (g) just downstream from the Capulin Canyon mouth (figs. 5 and 7). Each of these changes in mass loading appears to be related to the occurrence of debris fans or a narrowing of the canyon walls by bedrock or areas of mineralization close to the Red River. The amount of mass-loading increase varied, depending on constituent and time of year. There were clear differences between the two studies caused by two events in 2002: (1) more ground-water pumping along the mine-site portion of the reach (for milling) and (2) drier climatic conditions. The pumping and dry conditions virtually eliminated the large increase in manganese loading in the Columbine Park area that was observed in the 2001 study. By comparing and contrasting the two studies, the effect of pumping and seasonal trends on mass loading was clearly demonstrated.

The discharge of ground water to the Red River appears chemically analogous to an acid-base titration. The Red River begins upstream as a dilute, carbonate-buffered river and becomes less buffered as it moves through the study reach. Surface and alluvial ground water of the Red River upstream from the town of Red River (upstream from the study reach) has a more basic pH (higher than 8). As it moves down the valley, it receives acid influx from Bitter Creek, Hottentot Creek, Straight Creek, Hansen Creek, Sulphur Gulch, mine-waste piles, Goat Hill Gulch, and Capulin Canyon. The acid influx gradually consumes the buffering capacity of the Red River, though not completely. Figure 7 shows the values of pH for the Red River decreased from 8.2 at the town of Red River to 7.9 at the Questa stream gage in August 2001. In March–April 2002, the pH values decreased from 8.5 to 7.8 for the same locations.

Sulfate and soluble metal concentrations such as zinc, manganese, and total recoverable aluminum have increased continually with downstream transport. Figure 7 shows the changes in discharge, pH, and the concentrations of alkalinity, SO_4, Mn, Zn, total recoverable Al, and dissolved Al with

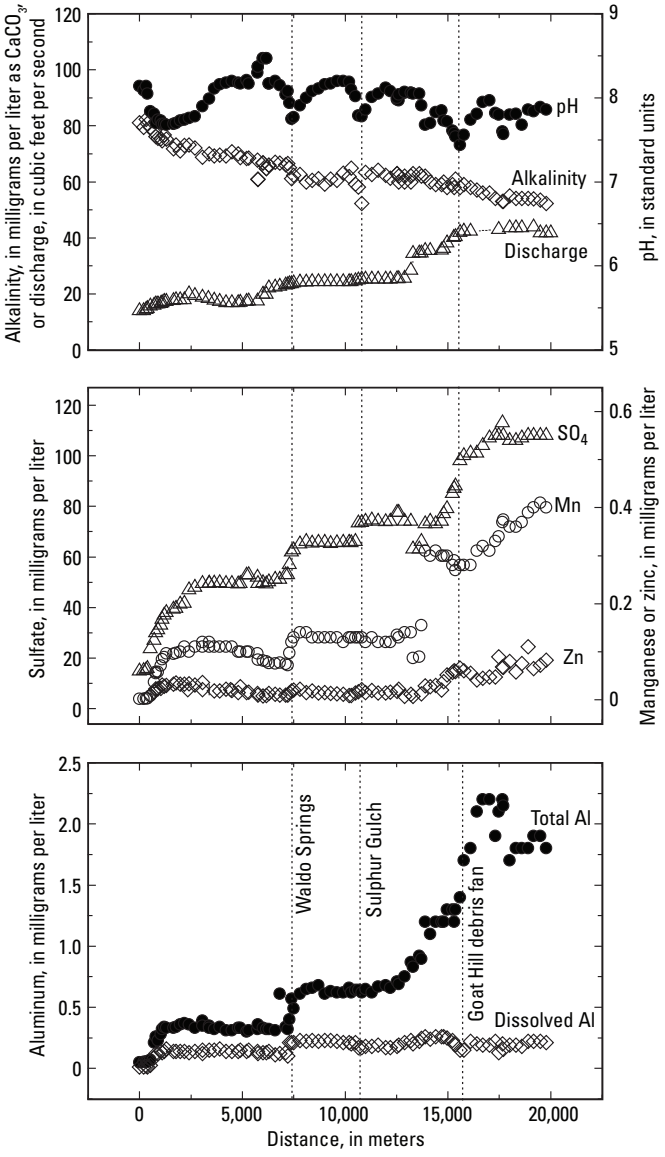

Figure 7. Longitudinal profiles of discharge, pH, alkalinity, dissolved sulfate, manganese, zinc, total recoverable aluminum, and dissolved aluminum with distance from the synoptic/tracer study of 2001 (from Nordstrom, 2005).

downstream distance in the Red River from the synoptic/tracer study of 2001. Abrupt decreases in pH and increases in SO_4, Zn, Mn, and total recoverable Al concentrations can be observed at three distinct locations, at Waldo Spring, Sulphur Gulch, and upstream from the Goat Hill debris fan. For manganese, total recoverable aluminum, and discharge, there is an additional increase in the Columbine Park–Cabin Springs area (plate 1) from ground-water emergence that did not appear in the 2002 synoptic-tracer study.

The results from the synoptic-tracer studies showed the complexity of the physical and chemical interactions of ground water with the Red River. Acidic ground waters with

high solute concentrations from both natural processes and mine-related activities have entered the Red River alluvium and the Red River itself at distinct locations related to landform features, not at the juncture of each catchment with the Red River. These locations of ground-water emergence into Red River water are often 2 to 3 km (1 to 2 mi) downstream from the catchment junctures.

Reactive-Transport Modeling in the Red River

Reactive-transport modeling not only integrates quantitatively the combined processes of ground- and surface-water influx, but it also considers quantitatively the in-stream processes of oxidation, sorption, and mineral precipitation/dissolution. The basic constraining principles and theories are those of chemical thermodynamics, fluid flow, and mixing. Ball and others (2005) used the synoptic/tracer data of both 2001 and 2002 to model mixing and in-stream chemical processes in the Red River with the OTIS/OTEQ code (Runkel, 1998; Runkel and Kimball, 2002).

In-stream reactive processes were necessary to model the behavior of hydrogen ion, iron, aluminum, copper, and zinc. Other constituents were sufficiently conservative to be modeled without reaction. Mineral precipitation (with formation of colloidal-size particles) can account for the low dissolved aluminum and iron concentrations in the Red River. Iron precipitation was simulated with ferrihydrite and $Fe(OH)_3$ solubility, and aluminum precipitation was simulated with microcrystalline to amorphous $Al(OH)_3$ solubility. Copper and zinc concentrations are kept low by sorption and were modeled by sorption onto hydrous ferric oxides. Aluminum hydroxide precipitates at pH values of about 5 until a pH of 7.5 is reached (Nordstrom and Ball, 1986; Ball and others, 2005). At this point, inorganic mineral precipitation is no longer effective because the aluminum concentration is virtually constant from pH 7.5 to 8.5 at a value much higher than that imposed by any $Al(OH)_3$ mineral solubility. Organic-aluminum complexing is proposed to explain the departure from mineral solubility controls (Ball and others, 2005).

Values of pH in the Red River oscillate between lower values resulting from inflow of acid water and higher values that appear to be caused by kinetically controlled degassing of carbon dioxide after acidification or possibly neutralization from reaction with carbonate minerals.

During this study, the chemical relationship among the inflow ground-water compositions (ground water discharging into the Red River), the Red River water compositions, and ground-water compositions from wells were examined. Inflow compositions can be obtained from (a) analyses of seeps and springs that are sampled next to the Red River (see McCleskey and others, 2003), (b) changes in constituent ratios, such as Ca/SO_4, upstream and downstream from emergent points, and (c) calculating the composition from the change in mass flux and discharge in the Red River upstream and downstream from emergent points.

Mixing lines, using conservative constituents, were found to reveal the chemical similarity between ground waters, inflow compositions, and changes in river-water composition. The mathematical basis for the mixing lines is given in the Appendix. An example is shown in figures 8 and 9 for (a) ground water upgradient from La Bobita (Straight, Hansen, and Hottentot Creeks), (b) the La Bobita well, (c) the Red River upstream from ground-water emergence, and (d) the Red River downstream from ground-water emergence. The reach of ground-water emergence can be seen in figure 7 in the vicinity of Waldo Springs from changes in metals concentrations. The other locations can be found on plate 1.

Two constituents, calcium and magnesium, are used for these examples. Constituent ratios to sulfate (such as calcium to sulfate ratio) plotted against sulfate concentration were found to reveal differences in the end-member water compositions. The calcium to sulfate ratio is plotted as a molar ratio so that the 1:1 molar ratio, representing pure gypsum dissolution, could be shown. Data plotting higher than the gypsum line are enriched in calcium from calcite dissolution that neutralizes acid drainage, indicating circumneutral-pH values. Data plotting lower than the gypsum line have additional sulfate from acid-sulfate waters derived from pyrite oxidation. The end members for the mixing line are the alluvial well water at SC–1A and the Red River upstream from the point of ground-water emergence. These two points anchor the mixing line with 100-percent source water represented by SC–1A composition and 0 percent represented by Red River at 7,200 m downstream from the town of Red River (distance points used in the synoptic/tracer study, McCleskey and others, 2003). All other data points are independent of the mixing-line calculation. The fact that all the water-chemistry data, with two exceptions (SC–5B and MMW–43A), lie along the mixing line suggests that the water mixing into the Red River near La Bobita is consistent with naturally acidic ground waters from scar areas as the source. Further, it suggests that the seepage water diluting SC–1A water to produce water compositions in wells SC–3A, SC–4A, and SC–6A are dilute and similar in composition to the Red River alluvial aquifer ground water.

Near La Bobita, part of the ground water emerges and the rest remains in the Red River alluvial aquifer. An important question is: How far downgradient from La Bobita can the same chemical signature be observed in the alluvial ground water? The next Red River alluvial well is MMW–17A. As shown in figures 8 and 9, its calcium and magnesium to sulfate ratios, respectively, are virtually identical to those for La Bobita (and other inflow waters). The next well water downstream from MMW–17A is that from MMW–43A. It shows a different signature from the mixing line for both calcium and magnesium to sulfate ratios at a much higher sulfate concentration than the La Bobita water, so it must be strongly affected by a different source composition of higher calcium, magnesium, and sulfate concentrations and higher ratios. The other exception to this mixing trend is water from well SC–5B (bedrock well). It was plotted to show that circumneutral-pH

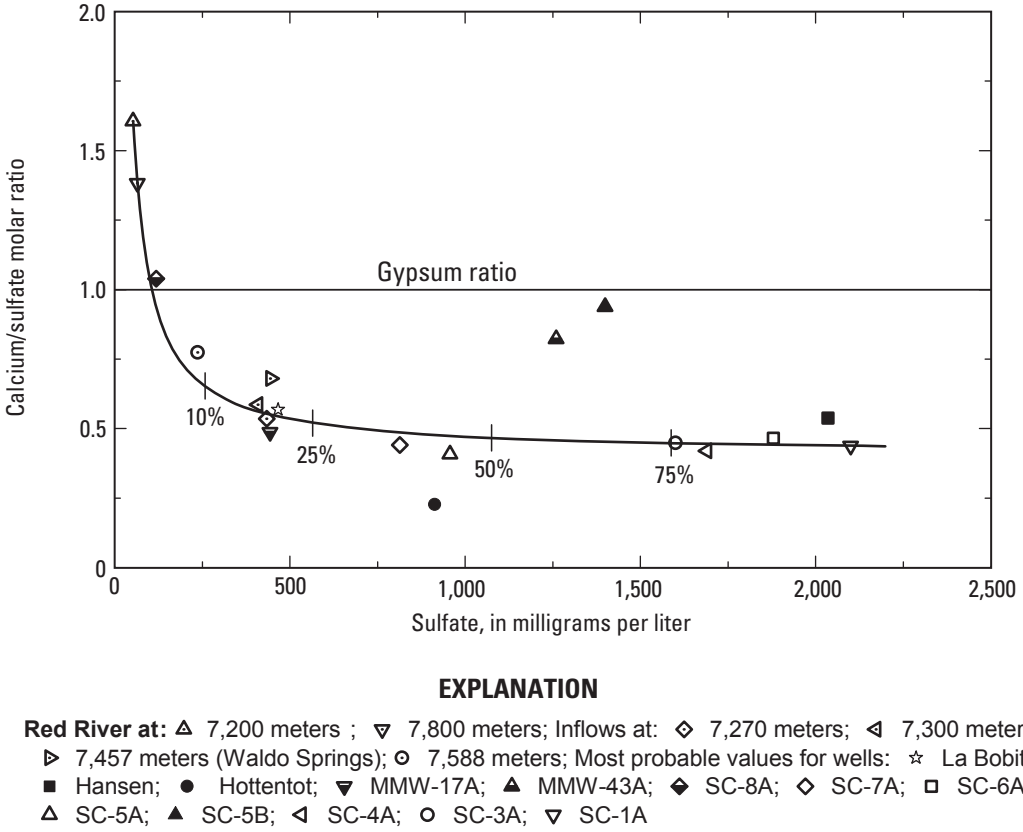

Figure 8. Mixing line constructed between Red River upstream from ground-water emergence (7,200 meters) and well water from SC–1A, using calcium/sulfate molar ratios relative to sulfate concentrations. Other ground waters from Straight Creek, Hottentot Creek, Hansen Creek, La Bobita, MMW–17A, MMW–43A, and seeps in this reach are also plotted. Vertical bars indicate percentage of SC–1A water that has mixed with Red River (or similar) water (from Ball and others, 2005).

bedrock ground water in the Straight Creek catchment does not have the same chemical signature as the acid alluvial ground water. Its calcium to sulfate ratio is much higher than that for the alluvial ground water, and the magnesium to sulfate ratio is much lower than that for the alluvial ground water.

The well water at SC–7A also was used instead of SC–1A as the end-member source of acid water, and it makes no difference in the position of the mixing line. The observation that the Red River during mixing lies on the mixing line, as do the Waldo Springs discharge, La Bobita well water, and Straight Creek well-water compositions, indicates that the chemical signature is consistent with a flow path from the natural scar drainages to emergence in the Red River near La Bobita. This consistency in chemistry shows that the acid-scar drainages that become alluvial ground water do not mix with the alluvial ground water and emerge into the river until the narrowing of the canyon at La Bobita is reached. Well water from MMW–17A (just beyond the narrowing of the canyon) also is consistent with La Bobita, but the next downstream alluvial well, MMW–43A, has distinctly different chemistry. New sources of sulfate-rich water are entering the aquifer between MMW–17A and MMW–43A. The inflow compositions (seeps and springs near the banks of the river), from which one sample was chosen for the mixing calculations in the reactive-transport modeling, are also consistent with the mixing-line composition. The percent mixing indicates that less than 2 percent of SC–1A water was needed to mix with Red River water to cause the change in water chemistry of the Red River at La Bobita.

Diel, Storm Event, and Long-Term Trends in Red River

Variations in water chemistry at any one location can be caused by dynamic hydrologic events (snowmelt, rainstorms, floods), droughts, and anthropogenic activities (such as irrigation, water management with dams and canals, and wastewater discharge). Solar cycles regulate biological activity and consequently can affect water chemistry. During this investigation, water-chemistry variations in the Red River were observed by Verplanck and others (2006) and compared with historical

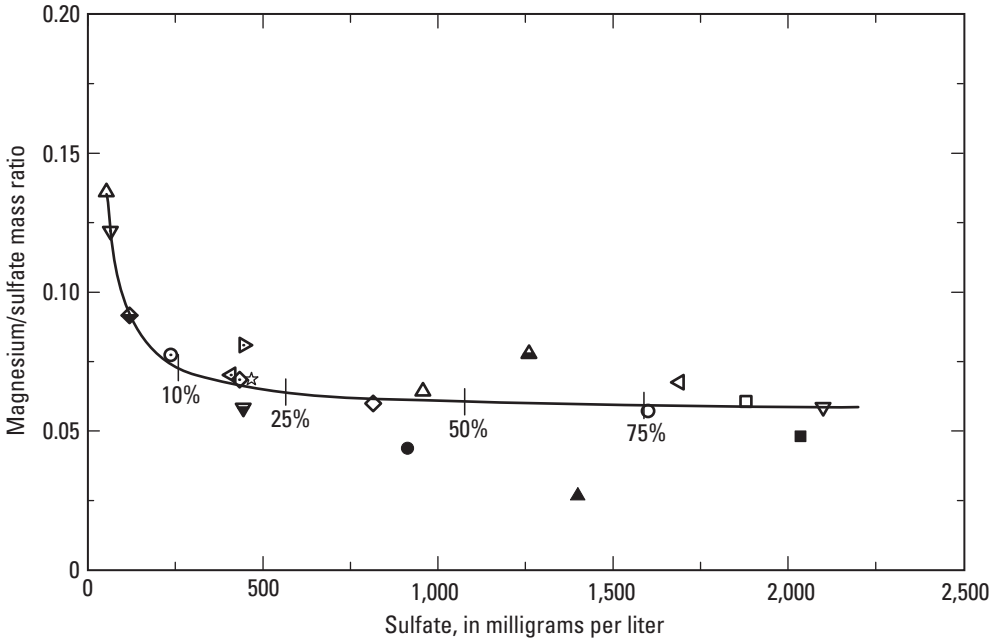

EXPLANATION

Red River at: △ 7,200 meters; ▽ 7,800 meters; Inflows at: ◇ 7,270 meters; ◁ 7,300 meters; ▷ 7,457 meters (Waldo Springs); ⊙ 7,588 meters; Most probable values for wells: ☆ La Bobita; ■ Hansen; ● Hottentot; ▼ MMW 17A; ▲ MMW 43A; ◆ SC-8A; ◇ SC-7A; □ SC-6A; △ SC-5A; ▲ SC-5B; ◁ SC-4A; ○ SC-3A; ▽ SC-1A

Figure 9. Mixing line constructed between Red River upstream from ground-water emergence (7,200 meters) and well water from SC–1A using magnesium/sulfate mass ratios relative to sulfate concentrations. Other ground waters from Straight Creek, Hottentot Creek, Hansen Creek, La Bobita, MMW–17A, MMW–43A, and seeps in this reach are also plotted (from Ball and others, 2005).

water-chemistry trends. They also reported on water-chemistry results from the Straight Creek and other scar drainages.

Water-chemistry variations in the Red River were found to be caused primarily by snowmelt and rainstorms and secondarily by length and degree of dry periods. Diel samples were collected during high flow (May 2003) and low flow (October 2003). Only at low flow and only for dissolved zinc and manganese was there a discernible diel cycle. Again, these diel trends were minor compared to snowmelt and rainstorm variations (Verplanck and others, 2006).

One series of samples collected before, during, and after the rainstorm of September 18, 2002, demonstrates the effect of natural scar drainage water on the water quality of the Red River at the Questa gage (Verplanck and others, 2006). In a matter of hours, discharge increased from 10 to 100 ft^3/s and the pH changed from 7.8 to 4.8 (fig. 10). The highest concentrations of iron, aluminum, zinc, and sulfate collected for the period 2001–2004 occurred during this storm. A greater change in chemistry of the Red River at the gage was found in the historical record (Maest and others, 2004) with a decrease in pH to 3.8.

Maest and others (2004) noted that when only the "low-flow" sulfate concentrations at the Questa gage were separated from the rest of sulfate concentration data set, there was an overall long-term trend of increasing concentration for the time period 1965–93 and then a small decrease after that time. More recent data from 2001 to 2004 from Verplanck and others (2006) were included to determine if the indication of a downward trend since 1993 was observed. These data indicate that there is no significant decrease in sulfate concentration since peak values were attained about 1993. The water-chemistry effects of drought years compared to wet years complicates the interpretation of discerning natural weathering processes from the effects of mining. A preliminary examination of the historical data suggests that prolonged dry periods can cause overall increases in solute concentration compared to wet periods because the relative proportion of surface flows, such as Columbine Creek and the portion of Red River upstream from the study reach, decreases more proportionally than the inflows of acidic ground water. Conversely, when surface-water flows increase, solute concentrations decrease except for momentary acid flushes, as shown in figure 10.

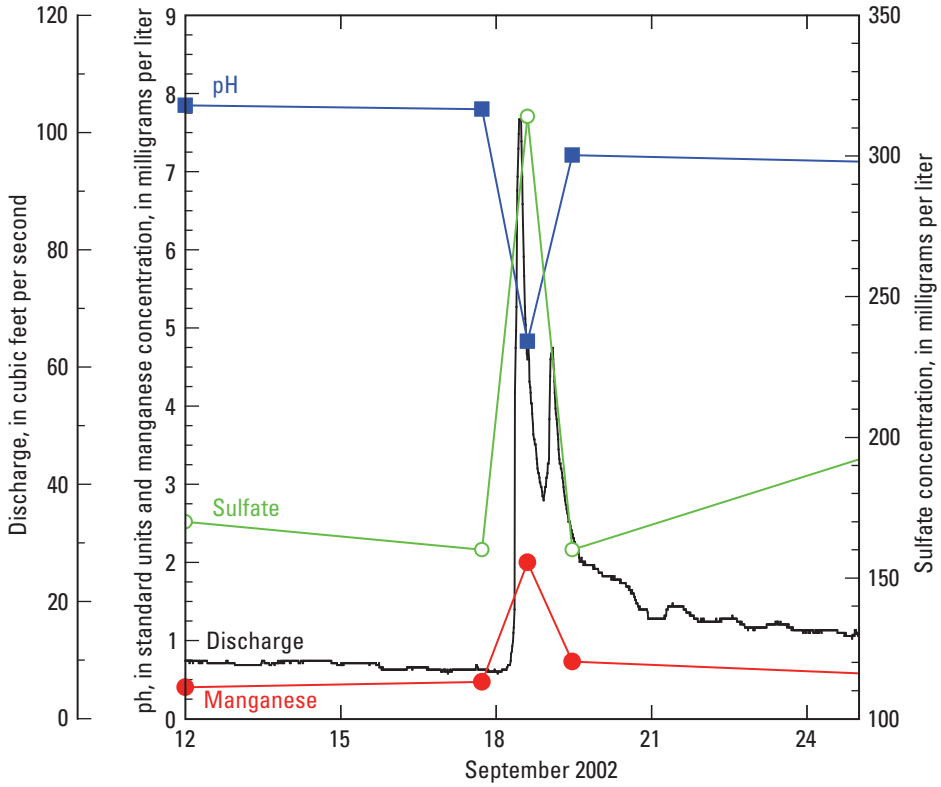

Figure 10. Changes in discharge, pH, and sulfate and manganese concentrations at the U.S. Geological Survey Questa gage during the storm of September 17–18, 2002 (Verplanck and others, 2006).

Ground Water

Ground-water geochemistry is described in the "Interpretation of Ground-Water Geochemistry" section. All of the ground-water results are integrated to summarize weathering controls and mineral solubility controls on solute composition. Results of well installation and development and methods and results of water-level collection are found in Naus and others (2006) and in Blanchard and others (2007). Methods of sample collection for water analyses are found in Naus and others (2006) and QA/QC, which applies to all water analyses in this investigation, is found in McCleskey and others (2004). Sampling and preservation procedures are consistent with those found in the USGS National Field Manual for the Collection of Water-Quality Data (*http://water.usgs.gov/owq/FieldManual/*).

Water Balances

Straight Creek

Considering the problems associated with aquifer tests on perched aquifers at Straight Creek and the inability to develop a ground-water model with such a spatially heterogeneous system, the effort was put into developing a ground-water budget (McAda and Naus, in press). Some 77 percent of precipitation was lost by evapotranspiration, leaving about 17 percent for ground-water infiltration in the debris fan and underlying regolith and about 5 percent for deeper bedrock ground water. This study indicated that the amount of ground-water flow to the Red River alluvium from Straight Creek is small, only about 156 liters per minute (0.347 ft^3/s) or about 3 percent of the Red River alluvial flow at Straight Creek. If only debris-fan (and underlying regolith) ground water is considered, then ground water is only about 2 percent of Red River alluvial flow. This small proportion of flow adds to the difficulty of finding the mixing zone in the Straight Creek debris fan. This proportion of flow is also consistent with estimates from chemical data and mixing curves, indicating that scar drainage accounts for only about 2 percent of the water in the Red River near La Bobita where ground water emerges.

Estimates for ground-water emergence to the Red River near the La Bobita area have been obtained from several studies (Borland and others, 1990; Vail Engineering, Inc., 2000; Kimball and others, 2006), and their values range from 1.4 to 5 ft^3/s. This range is better than expected because different methods were used, the study was done in different water years, and the studies were done at different times of the year. These results show that ground-water emergence appears consistently in this part of the river, independent of water year.

Red River Valley

A basinwide water balance was completed to achieve a better understanding of the relation between ground-water chemistry and flow of tributary basins to changes in flow and chemistry in the Red River (Naus and others, 2006). This study is another approach to understanding ground-water/surface-water interactions in complex terrain and relates to the mixing lines shown for ground waters and surface waters (figs. 8 and 9), but is a more quantitative approach. Both approaches should be consistent with each other. This study also is consistent generally with previous studies such as the Borland and others (1990) seepage investigation, the Vail Engineering, Inc. (2000) flow and load-balance investigation, the Vincent (in press) geomorphological analysis, and the Kimball and others (2006) synoptic/tracer/loading investigation. A series of natural barriers to alluvial ground-water flow repeatedly causes ground-water emergence into the river (Vincent, in press), but the flow balance can vary with the seasons and with prolonged wet periods or prolonged dry periods. Each study was done at a different time period except for the Vincent (in press) study, which was done with data that corresponded to the same time period as the Kimball and others (2006) study. The Naus and others (2006) study was based on annual averages over long time periods. Vail Engineering, Inc. (2000), derived an October 1999 flow balance that included Red River discharge measurements and sulfate concentrations for a sulfate load balance.

Naus and others (2006) reexamined precipitation, evapotranspiration, and different regression equations previously used for estimating yields. Long-term mean annual precipitation for subbasins in the valley is estimated to range from 330 to 890 mm. Using this range of precipitation in empirical equations relating precipitation to elevation and catchment areas, three estimates were obtained for yields for each subbasin. Alternatively, yield was estimated by subtracting evapotranspiration estimates from precipitation and by the chloride balance method. Long-term mean annual catchment yields ranged from 45 to 52 ft^3/s. Ground water was shown to be 80 to 94 percent of total yield, depending on the amount of surface-water flow.

Integrating Water-Flow and Sulfate Mass-Load Balances for the Hottentot–La Bobita Reach

There is sufficient information to attempt a water and sulfate load balance in the reach upstream from the mine site (from Hottentot debris fan to the La Bobita area). The results shed light on the process of ground-water mixing and discharge to the Red River and the consequences for downstream transport of solutes from natural sources to the reach along the mine site.

McAda and Naus (in press) have estimated from seismic data and hydraulic conductivity that the ground-water flow in the Red River alluvium adjacent to the Straight Creek fan (at seismic line 7 in Powers and Burton, 2007) is 11.65 ft^3/s based on water levels in September 2003. This flow is assumed to be the ground-water flow before any water from the natural scar drainage (or adjacent catchment drainage) enters the Red River alluvium. The surface-water flow in the Red River measured by Kimball and others (2006) for the 2001 tracer study was 17.12 ft^3/s. Hence, the total flow was 28.8 ft^3/s, which compares well with the estimated yield (ground water plus surface water) for that location in the Red River Valley of 32.3 ft^3/s (based on data in Naus and others, 2005). However, a better approximation of alluvial ground-water flow for August 2001, when the 2001 tracer study was obtained, would be 11.87 ft^3/s, assuming that conditions of August 2003 were similar to those of August 2001 (D.P. McAda, U.S. Geological Survey, written commun., 2005). Hence, the combined flow would be about 30 ft^3/s, only 7 percent different from the yield estimate. Similar estimates were made for water-level data that most closely approximate the conditions for the March/April 2002 synoptic/tracer.

The yield estimates can be used to calculate the yield from all catchments along the reach from Hottentot catchment to the end of ground-water emergence just downstream from the La Bobita campground. When the yields are summed from catchments 4–7 and 25–28 (catchment numbers from Naus and others, 2005), the result is 1.54 ft^3/s, of which about 0.89 ft^3/s is primarily from scar drainage. Hence, of the total flow (32.3 ft^3/s), scar drainage base flow constitutes 2.8 percent. Of the ground-water flow in this section (13.19 ft^3/s), the scar drainage constitutes 6.7 percent.

The results from the 2001 synoptic/tracer study by Kimball and others (2006) show two sections of ground-water emergence in this part of the study reach, one at about 4,800 to 5,735 m (using the east end of the town of Red River as the zero point; Kimball and others, 2006) and the other at about 5,765 to 8,700 m. The sum of those two flow increases is 5.03 ft^3/s. For the 2002 synoptic/tracer study, the sum of these flow increases is 3.65 ft^3/s. The alluvial outflow is simply the difference between ground-water emergence and the total flow before emergence. The resulting flow balance for the Red River alluvial aquifer along this reach is shown diagrammatically for both years in figure 11.

As a check on these calculations, an independent estimate of the alluvial outflow was obtained from Darcy's law by considering the cross-sectional area of the canyon at the narrowing just downstream from the La Bobita campground (about 3,000 m^2), the hydraulic conductivity (about 0.3 cm/s), and the gradient (about 0.017 m/m by topography and about 0.029 m/m with pumping in the mill reach). The range of alluvial outflow is then 5.4 ft^3/s without pumping and 9.2 ft^3/s with pumping (Kirk Vincent, written commun., 2005). Not only are the values estimated by difference within 50 percent of the Darcy calculation, but the estimate for 2002 when there was more pumping is within about 3 percent of the Darcy

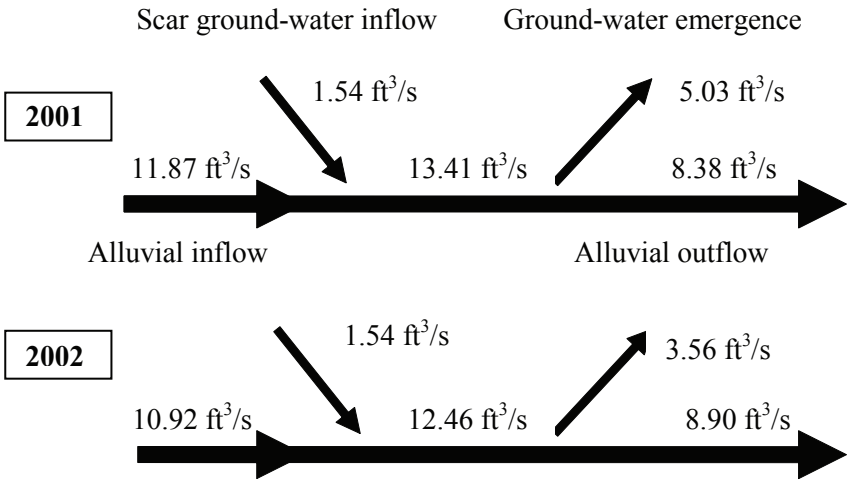

Figure 11. Water-flow balance for the Red River alluvial aquifer shown schematically for synoptic/tracer studies of 2001 and 2002 for the reach from Hottentot debris fan to La Bobita (from Kimball and others, 2006).

calculation. Consequently, a high degree of confidence can be attributed to the flow balances.

For the sulfate mass-load balance, it was assumed that the average sulfate concentration in the Red River alluvial ground water, before any water from the scar area mixed into it, was 119 mg/L based on the concentration of sulfate in ground water from well SC–8A. This well appears to be unaffected by the acid alluvial ground water from Straight Creek and should contain Red River alluvial ground water. Hence, the sulfate mass-load inflow in the Red River alluvium, before it mixed with scar-drainage inflow, was 3,454 kg/day for conditions of August 2001.

Scar-drainage sulfate loads were calculated by taking the yields from each catchment (Naus and others, 2005) and multipying them by the median sulfate concentrations from each respective wel1. Catchments that have little or no scars and no wells are more difficult to assess. The catchment to the west of the Hansen scar drainage (number 7 in Naus and others, 2005) has a small amount of scar from Little Hansen, and the catchments on the south side of the Red River have some small scars, but most of these areas are without scars or wells. Seepages along the banks of the Red River near La Bobita have sulfate concentrations of about 400 mg/L (McCleskey and others, 2003; Ball and others, 2005), and a spring sampled to the west of Little Hansen contained 412 mg/L of sulfate. Hence, a sulfate concentration of 400 mg/L was assumed for these other catchments. The sulfate mass loads for each catchment are shown in table 3. The scar drainages (numbers 4–6) contribute 5 percent of the water flow in this reach of the Red River but 33 percent of the sulfate load. Fifty-four percent of the sulfate load [(3,454/6,426) × 100] is carried by the Red River alluvium as it enters this reach.

For the 2001 synoptic/tracer study, the increase in sulfate load in the Red River was 1,843 kg/day. For the 2002 study, the increase was 1,159 kg/day. The schematic sulfate mass-load balance is shown in figure 12.

From these calculations, the concentration of sulfate in the ground water of the Red River alluvium would increase from 119 to 196 mg/L. However, if the sulfate concentrations are calculated for the emerging ground water and the nonemerging ground water, a problem arises. The concentrations should be the same because they originate from the same source, but they are not. The emerging ground water contains 150 mg/L sulfate, whereas the nonemerging ground water contains 244 mg/L. This difference occurs because the emergent ground-water flow and mass load are derived from separate measurements than the inflow of ground water from the catchments. It could be argued that this concentration difference is not of consequence considering all the uncertainties in the data; however, the consequences for the load balance is quite serious. This model will be named Model I and is based on “best available data.”

A different model (Model II) can be derived by making the mass loadings and concentrations consistent with the concept that the concentrations of both emerging and nonemerging water originate from the same source and must have the same concentration of sulfate. This model is the “completely mixed model.” This model begins with data that are most certain, such as the emerging ground-water flow and loading, and adjusts the least certain data, such as the sulfate mass loading from the catchments, so that there are no inconsistencies in the concentrations. For this model, all the flows are kept the same as before, only the concentrations are changed. The loading for the alluvium is calculated by working backward from the emerging ground water. Using the loading of 1,843 kg/day for

Table 3. Catchments that contribute ground water and sulfate loads to the Red River alluvium near natural scar drainages (Hottentot to La Bobita) for August 2001.

[ft^3/s, cubic feet per second; mg/L, milligrams per liter; kg/day, kilograms per day; --, not available]

Catchment number	Catchment	Yield (ft^3/s)	Sulfate concentration (mg/L)	Sulfate mass load (kg/day)
4	Hottentot	0.30	913	670
5	Straight	.24	1,300	763
6	Hansen	.14	2,035	697
7	--	.21	400	205
25–28	--	.65	400	636
			Total	**2,972**
Alluvium at Straight Creek	Upstream	11.87	119	**3,454**
			Grand total	**6,426**

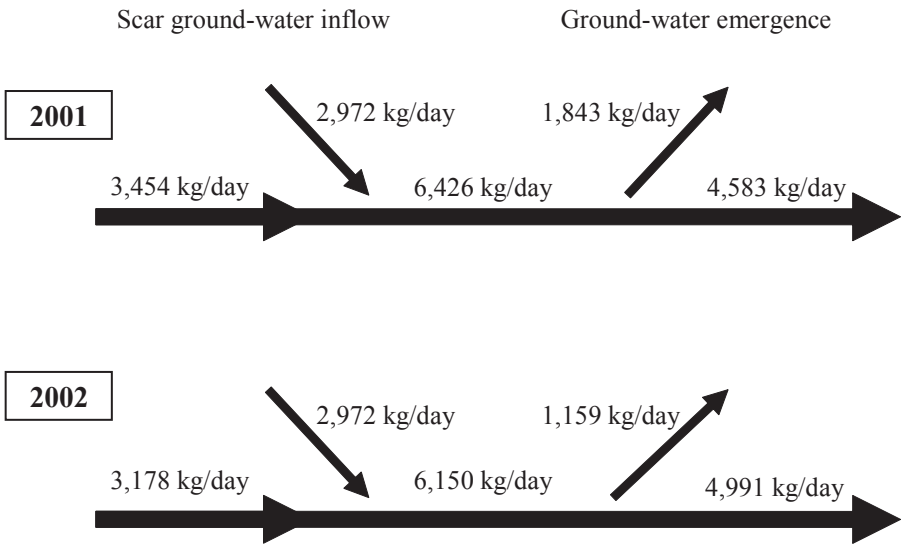

Figure 12. Sulfate mass-load balance for the Red River alluvium shown schematically for the synoptic/tracer studies of 2001 and 2002 for the reach from Hottentot debris fan to La Bobita.

the sulfate load of the emerging ground water and adding to that the loading of the nonemerging ground water (the flow of the alluvial outflow ground water times 150 mg/L) gives 4,914 kg/day for the alluvium sulfate load before emergence but after catchment waters have mixed. The flow and sulfate concentration of the alluvium before mixing with catchment yields are kept constant and, consequently, the sulfate mass load from the catchments must be found by difference to be 1,460 kg/day. Rather than attempting to justify adjustment in every single catchment, they were all decreased proportionally. The consequent concentrations for the catchment yields from Model II are shown in table 4, and the schematic flow diagram is in figure 13.

In Model I the concentrations in the two outflows are inconsistent with each other; in Model II the concentrations remain constant in the outflows but inconsistent with measured concentrations in the inflow catchment water. A third model, Model III, assumes sulfate concentration is incorrect for the Red River alluvial inflow. Keeping Model I for the catchment sulfate inflows and Model II for the outflows, then Model III changes the concentration of the alluvial inflow so that everything else balances. For this mass flux to balance, the sulfate concentration has to be 67 mg/L (for 2001) and

Table 4. Catchment yields, sulfate concentrations, and sulfate mass loads using Model II for 2001.

[ft^3/s, cubic feet per second; mg/L, milligrams per liter; kg/day, kilograms per day; --, not available]

Catchment number	Catchment	Yield (ft^3/s)	Sulfate concentration (mg/L)	Sulfate mass load (kg/day)
4	Hottentot	0.30	450	330
5	Straight	.24	637	374
6	Hansen	.14	998	342
7	--	.21	197	101
25–28	--	.65	197	313
			Total	**1,460**
Alluvium at Straight Creek	Upstream	11.87	119	**3,454**
			Grand total	**4,914**

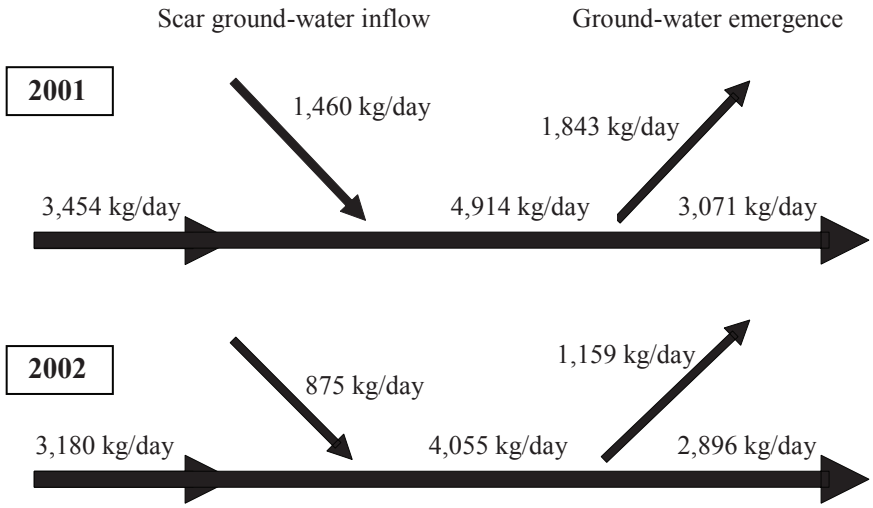

Figure 13. Sulfate mass loads for Model II in which the sulfate mass loads of the catchments are back-calculated from the ground-water emergence mass loads.

41 mg/L (for 2002). The sulfate mass balance for Model III is shown in figure 14.

There are several sources of uncertainty that could be causing these inconsistencies. Concentrations for both the inflowing alluvial ground water and the inflowing catchment ground water may not be low enough. The waters may not be adequately mixed for this type of evaluation. Because of heterogeneities in the real system and the inability of the data to define these fine-scale gradients, the actual fluxes cannot be constrained much more than by using these three models.

It is important to realize that there is no logical basis or independent criterion to allow a best choice between these models without further data. The ground waters do not completely mix because of the tendency for acid ground water from the north catchments to hug the north side of the alluvial aquifer, and not enough is known about mixing to say at what point or along what reach it becomes mostly or completely mixed. Hence, Model II is not necessarily correct. Alternatively, Model I relies on complete mixing among catchment ground-water inflows and the Red River alluvial aquifer to calculate the mass balances, so it may not be correct either. What one can infer from this analysis is that about 20–40 percent of the sulfate loads in the alluvium are emerging in the La Bobita area. The remainder continues on downstream in the alluvial flow. In the reach from the mill site to Thunder Bridge, the emerging ground water contains sulfate loads that are severalfold greater than what remains in the alluvial ground water from the scar areas upstream from the mine site. Hence, new sources must have entered from the mine site to account for the load of sulfate entering in this reach of the Red River. These sources would be a mixture of loads from natural scars and from waste rock.

Vail Engineering, Inc. (2000), concluded that at least one-half of the sulfate load that emerged in the Columbine Park area was from natural scar drainage areas upstream from the mine site. Studies by Kimball and others (2006) indicate

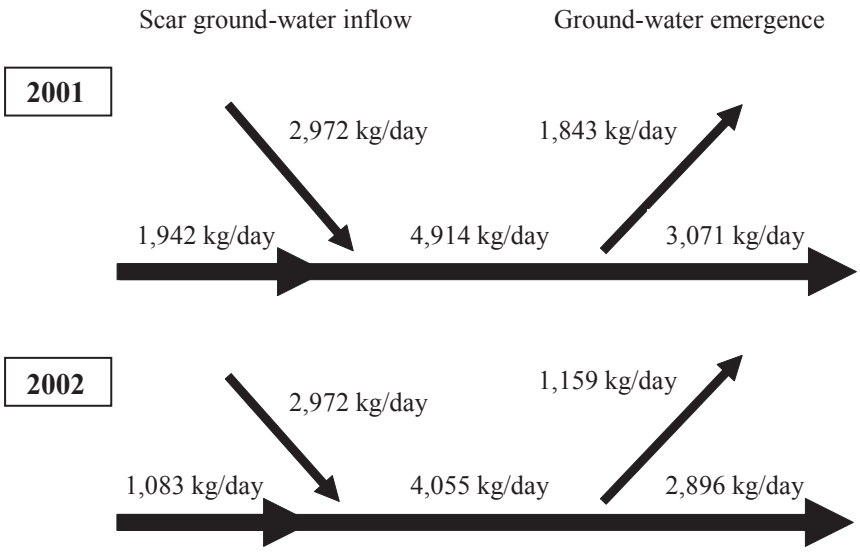

Figure 14. Sulfate mass loads for Model III in which the sulfate mass load of the alluvial ground-water inflow is back-calculated from the ground-water emergence mass loads and the catchment inflows are kept constant.

that most of the emerging solute load near Columbine and the Goat Hill debris fan originate from the reach along the mine site (from the mill site to Thunder Bridge) for the time periods of August 2001 and March–April 2002. The analysis shown here helps to constrain this problem. Of the 4,055–6,426 kg/day of sulfate (the total sulfate flux) that flows in the alluvium along the Hottentot-Straight-Hansen Creek scars, perhaps 875–2,972 kg/day (22–73 percent) is directly derived from Hottentot-Straight-Hansen Creek scar drainages. About 20 to 40 percent of the total emerges near La Bobita and the remainder (60–80 percent) continues downstream in the Red River alluvium. In other words, the ground-water flux leaving the La Bobita area after ground-water emergence is 8 to 9 ft^3/s, and the sulfate flux, depending on the year and time of year, is 2,896 to 4,991 kg/day.

The water and sulfate flux in the ground water of the Columbine Park area (downstream from Columbine Creek) is not known, but Vincent's (in press) analysis indicates that, for flows to balance under steady-state conditions, ground-water flow should be about 9.7 ft^3/s before ground water emerges near the Goat Hill fan and before pumping. About 8 ft^3/s of ground water emerges at Cabin Springs (about 0.8 ft^3/s) and just upstream from the Goat Hill fan (about 7.2 ft^3/s). These crude estimates indicate that 82 percent of the ground water is emerging here. From the mass-loading results, the emergent sulfate flux is about 4,300 kg/day in this same area. Using simple proportions, 100 percent of the sulfate flux would be 5,244 kg/day, and the sulfate flux from upstream from the mine site would be 55 to 95 percent of this amount. However, sulfate concentrations at La Bobita are 400–500 mg/L, and they are the same at wells MMW–17A and MMW–28A (between Sulphur Gulch and La Bobita), but wells in the Red River alluvium downstream from Sulphur Gulch contain concentrations of sulfate that are higher, sometimes more than 1,000 mg/L. Such a large increase in solute concentration indicates that the loading upstream from the mine site cannot account for most of the loading in the reach of the mine site. Further, there are ground-water inflows with high sulfate concentrations and ground-water emergences between the mill site and Goat Hill Gulch that must be included in the mass balances. Estimates can vary considerably because of large uncertainties in the data and because part of the variability in the data is caused by seasonal and climatic fluctuations and by the amount of ground-water pumping. Better measurements for hydraulic conductivity from aquifer tests, seismic profiles to define the alluvium geometry, and geoprobe measurements to define water levels and to collect samples for analysis along this reach of the Red River combined with water-quality data from existing wells and a detailed tracer study could likely define the sources and fate of solute flux in this area. Further work along these lines is needed. It must be remembered that simply stating that some portion of the increased sulfate loading in the Red River is derived from the mine-site reach does not indicate how much loading is from mining activities and how much is from natural scars and natural mineralized areas that exist on the mine site. A focused study might resolve this question.

Interpretation of Ground-Water Geochemistry

The Straight Creek analog site provided an opportunity to study in detail the hydrology, geology, and geochemistry of water/rock interactions in a Red River Valley catchment unaffected by mining activities. The geochemical processes determined from the Straight Creek study were then compared to other catchments unaffected by mining to ascertain the applicability of the Straight Creek results beyond the Straight Creek catchment. The valleywide comparison is fundamentally a scientific evaluation of the geochemical processes that were interpreted to occur in the Straight Creek catchment. From this comparison, generalizations can be formulated about water/rock interactions given the known geologic and hydrologic properties of the valley. With this broader understanding of the water/rock interactions that led to the observed ground-water chemistry in the Red River Valley, the same concepts can be applied to the mine site with appropriate modifications that account for any geologic and hydrologic characteristics of the mine site that are substantially different from the other sites.

The Straight Creek catchment is shown in figure 15 with well locations designated. Well SC–9A was a temporary geoprobe installation from which no water samples were collected for analysis.

Median Concentrations from Monitoring Data

Water analyses from individual monitor wells showed relatively small variations over time with few exceptions. To represent averages of these solute concentrations the median value is used for purposes of graphical representation and interpretation. The median pH was obtained by taking the antilogarithm of the pH values, finding the median of the proton activities, then taking the logarithm of that median. The variance of the values around the median is shown by the mean absolute deviation (MAD, the absolute value of the mean of deviations about the median). The median is chosen instead of the mean because it is much less affected by outliers. Table 5 lists the medians and MADs for the monitoring data from this study. These values are used in the following sections that describe the general trends in water chemistry from which the pre-mining concentrations are derived.

The analyses from which table 5 is derived are in Naus and others (2005) and in Nordstrom and others (2005). There were two exceptions to the procedure previously mentioned for obtaining the median values. Wells SC–1B and SC–5B have evidence of contamination from unknown additives that were used to assist well development. The main contaminants are reflected in high and variable sodium, iron, and dissolved organic carbon (DOC) concentrations. The concentrations of these constituents tended to increase over time, reach a peak, and then decrease. The decreasing concentrations tended to reflect exponential decay, so we assume the last measured concentrations were closest to the true ground-water concentration before the additives were introduced.

Chemistry of Water Developed from Scar Weathering

During the course of these investigations, a notable consistency in the pH of scar-drainage water was observed. If just the pH values from water derived from scar weathering are compiled, excluding those which have traveled over, under, or through any sizable volume of debris fan or other rock material, the pH values are consistently near 3. Figure 16A shows a frequency distribution plot of pH values from a literature compilation of scar-seep chemistry (LoVetere and Nordstrom, in press). The mean and median are nearly the same, 2.97 and 2.93, respectively, for 121 samples. The close correspondence of mean and median indicates a symmetrical distribution, and it is a necessary condition for normal distributions.

Similarly, the sulfate concentrations for scar drainage are also consistent with a mean of 2,014 mg/L and a median of 2,000 mg/L (fig. 16B). This consistency in sulfate concentrations for scar-drainage water helps to differentiate them from waste-rock drainage, which frequently is greater than 5,000 mg/L in sulfate concentration (LoVetere and Nordstrom, in press). However, two notes of caution must be applied. Waste-rock water compositions overlap with scar-drainage compositions (that is, they can be less than 5,000 mg/L sulfate), and there is one scar-drainage example not sampled in the USGS study that has sulfate concentrations up to about 15,000 mg/L. This drainage is from the Bitter Creek scar and was considered outside the study area but was sampled by Robertson Geoconsultants, Inc. (2000a). It is unclear why the Bitter Creek water had such a high concentration. Evaporation or unusually high residence times are possibilities; because no isotopes or age dates were obtained, we could not determine why these waters are anomalous compared to all the others.

Water-Chemistry Classification for the Red River Valley Ground Water

Using medians to summarize the pH values and sulfate concentrations from all the wells and Straight Creek surface waters sampled in this study (fig. 17), the waters divide into three groups: Group I are dilute, neutral-pH, Ca-HCO_3 type waters; Group II are neutral-pH, mineralized Ca-SO_4 type waters; and Group III are acid, scar-derived, mineralized Ca-SO_4 type waters. The La Bobita well water is shown outside of Group III because it is a mixture of Group I with Group III waters. Group I waters are typical of surface and alluvial ground waters of the Red River upstream from Bitter Creek. They would be typical of water draining rocks with no more than propylitic alteration that are found as occasional outcrops along the north side of the valley and along areas

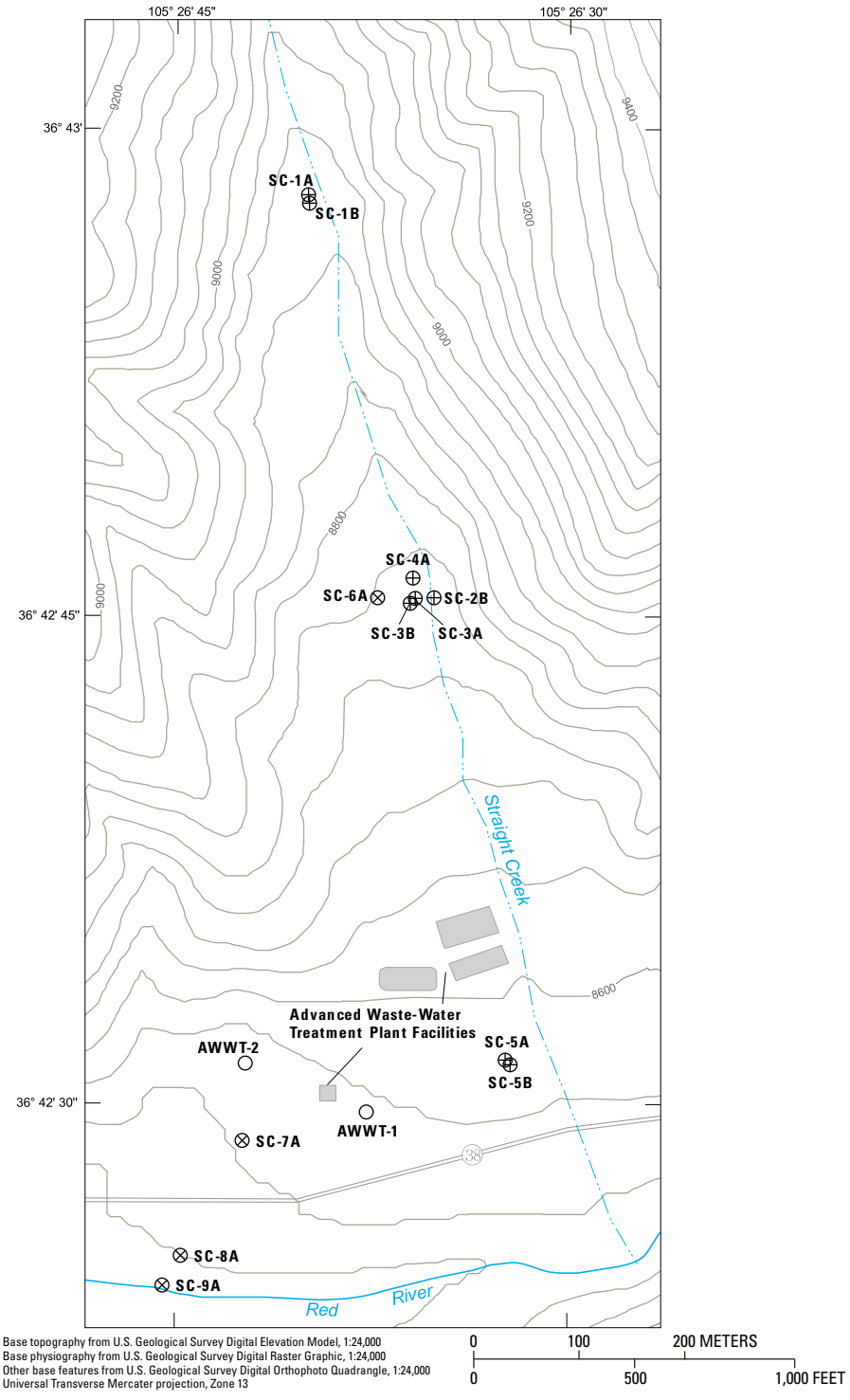

EXPLANATION

- ⊕ Early observation well
- ⊗ Late observation well
- ○ Advanced Waste-Water Treatment (AWWT) Plant Facilities
- 9000 Topographic contour — Shows altitude of land surface in feet above the National Geodetic Vertical Datum of 1929 (NGVD 29). Contour interval 40 feet. Horizontal coordinate information is referenced to the North American Datum of 1927 (NAD 27)

Figure 15. Location of observation wells in Straight Creek catchment and Advanced Waste-Water Treatment facilities.

Table 5. Median values for pH, temperature, specific conductance (SC), redox potential, dissolved oxygen (DO), dissolved solute concentrations, dissolved organic carbon (DOC), cation- and anion-equivalent sum, and speciated charge imbalance for Straight Creek drainage water and ground water analyzed in this study.

[ID, identifier; CI, charge imbalance; D.L., detection limit; MAD, median absolute deviation; meq/L, milliequivalents per liter; Lab, laboratory; µS/cm, microsiemens per centimeter; mg/L, milligrams per liter; n, number of analyses; V, volts; °C, degrees Celsius; Eh, redox potential; %, percent; ---, not determined; <, less than]

Sample ID	Straight Creek n=14		SC–1A n=15		SC–1B n=14	
	Median	MAD	Median	MAD	Median	MAD
pH (standard units)	2.98	0.13	3.64	0.04	6.75	0.06
pH Lab (standard units)	2.70	.06	3.15	.03	7.93	.06
Specific conductance (µS/cm)	3,085	274	2,790	59	3,300	119
Specific conductance Lab (µS/cm)	3,200	74	2,850	44	2,940	59
Temperature (°C)	7.7	5.2	7.5	.9	7.6	1.6
Eh, V	.781	.060	.580	.021	.087	.160
DO (mg/L)	5.59	1.1	.3	.1	.5	.2
			Constituent, mg/L			
Ca	349	55	384	10	503	12
Mg	113	16	123	4	215	7
Na	8.08	1.5	16.7	1.7	66.1	12.3
K	.753	.43	1.10	.13	11.2	3.56
SO_4	2,030	460	2,100	59	1,850	104
Alkalinity as HCO_3	---	---	---	---	493	29
F	7.71	5.9	9.46	1.5	.740	.2
Cl	2.98	1.7	3.21	1.8	13.9	9.7
SiO_2	74.2	15.8	94.7	3.6	25.4	2.1
Al	91.5	15.6	94.1	3.4	.012	.005
Fe	65.0	27.1	28.8	1.5	[1]1.85	[1].12
Fe(II)	[2].475	[2].361	26.9	1.4	[1]1.83	[1].13
Li	.181	.057	.217	.007	.159	.019
Sr	.612	.115	.867	.021	11.0	.297
Ba	[2].002	[2].002	.002	0	.008	.001
Mn	2.8	3.4	19.8	.7	6.07	.18
Zn	7.63	1.05	7.17	.25	[2].005	[2].178
Pb	[3].012	[3]---	[3].009	[3]---	.0012	[3]---
Ni	.727	.107	.730	.016	[2].004	[2].003
Cu	1.87	.28	.929	.044	<.0005	---
Cd	.039	.007	.038	.009	<.0002	---
Cr	.040	.005	.031	.006	<.0005	---
Co	.325	.046	.326	.015	[3]<.0008	---
Be	.026	.004	.025	.003	[2].001	[2]0
DOC	1.44	.36	1.20	.1	[1]6.5	.3
Sum cations (meq/L)	26.9		27.2		33.5	
Sum anions (meq/L)	26.2		28.5		34.1	
Speciated CI (%)	2.6		–4.8		–1.7	

Table 5. Median values for pH, temperature, specific conductance (SC), redox potential, dissolved oxygen (DO), dissolved solute concentrations, dissolved organic carbon (DOC), cation- and anion-equivalent sum, and speciated charge imbalance for Straight Creek drainage water and ground water analyzed in this study.—Continued

[ID, identifier; CI, charge imbalance; D.L., detection limit; MAD, median absolute deviation; meq/L, milliequivalents per liter; Lab, laboratory; µS/cm, microsiemens per centimeter; mg/L, milligrams per liter; n, number of analyses; V, volts; °C, degrees Celsius; Eh, redox potential; %, percent; ---, not determined; <, less than]

Sample ID	SC–2B n=11		S–3A n=14		SC–3B n=14	
	Median	MAD	Median	MAD	Median	MAD
pH (standard units)	6.44	0.10	3.31	0.06	5.88	0.10
pH Lab (standard units)	7.59	.34	3.41	.02	4.19	.22
Specific conductance (µS/cm)	2,420	104	2,375	67	2,850	89
Specific conductance Lab (µS/cm)	2,300	30	2,275	37	2,770	37
Temperature (°C)	8.3	1.8	7.9	.5	7.8	1.3
Eh, V	.267	.049	.765	.016	.343	.046
DO (mg/L)	.3	.2	4.8	.3	.6	.2
Constituent, mg/L						
Ca	439	7	299	7	481	11
Mg	105	3	91	6	150	5
Na	22.1	1.8	16.5	1.8	33.0	2.5
K	3.39	.28	.79	.07	2.92	.59
SO_4	1,480	59	1,600	44	1,920	82
Alkalinity as HCO_3	144	26	---	---	74	17
F	6.14	.61	6.82	.06	6.58	.70
Cl	3.91	.53	3.34	1.56	5.23	2.11
SiO_2	1.6	.9	92.8	3.3	18.1	1.2
Al	.636	.338	79.3	2.4	5.38	.33
Fe	33.2	.4	.549	.036	58.9	1.6
Fe(II)	33.2	1.1	.027	.012	58.9	1.4
Li	.313	.024	.158	.016	.197	.022
Sr	2.32	.074	.334	.019	3.60	.133
Ba	.006	.001	.002	0	.005	.001
Mn	17.3	1.2	15.3	.4	27.1	1.2
Zn	1.53	.28	5.44	.19	4.57	.25
Pb	[3].006	[3]---	<.0003	---	[3].011	[3]---
Ni	.480	.028	.543	.022	.463	.019
Cu	[2].0005	[2].0022	.818	.033	[3]<.0005	---
Cd	[2].001	[2]0	.025	.003	[2].002	[2]0
Cr	[2].008	[2]0	.020	.002	[2].006	[2].003
Co	.157	.024	.230	.019	.233	.018
Be	.021	.003	.017	.001	.023	.004
DOC	1.55	.44	2.00	.30	2.70	.30
Sum cations (meq/L)	24.1		21.8		28.9	
Sum anions (meq/L)	24.1		22.0		28.8	
Speciated CI (%)	.1		–.8		.2	

Table 5. Median values for pH, temperature, specific conductance (SC), redox potential, dissolved oxygen (DO), dissolved solute concentrations, dissolved organic carbon (DOC), cation- and anion-equivalent sum, and speciated charge imbalance for Straight Creek drainage water and ground water analyzed in this study.—Continued

[ID, identifier; CI, charge imbalance; D.L., detection limit; MAD, median absolute deviation; meq/L, milliequivalents per liter; Lab, laboratory; µS/cm, microsiemens per centimeter; mg/L, milligrams per liter; n, number of analyses; V, volts; °C, degrees Celsius; Eh, redox potential; %, percent; ---, not determined; <, less than]

Sample ID	SC–4A n=15		SC–6A n=5		S–5A n=15	
	Median	MAD	Median	MAD	Median	MAD
pH (standard units)	3.58	0.18	3.51	0.04	3.44	0.04
pH Lab (standard units)	3.20	.15	3.24	.03	3.45	.03
Specific conductance (µS/cm)	2,450	30	2,670	44	1,630	311
Specific conductance Lab (µS/cm)	2,470	119	2,640	0	1,570	178
Temperature (°C)	8.0	1.2	11.6	2.8	7.8	.7
Eh, V	.604	.025	.664	.006	.755	.027
DO (mg/L)	1.7	1.1	.9	.4	.9	.4
Constituent, mg/L						
Ca	296	10	365	6	163	25
Mg	114	10	114	10	61.4	13.5
Na	21.7	2.4	17.4	1.6	16.2	2.4
K	1.98	.39	1.11	.13	1.85	.09
SO_4	1,690	59	1,880	74	957	62
Alkalinity as HCO_3	---	---	---	---	---	---
F	6.72	.43	8.78	.06	3.24	.68
Cl	5.16	1.24	3.10	.56	5.18	1.31
SiO_2	73.6	8.2	93.2	5.2	76.3	3.9
Al	68.0	5.5	85.1	2.7	52.0	4.9
Fe	23.6	15.1	12.1	1.3	.450	.033
Fe(II)	21.2	14.9	1.4	1.5	.016	.013
Li	.178	.015	.212	.007	.074	.018
Sr	.649	.111	.430	.006	.507	.071
Ba	.003	0	.002	0	[2].0008	[2].0001
Mn	17.1	1.5	19.0	.3	7.64	1.36
Zn	5.28	.12	6.51	.30	2.67	.36
Pb	.0021	[3]---	[3].0009	[3]---	<.0003	---
Ni	.551	.018	.668	.053	.333	.077
Cu	.362	.200	.639	.036	.215	.046
Cd	.020	.003	.031	.001	.012	.006
Cr	.013	.001	.021	.001	.008	.001
Co	.234	.016	.277	.037	.136	.042
Be	.016	.001	.018	.001	.008	.001
DOC	1.6	.3	1.40	.22	1.25	.67
Sum cations (meq/L)	22.9		25.3		14.2	
Sum anions (meq/L)	23.7		25.2		13.8	
Speciated CI (%)	–3.5		.4		2.8	

Table 5. Median values for pH, temperature, specific conductance (SC), redox potential, dissolved oxygen (DO), dissolved solute concentrations, dissolved organic carbon (DOC), cation- and anion-equivalent sum, and speciated charge imbalance for Straight Creek drainage water and ground water analyzed in this study.—Continued

[ID, identifier; CI, charge imbalance; D.L., detection limit; MAD, median absolute deviation; meq/L, milliequivalents per liter; Lab, laboratory; µS/cm, microsiemens per centimeter; mg/L, milligrams per liter; n, number of analyses; V, volts; °C, degrees Celsius; Eh, redox potential; %, percent; ---, not determined; <, less than]

Sample ID	SC–5B n=15		SC–7A_1 n=4		SC–7A_2 n=4	
	Median	MAD	Median	MAD	Median	MAD
pH (standard units)	7.52	0.12	3.90	0.05	3.95	0.04
pH Lab (standard units)	7.94	.13	3.10	.01	3.11	.01
Specific conductance (µS/cm)	2,480	89	1,505	22	1,395	82
Specific conductance Lab (µS/cm)	2,270	59	1,670	52	1,565	59
Temperature (°C)	8.1	.7	7.9	.7	9.5	2.4
Eh, V	.014	.124	.566	.010	.556	.008
DO (mg/L)	.2	.1	.4	.2	.3	0
			Constituent, mg/L			
Ca	548	34	187	5	162	2
Mg	37.4	4.9	6.2	1.3	5.1	1.5
Na	62.4	31.4	18.7	2.0	15.6	1.6
K	4.84	1.50	3.02	.11	2.67	.11
SO_4	1,400	59	950	27	849	38
Alkalinity as HCO_3	226	69	---	---	---	---
F	1.06	.03	2.80	.37	2.40	.25
Cl	8.63	5.43	3.93	.41	4.24	.47
SiO_2	21.5	2.5	58.1	1.3	57.6	.3
Al	[2].004	[2].004	36.4	1.6	33.3	1.0
Fe	[4].468	[4].013	3.3	.6	29.5	.2
Fe(II)	[4].462	[4].004	3.2	.4	29.2	.5
Li	.054	.013	.070	.002	.057	.004
Sr	8.33	.504	1.05	.052	.850	.032
Ba	.025	.006	.004	.001	.005	0
Mn	2.68	.44	6.79	.33	5.62	.23
Zn	<.005	---	2.12	.10	1.82	.04
Pb	<.0003	---	<.0003	---	<.0003	---
Ni	[2].003	[2].003	.244	.012	.219	.016
Cu	<.0005	---	.060	.004	.056	.006
Cd	<.0002	---	.007	0	.006	.001
Cr	<.0005	---	.005	0	.004	0
Co	<.0008	---	.100	.006	.092	.011
Be	<.001	---	.006	.001	.005	.001
DOC	[4]2.0	---	1.31	.52	1.10	.44
Sum cations (meq/L)	24.6		14.9		13.0	
Sum anions (meq/L)	24.2		14.1		12.7	
Speciated CI (%)	1.7		5.6		1.8	

Table 5. Median values for pH, temperature, specific conductance (SC), redox potential, dissolved oxygen (DO), dissolved solute concentrations, dissolved organic carbon (DOC), cation- and anion-equivalent sum, and speciated charge imbalance for Straight Creek drainage water and ground water analyzed in this study.—Continued

[ID, identifier; CI, charge imbalance; D.L., detection limit; MAD, median absolute deviation; meq/L, milliequivalents per liter; Lab, laboratory; µS/cm, microsiemens per centimeter; mg/L, milligrams per liter; n, number of analyses; V, volts; °C, degrees Celsius; Eh, redox potential; %, percent; ---, not determined; <, less than]

Sample ID	SC–7A_3 n=4		SC–7A_4 n=4		AWWT1 n=14	
	Median	MAD	Median	MAD	Median	MAD
pH (standard units)	3.89	0.08	3.91	0.04	3.86	0.02
pH Lab (standard units)	3.11	.02	3.12	.01	3.07	.04
Specific conductance (µS/cm)	1,370	52	1,345	52	1,470	22
Specific conductance Lab (µS/cm)	1,480	22	1,495	30	1,630	30
Temperature (°C)	1.5	4.2	1.4	4.4	9.9	1.0
Eh, V	.561	.004	.560	.015	.555	.052
DO (mg/L)	.3	.1	.3	.1	.4	.2
Constituent, mg/L						
Ca	151	3	150	8	158	3
Mg	5.7	.8	48.8	1.8	53.6	2.3
Na	15.5	1.3	17.3	2.2	16.6	.7
K	2.82	.22	2.83	.26	2.77	.25
SO_4	821	39	815	26	893	23
Alkalinity as HCO_3	---	---	---	---	---	---
F	2.55	.15	2.55	.07	2.60	.16
Cl	4.33	.51	4.44	.42	5.56	1.16
SiO_2	58.8	.9	56.7	1.9	62.4	1.7
Al	31.4	2.0	31.0	1.4	36.3	.7
Fe	27.2	.6	26.9	1.2	33.4	.9
Fe(II)	26.8	.3	26.7	.4	33.3	1.0
Li	.056	.003	.056	.002	.059	.002
Sr	.766	.023	.754	.056	.758	.024
Ba	.005	0	.005	.001	.005	0
Mn	5.30	.19	5.22	.44	5.90	.15
Zn	1.82	.05	1.85	.02	2.06	.04
Pb	<.0003	---	<.0003	---	[3].0003	[3]---
Ni	.199	.022	.211	.021	.265	.026
Cu	.065	.012	.067	.013	<.0005	---
Cd	.006	.001	.005	.001	.006	0
Cr	.004	0	.004	0	.082	.007
Co	.082	.004	.087	.005	.102	.010
Be	.005	0	.005	.001	.005	.001
DOC	1.15	.36	1.05	.30	1.25	.37
Sum cations (meq/L)	12.4		12.3		13.3	
Sum anions (meq/L)	12.4		12.4		13.4	
Speciated CI (%)	.3		–.4		–.6	

Table 5. Median values for pH, temperature, specific conductance (SC), redox potential, dissolved oxygen (DO), dissolved solute concentrations, dissolved organic carbon (DOC), cation- and anion-equivalent sum, and speciated charge imbalance for Straight Creek drainage water and ground water analyzed in this study.—Continued

[ID, identifier; CI, charge imbalance; D.L., detection limit; MAD, median absolute deviation; meq/L, milliequivalents per liter; Lab, laboratory; µS/cm, microsiemens per centimeter; mg/L, milligrams per liter; n, number of analyses; V, volts; °C, degrees Celsius; Eh, redox potential; %, percent; ---, not determined; <, less than]

Sample ID	AWWT2 n=1	SC–8A n=5		HANSEN n=4	
		Median	MAD	Median	MAD
pH (standard units)	6.78	6.63	0.01	3.79	0.07
pH Lab (standard units)	7.93	8.02	.06	3.75	0
Specific conductance (µS/cm)	3,110	384	24	2,795	15
Specific conductance Lab (µS/cm)	2,860	365	13	2,700	15
Temperature (°C)	8.7	6.9	.9	8.4	.4
Eh, V	.351	.524	.154	.731	.012
DO (mg/L)	.54	6.1	.7	5.2	.3
Constituent, mg/L					
Ca	406	52	4	457	7
Mg	266	11	1	98	4
Na	50.0	5.7	.4	16.3	2.7
K	4.74	1.01	.12	3.80	.34
SO_4	1,830	119	9	2,035	7
Alkalinity as HCO_3	353	64	1	---	---
F	4.07	.26	.01	3.60	.10
Cl	5.03	2.93	.10	1.87	.40
SiO_2	21.0	12.9	.7	55.4	1.3
Al	.0068	.007	.002	8.6	3.4
Fe	.101	[2].001	[2]0	.064	.011
Fe(II)	.076	<.002	---	[2].009	[2].006
Li	.177	.004	.001	.091	.004
Sr	7.38	.31	.043	2.82	.178
Ba	.006	.022	.003	.003	0
Mn	5.7	.002	[3]---	11.9	1.0
Zn	.528	[2].037	[2].024	2.73	.13
Pb	<.008	<.0003	---	[3].0009	[3]---
Ni	.211	.004	0	.584	.019
Cu	<.0005	<.0005	---	.114	.007
Cd	<.001	[2].0002	[2].0046	.006	0
Cr	<.0005	<.0005	---	.003	0
Co	.115	<.0008	---	.177	.016
Be	.005	<.001	---	.016	.001
DOC	2.00	.70	.15	.70	.18
Sum cations (meq/L)	32.1	3.4		26.3	
Sum anions (meq/L)	31.4	3.3		27.4	
Speciated CI (%)	2.0	4.1		–4.2	

Table 5. Median values for pH, temperature, specific conductance (SC), redox potential, dissolved oxygen (DO), dissolved solute concentrations, dissolved organic carbon (DOC), cation- and anion-equivalent sum, and speciated charge imbalance for Straight Creek drainage water and ground water analyzed in this study.—Continued

[ID, identifier; CI, charge imbalance; D.L., detection limit; MAD, median absolute deviation; meq/L, milliequivalents per liter; Lab, laboratory; µS/cm, microsiemens per centimeter; mg/L, milligrams per liter; n, number of analyses; V, volts; °C, degrees Celsius; Eh, redox potential; %, percent; ---, not determined; <, less than]

Sample ID	Hottentot n=5		La Bobita n=4		CC–2A n=5	
	Median	MAD	Median	MAD	Median	MAD
pH (standard units)	2.99	.01	4.35	0.22	6.05	0.13
pH Lab (standard units)	2.59	.01	4.24	.00	4.94	.18
Specific conductance (µS/cm)	1,670	59	900	0	1,520	15
Specific conductance Lab (µS/cm)	1,930	44	856	9	1,400	59
Temperature (°C)	7.5	.0	8.6	3.0	16.0	.9
Eh, V	.630	.006	.578	.067	.348	.110
DO (mg/L)	.2	.1	3.7	.4	5.1	.9
Constituent, mg/L						
Ca	86.9	2.2	111	4	225	38
Mg	39.9	3.0	32.1	1.0	13.2	2.4
Na	8.14	.56	13.0	.4	34.5	6.8
K	2.06	.18	1.81	.39	6.87	1.02
SO_4	913	13	467	2	816	50
Alkalinity as HCO_3	---	---	---	---	64	10
F	4.10	.06	2.65	.22	19.07	1.45
Cl	1.81	.24	5.00	.73	2.98	.28
SiO_2	92.1	1.3	33.4	.4	26.7	2.8
Al	62.3	4.7	12.3	.7	5.42	.13
Fe	87.7	2.5	.037	.020	33.6	4.0
Fe(II)	85.6	2.5	.010	.010	33.6	4.0
Li	.074	.016	.034	.005	.039	.004
Sr	[2].010	[2].006	.814	.012	.825	.147
Ba	[2].001C	[2]0	.022	.002	.005	.001
Mn	7.99	.77	2.67	.10	4.9	9.6
Zn	3.70	.31	.96	.06	3.96	2.22
Pb	<.0003	---	.0009	0	[3].0007	[3]---
Ni	.345	.009	.133	.002	[2].028	[2].005
Cu	.118	.006	.031	.002	[2].0005	[2].0004
Cd	.005	0	.004	0	.003	0
Cr	.012	0	.006	.007	[2].0007	[2].0003
Co	.123	.016	.019	.001	.016	.004
Be	.011	0	.006	.001	.078	.009
DOC	1.10	0	1.25	.36	1.35	.37
Sum cations (meq/L)	13.7		8.1		12.8	
Sum anions (meq/L)	13.0		7.8		14.5	
Speciated CI (%)	5.5		4.3		–12	

Table 5. Median values for pH, temperature, specific conductance (SC), redox potential, dissolved oxygen (DO), dissolved solute concentrations, dissolved organic carbon (DOC), cation- and anion-equivalent sum, and speciated charge imbalance for Straight Creek drainage water and ground water analyzed in this study.—Continued

[ID, identifier; CI, charge imbalance; D.L., detection limit; MAD, median absolute deviation; meq/L, milliequivalents per liter; Lab, laboratory; µS/cm, microsiemens per centimeter; mg/L, milligrams per liter; n, number of analyses; V, volts; °C, degrees Celsius; Eh, redox potential; %, percent; ---, not determined; <, less than]

Sample ID	CC–2B n=4		CC–1B n=4		Ranger station n=1
	Median	MAD	Median	MAD	
pH (standard units)	6.91	0.11	7.16	0.16	6.50
pH Lab (standard units)	7.82	.04	8.06	.24	---
Specific conductance (µS/cm)	1,770	30	640	30	490
Specific conductance Lab (µS/cm)	1,525	7	464	35	---
Temperature (°C)	8.7	.7	9.7	3.1	8.8
Eh, V	.329	.099	.449	.046	.450
DO (mg/L)	1.0	.9	.3	.2	5.55
Constituent, mg/L					
Ca	376	19	96	2	71.8
Mg	21	1	13	0	15
Na	4.8	5.4	23.0	1.6	8.5
K	4.56	.27	1.90	.16	1.32
SO_4	852	13	119	7	223
Alkalinity as HCO_3	303	3	242	4	45.8
F	2.00	.02	1.35	.23	.92
Cl	2.59	.16	6.24	.53	5.00
SiO_2	23.2	.2	14.2	.7	17.6
Al	.011	.004	.005	.001	.087
Fe	1.33	1.01	[2].032	[2].013	.142
Fe(II)	1.26	1.01	[2].027	[2].017	.135
Li	.070	.010	.023	.001	.004
Sr	4.73	.059	1.27	.082	.509
Ba	.013	.001	.026	.003	.048
Mn	5.01	.38	.219	.028	.014
Zn	[3]---	[3]---	[3]---	[3]---	.035
Pb	<.0003	---	<.0003	---	<.0003
Ni	[2].002	[2].001	[2].002	[2].002	.005
Cu	<.0005	---	[2].0007	[2].0004	.0010
Cd	<.0002	---	<.0002	---	.0002
Cr	[2].0007	[2].0002	<.0005	---	<.0005
Co	[2].002	[2]0	<.0008	---	<.0007
Be	<.001	---	<.001	---	<.001
DOC	1.20	.27	2.15	.07	.87
Sum cations (meq/L)	17.7		6.48		4.55
Sum anions (meq/L)	17.9		6.20		4.91
Speciated CI (%)	–.9		4.5		–7.6

[1]Last four sampling trips used.

[2]Values below D.L. set equal to D.L.

[3]Highly variable results.

[4]Last two sampling trips used.

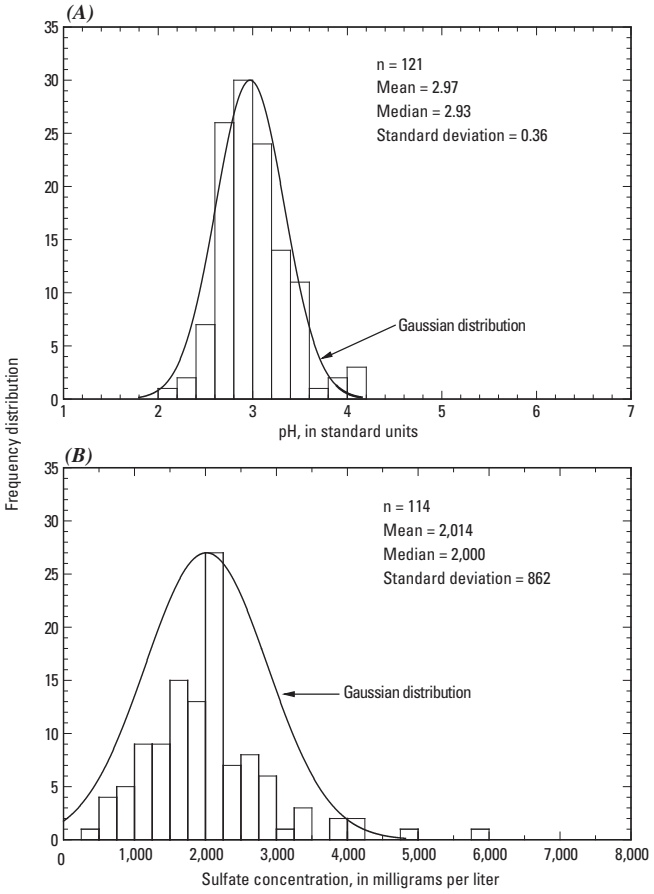

Figure 16. (A) Frequency distribution plot of pH for scar-drainage water in the Red River Valley and (B) frequency distribution plot of sulfate concentrations for scar-drainage water in the Red River Valley (excluding Goat Hill water).

of the south side. Indeed these waters are typical of shallow recharge water in many geologic settings.

The common occurrence of scar water with pH averaging close to 3.0 can be explained as water that has developed from pyrite oxidation with relatively small amounts of precipitated hydrous ferric oxides, gypsum dissolution, and minor amounts of aluminosilicate dissolution. Figure 18 shows a simulation of pyrite oxidation alone (Nordstrom, 2004) using the computer code PHREEQC (Parkhurst and Appelo, 1999). The pH of the resultant solution is plotted as a function of the amount of pyrite oxidized under four scenarios: (1) no oxidation of the resultant acid iron-sulfate solution, (2) oxidation to an acid ferric-sulfate solution but no precipitation of hydrous ferric oxides, (3) oxidation with precipitation of ferrihydrite, and (4) oxidation with precipitation of goethite. The important point about this diagram is to notice the crossover points at pH values of 3.3 and 2.4 because they represent inflection points or regions of buffering capacity. That is, if only pyrite is weathered there will be a tendency for the resultant solutions to reach pH values of 2.4–3.3 depending on how much iron is oxidized and precipitated. The median pH value of 3 for scar leachates lies in between these values although more toward the value of 3.3, which reflects oxidation but little or no precipitation of hydrous ferric oxides (HFO). Our observations of scar-water chemistry also show that these waters contain fully oxidized iron, but precipitated HFO seems to be minimal. If aluminosilicate dissolution was substantial, then the pH would be different. In scars, the mineral assemblage is primarily QSP. The quartz is insoluble, and sericite (or illite) does not weather substantially (as evident in the low concentrations of potassium). Gypsum dissolution also has no significant effect on these pH values. The simulation indicates that we understand the main compositional features of water derived from natural scar weathering.

Geochemical Mass Balance on Straight Creek Drainage

A simple mass-balance calculation to estimate the amount of minerals dissolved and precipitated to produce the Straight Creek scar-drainage water is derived by using the inverse modeling method of Plummer and others (1983), also described by Parkhurst (1997), Bricker and others (2004), Nordstrom (2004), and Bowser and Jones (2002). Assuming the initial water is rainwater, which can be approximated by pure water, and the final water is the median water-chemistry analysis for Straight Creek drainage water from table 5, and using idealized mineral compositions based on petrography and X-ray diffractometry (Plumlee and others, 2005), the results are two models shown in table 6. For example, for the dolomite model, dolomite or magnesian calcite could be substituted for chlorite as a source of magnesium, but the amount of dolomite that is required (4.64 mmol/kg_{H_2O}) seems unreasonable in this environment because dolomite is not abundant at Straight Creek. Chlorite is abundant, however (Ludington and others, 2005; Plumlee and others, written commun., 2004), and the mass balance in the dolomite model has more dolomite dissolving than gypsum, which does not seem reasonable. From these two models it is clear that gypsum and pyrite dissolution dominate the weathering reactions. Dissolution of chlorite, kaolinite, and oligoclase will raise the pH slightly from that predicted in figure 18. This neutralization capacity is overcome by the greater amount of pyrite oxidized in the chlorite model shown in table 6 (6.2 mmol/kg_{H_2O}) compared to the range indicated by figure 18 (0.5 – 3 mmol/kg_{H_2O}). Using dolomite for a magnesium source instead of chlorite potentially develops more neutralization capacity, but the mass balance requires more pyrite to be oxidized with the resultant pH about the same. Unfortunately, these two models are mutually exclusive, whereas magnesium probably is derived from both sources. Laboratory and field data demonstrate that calcite and dolomite dissolution rates (Brown and Glynn, 2003) are at least a couple of orders of magnitude faster than chlorite dissolution rates (Brandt and others, 2003) so that a dolomite model would be preferred.

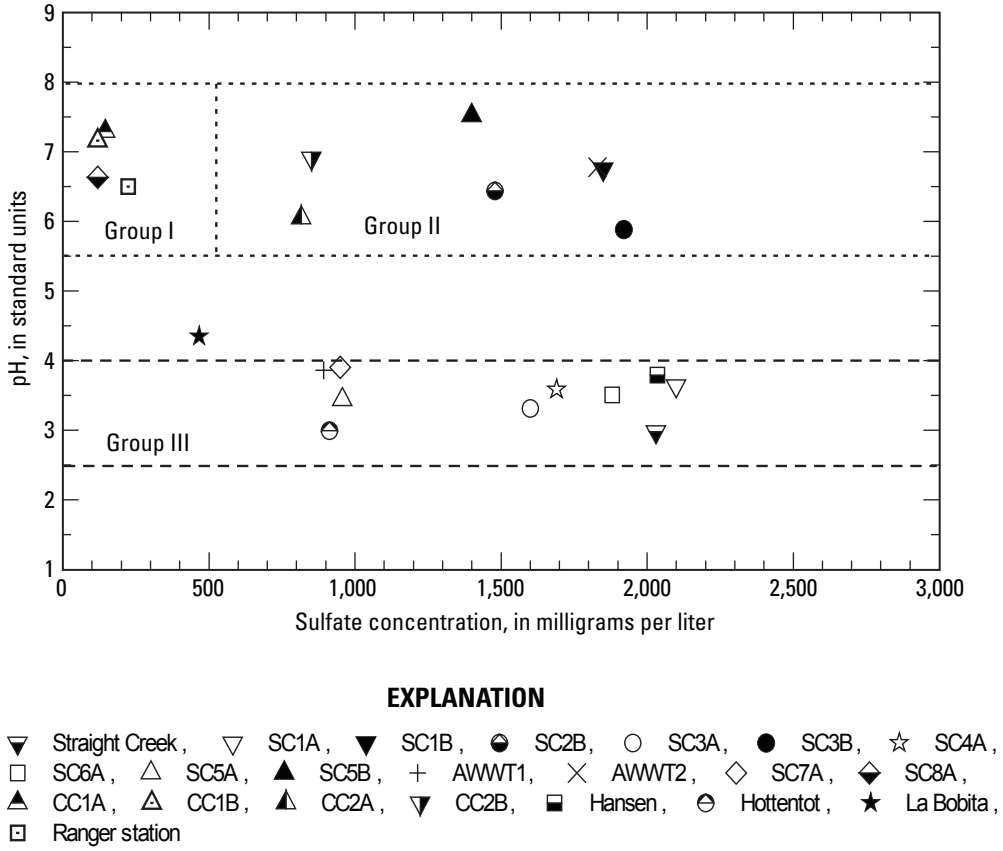

Figure 17. Plot of pH against median sulfate concentration for all ground waters and Straight Creek surface water. Group I are dilute, nonmineralized, Ca-HCO_3 type waters; Group II are mineralized, carbonate-buffered, Ca-SO_4 type waters; and Group III are acid, scar-derived, Ca-SO_4 type waters.

The water chemistry evolves according to the presumed flow paths shown in figure 19 with the largest mass transfer, as noted by Robertson Geoconsultants, Inc. (2001b) and Shaw and others (2003), in the scar area. Several observations have shown that the Straight Creek surface water is the main input flow and source of constituents that appear in both the alluvial and bedrock ground waters as described by Shaw and others (2003). The Straight Creek drainage sinks into the debris-flow fan almost all year round (the only exception is during the rare intense monsoon rainstorm when the overland flow actually reaches the Red River). The median chemistry of Straight Creek surface water is nearly identical to the median chemistry for water in the most upgradient well (SC–1A). Water levels in SC–1A fluctuate with the change in discharge of Straight Creek, and no other obvious sources are visible. The main change between Straight Creek water and SC–1A water is iron reduction along with some copper and chromium removal (also probably by reduction) and some gain in silica.

Water in well SC–6A is closer in chemical composition to those in SC–1A than water in SC–3A and SC–4A. Furthermore, the ground-water ages from youngest to oldest are SC–1A to SC–6A to SC–5A to AWWT1 and SC–7A (Naus and others, 2005; Nordstrom and others, 2005). Water from SC–3A and SC–4A is apparently much younger than any of these. These results indicate mixing with younger water. Indeed, water from SC–4A appears to be SC–3A water with a small amount of admixed SC–3B water that produces a greater age (than SC–3A) and an increase in solute concentrations. This unexpected result indicates how bedrock aquifers and debris-flow aquifers can mix to some extent even though their permeabilities appear to be quite different. Water from SC–8A is not shown on the diagram, and it appears to be Red River alluvial aquifer water unaffected by acidic scar-drainage water. From the reported data, there appears to be little or no hydraulic connection between SC–7A and SC–8A.

Water chemistry from the La Bobita well has much in common with the water chemistry at Hansen and Straight Creek debris-fan ground water; its composition is consistent with a diluted version of these waters from mixing with some Red River alluvial water and with removal of some iron, silica, and aluminum. This result is consistent with the tracer study that showed an increase in solute concentrations and loads in this reach of the Red River near La Bobita.

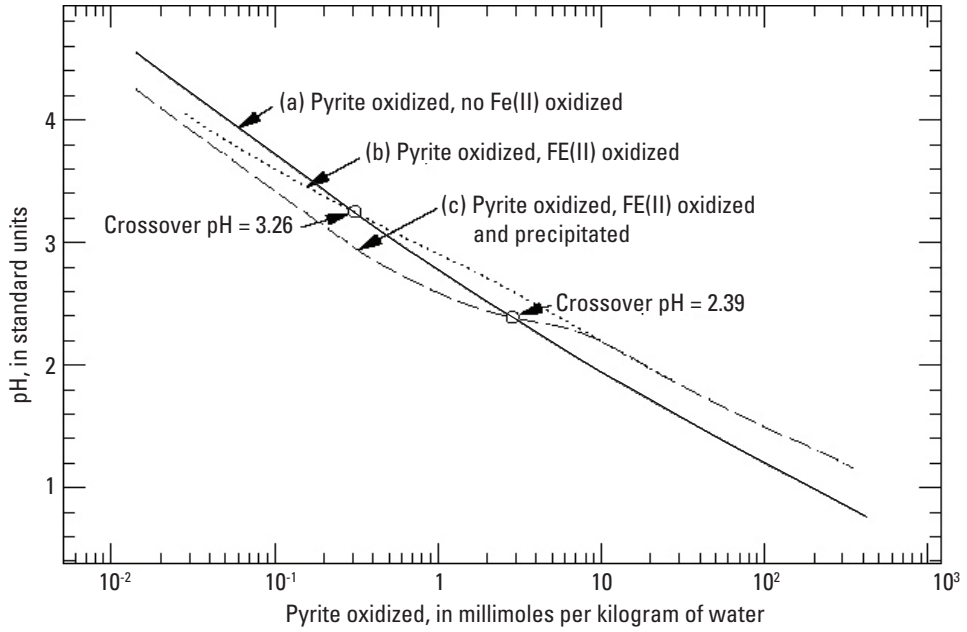

Figure 18. Decrease in pH with the incremental oxidation of pyrite to (a) an acid ferrous sulfate solution with no dissolved iron oxidation, (b) oxidation of the dissolved iron sulfate solution but no precipitation of hydrous ferric oxides, and (c) oxidation with precipitation of ferrihydrite.

Table 6. Weathering mass balances of minerals that can account for the median chemistry of Straight Creek scar-drainage water.

[--, not available]

Mineral phase at Straight Creek (idealized chemical formula in parentheses)	Millimoles of mineral transferred per kilogram of water; positive = mass mineral dissolved, negative = mass mineral precipitated	
	Chlorite model	Dolomite model
Gypsum ($CaSO_4 \cdot 2H_2O$)	8.51	3.78
Pyrite (FeS_2)	6.21	8.66
Chlorite ($Mg_5Al_2Si_3O_{10}[OH]_8$)	.93	--
Dolomite ($CaMg[CO_3]_2$)	--	4.64
Kaolinite ($Al_2Si_2O_5[OH]_4$)	.47	1.40
Oligoclase ($Na_{0.8}Ca_{0.2}Al_{1.2}Si_{2.8}O_8$)	.44	.44
Fluorite (CaF_2)	.20	.20
Sphalerite (ZnS)	.11	.11
Illite ($K_{0.6}Mg_{0.25}Al_{2.3}Si_{3.5}O_{10}[OH]_2$)	.032	.032
Chalcopyrite ($CuFeS_2$)	.029	.029
Goethite (FeOOH)	–5.08	–7.40
Silica (SiO_2)	–3.82	–2.89

Geochemical Controls on Solute Concentrations

Trends in Specific Conductance

Specific conductance correlates well with sulfate concentration for most surface and ground waters within the Red River Valley because the waters are dominated by dissolution of gypsum and pyrite, and sulfate is the dominant anion almost everywhere. In terms of equivalents per liter, sulfate is 50 to 99 percent of the anion equivalents for all samples, and sulfate approaches 50 percent for the most dilute, upstream samples in the Red River with pH values around 8. The correlation of specific conductance with sulfate concentrations for water in the Straight Creek catchment is shown in figure 20A, and other ground waters sampled in this study are shown in figure 20B. For Straight Creek surface and alluvial ground waters, the equation of best linear fit is:

Specific conductance (microsiemens per centimeter) = 1.197(SO_4, milligrams per liter) + 391.

The linear fit is a reasonable approximation in the range of about 400 to 3,000 mg/L. The linear fit is not a good fit at very low or very high sulfate concentration. As higher concentrations are reached, the extent of ion pairing increases, which effectively decreases the rate of increase of specific

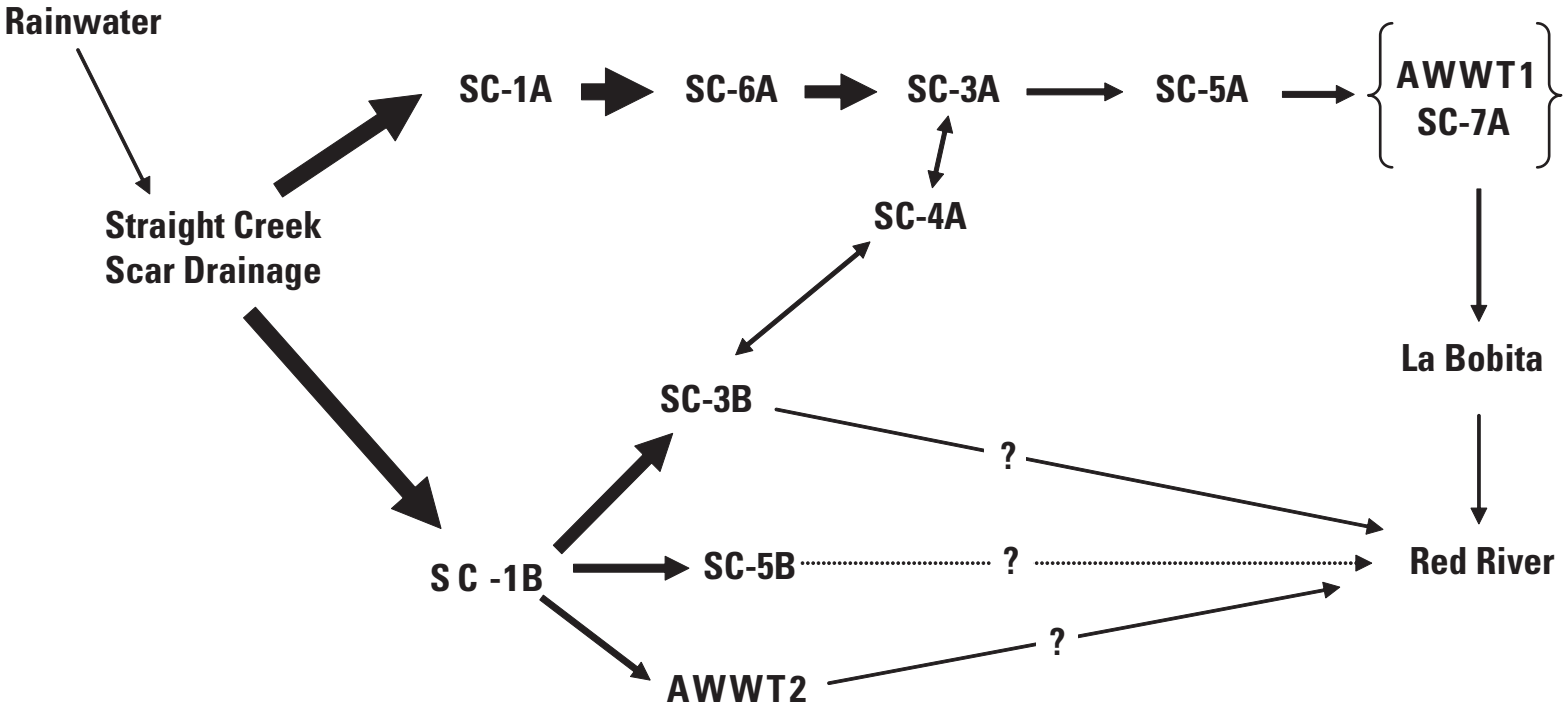

Figure 19. Evolutionary flow paths based on changes in ground-water chemistry with downstream gradient. Arrows point in the direction of downstream gradient and more dilute water. Thicker arrows indicate higher solute concentrations. The double-headed arrows shown for interactions between SC–4A and SC–3B and SC–4A and SC–3A reflect the fact that bedrock water chemistry of SC-3B influences the chemistry of SC–4A but to a lesser extent than that from SC–3A.

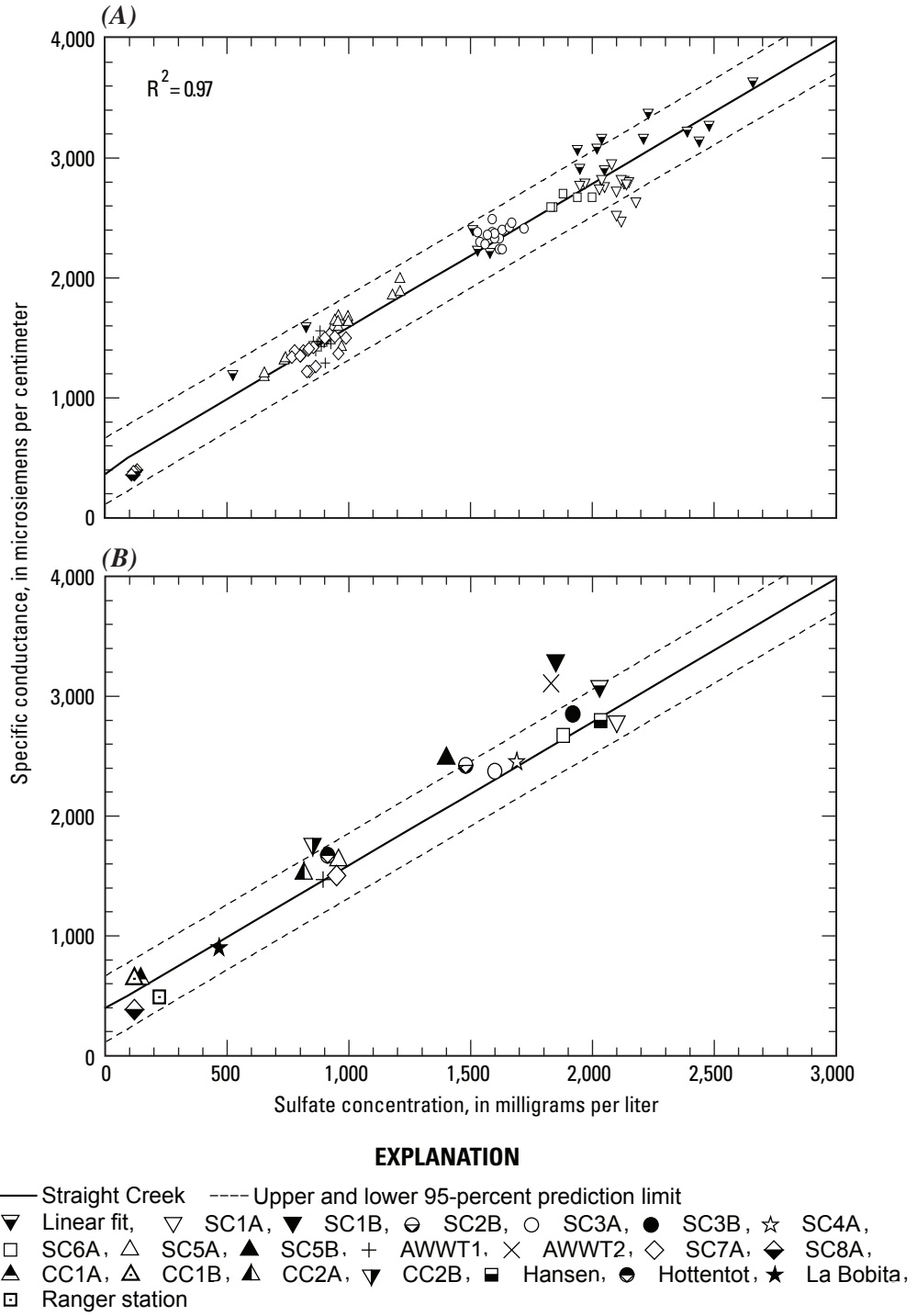

Figure 20. Plot of specific conductance against sulfate concentrations for (A) Straight Creek surface and alluvial ground waters and (B) median values for ground waters and Straight Creek surface water.

conductance per unit increase in sulfate concentration. Acid sulfate water of even higher sulfate concentration than shown here clearly shows a tendency to plateau with increasing concentration. However, an analysis of this refinement is beyond the scope of this study.

A more important trend is the bias of other ground-water samples shown in figure 20B toward the upper confidence limit. This bias is caused by ground waters, such as SC–1B and SC–5B, which have circumneutral pH and high alkalinity values. These ground waters have higher specific conductance

than the best linear fit to the sulfate-dominated waters in figure 18(a) because dissolved inorganic carbon is contributing substantially to the anion equivalents and to the conductivity of these solutions. Nevertheless, all samples except those from SC–1B, SC–5B, and CC–2B are at or within the prediction limits that express a 95-percent confidence for the variation in the data from the best fit. Because dilute waters may have a substantially higher proportion of free ions than the high-sulfate ground waters, this correlation should not be used for sulfate concentrations less than about 400 mg/L such as those for the Red River.

The correlation of specific conductance with sulfate concentrations for the Red River surface water (McCleskey and others, 2004; Verplanck and others, written commun., 2004) has been obtained separately from Red River ground water and is shown in figure 21. The correlation coefficient of 0.97 demonstrates how well the specific conductance responds to changes in sulfate concentration and can be used to predict the sulfate concentration for dilute water samples. The best fit equation for this line is:

Specific conductance (microsiemens per centimeter) = 1.46(SO_4, milligrams per liter) + 179,

which should give an estimate of the sulfate concentration from measured conductivity within about ±20 percent at the 95-percent confidence level.

Geochemical Controls on Dissolved Sulfate Concentrations

There are only two substantial sources of dissolved sulfate in surface and ground waters of the Red River Valley—gypsum dissolution and pyrite oxidation. If both the gypsum and the pyrite were formed under similar hydrothermal conditions, then these sources could be differentiated based on stable isotope compositions of the dissolved sulfate (Seal and others, 2000; Seal, 2003). Unfortunately, the gypsum is secondary; that is, it has formed from the weathering of pyrite and calcite (Ludington and others, 2005). Under these conditions gypsum inherits nearly the same $\Sigma^{34}S$ value as the pyrite. The $\Sigma^{18}O$ composition of the gypsum will also be the same as that in sulfate derived from pyrite oxidation so that stable sulfate isotope data of dissolved sulfate does not distinguish between these sources. However, chemical data can differentiate these sulfate sources, and it was used to do that in the mass-balance calculations.

The dissolved sulfate concentration in Red River Valley ground water should be dependent on the residence time of the ground water as well as on the source of the sulfate. The longer the water is in contact with gypsum and the longer that water and oxygen contact pyrite surfaces, the higher the concentration of sulfate should be if there were no other processes (up to the solubility limit). As a consequence, one might predict that there would be higher sulfate concentrations the

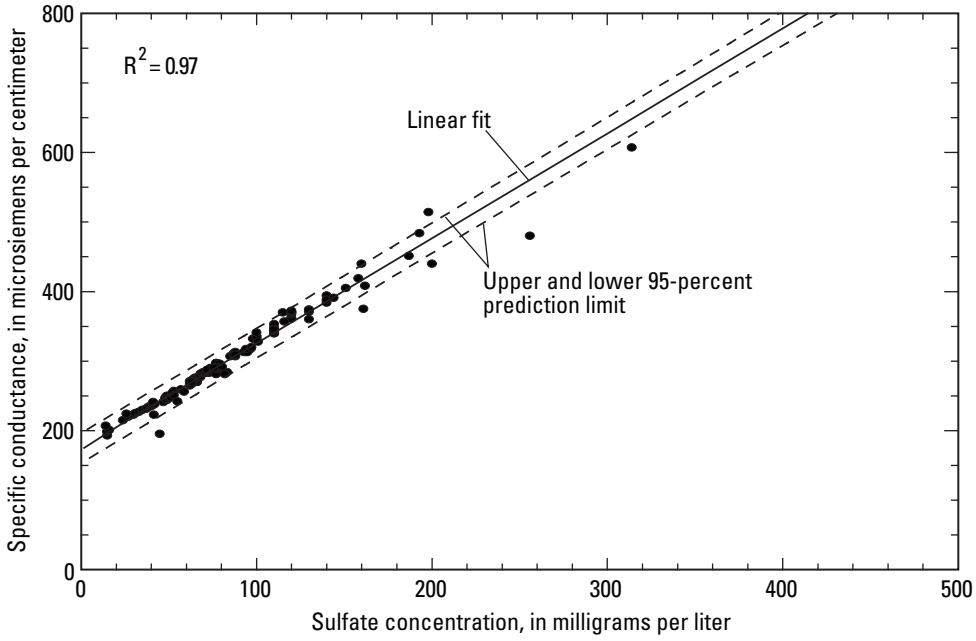

Figure 21. Correlation between specific conductance and sulfate concentration for Red River surface-water samples from this study.

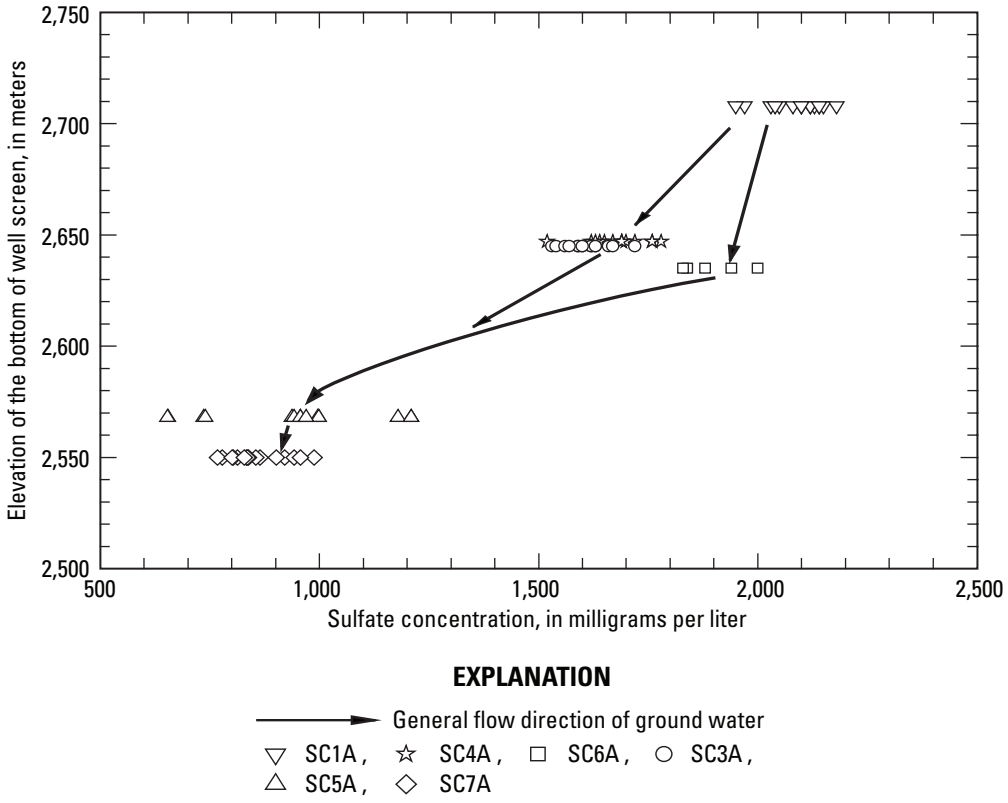

Figure 22. Relation between sulfate concentrations of Straight Creek well waters and elevation of the bottom of the screened interval for each well.

longer ground water has resided in a debris fan derived from a scar, but this prediction would be incorrect. As demonstrated in the Straight Creek debris-fan ground water, there is uniform dilution from the uppermost well in the fan to the lowermost well (Naus and others, 2005). Sulfate concentrations in water from well SC–1A are more than 2,000 mg/L and decrease to about 800 mg/L in the lower portion of well SC–7A, less than one-half of the original input concentration. This trend is shown in figure 22 in which the sulfate concentrations of the Straight Creek alluvial ground waters are plotted relative to the elevation of the bottom of the screened well. The main alluvial ground-water flow follows the contact between the bedrock and the alluvium. This "bedrock surface" has an identifiable channel, as shown from seismic studies, and would be expected to carry the major portion of the alluvial flow. That channel shows that well SC–6A is located within the deeper portion of the channel, whereas wells SC–3A and SC–4A are not. Wells SC–3A and SC–4A are in a perched bedrock position relative to the main channel, and consequently, their water tables are perched with respect to that in well SC–6A. The positions of wells SC–3A and SC–4A explain why their solute concentrations are less than those in well SC–6A even though they are close together and at the same ground-surface elevation. They are in a perched position to the side of the drainage where they would receive more dilution from dilute-water seepage along the side of the canyon, whereas well SC–6A receives more direct flow from water in the scar area and by water in well S–1A without as much dilution. By the time ground water reaches wells SC–5A and SC–7A, it is diluted with Red River alluvial ground water. Regardless of the source of diluting water, continual dilution is apparent all the way to the Red River alluvium. Samples from SC–8A appear to have little or no acid water. It is likely to be representative of uncontaminated Red River ground water. These flow paths have been shown schematically with the use of arrows in figure 22.

Similar trends are apparent in the other debris fans receiving scar-drainage water (Naus and others, 2005; Nordstrom and others, 2005). The source of this dilution appears to be more dilute ground water seeping in from the sides of the drainage. Such seepage would be expected based on the steep topography of the canyon. Dilution from the east tributary of Straight Creek and from vertical infiltration during snowmelt and floods might also contribute, but this dilution is not likely to be the main source of dilution because snowmelt and floods

are more episodic and infrequent events compared to side seepage. For this reason, key constituent concentrations are plotted against sulfate concentrations in subsequent sections of this report to reveal the extent to which they change either by dilution (conservative and nonreacting) or by reaction (nonconservative). Hydrogeochemistry cannot predict the exact flow path of ground water, nor the exact minerals along that flow path, nor the exact dissolution rate for those conditions in the aquifers of the Red River Valley. Hence, empirical data (direct measurements) on ground-water chemistry and weathering conditions are used for those conditions that are not defined by mineral solubility limits. It is not strictly empirical because the main minerals that weather to form the ground-water composition and their relative weathering rates are known. Also, the change in mineral abundance with location and trace-element content of those minerals is known.

The regular dilution trends found for specific conductance relative to sulfate concentrations in Straight Creek surface and ground waters (figs. 20 and 22) were so linear that it was useful to plot every inorganic solute concentration relative to sulfate concentration. These linear correlations served several purposes: (1) They distinguished conservative constituents (those undergoing dilution only) from nonconservative, or reactive, constituents (those undergoing mineral precipitation/dissolution or redox reactions), (2) they identified constituents added or removed from the Straight Creek surface drainage upon entering the debris-fan aquifer, and (3) they provided a framework for a comparison of solutes in other catchments and, ultimately, a reference framework for estimating pre-mining ground-water solute concentrations at the mine site. The linear equations and their correlation coefficients are in table 1–2 of Appendix 1.

Geochemical Controls on Dissolved Iron Concentrations

Dissolved iron concentrations, particularly in surface and ground waters of the Red River Valley, are complicated functions of both pH and redox (reduction-oxidation) chemistry. Water of low pH usually contains high iron concentration, but iron can precipitate from solution if it is oxidized and the pH is about 2.5 or higher, thus lowering the concentration. The primary source of dissolved iron in the Red River Valley

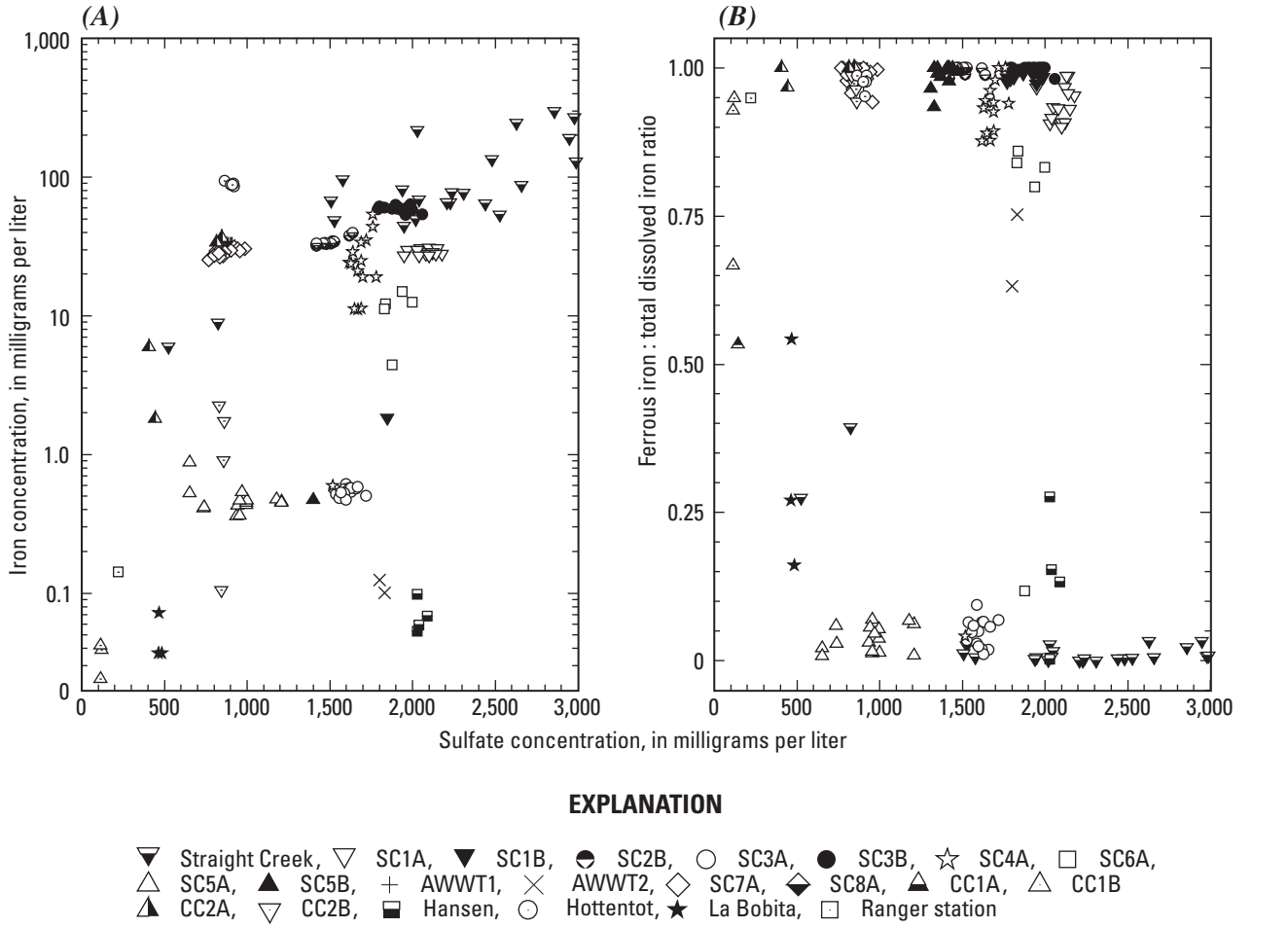

Figure 23. (A) Iron concentrations plotted against sulfate concentrations for all ground waters and Straight Creek surface water. (B) Ferrous iron:total dissolved iron molar ratio plotted against sulfate concentrations for all ground waters and Straight Creek surface water.

is from the oxidation of pyrite. Hence, the concentrations of iron in surface and ground waters depend on (1) the amount of pyrite oxidized, (2) the extent to which the dissolved iron is oxidized, (3) any mineral-precipitation reactions that can provide an upper limit to iron concentrations, and (4) any changes in pH caused by other reactions such as carbonate dissolution or feldspar dissolution. As shown in figure 23A, iron concentrations cover a large range of values (less than detection to 300 mg/L) and do not reflect a predictable correlation with sulfate concentrations although, qualitatively, the iron concentrations do decrease generally with decreasing sulfate concentration.

The iron concentrations for well SC–1A average slightly less than those of Straight Creek, but the sulfate concentrations average about the same. Hence, Straight Creek drainage water can be the input for iron mass flux to the alluvial ground water if some iron is precipitated. Iron precipitation would seem reasonable because most of the dissolved iron in Straight Creek is already oxidized (see fig. 23B), and the larger mineral surface area in the debris fan should encourage precipitation.

Figure 23B shows the dissolved Fe(II)/Fe(total) redox ratio discriminates the ground water into primarily two groups, those that are largely reduced (SC–1A, SC–1B, SC–2B, SC–3B, SC–4A, SC–5B, SC–7A, AWWT1, CC–1B, CC–2A, CC–2B, and Hottentot) and those that are largely oxidized (Straight Creek drainage, SC–3A, and SC–5A). Very few waters sampled have intermediate Fe(II/III) redox ratios (La Bobita, CC–1A, AWWT2, and Hansen).

Ferric Iron Concentrations

Figure 24A shows that when ground-water concentrations of ferric iron are plotted against pH there is a substantial decrease in concentration by two orders of magnitude as the pH increases from 2.5 to 4. This decrease is far greater than that afforded by ground-water dilution alone and is strong evidence for precipitation of iron minerals.

The most generally applicable control on the upper limit of iron concentrations in oxic waters is HFO precipitation, represented by the formula $Fe(OH)_3$. Although the mineral that precipitates is not a single phase but often a mixture of schwertmannite, ferrihydrite, and microcrystalline goethite, all with slightly different stoichiometries from $Fe(OH)_3$, it is more straightforward to model it as $Fe(OH)_3$ or ferrihydrite precipitation. Determining the concentration of dissolved, oxidized iron (ferric iron) is challenging because precipitated HFO particles are commonly colloidal in size and are not easily filtered with 0.45 or even 0.1 μm pore size. Colloidal ferric iron particles then become included as part of the dissolved ferric iron concentrations, biasing the results. Consequently, this study compared the measured redox potential, or Eh, with the calculated Eh because the measured Eh will respond only to the truly electroactive, and, thus, dissolved activities of ferrous and ferric iron. Where the comparisons were in good agreement, the concentrations were then used to calculate the saturation indices (SI) for HFO (Nordstrom and others, 2005). The results plotted in figure 24B show the SI for HFO relative to pH for all the samples that met the Eh comparison criteria. This figure indicates that the ferrihydrite (HFO) saturation does provide an upper limit for iron concentrations in oxidized water. Figure 24C shows that as the dissolved iron concentrations increase there is a consistent plateau of the ferrihydrite saturation indices, independent of iron concentrations. At low pH, jarosite saturation is reached (fig. 25) and may provide a control on ferric iron concentrations.

Ferrous Iron Concentrations

Anoxic waters can maintain high concentrations of ferrous iron at any pH value, but a limit would be reached by siderite saturation in the presence of carbonate buffering and at neutral pH. Figure 26A shows that as alkalinity concentrations increase, the concentrations of ferrous iron decrease, an expected common-ion effect if siderite solubility limits ferrous iron concentrations. Figures 26B and 24C show the SI values for siderite relative to pH and to calcium concentrations. As with all carbonates, equilibrium solubility requires near-neutral pH values. A trend that will be recurring with the carbonate equilibrium mineral solubilities and demonstrated in figure 26C is that a uniform approach to saturation is seen with increasing calcium concentration. Siderite has not been found as a primary hydrothermal mineral. The preferred hypothesis is that with continued dissolution of known carbonates, primarily calcite and possibly some ankerite, the high ferrous iron concentrations eventually reach siderite saturation and begin to precipitate as thin coatings on carbonate minerals. Within reasonable uncertainties, siderite appears to provide an upper limit for ferrous iron concentrations.

Consequently, iron concentrations in ground water can vary considerably depending on the amount of pyrite weathering and the amount of dissolved ferrous iron oxidation. Surface water originating in scar areas contains high concentrations of iron that are rapidly oxidized, but most ground water contains predominantly reduced iron, depending on proximity to the water table. Some alluvial ground waters are well aerated and contain nearly all ferric iron. The solubility of HFO provides an upper limit to ferric iron concentrations at moderately acidic to neutral pH values (3.5–8), jarosite provides an upper limit to ferric iron concentrations at low pH (1–3), and siderite solubility provides an upper limit to ferrous iron concentrations at circumneutral pH.

Geochemical Controls on Dissolved Manganese Concentrations

Dissolved manganese concentrations behave somewhat similarly to dissolved iron concentrations in that manganese occurs in a more-soluble reduced form, manganous ion, and a less-soluble oxidized form, manganic ion. Manganese, however, is more easily reduced in anoxic water than iron and is generally more mobile. Hence, manganese concentrations

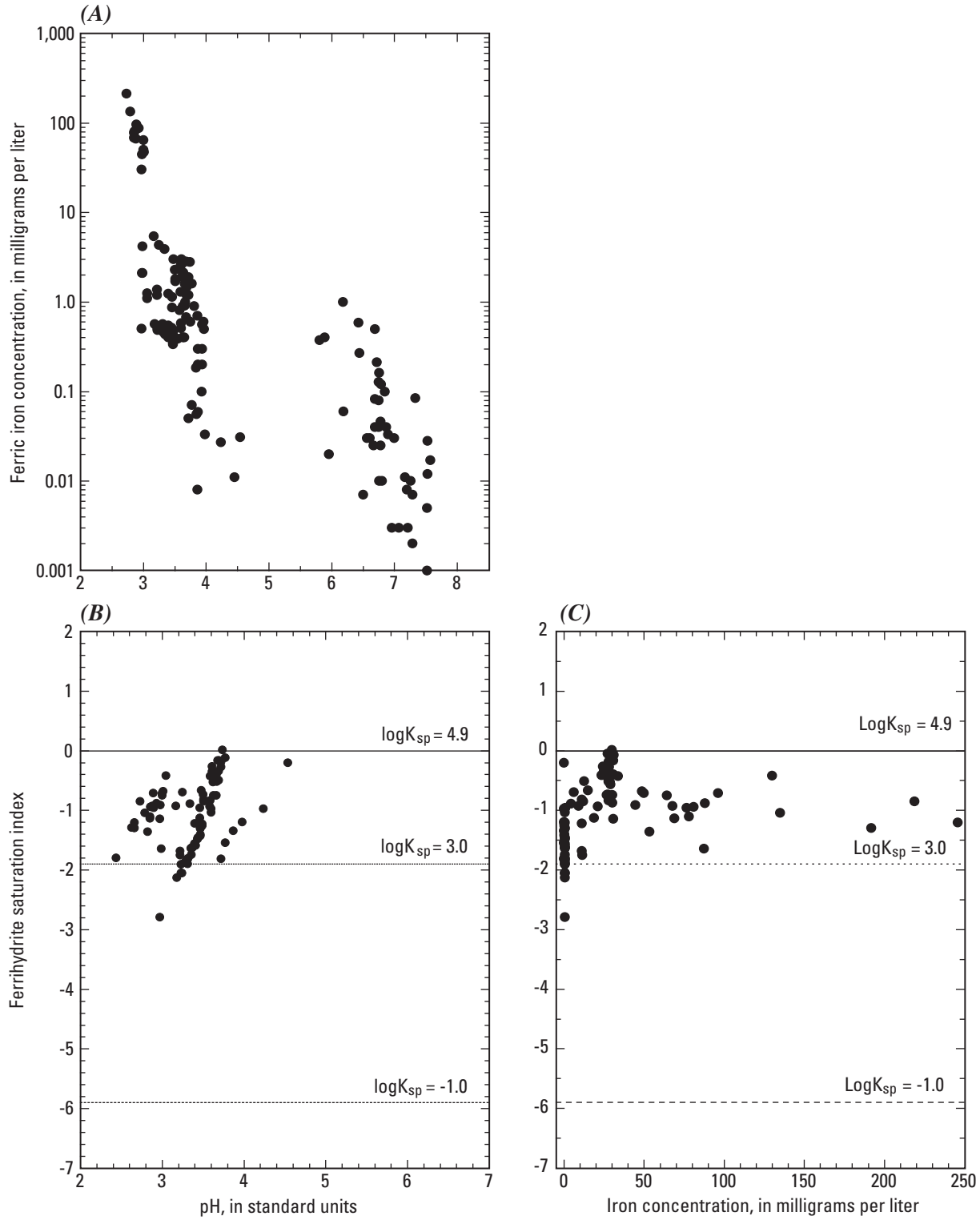

Figure 24. (A) Ferric iron concentrations plotted against pH for all ground waters and Straight Creek surface water. Ferrihydrite saturation index plotted against (B) pH and (C) iron for all ground waters and Straight Creek surface water fulfilling the Eh measurement requirements described in Naus and others (2005) and in Nordstrom and others (2005). The $\log K_{sp}$ = 4.9 and 3.0 represent the upper and lower bounds, respectively, on the solubility of HFO (Nordstrom and others, 1990).

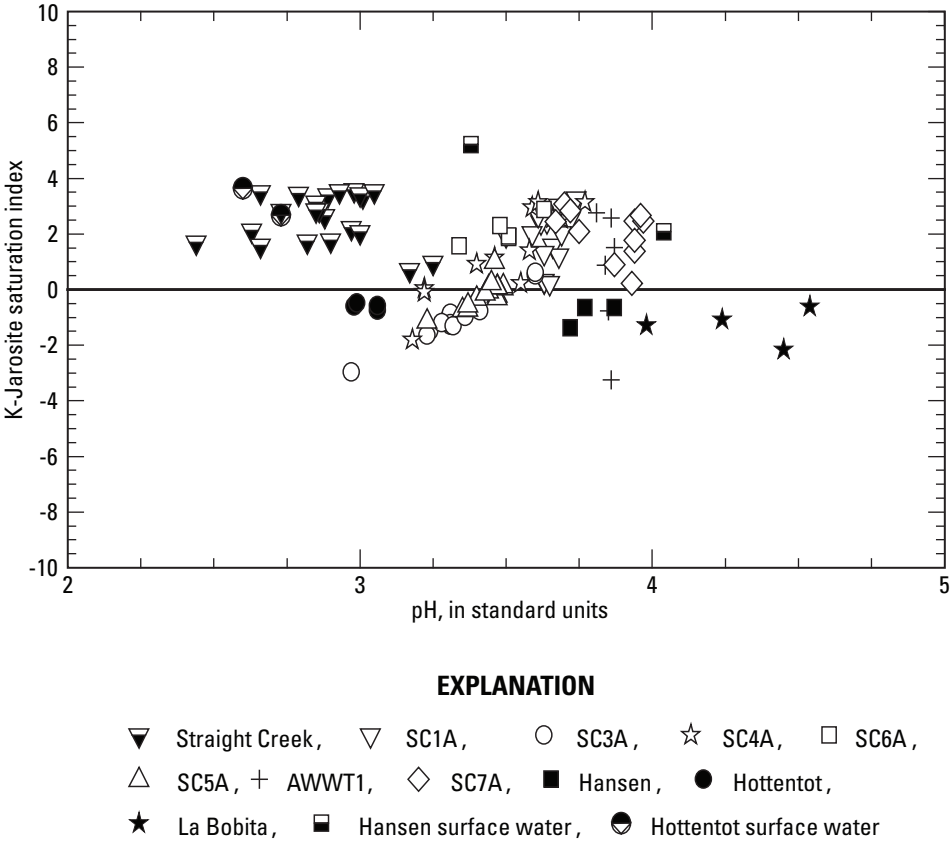

Figure 25. Saturation indices for potassium jarosite plotted relative to pH.

show a good correlation with sulfate concentrations as shown in figure 27A for the Straight Creek surface and alluvial ground waters. Figure 27A includes a 95-percent confidence for the prediction limits about the linear best fit. Statistics of best linear fit for all the correlation lines shown in this paper are provided in table 1–2 in the Appendix and were originally derived from the Straight Creek study (Naus and others, 2005). Water from SC–8A is circumneutral pH, dilute, Red River alluvial ground water and would not necessarily correlate in metal concentration with the acidic alluvial ground waters of Straight Creek. Hence, it was included in the linear fit if it was consistent with acidic ground-water data, and otherwise it was not used. The best fit line with the confidence intervals and median values of the Straight Creek alluvial ground waters were then used to compare with the median values of other ground waters (Straight Creek bedrock ground waters and Hansen Creek, Hottentot Creek, La Bobita, and Capulin Canyon ground waters) and Straight Creek drainage water (fig. 27B). Manganese concentrations in the Straight Creek surface water are nearly the same as those from SC–1A. Most other constituents show the same correspondence and provide evidence that Straight Creek is the main flow input for the Straight Creek alluvial ground water.

Most of the other ground waters have manganese concentrations that agree well with the Straight Creek alluvial ground-water trend, but some important differences must be noted. Water from well CC–2A contains considerably more manganese than the Straight Creek trend, and water from well SC–3B contains slightly more manganese than the trend. Water from CC–2A (Capulin Canyon) also is anomalously high in beryllium and fluoride concentrations. No other outstanding anomalies have been observed for CC–2A ground water. It would seem reasonable to conclude that there is more rhodochrosite, fluorite, and beryllium mineralization found locally at CC–2A (and rhodochrosite only at SC–3B) than in the Straight Creek catchment. The lack of other solute anomalies at CC–2A probably reflects the circumneutral pH conditions, which should reduce the aqueous mobility of elements such as aluminum, copper, cobalt, and nickel. The high reduced iron, high sulfate, and elevated zinc concentrations indicate there is sulfide mineralization in this part of Capulin Canyon but not enough oxidation of pyrite to lower the pH values substantially.

Another departure from the Straight Creek manganese-sulfate trend in alluvial ground water is the anomalously low manganese concentrations for waters from wells SC–1B, SC–5B, AWWT2, and Hansen. This consistent trend of lower manganese concentrations for ground water with circumneutral pH and substantial carbonate alkalinity (not Hansen) indicates that aqueous saturation is reached with respect to rhodochrosite. Furthermore, this trend shows that although manganese concentrations are limited by rhodochrosite satura-

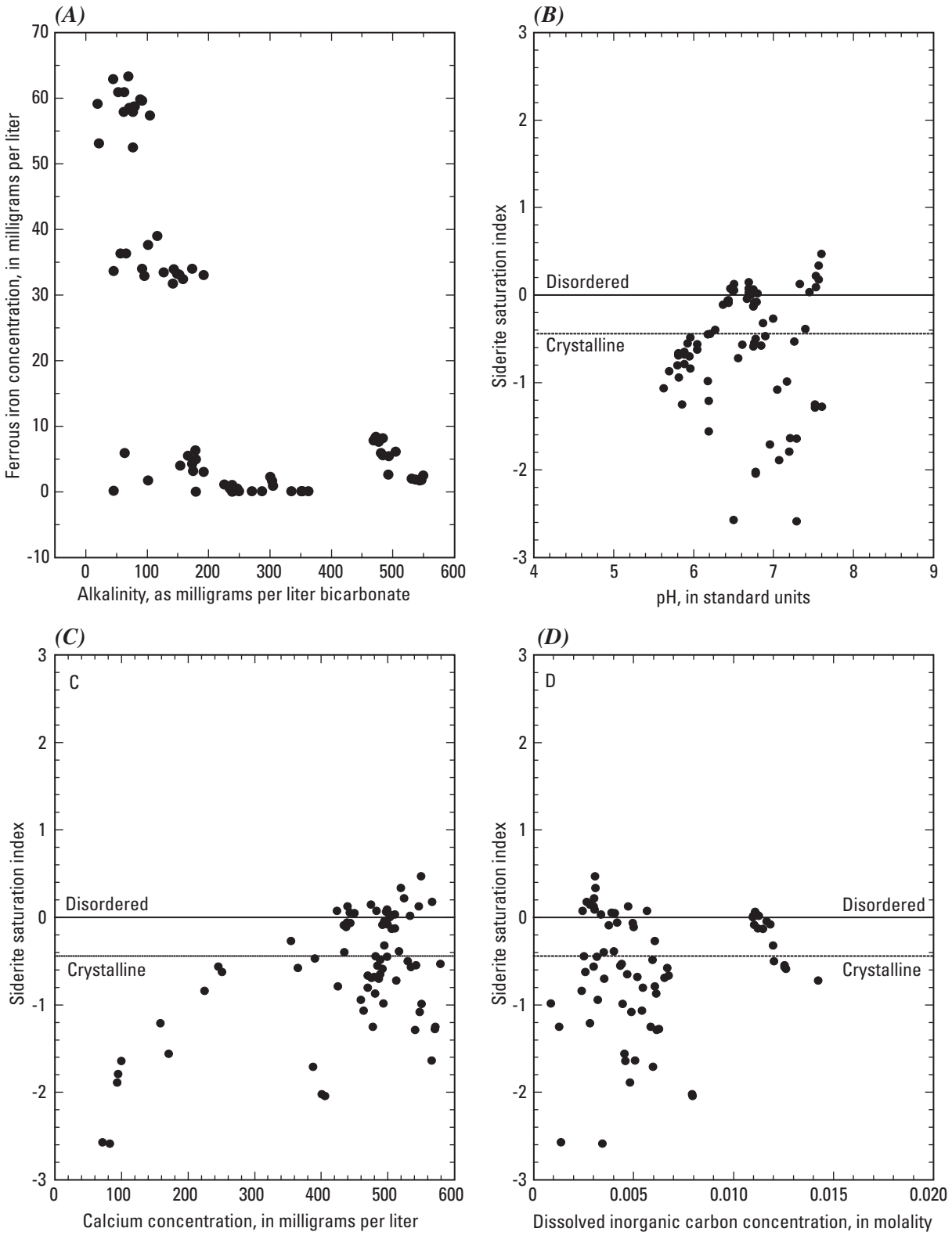

Figure 26. (A) Ferrous iron plotted against alkalinity. Siderite saturation index plotted against (B) pH, (C) calcium concentrations, and (D) dissolved inorganic carbon concentrations for all ground waters and Straight Creek surface water.

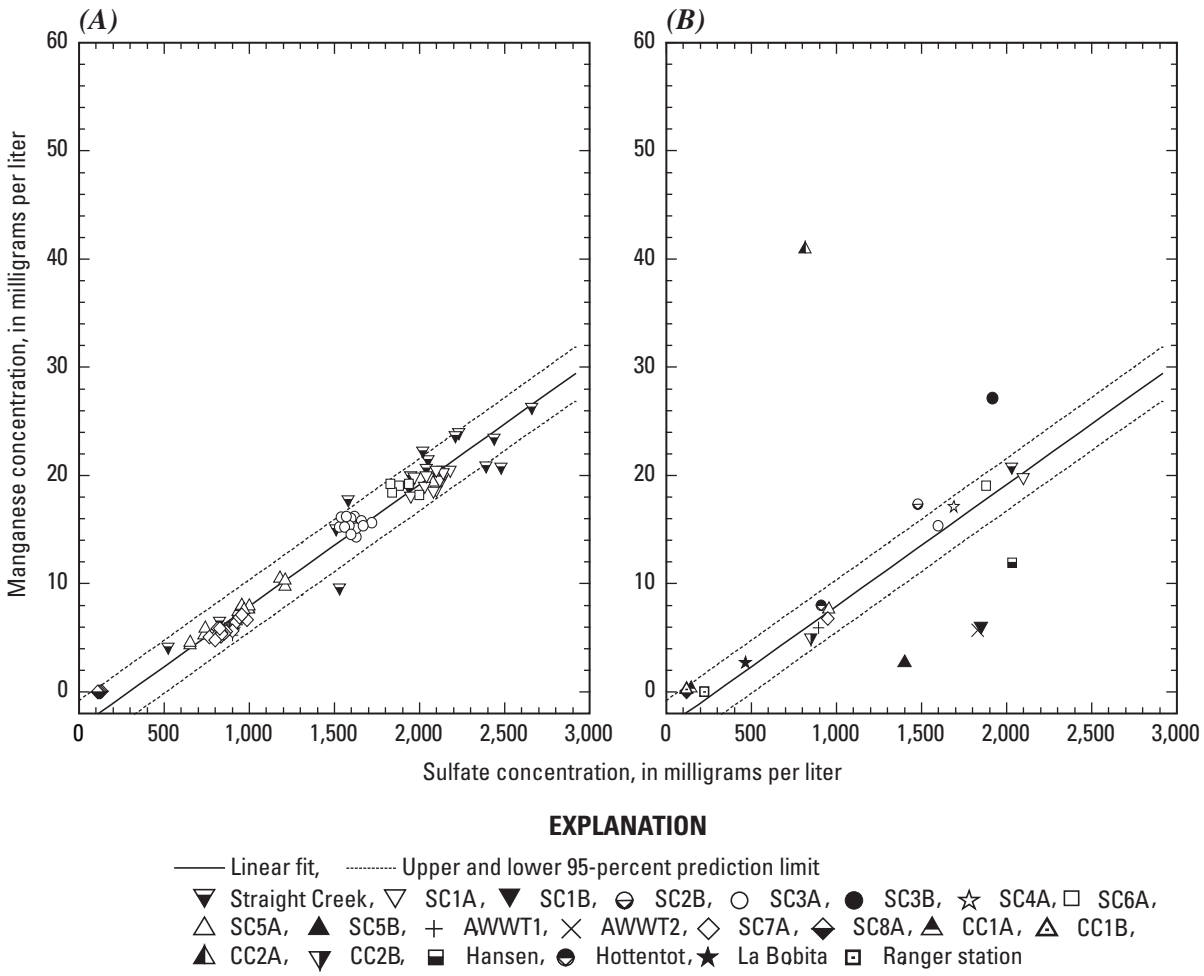

Figure 27. Manganese concentrations plotted against sulfate concentrations for (A) Straight Creek surface and alluvial ground waters and (B) median manganese and sulfate concentrations for all ground waters and Straight Creek surface water. Linear fit and prediction limits at 95-percent probability for Straight Creek data only were used for both A and B (from Naus and others, 2005; Nordstrom and others, 2005).

tion, the dissolution of other carbonate minerals, such as calcite, keeps the alkalinity elevated. The manganese concentrations are plotted with respect to alkalinity in figure 28A and, similar to ferrous iron concentrations, demonstrate a common-ion effect of decreasing manganese with increasing alkalinity. Figures 28B and 28C show the saturation indices for rhodochrosite from all well waters relative to the total dissolved inorganic carbon (DIC) concentrations and the pH, respectively. Saturation with respect to disordered rhodochrosite is maintained for many of the waters over a wide range of DIC, supporting the concept that rhodochrosite saturation limits the manganese concentrations in ground water. The SI values of rhodochrosite as a function of pH demonstrate that this solubility control is only operative at circumneutral pH values (greater than 6.5). The pH effect holds for most all carbonate mineral solubilities. Because the water from the Hansen well is acidic, the relatively low manganese concentrations cannot be a result of rhodochrosite solubility equilibrium. It is apparent that the relative abundances of soluble manganese-rich minerals such as rhodochrosite and manganiferous calcite (or dolomite) (Plumlee and others, 2005) vary substantially in the Red River Valley and can be expected to vary according to the alteration zones outlined by Ludington and others (2005). If the Hansen catchment is more distal from the thermal core of the alteration, and the core was more centered near the Straight Creek catchment or to the east of Straight Creek, then there should be less manganese mineralization in the weathering zone of the Hansen catchment relative to the Straight Creek or Hottentot catchments. It is noteworthy that, although the Hansen well water contains lower manganese to sulfate ratios than the waters from the Straight Creek alluvial wells, the concentration of manganese is higher than that in Hottentot well water and in waters from wells SC–5A, SC–7A, and AWWT1. These observations indicate that the ratio of rhodochrosite to pyrite available to weathering can vary significantly between some catchments. In the CC–2A

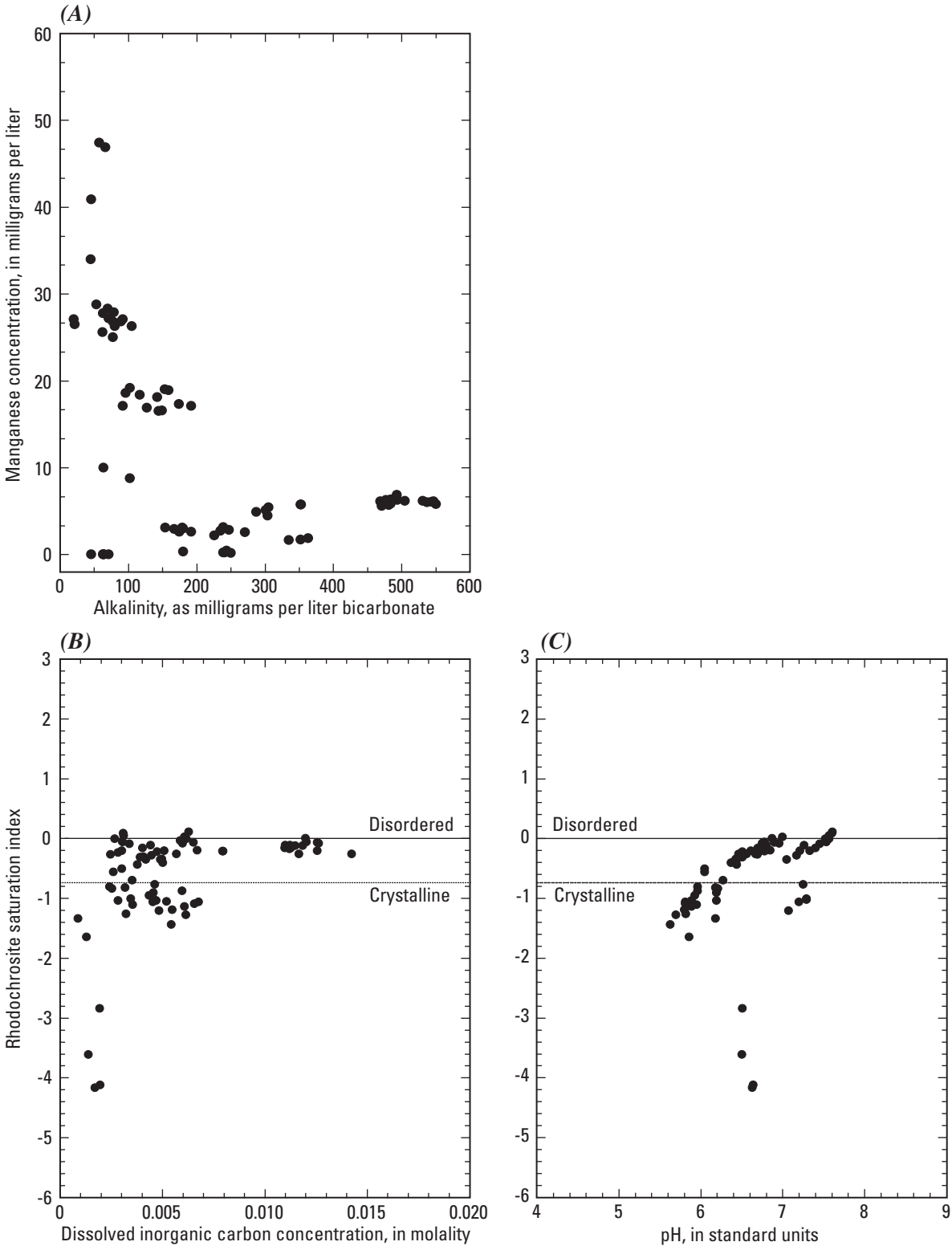

Figure 28. (A) Dissolved manganese concentrations plotted against alkalinity. Rhodochrosite saturation index plotted against (B) dissolved inorganic carbon concentrations and against (C) pH for all ground waters and Straight Creek surface water.

well, the rhodochrosite to pyrite ratio is high, whereas in the Hansen catchment the ratio is low. The ratios represented by the Straight Creek alluvial ground waters are probably average values between these extremes.

Important generalizations can be drawn from these results for the behavior of manganese mobility in ground water of the Red River Valley. First, manganese is readily available in the weathering zone from the common occurrence of rhodochrosite or manganiferous calcite. Second, for circumneutral pH water with adequate alkalinity, rhodochrosite equilibrium provides an upper limit to manganese concentrations. Third, manganese to sulfate ratios can vary substantially because of the variability of abundance of rhodochrosite to pyrite in the weathering zone.

Geochemical Controls on Dissolved Aluminum and Silica Concentrations

Although the State of New Mexico has a ground-water quality standard for aluminum and not for silica, these two constituents must be discussed together because they have geochemical similarities. They both change solubility with pH, but for different reasons, and they tend to react with each other to form clay minerals.

Aluminum

The concentration and speciation of dissolved aluminum in natural waters is primarily controlled by pH. Under acid conditions, aluminum is highly soluble, and at circumneutral pH, aluminum is insoluble. This behavior is directly related to the value of the first hydrolysis constant, $-\log K_1 = pK_1 = 5.0$. When the pH of an acid, aluminum-rich solution increases and approaches the pK_1, aluminum begins to hydrolyze and precipitate, generally in the pH range 4.5–5.0 (Nordstrom and Ball, 1986). Not only does the amount of hydrolysis increase with increasing pH values, but the rate of hydrolysis also increases in this pH range (Hem and Roberson, 1990). In acid sulfate water, the actual precipitate is more of an aluminum hydroxysulfate compound rather than a pure aluminum hydroxide (Bigham and Nordstrom, 2000) because of the high concentrations of sulfate. This geochemical reaction has often been observed in surface water but has not been as well documented for ground water. Blowes and others (2003) report a buffering of tailings water pH under mildly acidic conditions that they ascribe to aluminum hydrolysis at a pH of about 4.5.

These concepts can be further evaluated because of the numerous reliable aluminum analyses from this study that span a wide range of pH. Figure 29A plots aluminum concentration against sulfate concentration from the alluvial wells in Straight Creek, excluding wells AWWT1 and SC–7A. The linear fit correlates well with a correlation coefficient of $R^2 = 0.93$. Hence, aluminum is behaving conservatively for these waters. The analyses from AWWT1 and SC–7A were not included because they deviate noticeably from the linear fit, as can be seen in figure 29B. La Bobita ground waters are also below the correlation line and their pH values average 4.35, close to the range where aluminum hydrolysis begins. Bedrock ground waters, circumneutral in pH, are also considerably lower in aluminum concentration. These results are consistent with aluminum concentrations governed by pH. This sensitivity to pH is seen most clearly in figure 29C in which aluminum concentrations decrease rapidly as pH increases to 4.

Possible solubility controls by amorphous to microcrystalline $Al(OH)_3$ and by alunite, $KAl_3(SO_4)_2(OH)_6$, are shown by the saturation indices plotted in figures 30A–30D. The logarithm of the speciated free aluminum ion, $\log a_{Al^{3+}}$, is plotted against pH in figure 30A to compare with similar figures for other sites (for example, Nordstrom and Ball, 1986; Driscoll and others, 1984). At low pH (below 4.5), a linear trend is apparent with a shallow slope, parallel to the linear fit for the Straight Creek alluvial ground waters (Naus and others, 2005) but with a slightly lower intercept. These results, along with the excellent correlation of aluminum with sulfate concentrations in figure 29A, indicate conservative behavior of aluminum for these acid waters. Conservative behavior does not mean necessarily that minerals such as alunite are not forming under these conditions; rather, if alunite is forming, the amount of mass transfer is too small to affect the aqueous concentrations of aluminum and sulfate.

At circumneutral pH values, the aluminum decreases within the field-temperature range of crystalline gibbsite to amorphous $Al(OH)_3$. Figure 30B shows the saturation indices for crystalline gibbsite to amorphous $Al(OH)_3$ plotted as a function of pH. Again, a simple mixing line with conservative behavior is indicated for the tightly correlated values at low pH. A plateau of SI values is observed at circumneutral pH. These results show that hydrolysis and precipitation of a form of hydrolyzed aluminum controls aluminum concentrations as described by Nordstrom and Ball (1986). Aqueous aluminum behaves conservatively at low pH values and reacts rapidly at high pH values to form an insoluble precipitate. The same process is seen along the banks of the Red River where white precipitates form as a result of mixing of low-pH, aluminum-rich seepage water with the neutral-pH water of the river. There is a noteworthy difference between surface water and ground water for the transition pH from conservative to nonconservative behavior. For surface water the transition pH is consistently in the range of 4.5 to 5.5 (fig. 30A; Nordstrom and Ball, 1986). Using the data from Straight Creek (Naus and others, 2005) as shown in figure 29B, the transition pH is lower, closer to 4. Wells SC–7A and AWWT1 consistently show lower aluminum concentrations relative to sulfate (fig. 29B) than all the other alluvial waters in Straight Creek, and these waters have pH values in the range of 3.8–4.0. These data indicate that the transition pH to nonconservative behavior for aluminum is more than 0.5 of a pH unit lower than that observed in surface water. This difference might be expected because of the higher available surface area of solids contacting water in aquifers compared to sediments in surface water. Another possibility is that hydrous aluminosilicate (or amorphous aluminosilicate

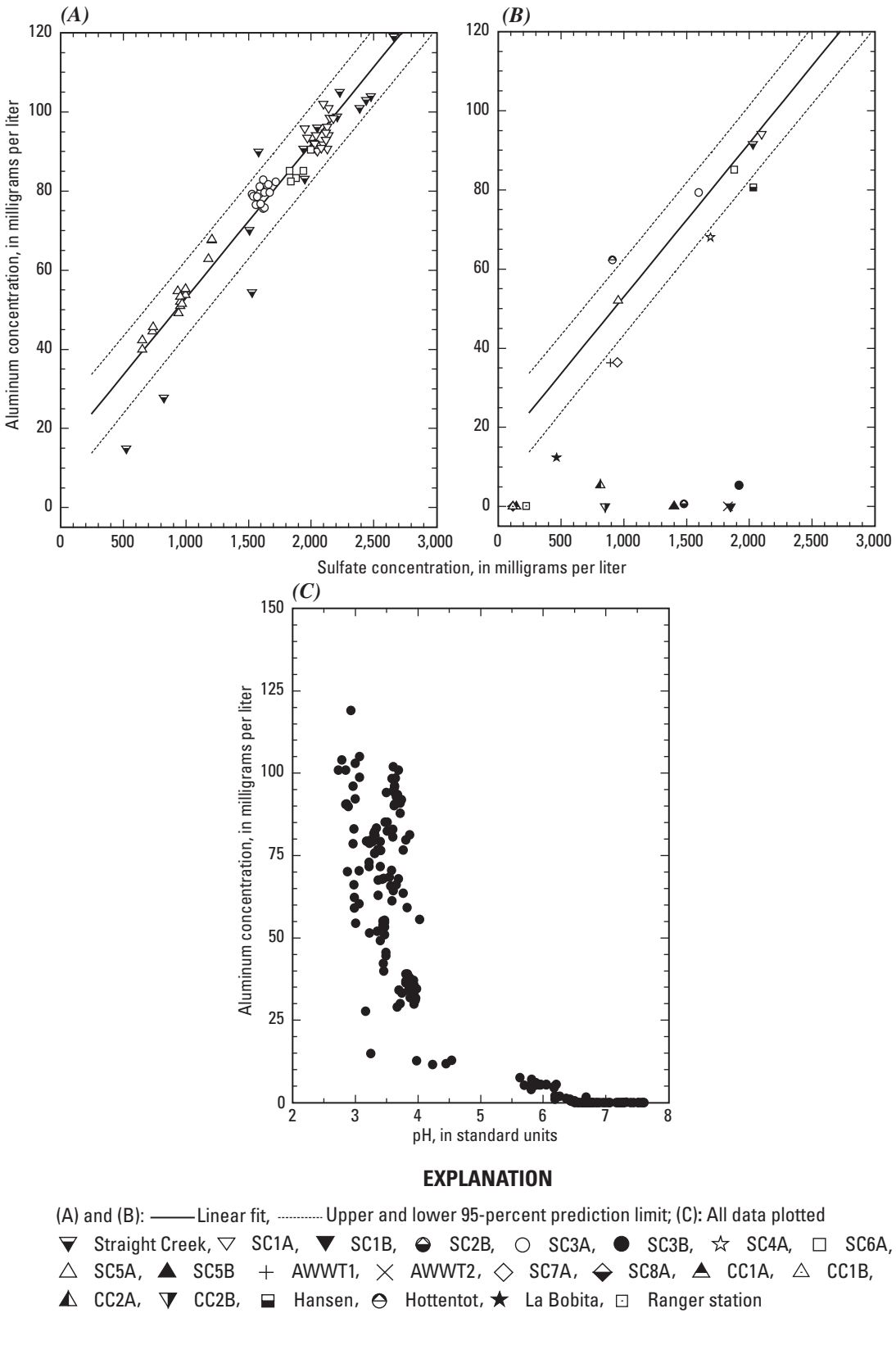

Figure 29. Dissolved aluminum concentrations plotted against sulfate concentrations for (A) Straight Creek surface and alluvial ground waters, (B) median aluminum and sulfate concentrations for all ground waters and Straight Creek surface water, and (C) dissolved aluminum concentrations plotted against pH. Linear fit and prediction limits at 95-percent probability for Straight Creek data only were used for both A and B (from Naus and others, 2005; Nordstrom and others, 2005).

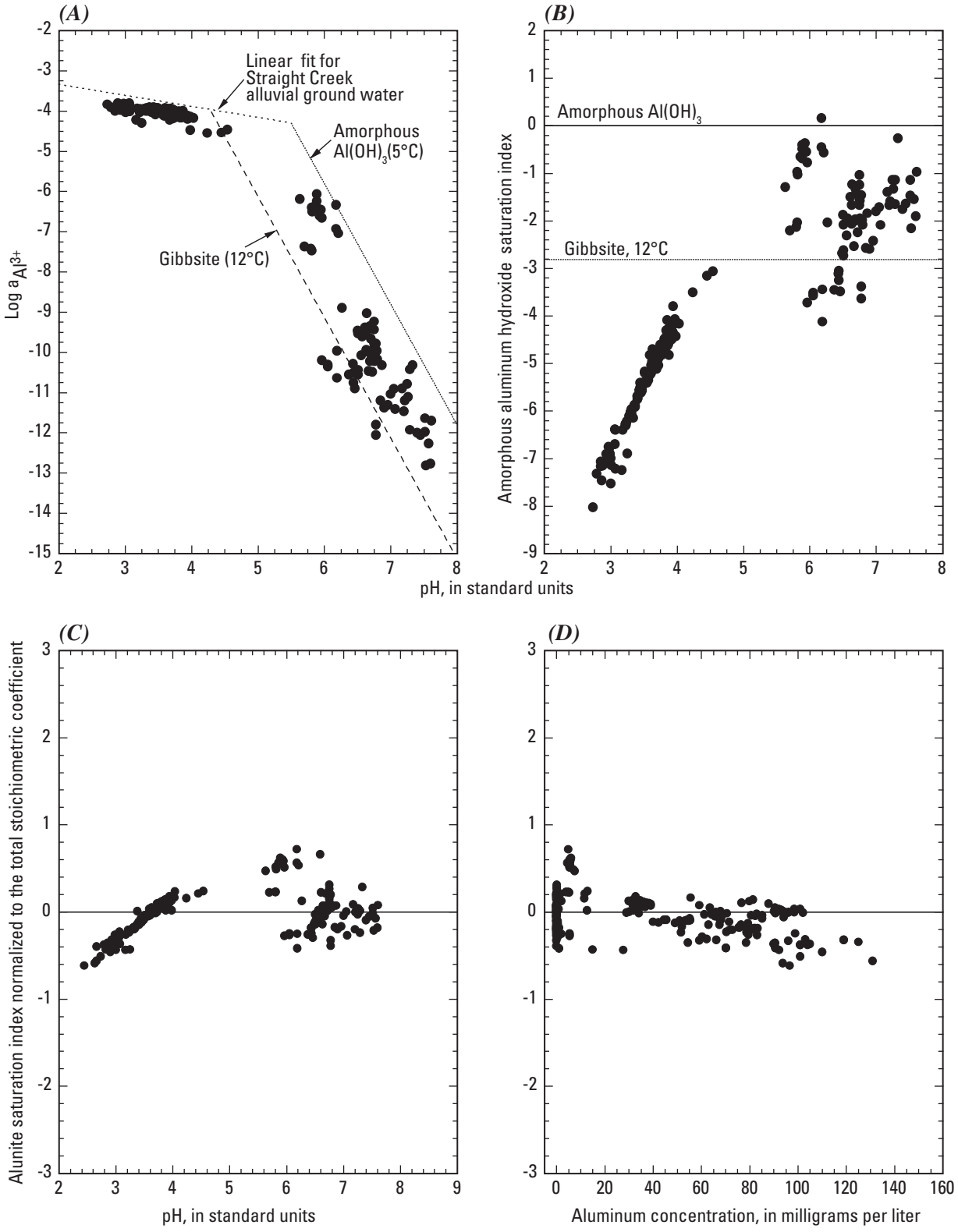

Figure 30. (A) The log of the activity of free Al^{3+} plotted against pH for all ground waters and Straight Creek surface water. Solubility limits for amorphous aluminum hydroxide (maximum value for temperature range and crystalline gibbsite (lowest value for temperature range) are shown. (B) Amorphous aluminum hydroxide saturation index plotted against pH for all ground waters and Straight Creek surface water. Alunite saturation index normalized to the total stoichiometric coefficient plotted against (C) pH, and (D) aluminum concentration.

gel) might be forming. This concept will be considered further in the next section.

Alunite SI values are plotted as a function of pH and aluminum concentration in figures 30C and D, respectively. The SI values are normalized to the total stoichiometric coefficient (for alunite, the total stoichiometric coefficient is 12; Nordstrom, 1999). Alunite is a stable mineral phase at low pH (<6; Nordstrom, 1982) and high sulfate concentrations that might provide a solubility limit. However, the linear, tightly clustered values at low pH that are not parallel to the horizontal line of constant saturation index do not reflect a solubility limit. Instead, the data reflect the same conservative mixing mentioned previously. Supersaturation is achieved at circumneutral pH, but alunite is not stable under these conditions. Again, though alunite may be forming, it does not provide an obvious solubility limit.

Silica

Silica concentrations in most ground waters are derived from dissolution of aluminosilicate minerals during weathering combined with some silica or clay mineral precipitation when concentrations are sufficiently high. Hence, under acid weathering conditions, both aluminum and silica can come from the same source, but dissolved silica is already fully hydrolyzed as $Si(OH)_4$ for all pH values in waters of the Red River Valley. Equilibrium thermodynamics and the known solubility of silica indicate that silica concentrations should not change as a function of pH; however, in figure 31A they clearly do. The silica concentrations decrease substantially as pH increases to 4, and then they decrease slightly or not at all. There is a kinetic explanation for this behavior. Dissolution of silica from silicate minerals easily occurs at low pH, but the silica precipitation rate is a slow process at low pH. Upon silicate mineral dissolution at low pH, a mixture of silica polymers and monomers appear in solution. The polymers dissociate to monomers, and the rate of the process is pH-dependent. It is much slower at pH 3 than at circumneutral pH values (Dietzel, 2000; Icopini and others, 2005). Silica precipitation requires polymerization of the individual silica molecules into chains and clusters, and polymerization rates are also dependent on pH (Iler, 1979). Again, low pH retards polymerization and precipitation. The result is that silica concentrations can be high in acid waters and above solubility limits with respect to stable silica or aluminosilicate mineral phases.

The aluminum and silica concentrations plotted in figure 31B correlate well, although not in a linear fashion and not for the same reason (although interactions between dissolved silica and dissolved aluminum are well established; Exley and others, 2002). Aluminum increases with decreasing pH because of increased dissolution rate for aluminosilicate minerals with increased acidity. Silica increases with decreasing pH because of the decreasing polymerization rate with increasing acidity. The silica concentration plotted against sulfate concentration for Straight Creek alluvial well waters except SC–7A and AWWT1 in figure 31C shows a dilution trend with sulfate. In the flow path that can be inferred from figure 31D, the silica increases in concentration from Straight Creek drainage water to SC–1A and gets diluted from SC–1A to SC–5A; then silica is attenuated, apparently by precipitation, and diluted flowing to AWWT1 and SC–7A. The attenuation indicated for silica is very similar to the attenuation pattern indicated for aluminum, and because these waters approach a pH of 4, this water chemistry might be amenable to the formation of a hydrous aluminosilicate colloid (Exley and others, 2002) or an aluminosilicate (clay mineral or gel) precipitation. If the saturation indices for various silica minerals are considered (fig. 32A), the high silica concentrations at low pH appeared to have reached a plateau that is the solubility limit of amorphous silica. At higher pH (5.5–8) a lower plateau of silica appears to have been reached that is slightly higher than chalcedony solubility and could represent some microcrystalline silica phase. Saturation indices for kaolinite and halloysite are shown in figure 32B (normalized by the stoichiometry). This figure shows that at circumneutral pH values the water chemistry has reached the range of halloysite to kaolinite solubility, and these SI values provide further evidence that some type of clay mineral (or gel) is forming in this pH range. Kaolinite is found in the weathering profile and with hydrothermal minerals. It is difficult to determine its origin without much more detailed work and isotopic studies. Halloysite has not been identified, but its saturation index is used to approximate fine-grained, poorly crystalline kaolinite. Because of the difficulty in eliminating all particles of colloidal aluminosilicates during filtration, it is not known whether the supersaturation observed for kaolinite and halloysite is real or an artifact.

Geochemical Controls on Dissolved Fluoride Concentrations

Fluoride concentrations showed a linear correlation with sulfate concentrations for the alluvial Straight Creek ground waters, indicating a dilution trend as shown in figure 33A. Little difference in fluoride concentration is apparent between Straight Creek drainage water and SC–1A and the other alluvial ground waters as seen in figure 33B. Possibly some small addition of fluoride from fluorite dissolution is indicated. Most of the other ground waters follow this trend, but there are some notable exceptions (fig. 33B). Waters from well CC–2A are anomalously high in fluoride relative to sulfate, consistent with the high manganese and relatively high sulfate concentrations that indicate mineralization near this well. Fluoride concentrations from Straight Creek bedrock ground waters SC–1B, SC–5B, and AWWT2 and from alluvial Hansen ground waters are low or depleted relative to sulfate compared to the Straight Creek alluvial ground waters. This depletion indicates a possible solubility control by fluorite. Similar correlation trends are seen in figures 33C and 33D in which fluoride concentrations are plotted against calcium concentrations for Straight Creek alluvial ground waters and all other well waters, respectively. The depletion in fluoride relative to

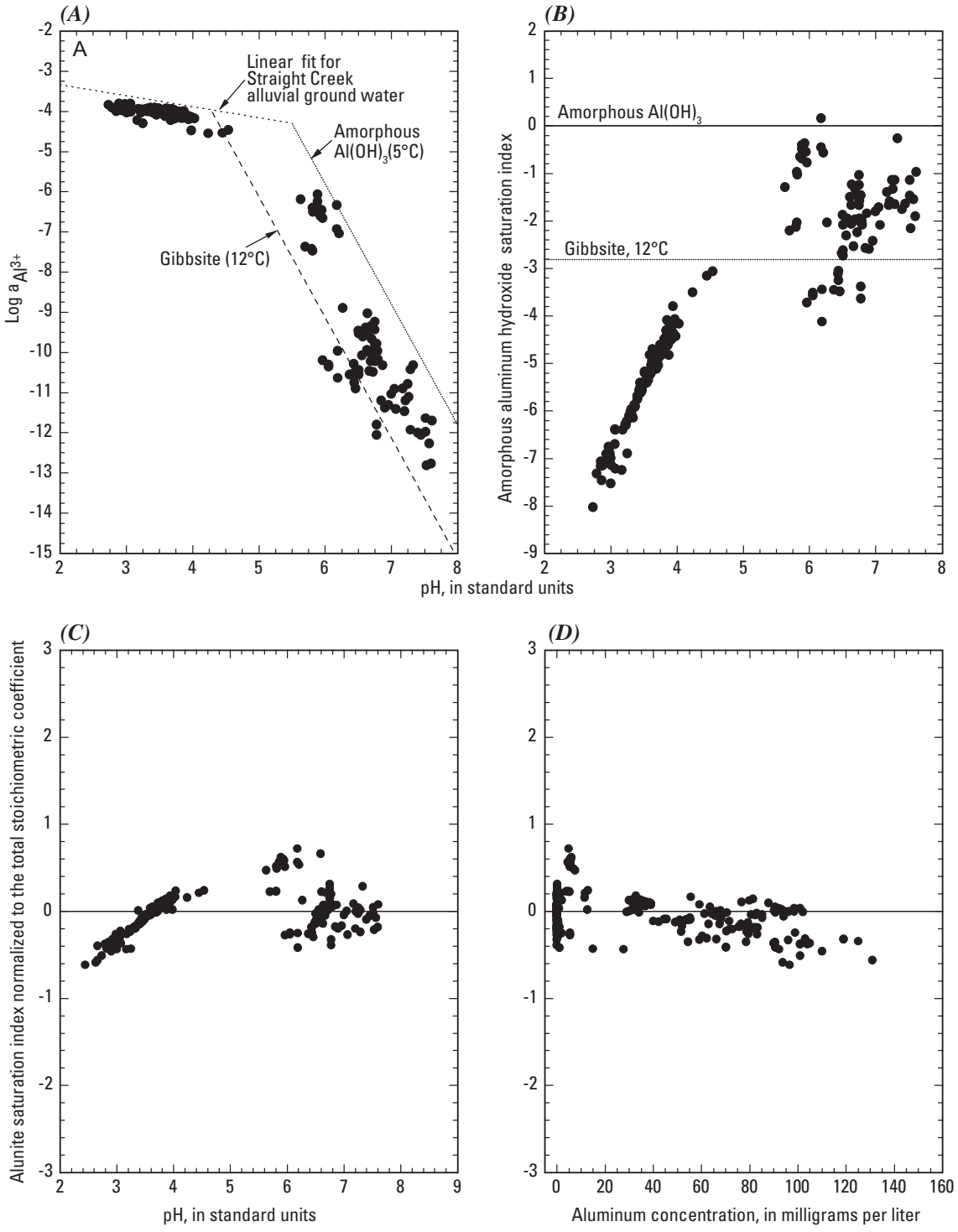

Figure 31. (A) Silica concentrations plotted against pH for all ground waters. (B) Silica concentrations plotted against aluminum concentrations for all ground waters. For samples having a pH value less than 4, silica concentrations plotted against sulfate concentrations for (C) Straight Creek alluvial ground water; and (D) median silica and sulfate concentrations for all ground waters and Straight Creek surface water. Linear fit and prediction limits at 95-percent probability for Straight Creek data only were used for both A and B (from Naus and others, 2005; Nordstrom and others, 2005).

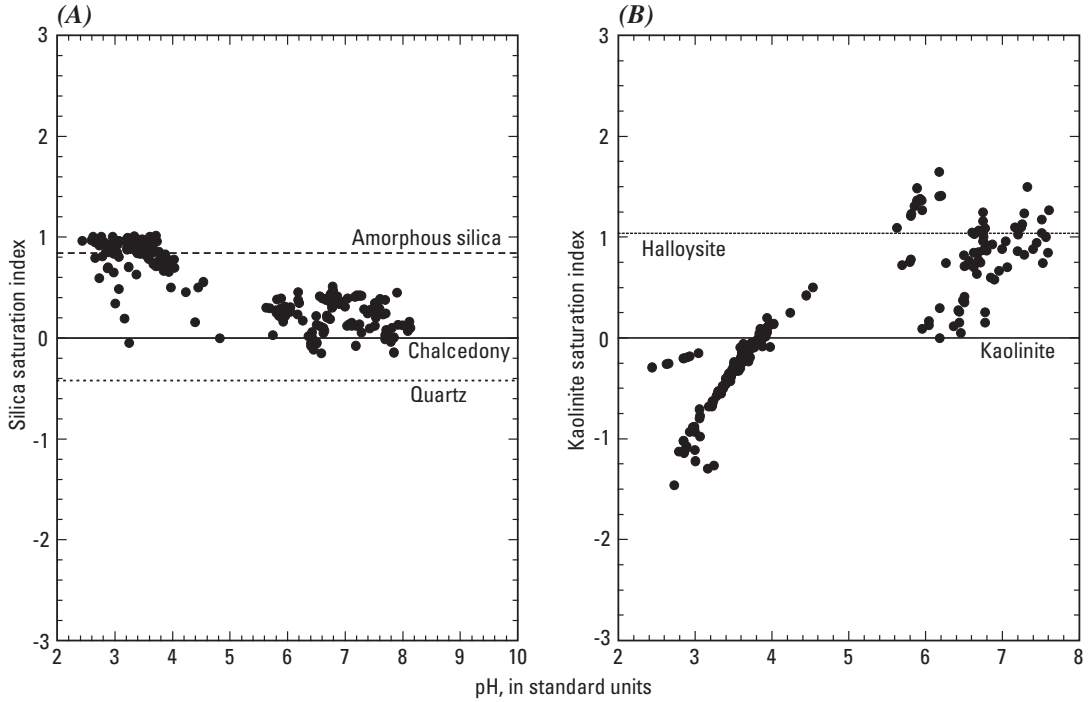

Figure 32. (A) Silica saturation index plotted against pH, and (B) kaolinite saturation index plotted against pH.

calcium is even more apparent in figure 33D, indicating that fluorite solubility equilibrium is a likely candidate for controlling the upper limit to fluoride concentrations in circumneutral pH ground waters.

Fluoride concentrations are plotted against calcium concentrations for all ground waters in figure 34A with two different symbols reflecting waters of low pH (<4.5) and high pH (>4.5). The trend of decreasing fluoride concentrations with increasing calcium concentrations is apparent for the higher pH ground waters and supports an upper fluoride concentration limit dictated by fluorite equilibrium mineral solubility. Saturation indices for fluorite plotted against pH in figure 34B confirm that fluorite solubility limits are reached at pH values of 6–7.5. A problematic trend in figure 34B is the degree of supersaturation up to nearly 1.5 orders of magnitude. Because dissolved aluminum is known to complex with large quantities of fluoride (Tagirov and others, 2002), fluorite saturation indices are plotted against aluminum in figure 34C. This plot clearly shows that high aluminum concentrations maintain strong undersaturation for fluorite solubility consistent with a high degree of complexing even though the concentrations of fluoride are more than 1 mg/L. Figure 34D details the low concentration range of aluminum from figure 34C and indicates that the samples that are supersaturated generally are those with low but detectable aluminum concentrations. There could be errors in the speciation calculations for this range of solute concentrations that would explain the supersaturation, or supersaturation could be real with precipitation inhibited by an unknown complex or other kinetic reasons.

Dissolved fluoride concentrations are plotted against dissolved aluminum concentrations in figure 35 with low pH samples shown in solid circles and high pH samples shown in open circles. This figure provides a further clue to the fluorite supersaturation effect because the high pH samples do not correlate with aluminum. Further, the highest fluoride concentrations at high pH are those that are supersaturated in figures 34C and 34D. This lack of correlation might have been considered as analytical errors, but that possibility is discounted because analyses were checked by two different methods, ion chromatography and ion-selective electrode potentiometry, passing rigorous laboratory quality control. Another possibility is that some unknown complexing, not accounted for in the speciation computations, is causing the supersaturation effect at high fluoride concentration. For the purposes of this study it is sufficient to note that fluorite saturation is reached and can limit fluoride concentrations in these waters.

Molling (1989) found that micas formed during the hydrothermal alteration of the volcanics were enriched in fluoride, up to 6 weight percent. This amount of rock fluoride could be comparable to or even greater than that contained in fluorite mineralization and could, therefore, be a source of fluoride to ground water during weathering. However, fluoride in the hydroxyl lattice site of phyllosilicates is released by high-pH water, not acid water; at low pH, fluoride tends to be adsorbed onto clay minerals (Harrington and others, 2003;

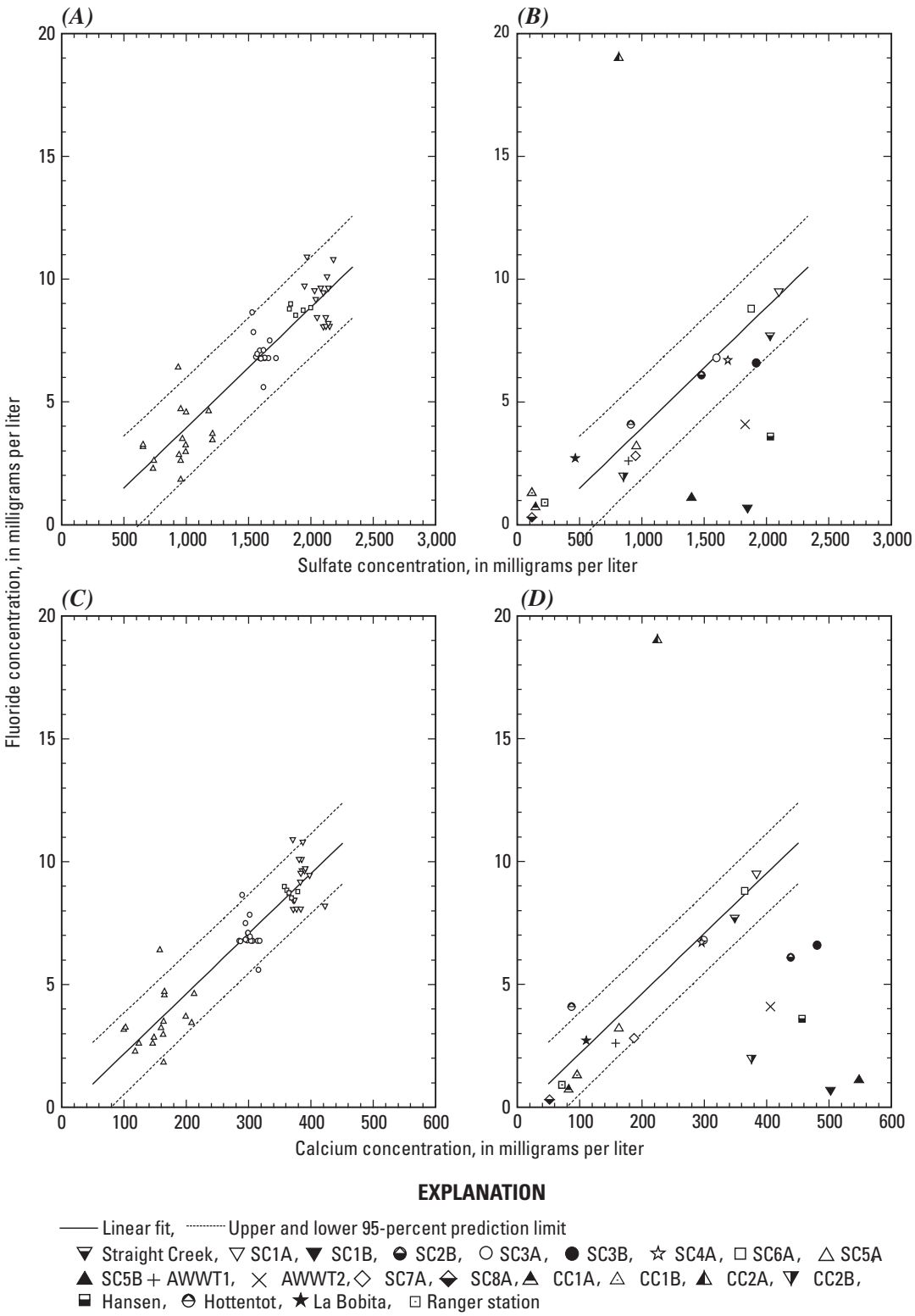

Figure 33. Fluoride concentrations plotted against sulfate concentrations for (A) Straight Creek alluvial ground waters and (B) median fluoride and sulfate concentrations for all ground waters and Straight Creek surface water. Fluoride concentrations plotted against calcium concentrations for (C) Straight Creek and alluvial ground water and (D) median concentrations for all ground waters and Straight Creek surface water. Linear fit and prediction limits at 95-percent probability for Straight Creek data only were used for all plots (from Naus and others, 2005; Nordstrom and others, 2005).

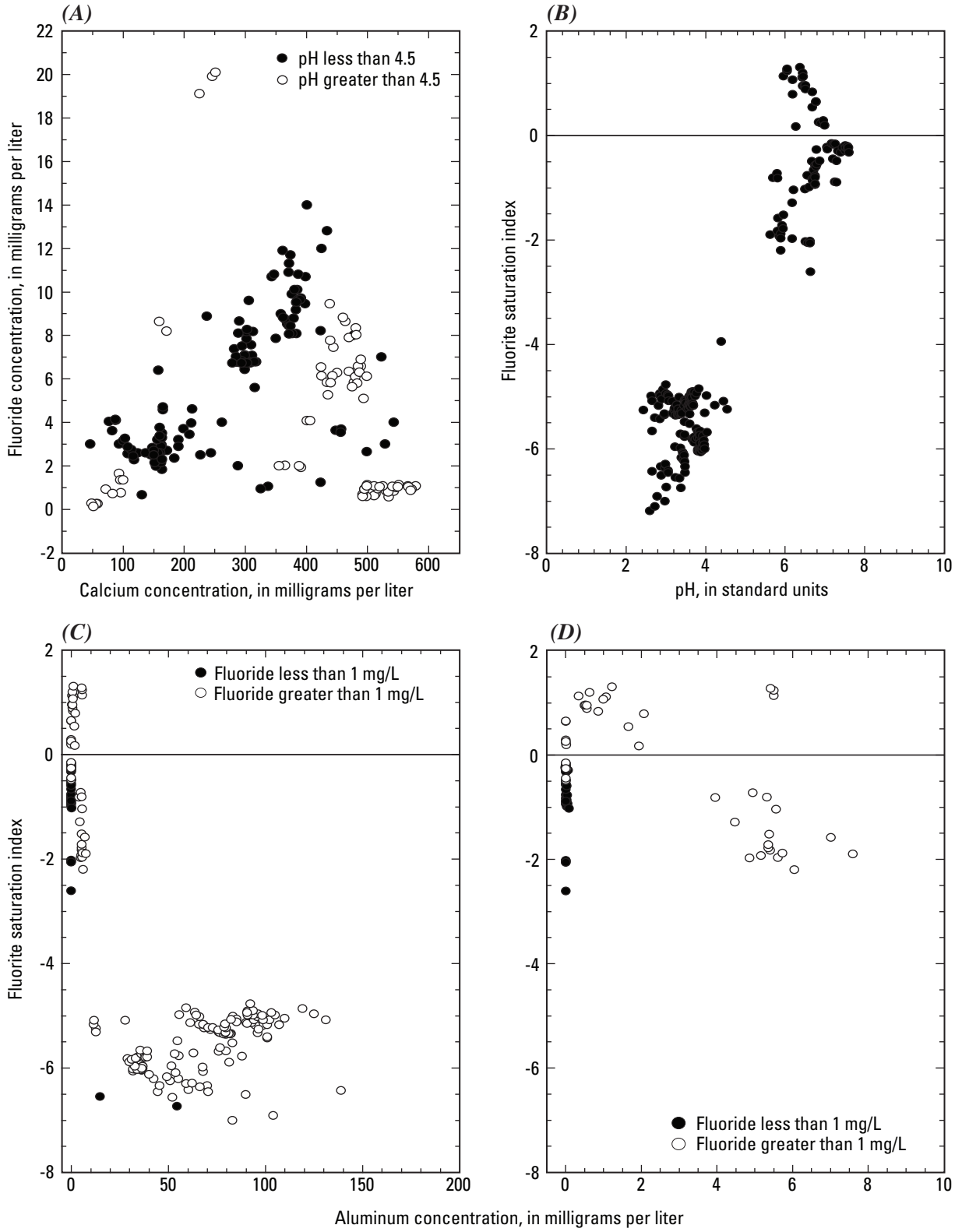

Figure 34. (A) Fluoride concentrations plotted against calcium concentrations. Fluorite saturation index plotted against (B) pH, (C) aluminum concentrations, and (D) aluminum concentrations less than 10 milligrams per liter for all ground waters and Straight Creek surface water.

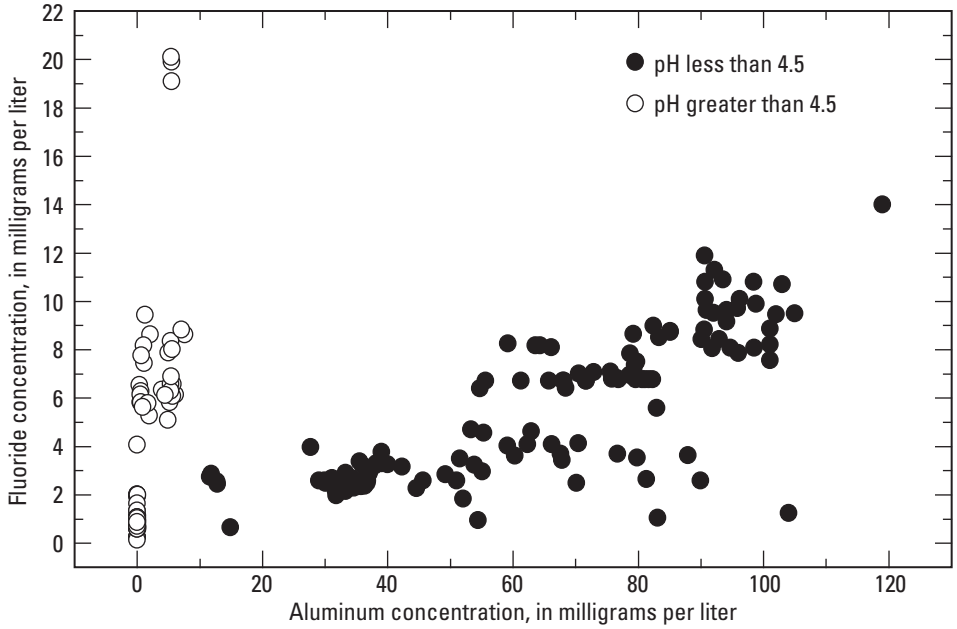

Figure 35. Fluoride concentrations plotted in relation to aluminum concentrations for all ground waters and Straight Creek surface water.

Zhu and others, 2006). Fluorite dissolves so readily in sulfuric acid solutions that it can be safely assumed to be the main source of dissolved fluoride. The reaction of sulfuric acid with fluorite to produce hydrofluoric acid has been known for a long time for etching glass; the reaction was discovered by Heinrick Schwanhard in 1670 (Emsley, 2001) and by Carl Wilhelm Scheele a few decades later (Ihde, 1984).

Geochemical Controls on Dissolved Calcium Concentrations

Dissolved calcium concentrations are derived primarily from gypsum dissolution and secondarily from calcite dissolution. These are the two most soluble calcium minerals in the Red River Valley, and they are abundantly and widely distributed (Ludington and others, 2005; Livo and Clark, 2002). The alluvial ground waters in the Straight Creek catchment show a dilution trend as seen in figure 36A. The best linear fit, with 95-percent confidence intervals from figure 36A, are plotted in figure 36B along with the median values for waters from all wells (table 5) and found to follow a similar trend except for bedrock Hansen and CC–2A. Straight Creek drainage waters also correlate well with the alluvial ground waters, indicating that the Straight Creek surface water can be the input for the alluvial water with no substantial additions nor depletions of calcium. Bedrock ground waters should have higher calcium:sulfate ratios because these waters have additional calcium from calcite (and possibly dolomite) dissolution that gives them circumneutral, carbonate-buffered pH values. A few wells even have water that has higher calcium:sulfate ratios than that from pure gypsum dissolution (figs. 36C and 36D) such as CC–1A, CC–1B, and CC–2B (fig. 33B). Figure 36D shows how the calcium:sulfate molar ratio varies with pH. At low pH values the ratio is low, indicating the preponderance of sulfate from pyrite oxidation. For ratios that approach 1 (indicative of stoichiometric gypsum dissolution), the pH must be about 6 or higher, and the highest ratios are only reached at pH values above 7. These trends all support the contentions described previously. In figure 36D the two lower horizontal dashed lines indicate the range found for water-chemistry dominance by gypsum dissolution based on isotopic compositions in the upper Animas River drainage basin (Nordstrom and others, in press). The trends seen for the Red River Valley data are consistent with those seen in the upper Animas River in that the marked shift to higher pH values occurs at a calcium:sulfate ratio of about 0.6. This range is where gypsum is more dominant as a source of sulfate over sulfate from pyrite oxidation and a more dominant source of calcium than that from calcite dissolution.

Gypsum is one of the most common minerals within mineralized areas of the study reach between the town of Red River and the USGS gaging station. Gypsum forms naturally through weathering from reaction between hydrothermal calcite and pyrite that commonly are present together in veins (Ludington and others, 2005). The widespread occurrence of gypsum in mineralized areas, scars, and debris fans combined with its relatively high solubility is reflected in the SI values for gypsum plotted in figures 37A, B, and C. In figure 37A the gypsum SI values are plotted relative to the calcium concentrations. The SI values are all close to saturation, and they progress continuously toward saturation with increasing calcium concentrations. Unlike calcite SI values that can be

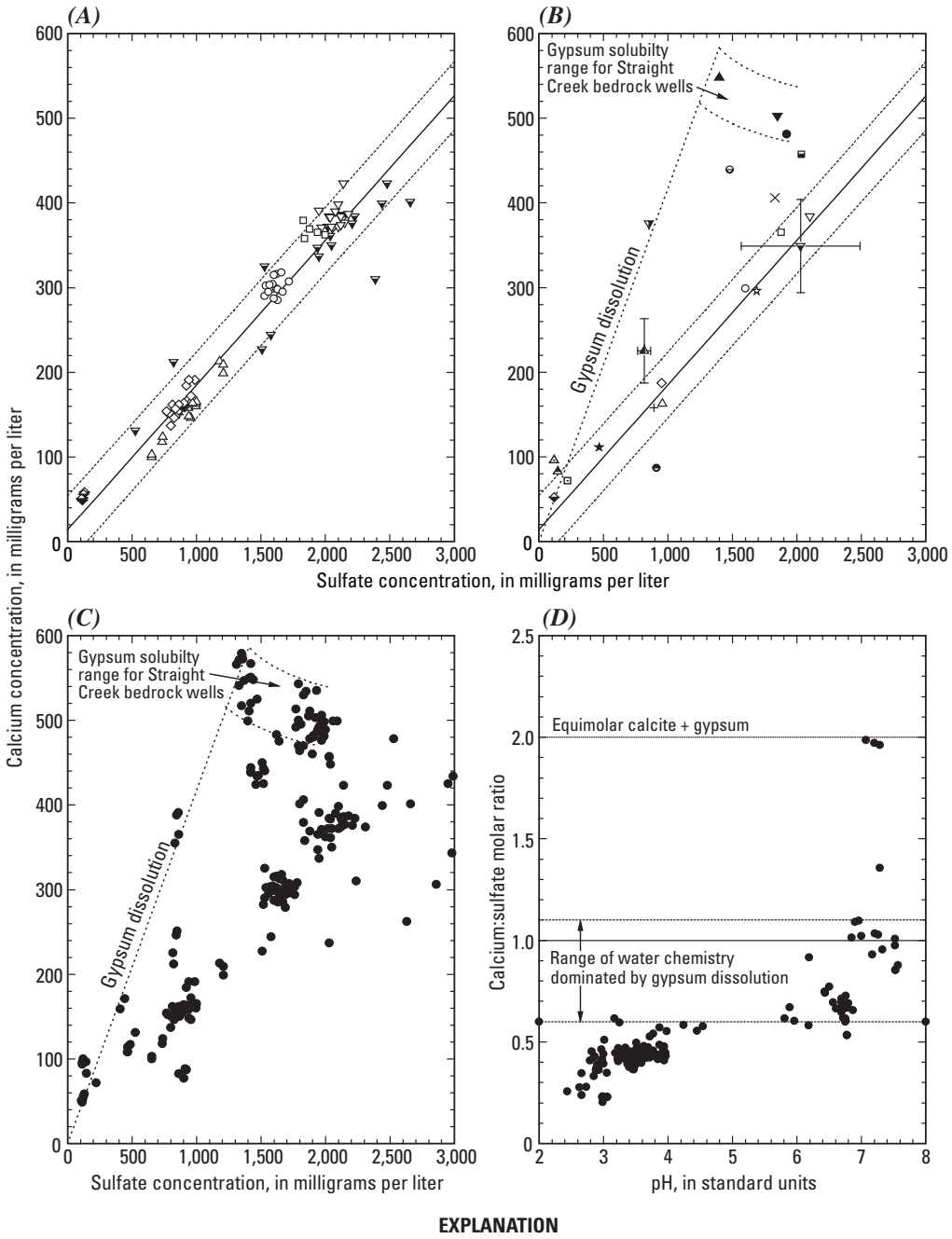

Figure 36. Calcium concentrations plotted against sulfate concentrations for (A) Straight Creek surface and alluvial ground waters and (B) for median ground-water concentrations and Straight Creek surface water. Linear fit and prediction limits at 95-percent probability for Straight Creek data only were used for both A and B (from Naus and others, 2005; Nordstrom and others, 2005). (C) Ground waters and Straight Creek surface water, all data. (D) Calcium:sulfate molar ratio plotted against pH for all ground waters and Straight Creek surface water. Dotted lines indicate the region of increasing dominance by gypsum dissolution (0.6 to 1.1 in calcium:sulfate molar ratio) and from calcium:sulfate molar ratio of 1.1 to 2 indicates increasing contribution of calcite dissolution to the calcium:sulfate ratio (based on Nordstrom and others, 2007).

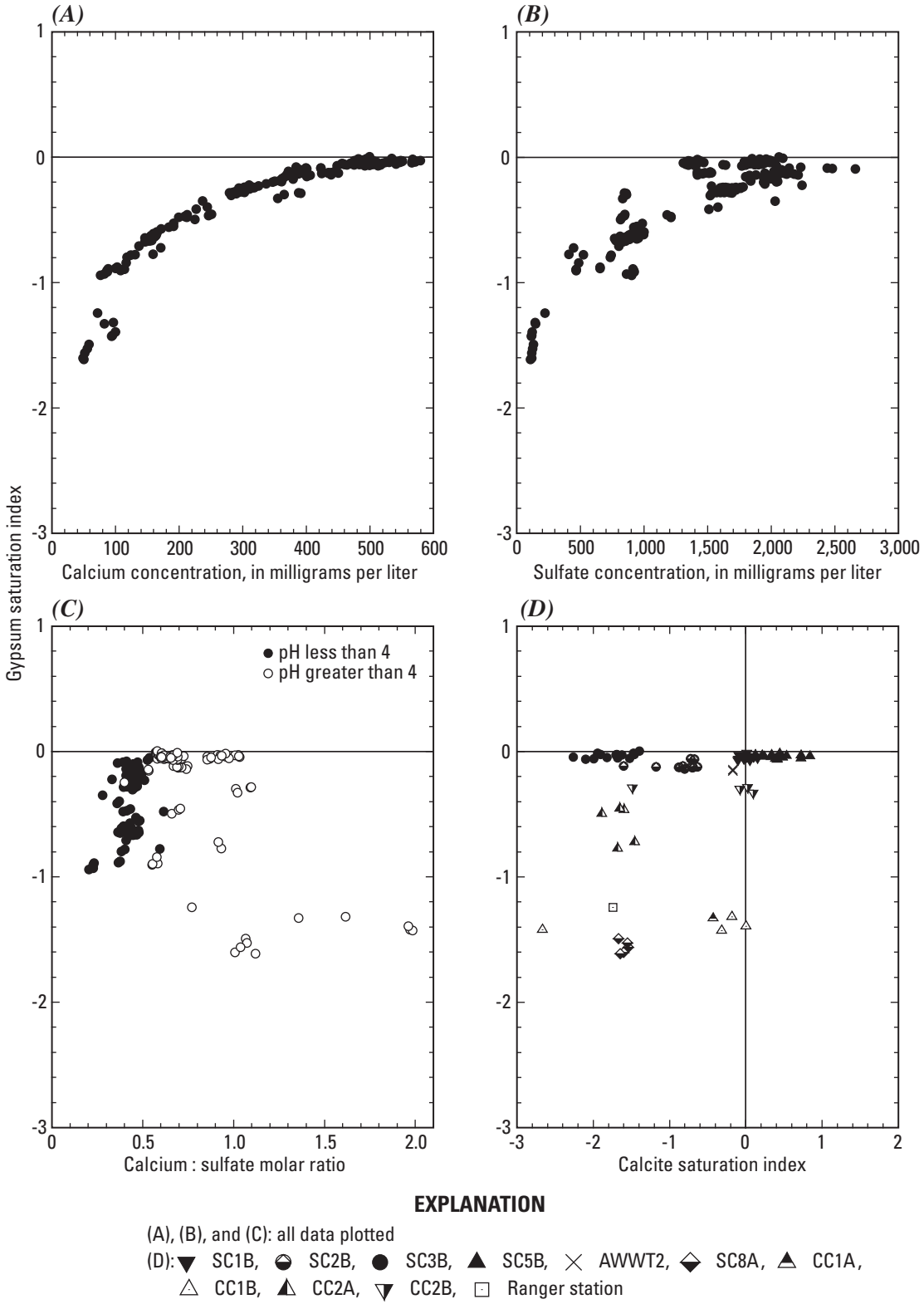

Figure 37. Gypsum saturation index plotted against (A) calcium concentrations, (B) sulfate concentrations, (C) the calcium:sulfate molar ratio for Straight Creek ground water and surface water. (D) Gypsum saturation index plotted against calcite saturation index.

supersaturated, gypsum SI values achieve equilibrium saturation and do not become supersaturated. The regular approach to gypsum saturation with increasing calcium concentration indicates the simple dependence on a single source for calcium, which is calcite. Whenever the calcium concentrations are at or in excess of 450 mg/L, the water can be expected to be at gypsum saturation. The gypsum SI values are plotted with respect to sulfate concentrations in figure 37B and do not show as regular a progression to saturation as when plotted against calcium concentrations. At sulfate concentrations greater than about 1,300 mg/L, gypsum saturation is reached, but not consistently for all waters.

In figure 37D, the SI values for gypsum and calcite are shown. Whereas gypsum provides a consistent solubility limit, calcite is supersaturated when gypsum is saturated but not when gypsum is undersaturated. The calcite supersaturation occurs for water high in magnesium and sulfate, both known to be inhibitors of calcite precipitation. Another possible reason for supersaturation is that the calcite in the Red River Valley is known to contain variably substituted magnesium, manganese, and iron. This solid substitution for calcium in calcite can also lead to apparent supersaturation when the saturation indices are computed with respect to pure calcite.

The SI values for calcite are plotted against pH in figure 38, showing that calcite saturation is reached only at pH values above 6.5, and supersaturation tends to occur at pH values above 7.2. Between the pH values of 6.5 and 7.2, calcite equilibrium solubility is maintained.

Geochemical Controls on Dissolved Magnesium Concentrations

Sources of dissolved magnesium in ground water include dolomite, magnesian calcite (and other magnesian carbonates), and chlorite. Carbonates are more soluble and weather more easily than silicates; hence, they are more likely the source of dissolved magnesium. Dissolution of chlorites cannot be discounted, however, because they are fine grained and abundant.

Concentrations of magnesium and sulfate correlate well for Straight Creek alluvial ground waters (fig. 39A), but notable deviations are observed when concentrations from ground waters in other catchments are compared to the same correlation (fig. 39B). Neither gain nor loss in magnesium is needed when comparing the Straight Creek drainage water with water from well SC–1A and the other Straight Creek alluvial ground waters. When magnesium concentrations are plotted against calcium concentrations for Straight Creek alluvial ground waters the correlation is obvious (fig. 39C) but not for all other well waters (fig. 39D). This variation in magnesium concentrations was seen in historical ground-water analyses (LoVetere and others, 2004) and seems to be related to sources and limitations on calcium and sulfate concentrations that do not apply to magnesium concentrations. Gypsum dissolves, which increases calcium and sulfate concentrations but does not affect magnesium concentrations for well waters SC–5B, CC–2A, and CC–2B. Gypsum equilibrium solubility limits calcium concentrations but not magnesium concentrations for

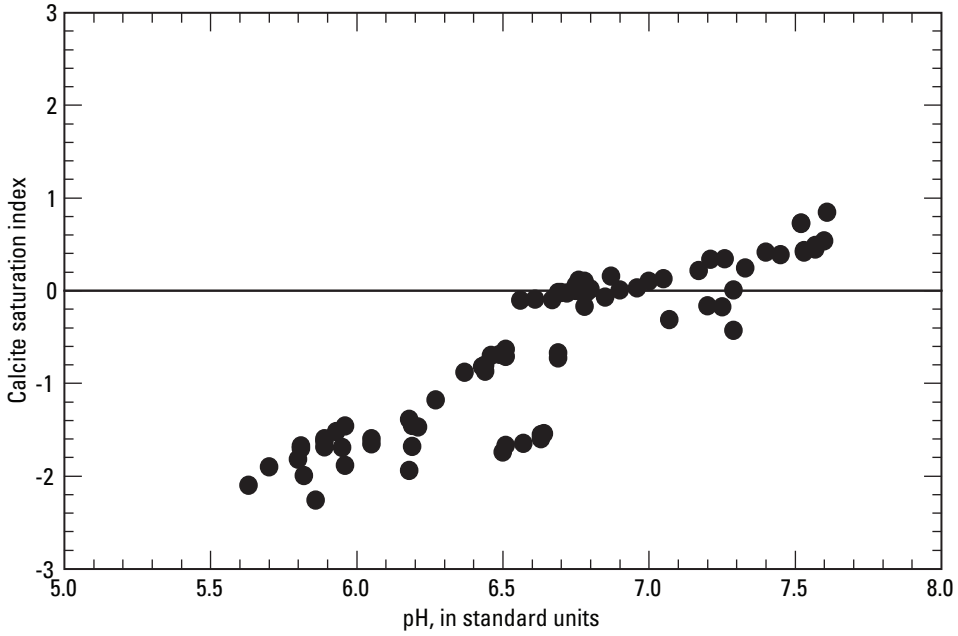

Figure 38. Calcite saturation index plotted against pH for all ground waters and Straight Creek surface water.

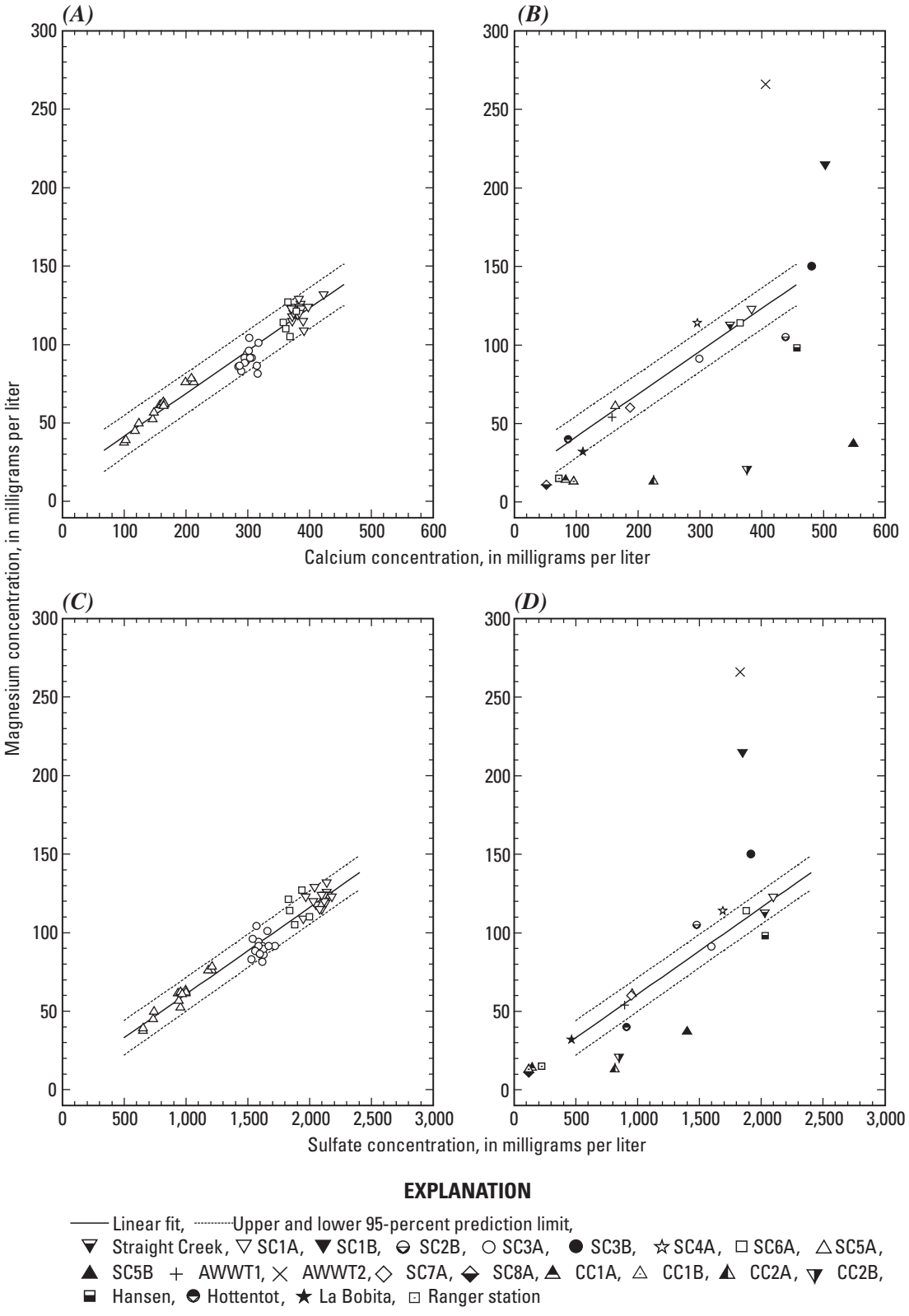

Figure 39. Magnesium concentrations plotted against calcium concentrations for (A) Straight Creek surface and alluvial ground waters and (B) median concentrations for all ground waters and Straight Creek surface water. Magnesium concentrations plotted against sulfate concentrations for (C) Straight Creek surface and alluvial ground waters and (D) all ground waters and Straight Creek surface water. Linear fit and prediction limits at 95-percent probability for Straight Creek data only were used for all plots (from Naus and others, 2005; Nordstrom and others, 2005).

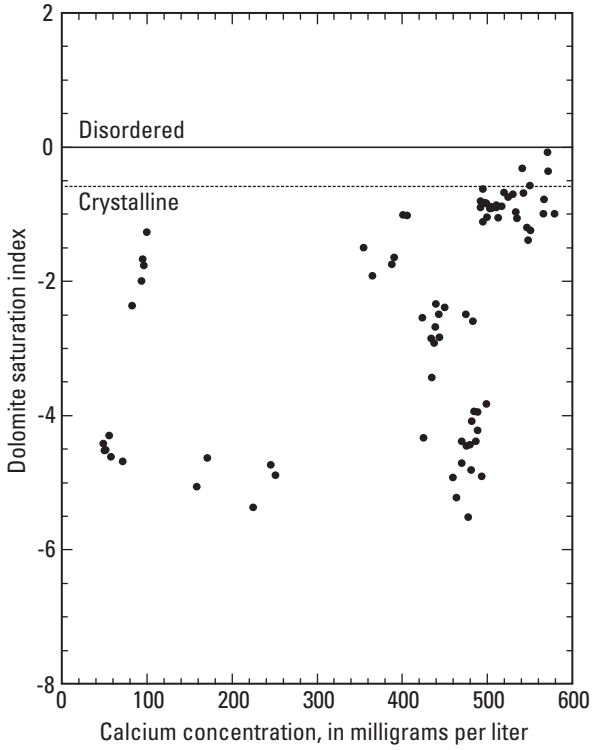

Figure 40. Dolomite saturation index plotted against calcium concentrations.

well waters AWWT2, SC–3B, and CC–1B. Dolomite has been found in hydrothermally altered areas (Ludington and others, 2005; Plumlee and others, 2005), and a plot of dolomite saturation indices as a function of calcium concentrations does show saturation achieved at the highest calcium concentrations (fig. 40).

Geochemical Controls on Dissolved Strontium Concentrations

Unlike most other elements, strontium does not correlate with sulfate concentrations (fig. 41A). Instead, strontium concentrations are low and constant until the highest concentrations of calcium are reached (fig. 41). As shown in figure 36D, the highest Ca:SO_4 molar ratios are indicative of increasing contribution of calcite dissolution relative to gypsum dissolution as a source for dissolved calcium. These results show that the main source of strontium is from the dissolution (or recrystallization) of calcite. Chemical analyses of carbonate minerals from the Red River Valley show that detectable strontium concentrations can range from 0.04 weight percent to as high as 0.6 weight percent (as SrO; Plumlee and others, 2005). These concentrations would correspond to Sr:Ca molar ratios of 0.0005 to 0.006. Molar ratios for Sr:Ca in ground water in the study area range from 0.00003 to 0.010. The highest Sr:Ca molar ratios are similar for carbonate minerals obtained from drill cuttings and for ground water. Indeed, the highest Sr:Ca molar ratios in ground water are found in Straight Creek wells SC–1B and SC–5B, and the highest Sr:Ca molar ratios in carbonate minerals are found in well cuttings from these same wells (Plumlee and others, 2005). These well waters also have reached saturation with respect to both gypsum and calcite. It would appear that high-Sr calcites are dissolving upgradient from SC–1B in the bedrock under anoxic conditions and that they have largely weathered out of the exposed bedrock and colluvial material that contribute solutes to the Straight Creek alluvial ground waters. Furthermore, gypsum is produced from the reaction of calcite with pyrite in the oxidizing part of the weathering zone, and it seems reasonable to assume that the gypsum will not incorporate as much strontium at low temperature as the original hydrothermal calcite (Glynn, 1991). Release of trace elements during recrystallization is a process used in chemical engineering to purify soluble materials. For example, ground waters from well SC–1B have neutral pH values, are at saturation with respect to gypsum and calcite, and have the highest Sr:Ca ratios. However, ground waters from SC–1A have only 20 percent less calcium but 92 percent less strontium. The chemistry indicates that most of the calcium in SC–1A comes from gypsum dissolution whereas calcium in SC–1B must come from both calcite and gypsum dissolution under anoxic conditions (no pyrite oxidation). Hence, strontium can be an indicator of calcite dissolution. But this hypothesis creates a dilemma. If the high sulfate concentration in SC–1B waters is derived solely from gypsum dissolution then there is insufficient calcium to balance sulfate, which is in excess of calcium by more than 13 meq/L. This excess indicates the bedrock ground waters originated with chemistry similar to Straight Creek surface water with acid pH values that infiltrated bedrock, became anoxic, and was neutralized by strontium-rich calcite. If the median sulfate concentration for Straight Creek is decreased to the median sulfate concentration for SC–1B (see table 5) and the calcium concentration for Straight Creek is decreased proportionally by the same amount, and that amount of calcium is assumed to result from gypsum dissolution, then 8 mmol/L of calcium out of 12.6 mmol/L for SC–1B must come from gypsum dissolution and the other 4.6 mmol/L must come from calcite dissolution. In this case, the Sr:Ca molar ratio for that calcite would have to be 0.027, or about 4.5 times the highest molar ratio found in any carbonate mineral. This result would indicate that either calcites with higher Sr:Ca molar ratios are present than have been analyzed, that some strontianite occurs in the carbonate minerals, or that there is another source of strontium.

Strontianite $SrCO_3$ and celestine $SrSO_4$ saturation indices are plotted against calcium concentrations in figures 41C and D, respectively. Strontium concentrations reach celestine saturation as a solubility limit whereas strontianite SI values appear to reach a limit at about 1 order of magnitude undersaturated. This limit was shown by Plummer and others (1990) to be a result of the phase rule and the fact that calcite, gypsum, and celestine all reach saturation (see Naus and others, 2005). Celestine, therefore, could be another source of strontium in the study area, but none has been identified in the mineralogical study (Plumlee and others, 2005).

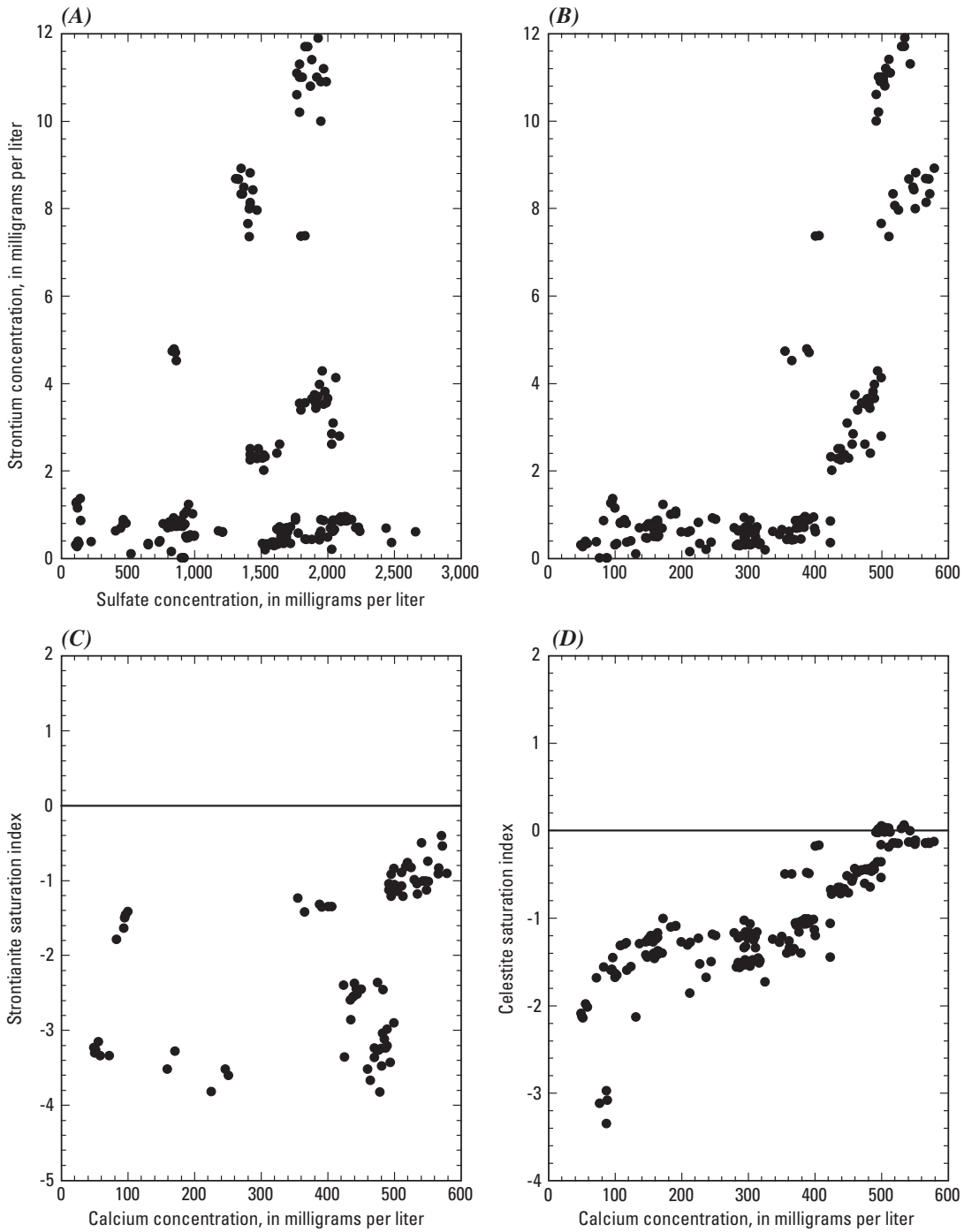

Figure 41. (A) Plot of strontium concentrations against sulfate concentrations for all ground waters and Straight Creek surface water. (B) Plot of strontium concentrations against calcium concentrations for all ground waters and Straight Creek surface water. (C) Strontianite saturation index relative to calcium concentrations for ground water and Straight Creek surface water. (D) Celestine saturation index relative to calcium concentrations for all ground waters and Straight Creek surface water.

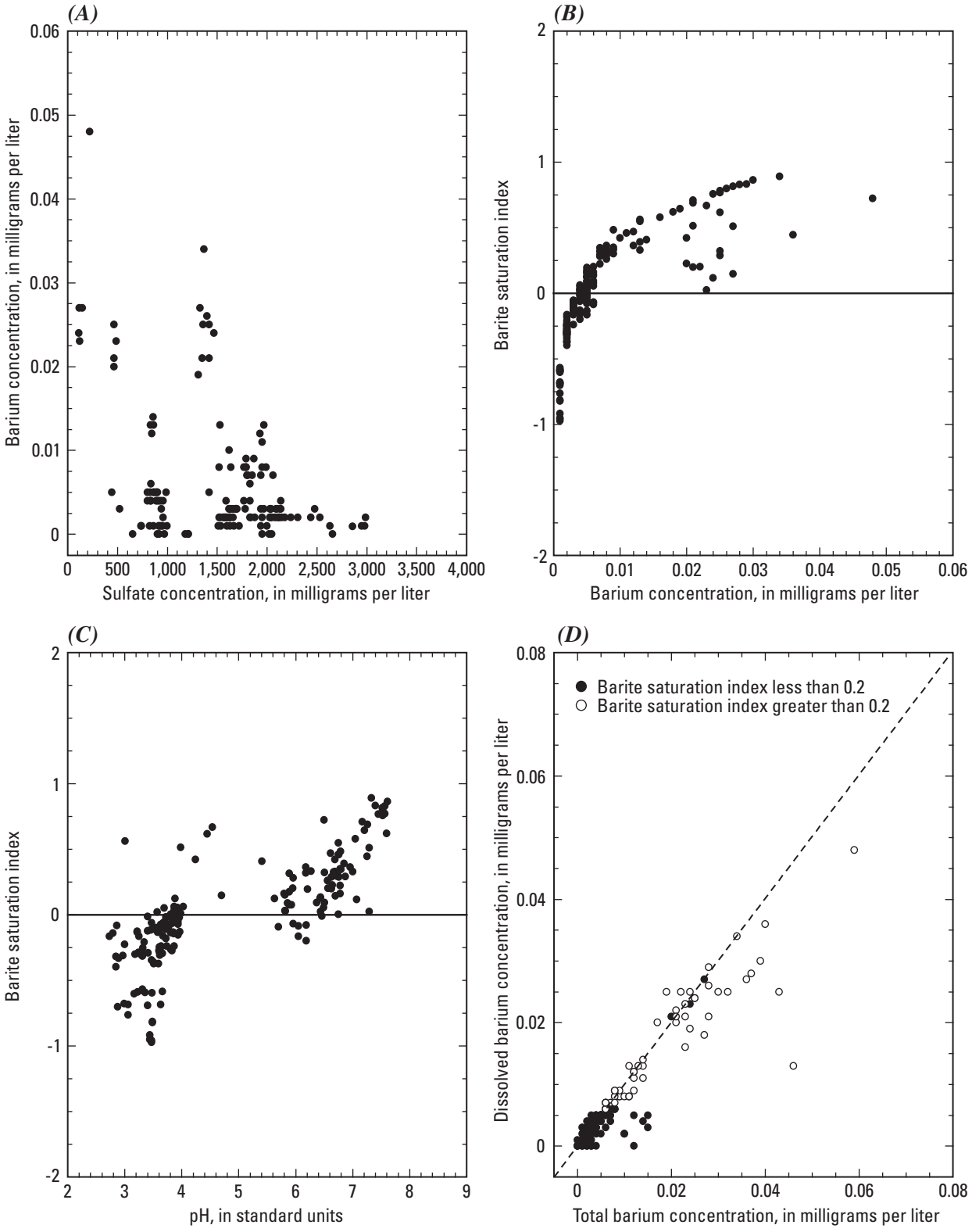

Figure 42. (A) Barium concentrations plotted against sulfate concentrations for all ground waters and Straight Creek surface water. Barite saturation index plotted against (B) barium concentration and (C) pH for all ground waters and Straight Creek surface water. (D) Dissolved (0.45-micrometer filtration) barium concentrations plotted against total recoverable barium concentrations for all ground waters and Straight Creek surface water; those data with SI for barite greater than +0.2 are shown with open circles, all others with filled circles.

Geochemical Controls on Dissolved Barium Concentrations

The most common source of barium in mineralized areas is barite, $BaSO_4$, because it commonly occurs as a gangue mineral. A gangue mineral is an accessory mineral that formed with the mineral deposit but does not have any economic value.

Barium concentrations in acid-sulfate water are often near detection limits because barite reaches solubility equilibrium, and the common-ion effect from sulfate, along with the low solubility of barite, minimizes barium concentrations. Solubility limits readily explain the lack of correlation in figure 42A in which barium concentrations are plotted with respect to sulfate concentrations. The only apparent trend is the tendency for barium concentrations to decrease at the higher sulfate concentrations, consistent with the common-ion effect for solubility control. In figure 42B the SI values for barite are plotted as a function of barium concentrations. Although the SI values level out to a plateau that would indicate a solubility limit, the values also are supersaturated by up to an order of magnitude. There are at least four possible reasons for this supersaturation. Freshly precipitated barite can be so fine grained that there is a grain-size, or surface-area, effect on the equilibrium solubility (Balarew, 1925; Hina and Nancollas, 2000). A related possibility is that colloidal particles of barite are not adequately filtered during field filtration. A third possibility is that the precipitating barite has a variable composition caused by solid substitution (for example, Felmy and others, 1993). A further, and less likely, possibility is that insufficient barium complexing is included in the speciation computations. Other research indicates that colloidal barite that can occasionally pass through filter membranes is the main cause (H.E. Taylor and D.K. Nordstrom, U.S. Geological Survey, oral commun., 2004).

When barite SI values are plotted relative to pH, as shown in figure 42C, no pH limitation is apparent. Barite provides a solubility limit to barium concentrations for a wide range of pH values, although most of the supersaturated values occur in the pH range 5.5–8.

In figure 42D, dissolved barium concentrations are plotted relative to total recoverable barium concentrations with open circles designating those samples that are supersaturated with respect to barite (SI values greater than +0.2). Nearly all the supersaturated values are those with the highest barium concentrations, and many of these have total recoverable barium concentrations greater than dissolved barium concentrations. This trend lends support to the possibility that fine-grained or colloidal barite particles are a cause for apparent supersaturation, but the other possibilities cannot be discounted at this time.

Geochemical Controls on Dissolved Zinc Concentrations

The most abundant and most easily weathered mineral that provides a source of zinc to ground water is the mineral sphalerite, ZnS.

For the Straight Creek alluvial ground waters, zinc concentrations correlate well with sulfate concentrations (fig. 43A), and there is little difference between Straight Creek drainage-water composition and alluvial ground-water composition. Upon comparing the Straight Creek alluvial ground-water zinc concentrations with those of other ground waters in figure 43B, no enriched anomalies are observed, but several examples of depletions in zinc are noteworthy. The wells depleted in zinc relative to sulfate for the Straight Creek alluvial ground waters are those of neutral pH and one acidic ground water, Hansen (probably less sphalerite mineralization because it is more distal from the hydrothermal source). There is no identifiable mineral solubility equilibrium that has been reached for zinc, although the possibility of a mineral solubility limitation such as hydrozincite $[Zn_5(CO_3)_2(OH)_6]$ or hemimorphite $[Zn_4Si_2O_7(OH)_2 \cdot H_2O]$, both of which would be stable under neutral to high pH, cannot be excluded. Empirically, zinc concentrations do not appear to exceed 2 mg/L for ground water of circumneutral pH.

Another element distinctive of mineralized areas is manganese, and zinc and manganese are both soluble enough to be found in ground water and surface water. Figure 43C shows a plot of zinc relative to manganese for the Straight Creek surface and alluvial ground waters. The correlation is the strongest of all elements ($R^2 = 0.99$) with little difference between the concentrations for Straight Creek surface water and those for ground water in well SC–1A. Other ground waters have similar zinc and manganese concentrations (fig. 43D) except for waters from wells SC–2B, SC–3B, and CC–2A.

Geochemical Controls on Dissolved Cadmium Concentrations

Cadmium concentrations also correlate well for the Straight Creek alluvial ground waters with little difference between Straight Creek surface water and water from well SC–1A (fig. 44A). The comparison for other ground waters is substantially similar to that for zinc and sulfate concentrations with depleted cadmium concentrations in circumneutral pH ground waters (fig. 44B). This similarity would be expected because the source of cadmium is sphalerite (Plumlee and others, 2005). The Zn:Cd weight ratios in sphalerite are often in the range of 50–200 (Fleischer, 1955). The ratios of Zn:Cd can vary with alteration zone, probably reflecting changing conditions with distance from the hydrothermal source, competition from other trace elements, and possibly differences in source abundance. Crystallochemical considerations such as ionic radius and bonding coordination also affect the amount of substitution.

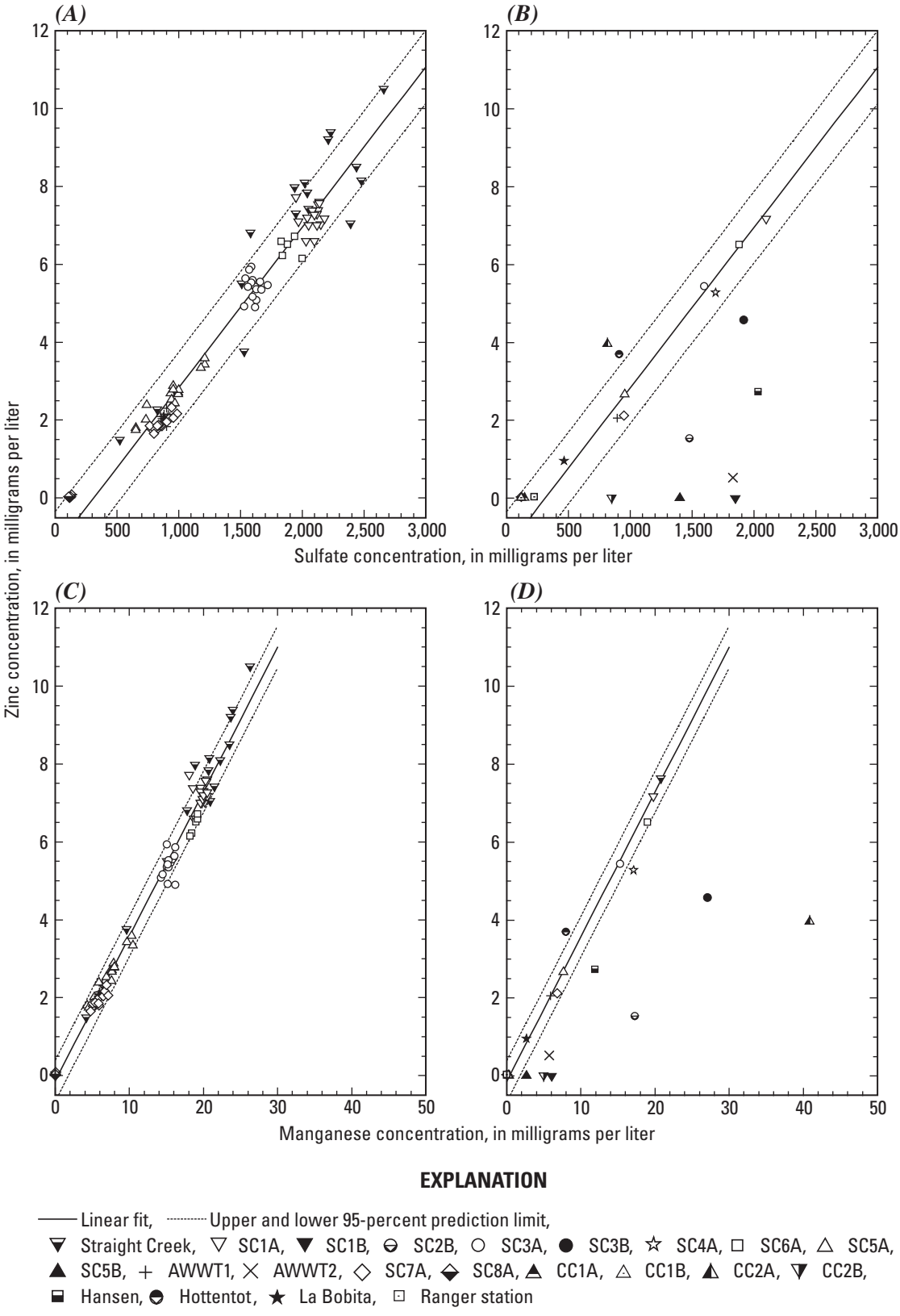

Figure 43. Zinc concentrations plotted against sulfate concentrations for (A) Straight Creek surface and alluvial ground waters and (B) median values for all ground and surface waters. Zinc concentrations plotted against manganese concentrations for (C) Straight Creek surface and alluvial ground waters and (D) median values for all ground and surface waters.

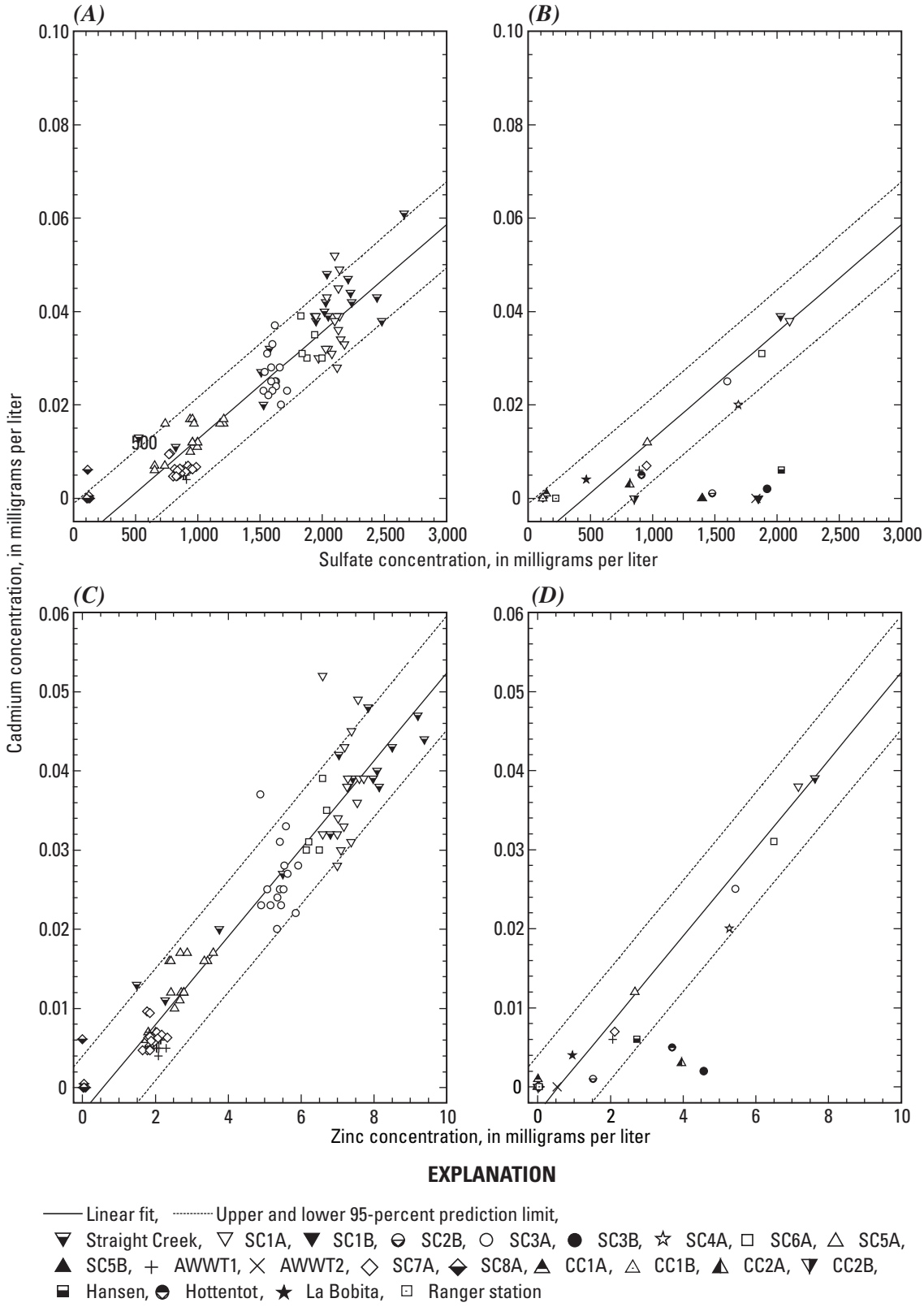

Figure 44. Cadmium concentrations plotted against sulfate concentrations for (A) Straight Creek surface and alluvial ground waters and (B) all ground and surface waters. Cadmium concentrations plotted against zinc concentrations for (C) Straight Creek surface and alluvial ground waters and (D) all ground waters and Straight Creek surface water.

Two samples of sphalerite from Molycorp's open pit, which were analyzed for cadmium, gave Zn:Cd weight ratios of 130 and 170, whereas three sphalerites from Straight Creek basin gave ratios of 54, 60, and 62 (Plumlee and others, 2005). The cadmium is much more enriched in Straight Creek sphalerites than in the open-pit sphalerites; however, the limited sampling makes it difficult to reach definitive conclusions.

From figure 44C the Zn:Cd weight ratio for the Straight Creek acidic, alluvial ground waters is about 180. This ratio also applies to other ground waters as shown in figure 44D except for waters from wells SC–3B, CC–2A, and Hottentot. Waters from CC–2A and Hottentot are slightly enriched in zinc relative to sulfate compared to the Straight Creek trend (fig. 44B) and depleted in cadmium relative to sulfate compared to the Straight Creek trend, suggesting cadmium-depleted sphalerites occur in these areas.

For cadmium, there are no substantial enrichments compared to the Straight Creek linear best-fit trend, only a few depletions. Consequently, the Straight Creek trend provides an upper limit to cadmium concentrations relative to sulfate and zinc concentrations.

Geochemical Controls on Dissolved Copper Concentrations

The primary natural source of copper in the Red River Valley is the mineral chalcopyrite, $CuFeS_2$ (Plumlee and others, 2005). There are minor to trace amounts of other copper sulfide minerals combined with tin, bismuth, and tellurium, but these cannot contribute much copper to the overall mass balance and transport of copper.

Although copper concentrations do follow a general dilution trend for the Straight Creek alluvial ground waters (fig. 45A), there is a poor correlation for other ground waters and a large decrease in copper concentration in going from the median Straight Creek copper concentration to the median copper concentration in water from well SC–1A (fig. 45B). This large decrease is caused by reduction processes. All of the dissolved iron in Straight Creek is in the ferric iron or oxidized form, but on entering the debris fan (well SC–1A) the dissolved iron is reduced to the ferrous iron form (fig. 23B). The same driving force for reduction would affect the redox state of the dissolved copper. This rapid reduction would precipitate copper out as cuprite (Cu_2O) or elemental copper, or by replacement in sulfide minerals in the debris fan, such as the replacement of sphalerite by covellite (CuS) and pyrite by chalcocite (Cu_2S) in a process known as supergene enrichment (Garrels and Christ, 1965; Krauskopf and Bird, 1995). For circumneutral-pH ground water, both strong adsorption and supergene enrichment would lower low copper concentrations in ground water such as shown in figures 45B and 45D. The strong tendency for copper sorption at moderately acidic pH values (4.5–6) is well established (for example, Krauskopf, 1956; Pickering, 1979; Dzomback and Morel, 1990).

An interesting observation can be made regarding the copper concentration data from well SC–6A. In the five water samples collected, the copper concentrations varied from 0.77 mg/L (the first sample taken) to 0.37 mg/L (the last sample taken). This concentration range is the largest for any well water for which the sulfate concentration is virtually constant. An examination of the data reveals that the iron redox species also vary widely with the copper concentrations. The highest copper concentration corresponds to the highest concentration (3.88 mg/L) of ferric iron and the largest percentage of ferric iron in the total dissolved iron (88 percent), indicating a strongly oxidized water, whereas the lowest copper concentration corresponds to the highest ferrous iron concentration (12 mg/L or 80 percent of the total), indicating a strongly reduced water. This trend of varying copper concentration according to the changing redox conditions over time within the same well water also supports the importance of redox in controlling copper concentrations.

Copper, like cadmium, tends to correlate well with zinc for the acidic ground waters of the Straight Creek alluvial aquifer (fig. 45C) and poorly for all ground waters (fig. 45D). The copper is higher in the Straight Creek alluvial ground waters than in any of the other ground waters, and this fact raises the question of whether Straight Creek as an analog site does not bias the conclusions for pre-mining copper concentrations in the direction of values that are too high. Information available at this time is insufficient to reach such a conclusion. Chalcopyrite is too ubiquitous in QSP alteration to observe any spatial differences in chalcopyrite mineralization (Plumlee and others, 2005). Hence, the upper limits to copper concentrations (relative to sulfate) are taken as those defined by the Straight Creek trend.

Geochemical Controls on Dissolved Nickel and Cobalt Concentrations

The source for nickel and cobalt in the Red River Valley is primarily pyrite (Plumlee and others, 2005). When a single mineral is the only substantive source of two or more constituents and those constituents dissolve congruently and are not affected by precipitation or sorption processes, then they should be highly correlated in the water chemistry. Furthermore, nickel and cobalt have one and only one stable oxidation state in natural waters, as divalent cations. The trivalent oxidation state of cobalt is not stable in aqueous solution, and it oxidizes water to form oxygen (Maki and Tanaka, 1985).

Nickel concentrations, for the Straight Creek alluvial ground waters, correlate strongly with sulfate concentrations (fig. 46A), and the Straight Creek median concentration is nearly identical to the median concentration for water from well SC–1A (fig. 46B). The other ground waters are represented in figure 46B, which continues to show a strong correlation, but only for acidic ground waters. Ground water of circumneutral pH is depleted in nickel. A similar correlation can be found for cobalt; but instead of displaying an almost

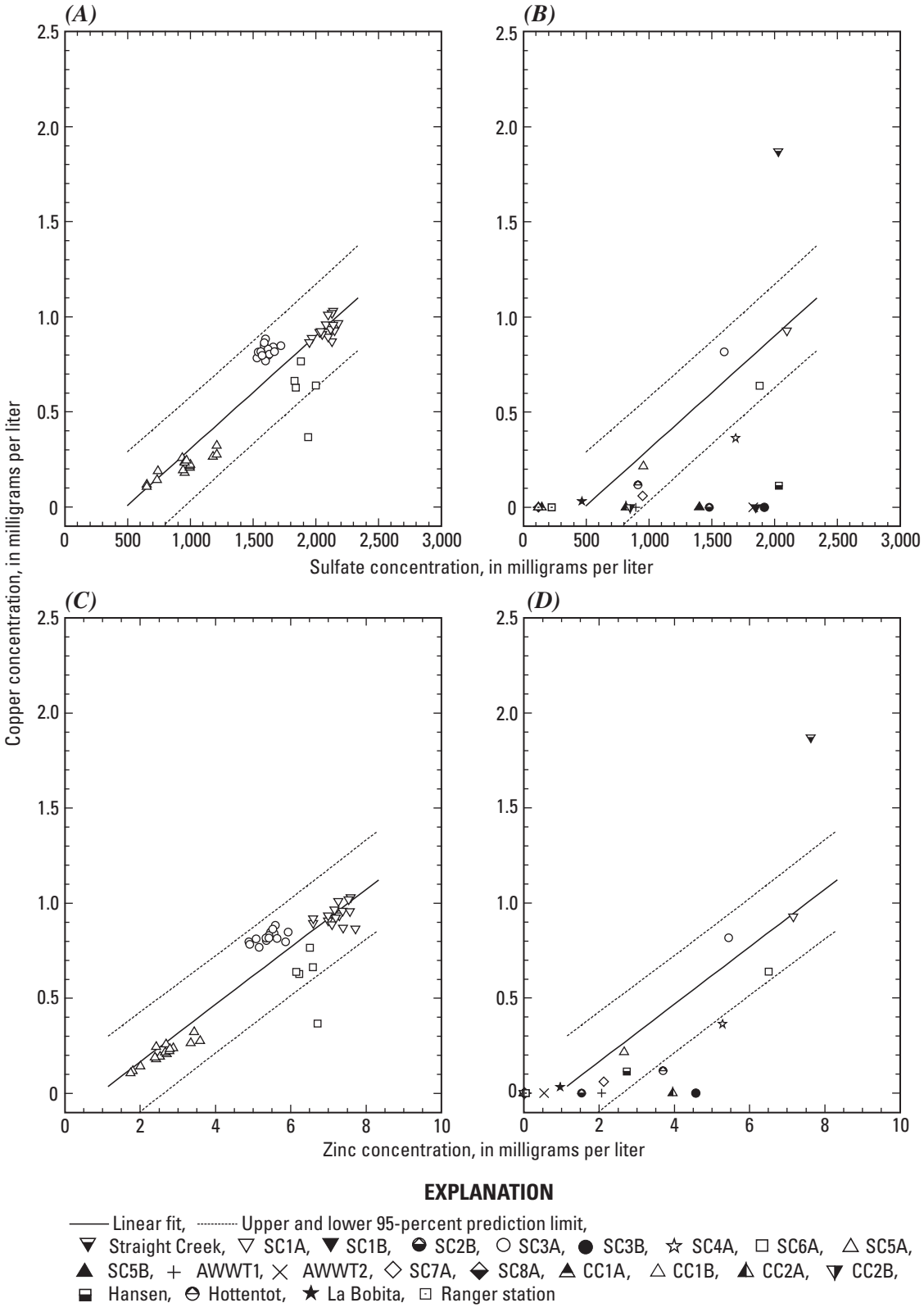

Figure 45. Copper concentrations plotted against sulfate concentrations for (A) Straight Creek surface and alluvial ground waters and (B) all ground and surface waters. Copper concentrations plotted against zinc concentrations for (C) Straight Creek surface and alluvial ground waters and (D) all ground waters and Straight Creek surface water.

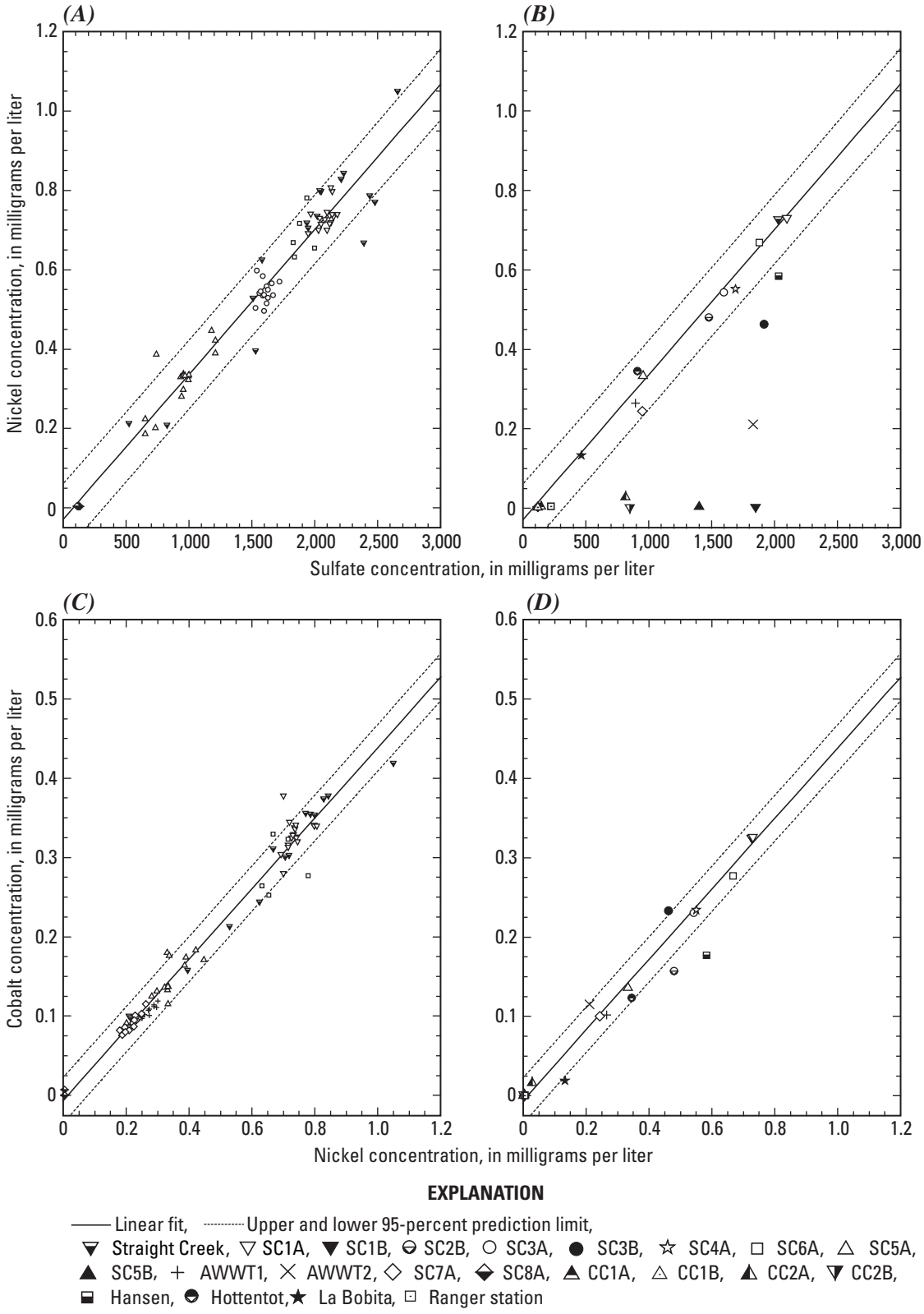

Figure 46. Nickel concentrations plotted against sulfate concentrations for (A) Straight Creek surface and alluvial ground waters and (B) all ground and surface waters. Cobalt concentrations plotted against nickel concentrations for (C) Straight Creek surface and alluvial ground waters and (D) all ground waters and Straight Creek surface water.

identical correlation, the correlation between cobalt and nickel is shown in figure 46C for Straight Creek surface and ground waters, and the median values for all ground waters are shown in figure 46D. These plots portray the strongest correlation ($R^2 = 0.98$) found for any two constituents except for the correlation for zinc and manganese.

For pyrite samples collected on the mine site, highly variable concentrations of cobalt were found, up to 0.58 weight percent, but nickel concentrations were mostly below detection (Plumlee and others, 2005). Pyrite samples from the Straight Creek catchment, however, averaged about 0.1 weight percent each in both cobalt and nickel. If the nickel and the cobalt in Straight Creek pyrite dissolved congruently and there were no attenuation processes downgradient in acid waters, the Co:Ni weight ratios in the water should be close to unity for the Straight Creek alluvial ground waters. Although the concentrations of these two elements are in the same range, the cobalt concentrations are typically about one-half of those for nickel (the slope of the linear fit is 0.44). Attenuation processes in these acid waters are unlikely for these elements. Hence, there are two possibilities for the lack of better agreement between the element ratios in the mineral and in the surface and ground waters. The first possibility is that limited sampling and analysis for trace elements in pyrite do not provide enough data to delineate the full range and meaningful average value. The other possibility could be that there is another source for nickel that could increase nickel concentrations over those for cobalt. Trace-element determinations for andesite collected in the Straight Creek catchment do indicate that nickel concentrations are higher than cobalt concentrations by a factor of 2 to 3. Whether this increased ratio is caused by pyrite or some other mineral is unknown. Nevertheless, the agreement between the Co:Ni ratios in pyrite and in the acidic ground water indicates, as hypothesized, that pyrite oxidation is the primary source of cobalt and nickel in ground water. Further, because most bedrock ground waters are anoxic and cannot oxidize pyrite, cobalt and nickel concentrations would have to be much lower than concentrations in acid ground waters.

Geochemical Controls on Dissolved Chromium Concentrations

Chromium originally resided in mafic minerals of the unaltered andesite that might include spinels, olivines, pyroxenes, biotites, and amphiboles. Hydrothermal alteration converted these minerals to chlorite, illite, and epidote. The chromium should mostly reside in the chlorite, probably substituting for trivalent iron and aluminum. Analyses of chlorites tend to support this hypothesis (Plumlee and others, 2005) with chromium concentrations in the range of 0.002 to 0.008 weight percent. In chlorites found in ultramafic rocks, chromium concentrations can average 0.3 weight percent (Oze and others, 2004). Consequently, dissolved chromium in ground water might be an indicator of chlorite dissolution. The three elements, chromium, cobalt, and nickel, also are commonly found together and in increasing concentration as rock types change in composition from andesitic to ultramafic. In natural waters, dissolved chromium can exist in two possible oxidation states—the reduced trivalent cation (Cr^{3+}) and the oxidized hexavalent anion (CrO_4^{2-}). Trivalent chromium is much less soluble than hexavalent chromium because of the low solubility of chromium (III) hydroxide. Water containing oxidized iron, such as Straight Creek surface drainage, would contain hexavalent chromium, and water containing reduced iron, such as the alluvial and bedrock ground waters in Straight Creek, would contain trivalent chromium.

Although chromium concentrations in the Straight Creek alluvial ground waters correlate with sulfate concentrations (fig. 47A), there is a decrease in chromium concentrations in ground water between Straight Creek drainage water to ground water from well SC–1A (fig. 47B). This decrease in concentration would be consistent with the change from oxidizing conditions to reducing conditions that are reflected in the Fe (II/III) ratio and in the decrease in copper concentrations. Further decreases in concentration would be expected for bedrock ground waters of circumneutral pH because of a longer residence time under anoxic conditions. This concept is corroborated by figure 47B in which the well waters with the lowest concentrations are in bedrock. The only enriched chromium anomaly is found in water from well AWWT1, the wastewater-treatment plant observation well. This concentration is so anomalous that it is highly likely to be from contamination from the use of chrome-plated parts or stainless steel from the well construction that would slowly dissolve in an acidic water. Hence, the upper limit of chromium concentrations relative to sulfate in acidic ground waters can be defined by the Straight Creek trend. Substantially lower concentrations are expected for anoxic ground water, especially if they are circumneutral in pH.

The correlation between chromium and nickel for the Straight Creek acid alluvial ground waters is shown in figure 47C with a correlation coefficient of 0.76. The same correlation accounts for other ground waters (fig. 47D) and supports the contention that chromium, nickel, and cobalt are strongly associated, even in altered rock

Geochemical Controls on Dissolved Lithium, Sodium, and Potassium Concentrations

Lithium is present in rocks and alteration minerals of the Red River Valley at higher concentrations than normally found in the same rocks lacking mineral deposits and hydrothermal alteration. It, along with beryllium, is one of the signature elements for molybdenum deposits. The minerals source for lithium is more dispersed than most other elements, and it is present in higher concentrations in some illites (sericite) than most other silicate phases that have been analyzed (Plumlee and others, 2005).

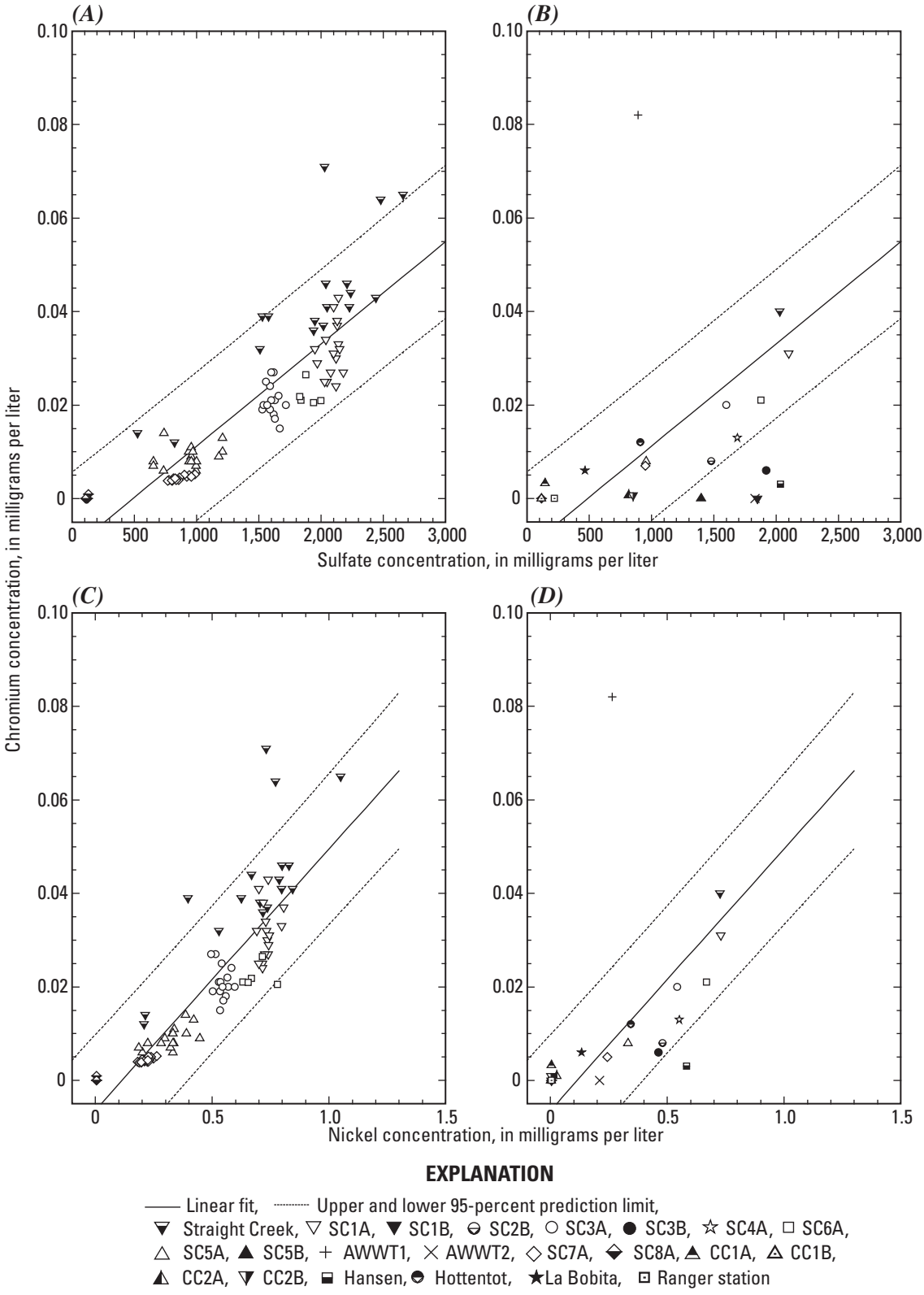

Figure 47. Chromium concentrations plotted against sulfate concentrations for (A) Straight Creek surface and alluvial ground waters and (B) all ground and surface waters. Chromium concentrations plotted against nickel concentrations for (C) Straight Creek surface and alluvial ground waters and for (D) all ground waters and Straight Creek surface water.

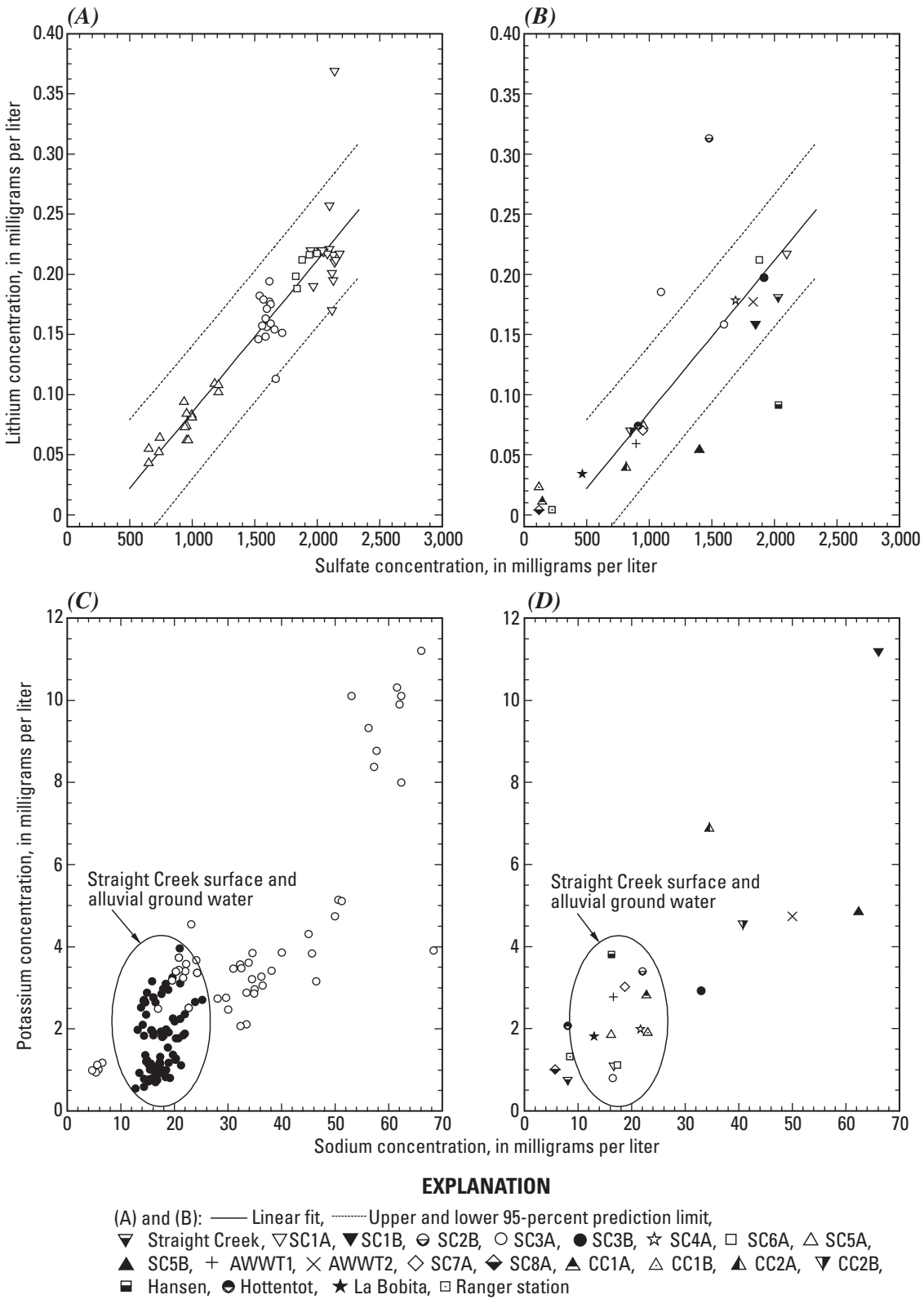

Figure 48. Lithium concentrations plotted against sulfate concentrations for (A) Straight Creek surface and alluvial ground waters and (B) all ground and surface waters. Potassium concentrations plotted against sodium concentrations for (C) Straight Creek surface and alluvial ground waters and for (D) all ground waters and Straight Creek surface water.

As shown in figure 48A, lithium correlates well with sulfate for the Straight Creek alluvial ground waters. That correlation also accounts for most of the lithium concentrations for the other ground waters (fig. 48B). One lithium-enriched water is from SC–2B, and two lithium-depleted waters are Hansen and SC–5B.

Sodium and potassium concentrations, although higher than lithium concentrations, are still low compared to most ground waters (Hem, 1985). The main source minerals for sodium are feldspars such as albite and other plagioclase feldspars. The main source minerals for potassium are illite (sericite) and potassium feldspars (orthoclase, adularia).

Figure 48C shows a plot of potassium relative to sodium concentrations for all ground waters, with filled circles designating the Straight Creek surface and ground waters. The concentration range for potassium is much lower than for sodium, which is typical for nearly all ground waters because sodium minerals are more soluble than their potassium counterparts. For example, albite ($NaAlSi_3O_8$) is more soluble and weathers more readily than orthoclase ($KAlSi_3O_8$). These two elements do generally occur together, indicating that increased weathering still maintains a roughly constant ratio for these elements. Figure 48D shows the median values for all well waters.

Geochemical Controls on Dissolved Beryllium Concentrations

Beryllium is another element found in high concentrations in areas of molybdenum ore deposits. The mineral beryl ($Be_3Al_2Si_6O_{18}$), although rare, has been found underground at the mine site (Bruce Walker, Molycorp, Inc., oral commun., 2003). The formation of emeralds, a particular green form of beryl, has been found to form at high temperature (greater than 300ºC) and from a brine with high fluoride concentration, at least for the deposits in Colombia (Banks and others, 2000). Wood (1991, 1992) has shown the importance of Be-F complexing for the speciation and transport of beryllium in hydrothermal fluids. Hence, beryllium should reflect this strong association with fluorine in water derived from the weathering of such deposits. More commonly, beryllium is found as a dispersed element with higher concentrations in some illites (Plumlee and others, 2005). Consequently, lithium, beryllium, and fluoride concentrations should correlate in acidic ground waters in the Red River Valley.

Beryllium correlates well with sulfate for the Straight Creek alluvial ground waters (fig. 49A), and that correlation holds generally for other ground waters (fig. 49B) with some exceptions. Water from well CC–2A is anomalously high in beryllium, and at Straight Creek ground waters from wells SC–1B, SC–5B, and AWWT2, all bedrock wells, are anomalously low in beryllium. It should be noted here that some ground waters monitored on the mine site have beryllium concentrations up to a few hundred micrograms per liter, and these are likely to be the highest concentrations ever reported for ground water (compare to Veselý and others, 2002).

The anomalously high concentration of beryllium at well CC–2A is associated with anomalously high fluoride concentration and might be caused by both abundance and by complexing between beryllium and fluoride. This relation can be seen in figures 50A and 50B. The correlation between beryllium and fluoride in the Straight Creek waters is quite good (R^2 =0.73 compared to 0.84 for the correlation with sulfate), but the correlation in figure 50B shows that high beryllium in CC–2A is expected based on the high fluoride concentration. Consequently, in interpreting the weathering of beryllium, the concentration of fluoride must also be taken into account.

In figures 50C and 50D, the correlations of beryllium with lithium are shown. The correlation coefficient for the Straight Creek alluvial ground waters is as strong as most of the other correlations (R^2 = 0.87).

Pre-Mining Ground-Water Chemistry at Molycorp's Questa Mine Site

Building on the information gained from the Straight Creek analog study and the additional information gained from wells located at Hottentot Creek, Hansen Creek, La Bobita Campground, and Capulin Canyon, the pre-mining ground-water chemistry at the mine site is derived next. For this analysis, the median values of water-chemistry constituents from the monitoring wells are used.

The primary constraints on chemical constituents for ground water in mineralized, but unmined, areas are (1) correlations found between constituents for the Straight Creek natural analog site, (2) applicable equilibrium mineral-solubility limitations, and (3) exceptionally high concentrations of constituents found at other undisturbed sites besides Straight Creek that can be explained by unusual geochemical circumstances.

Pre-Mining Ground Waters at Molycorp's Questa Mine

Molycorp's Questa mine site consists of three main drainages—Capulin Canyon, Goat Hill Gulch, and Sulphur Gulch. Sulphur Gulch is further divided into three tributary drainages—Spring Gulch, Blind Gulch, and Sulphur Gulch (fig. 51). There are four smaller, unnamed drainages between Goat Hill Gulch and Sulphur Gulch along the north side of the Red River that also must be considered. There are other smaller drainages to the east of the Sulphur Gulch drainage and within the mine-site boundaries that are small enough to be neglected and will not be considered further.

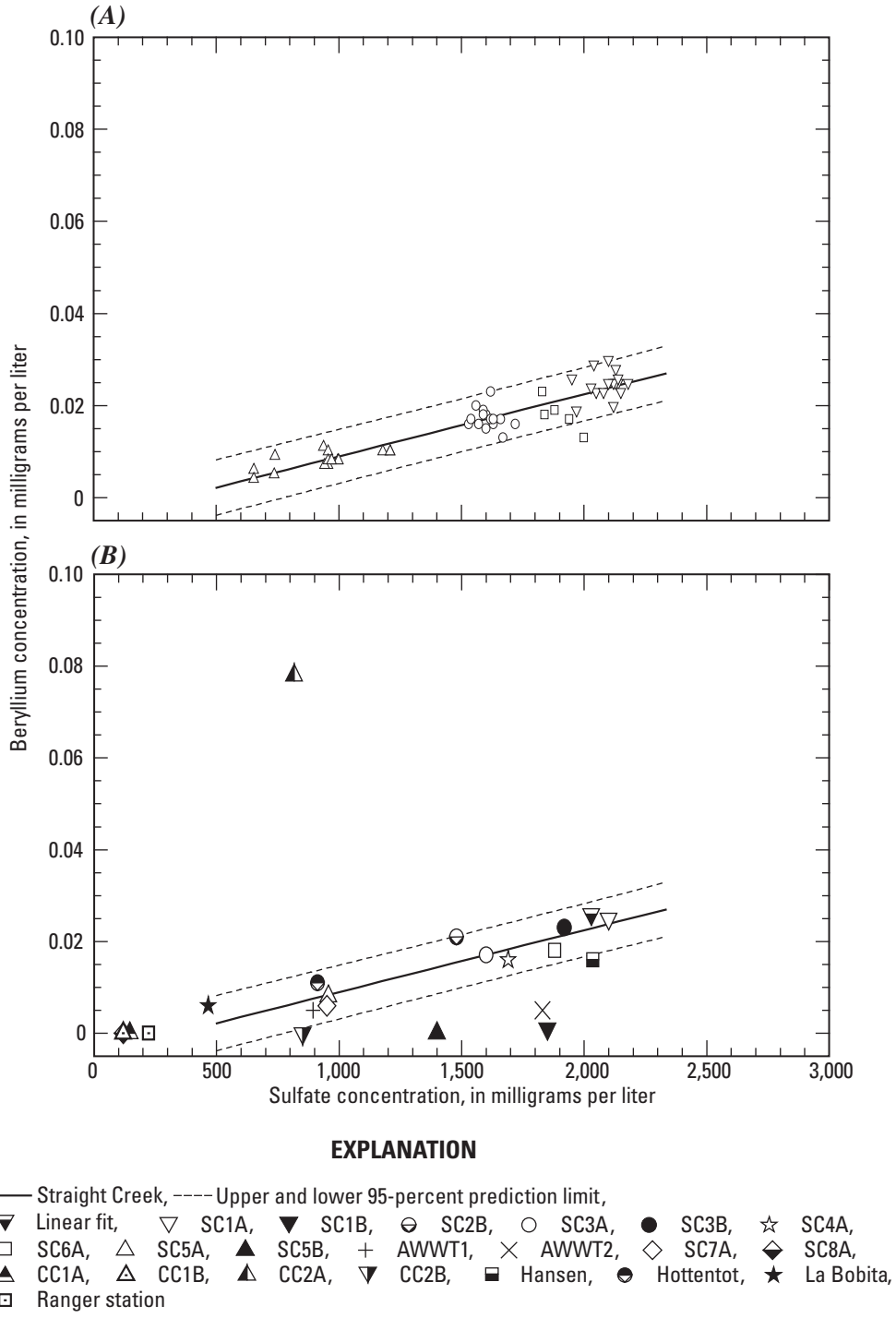

Figure 49. Beryllium concentrations plotted against sulfate concentrations for (A) Straight Creek surface and alluvial ground waters and (B) all ground and surface waters.

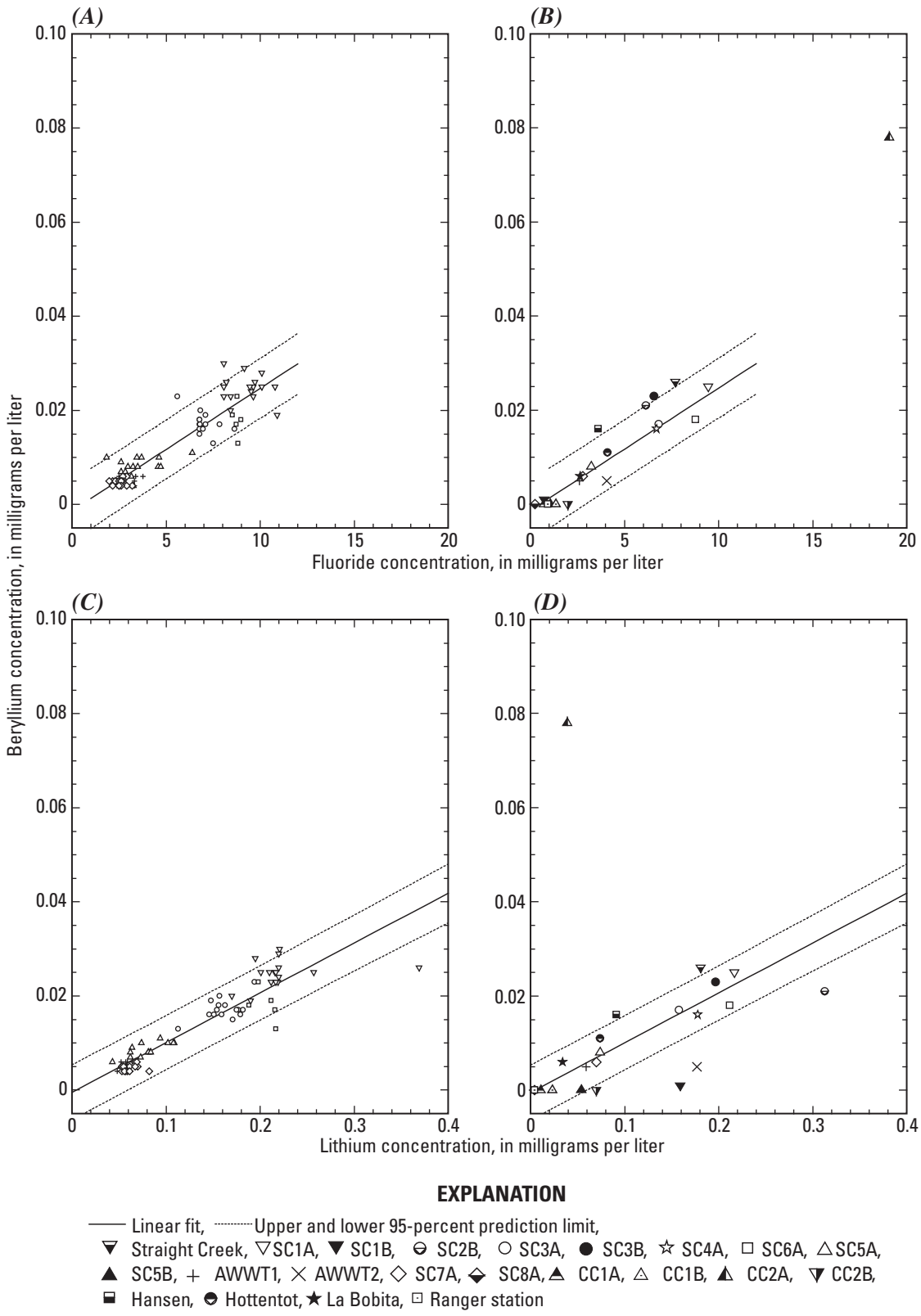

Figure 50. Beryllium concentrations plotted against fluoride concentrations for (A) Straight Creek alluvial ground waters and (B) all ground and surface waters. Beryllium concentrations plotted against lithium concentrations for (C) Straight Creek alluvial ground waters and for (D) all ground waters and Straight Creek surface water.

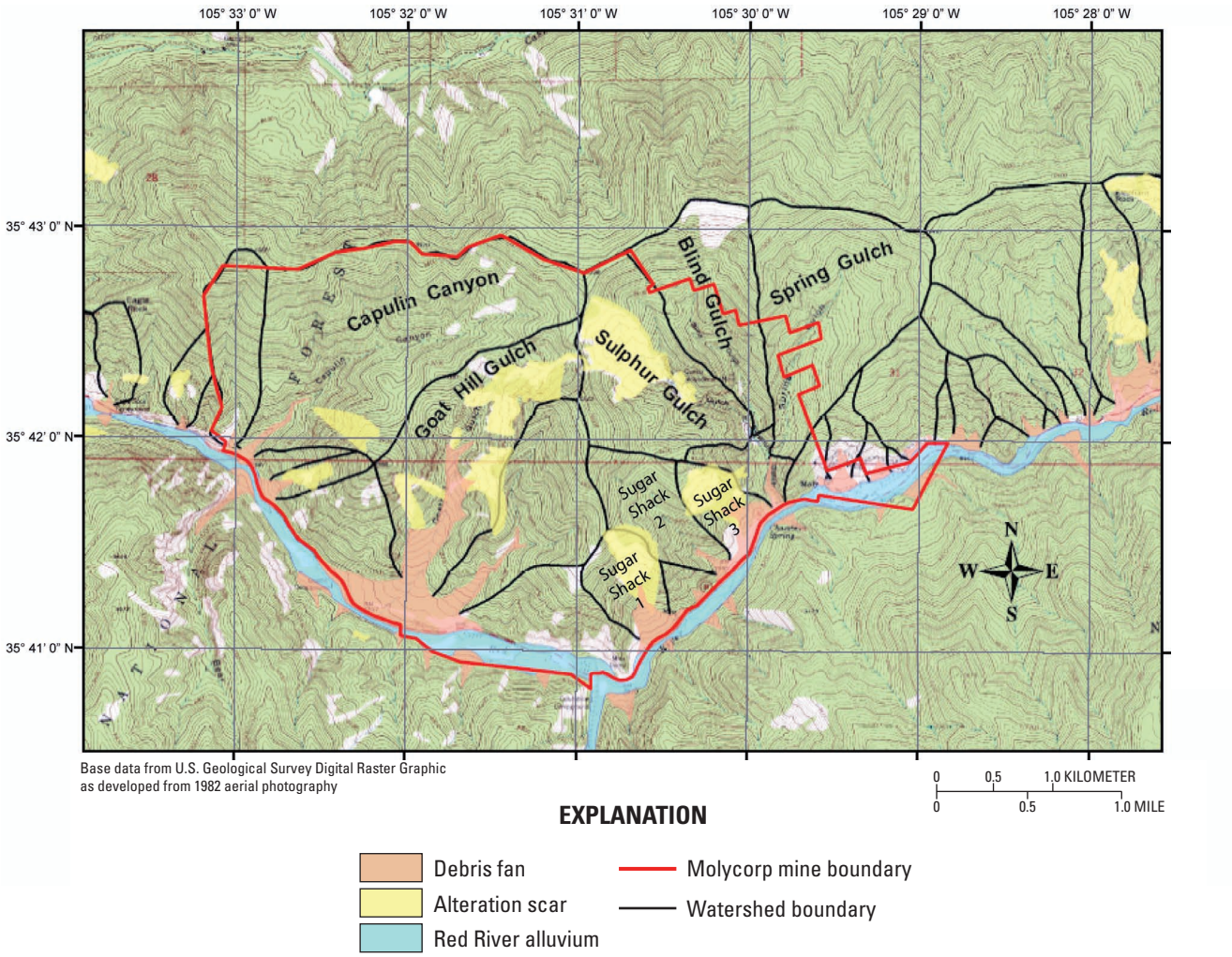

Figure 51. Topographic map of mine site with watershed boundaries, scar areas, debris fans, and Red River alluvium.

Each of the three main drainages is considered below in sequence from west to east of the mine-site property. Pre-mining solute concentrations for the mine site are based on the hydrogeochemical processes found to control the concentrations at the Straight Creek analog site modified by the differences observed between Straight Creek and mine-site mineralogy, lithology, and hydrology. These differences are primarily related to the position of the weathering surface with respect to the sequence of hydrothermal alteration zones that change with distance from the intrusion center (Ludington and others, 2005).

Capulin Canyon

Capulin Canyon is composed mostly of Amalia Tuff of rhyolitic composition with an exposure of andesite appearing in the upper part of the canyon and a mineralized zone in the lower part of the canyon. A portion of this mineralized zone forms a scar on the east side of the catchment. At the head of the canyon, waste piles reside from the open-pit operation, and their leachates were allowed to discharge into the canyon until the early 1990s when a collection impoundment contained these waters and a pump system discharged them to Goat Hill Gulch. This complex lithology with overlying waste rock from mining explains the wide range of ground-water compositions that have been recorded. It also means that there is not a simple pre-mining ground-water composition that can be assigned to Capulin Canyon.

Although Capulin Canyon contains waste-rock piles that have been weathering and leaching solutes into this drainage since the late 1960s, the waste-rock leachates were diverted with a collection system that was constructed beginning in 1992. In light of this diversion, it was thought possible that ground water monitored downgradient from the impoundment diversion in the canyon might be dominated by natural processes with little effect from mine wastes. Of the three main drainages in the mine area, Capulin Canyon has seen the least impact from mining and mineral processing activities and has been the least affected by the ground-water cone of depression around the open pit, underground mines, and the pumped alluvial aquifers. Consequently, plots of water chemistry were prepared with the specific objectives of determining

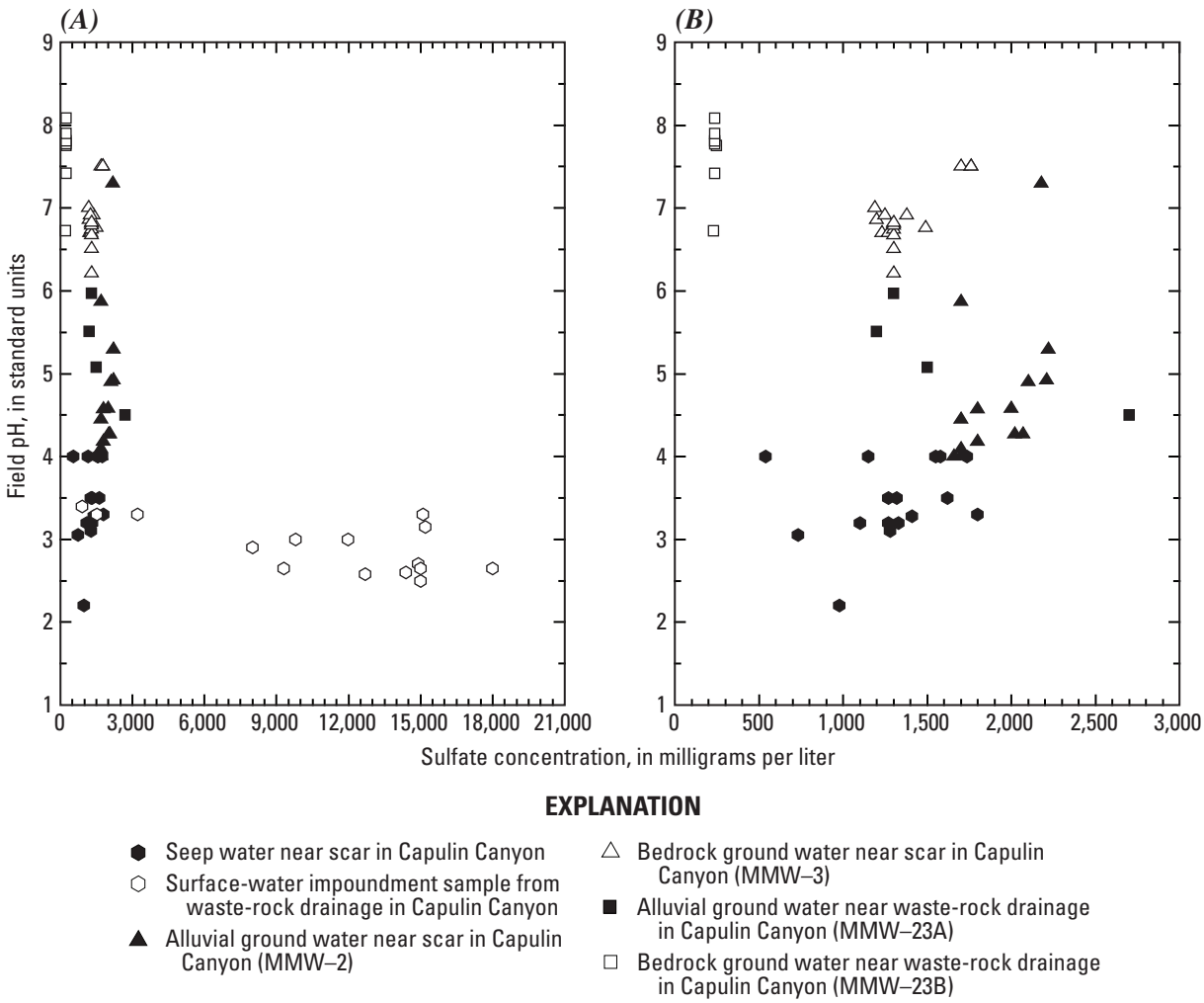

Figure 52. Plot of pH against sulfate concentration for (A) seeps and ground waters in Capulin Canyon with less than 3,000 milligrams per liter sulfate concentration and (B) same waters including those surface-water impoundment waters with greater than 3,000 milligrams per liter sulfate concentration.

(1) whether the chemistry of the waste-pile leachates could be distinguished from leachates from natural scar weathering and (2) the range of water chemistry from natural scar weathering in this canyon.

Those plots (figs. 52–54) reveal that the impoundment water collecting waste-rock leachates has generally higher concentrations of most constituents than the water derived from natural scar weathering. Sulfate concentrations are commonly 8,000 to 18,000 mg/L in the impoundment water compared to less than 2,500 mg/L for scar-weathering water. The pH values for both impoundment water and scar water are consistently low, between 2.5 and 3.5 (fig. 52B). It is unclear how much of the higher concentration is caused by evaporation compared to greater dissolution rate of minerals. Both factors could be significant.

Trace and minor elements, especially high beryllium and fluoride concentrations, seem characteristic of waste-pile leachates. Figures 53A and B plot the lower concentration range of fluoride against calcium and against sulfate, respectively. The impoundment waters shown in parallel figures 53C and 53D show the much higher concentrations of fluoride contained in the impoundment waters.

Figures 54A–54D show the low and high ranges of concentrations for zinc and manganese relative to sulfate and how much higher the concentrations in the impoundment are than in the ground waters and scar leachate seep waters. Figures 55A–55D show the low and high ranges of concentrations for nickel and cobalt relative to sulfate. Again, the highest concentrations are in the impoundment water. The strong correlation between cobalt and nickel is consistent with a single source for these elements, that is, pyrite (figs. 55B and 55D).

There is a distinct possibility that systematic sampling for water and sulfate stable isotopes in this canyon could reveal more quantitatively the differences between waste-pile weathering and natural-scar weathering and the influence of evaporation, but that remains to be studied. The chemical data do show that (1) alluvial well MMW–23A may contain some water derived from waste-pile leachates, (2) bedrock well

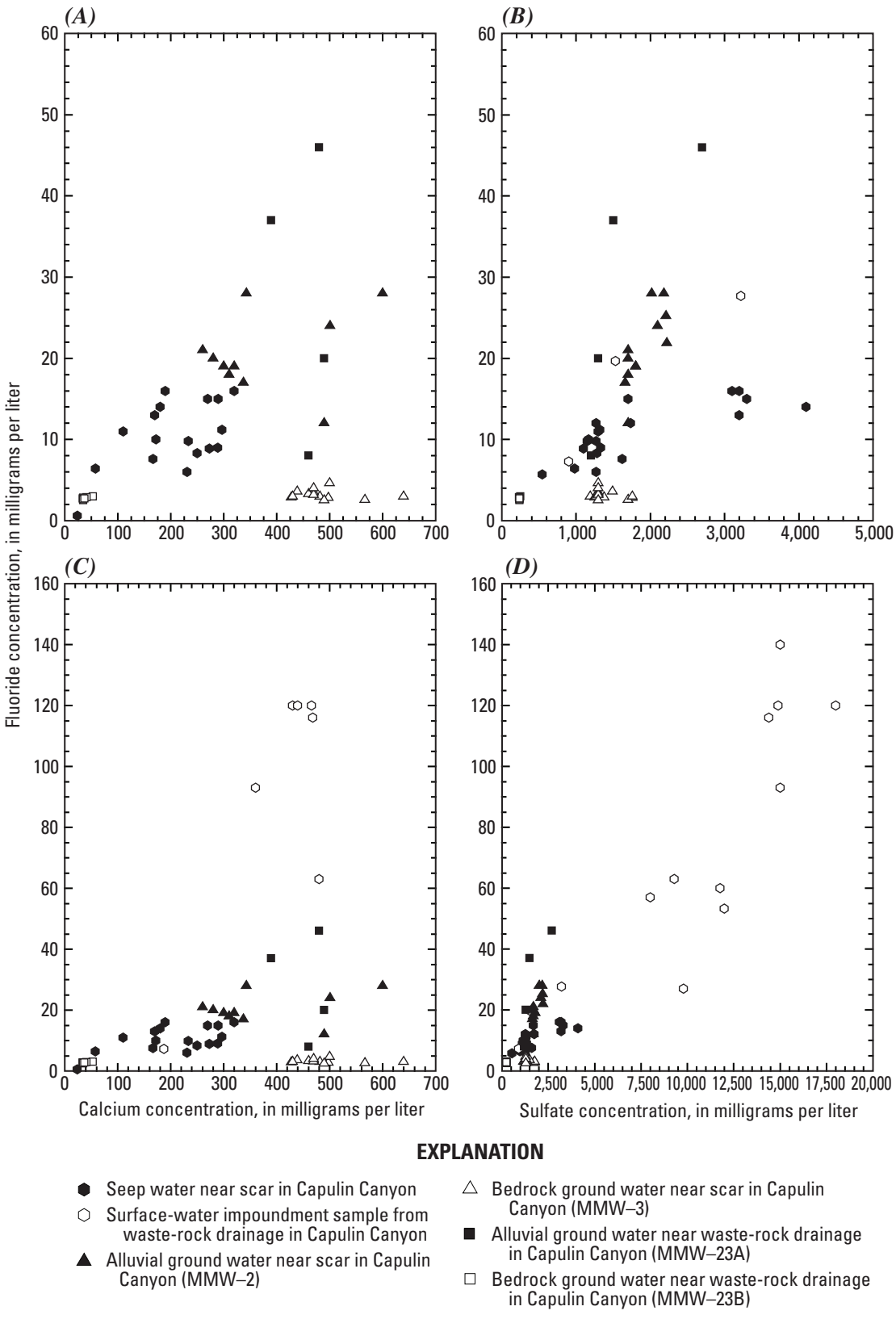

Figure 53. (A) Plot of fluoride concentrations (less than 60 milligrams per liter) against calcium concentrations for Capulin Canyon waters. (B) Plot of fluoride concentrations (less than 60 milligrams per liter) against sulfate concentrations (less than 5,000 milligrams per liter). (C) Same plot as figure 53A but showing the entire range of concentrations. (D) Same plot as figure 53B but showing the entire range of concentrations.

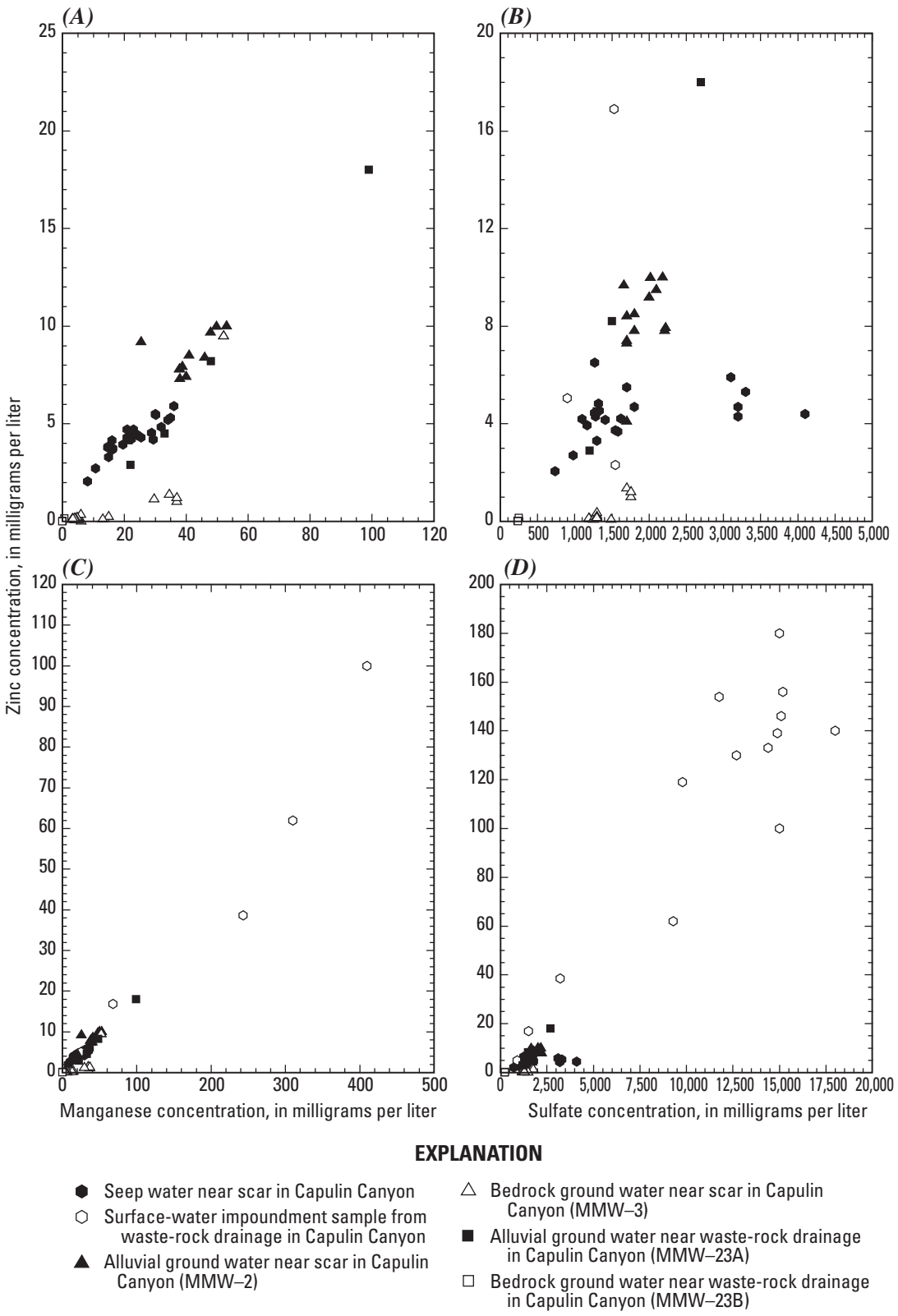

Figure 54. (A) Plot of zinc against manganese concentrations (less than 120 milligrams per liter) for Capulin Canyon waters. (B) Plot of zinc against sulfate concentrations (less than 5,000 milligrams per liter) for Capulin Canyon waters. (C) Same plot as figure 54A but showing the entire range of concentrations. (D) Same plot as figure 54B but showing the entire range of concentrations.

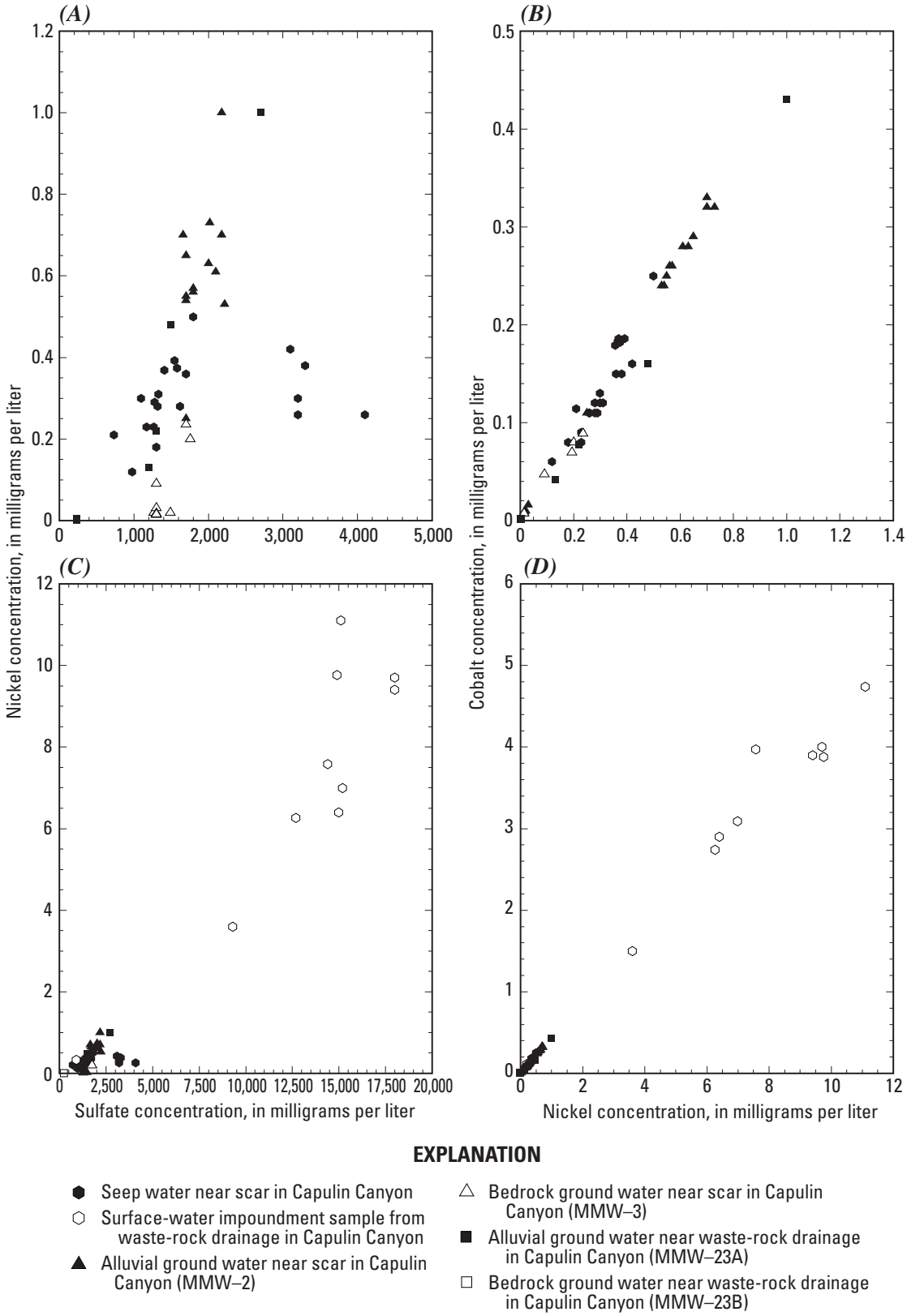

Figure 55. (A) Plot of nickel against sulfate concentrations (less than 5,000 milligrams per liter) for Capulin Canyon waters. (B) Plot of cobalt against nickel concentrations (less than 1.4 milligrams per liter) for Capulin Canyon waters. (C) Same plot as figure 55A but showing the entire range of concentrations. (D) Same plot as figure 55B but showing the entire range of concentrations.

MMW–23B appears to contain uncontaminated ground water, (3) alluvial well MMW–2 appears to be strongly influenced by scar drainage although influence from waste-rock leachates cannot be ruled out completely, (4) bedrock well MMW–3 is indicative of water in natural but mineralized bedrock, and (5) wells CC–1B, CC–2A, and CC–2B, located away from waste-rock influence, reflect water chemistry from both unmineralized and mineralized rock, indicating effects of mineralized rock on water chemistry away from obvious scar areas. Historical samples of ground-water chemistry were collected with objectives other than attempting to discern waste-water signatures with those from natural weathering. Consequently, it is difficult to assign specific pre-mining ground-water quality parameters in this catchment.

The range of concentrations for dissolved constituents in Capulin Canyon is much larger than expected because part of the canyon is largely unmineralized and other parts are strongly mineralized. Nonetheless, the following conclusions can be drawn:

1. The ground waters in Capulin Canyon can be divided into those alluvial waters unaffected by scar leachate (represented by CC–1B, CC–2A, and CC–2B), those affected by scar leachate (represented by MMW–2), and bedrock ground waters.

2. Analytical results for waters from uncontaminated Capulin Canyon alluvial aquifers reflect a large range of water compositions that tend to be high in concentration relative to New Mexico ground-water quality standards. The range of water-quality parameters is given in table 7 for the constituents of concern.

3. The range of values of ground-water chemistry demonstrates that Capulin Canyon contains mineralized tuff and andesite buffered by carbonate minerals where the pyrite content is low.

4. Most important, the main scar is located in the lower portion of the canyon and, consequently, acid waters with elevated metal concentrations dominate the water chemistry before entering the Red River alluvial system.

5. These concentrations are within or close to the range of concentrations found in the debris-flow aquifer at Straight Creek with two notable exceptions—fluoride and beryllium. The higher concentrations of these two elements found in the Capulin ground waters are likely a result of the more intense alteration and higher content of fluorite. Also, beryllium and fluoride tend to correlate well both in the chemistry of these alteration zones and in waters derived from these rocks. The abundance of these elements in the water is no doubt related to both abundance in the rocks and the strong aqueous complexation between fluoride and beryllium under acidic conditions.

6. The values for Capulin Canyon alluvium upgradient from the scar are based on the CC wells, bedrock wells at Straight Creek, and mineral solubility controls where applicable (table 7). The values for Capulin Canyon alluvium downgradient from the scar are based on MMW–2 and mineral solubility controls (table 8). The values for bedrock are based on MMW–3 and mineral solubility controls (table 9).

The bedrock ground waters in Capulin Canyon are buffered to circumneutral pH values and have substantially lower metal concentrations. The analytical data provided for bedrock wells MMW–23B and MMW–3 did not always have low enough detection limits for the purpose of quantifying trace-element concentrations of concern. Sulfate, manganese, cobalt, and fluoride are at concentrations greater than the ground-water quality standards. Sulfate could be as high as 2,000 mg/L and fluoride as high as 5 mg/L based on the available monitoring data.

Ground water from MMW–23B is substantially more dilute than that from MMW–3, which reflects the effect of mineralized zones in the lower part of the drainage. Sulfate concentrations for MMW–23B are about 250 mg/L and dissolved solids about 550 mg/L compared to average concentrations of 1,500 and 2,500 mg/L, respectively, for MMW–3. Ground water in MMW–23B would also be more dilute because it is closer to recharge, whereas ground water in MMW–3 is closer to discharge.

Goat Hill Gulch

Goat Hill Gulch has exposures of Amalia Tuff in the upper half of the catchment and Tertiary andesite in the lower half with an exposure of biotite-rich granite appearing near the middle. Large quantities of scar are exposed in steep canyons, and a large debris fan has aggraded and deposited sediment across part of the Red River. This catchment is dominated by QSP alteration. Physical erosion has been very rapid in the recent past such that unweathered pyrite can still be found in downgradient exposures of debris.

The weathering surface for Goat Hill Gulch with respect to the position of the alteration zones is very similar to that of Straight Creek as estimated by Ludington and others (2005), but the size of the debris fan is much larger. Consequently, the estimated values of pre-mining ground-water chemical constituents and properties should be no less in concentration than those in the Straight Creek study. For this catchment we have used the highest concentrations of constituents in the Straight Creek study, those measured in waters from well SC–1A; however, beryllium and fluoride concentrations should be as high as those in Capulin Canyon. The results are listed in table 10. If the concentration of a constituent from SC–1A was less than the highest concentration from Capulin alluvial water, then the Capulin value was used to replace it (for example, iron and manganese).

Following the development of the parameters in table 10, corroboration of the water chemistry in Goat Hill Gulch debris fan unaffected by mining became possible with water-quality

Table 7. Range of values for water-quality constituents of concern for Capulin Canyon alluvial ground waters unaffected by scar drainage.

[Values exceeding ground-water quality standards (table 1) shown in bold; mg/L, milligrams per liter; msc, mineral solubility control; calc'n, calculation; ≤, less than or equal to; <, less than; WATEQ4F speciation code, Ball and Nordstrom, 1991]

Water-quality constituent (Capulin alluvium above scar)	Range, in mg/L (except pH)	Source
Aluminum (Al)	0.005 – 5	CC wells, SC–1B, SC–5B, msc
Beryllium (Be)	0.001 – **0.08**	CC wells, SC–1B, SC–5B
Cadmium (Cd)	≤0.003	CC wells, SC–1B, SC–5B
Chromium (Cr)	<0.0007	CC wells, SC–1B, SC–5B
Cobalt (Co)	<0.016	CC wells, SC–1B, SC–5B
Copper (Cu)	0.0007	CC wells, SC-1B, SC-5B
Fluoride (F)	1 – **20**	CC wells, SC–1B, SC–5B, msc
Iron (Fe)	0.03 – **34**	CC wells, SC–1B, SC–5B, msc
Lead (Pb)	<0.001	CC wells, SC–1B, SC–5B
Manganese (Mn)	0.2 – **41**	CC wells, SC–1B, SC–5B, msc
Nickel (Ni)	<0.028	CC wells, SC–1B, SC–5B
Sulfate (SO_4)	100 – **850**	CC wells, msc
Zinc (Zn)	≤4	CC wells, SC wells
Dissolved solids	500 – **1,700**	CC wells; WATEQ4F calc'n
pH (standard units)	6 – 7.5	CC wells

Table 8. Range of values for water-quality constituents of concern for Capulin Canyon alluvial ground waters affected by scar drainage.

[Values exceeding ground-water quality standards (table 1) shown in bold; mg/L, milligrams per liter; msc, mineral solubility control; calc'n, calculation; <, less than; WATEQ4F speciation code, Ball and Nordstrom, 1991]

Water-quality constituent (Capulin alluvium below scar)	Range, in mg/L (except pH)	Source
Aluminum (Al)	**8 – 100**	MMW–2 well, msc
Beryllium (Be)	**0.015 – 0.08**	MMW–2 well
Cadmium (Cd)	0.004 – **0.04**	MMW–2 well
Chromium (Cr)	<0.007	MMW–2 well
Cobalt (Co)	**0.1 – 0.30**	MMW–2 well
Copper (Cu)	0.05 – 0.4	MMW–2 well
Fluoride (F)	**10 – 30**	MMW–2 well
Iron (Fe)	**20 – 50**	MMW–2 well
Lead (Pb)	0.003 – 0.010	MMW–2 well
Manganese (Mn)	**20 – 50**	MMW–2 well
Nickel (Ni)	0.2 – **0.8**	MMW–2 well
Sulfate (SO_4)	**1,700 – 2,200**	MMW–2 well, msc
Zinc (Zn)	4 – 10	MMW–2 well
Dissolved solids	**2,400 – 2,700**	MMW–2 well, WATEQ4F calc'n
pH (standard units)	**3.7 – 5.5**	MMW–2 well

Table 9. Range of values for water-quality constituents of concern for Capulin Canyon bedrock ground waters.

[Values exceeding ground-water quality standards (table 1) shown in bold; mg/L, milligrams per liter; msc, mineral solubility control; calc'n, calculation; <, less than; WATEQ4F speciation code, Ball and Nordstrom, 1991]

Water-quality constituent (Capulin bedrock)	Range, in mg/L (except pH)	Source
Aluminum (Al)	0.01 – 1	MMW–3, msc
Beryllium (Be)	0.001 – 0.0025	MMW–3
Cadmium (Cd)	0.004 – 0.007	MMW–3
Chromium (Cr)	0.0005 – 0.005	MMW–3
Cobalt (Co)	**0.07 – 0.10**	MMW–3
Copper (Cu)	0.001 – 0.005	MMW–3
Fluoride (F)	**2 – 5**	MMW–3, msc
Iron (Fe)	0.05 – 1	MMW–3, msc
Lead (Pb)	<0.001	MMW–3
Manganese (Mn)	**3 – 40**	MMW–3, msc
Nickel (Ni)	0.01 – 0.2	MMW–3
Sulfate (SO_4)	**1,000 – 2,000**	MMW–3, msc
Zinc (Zn)	0.005 – 0.5	MMW–3
Dissolved solids	**2,000 – 2,900**	MMW–3, WATEQ4F calc'n
pH (standard units)	6 – 7	MMW–3

Table 10. Preliminary values for water-quality constituents of concern for alluvial ground waters in Goat Hill.

[Values exceeding ground-water quality standards (table 1) shown in bold; mg/L, milligrams per liter]

Water-quality constituent (Goat Hill alluvium)	Values, in mg/L (except pH)	New Mexico standard, in mg/L (except pH)
Aluminum (Al)	**100**	5.0
Beryllium (Be)	**.08**	[1].004
Cadmium (Cd)	**.04**	.01
Chromium (Cr)	.03	.05
Cobalt (Co)	**.4**	.05
Copper (Cu)	1.0	1.0
Fluoride (F)	**30**	1.6
Iron (Fe)	**50**	1.0
Lead (Pb)	.009	.05
Manganese (Mn)	**50**	.2
Nickel (Ni)	**.75**	.2
Sulfate (SO_4)	**2,000**	600.0
Zinc (Zn)	10	10.0
Dissolved solids	**2,900**	1,000
pH (standard units)	**3–4**	6–9

[1] Federal standard, not New Mexico standard.

Table 11. Estimated preliminary values of pre-mining ground-water quality constituents for Goat Hill Gulch debris fan compared to the range of values from ground waters in wells MMW-42A and MMW-44A.

[mg/L, milligrams per liter]

Water-quality constituent (Goat Hill alluvium)	Estimated values, in mg/L (except pH)	Range of values for wells MMW–42A and MMW–44A, in mg/L (except pH)
Aluminum (Al)	100	130–350
Beryllium (Be)	.08	0.03–0.06
Cadmium (Cd)	.04	0.04–0.1
Chromium (Cr)	.03	0.03–0.6
Cobalt (Co)	.4	0.3–0.5
Copper (Cu)	1.0	3–6
Fluoride (F)	30	17–28
Iron (Fe)	50	1.5–5
Lead (Pb)	.009	0.001
Manganese (Mn)	50	20–41
Nickel (Ni)	.75	0.4–1.1
Sulfate (SO_4)	2,000	1,300–3,600
Zinc (Zn)	10	5.5–10
Dissolved solids	2,900	2,400–2,500
pH (standard units)	3–4	2.8–4.6

data from wells MMW–44A and MMW–42A. These wells were developed and sampled in 2002 and after. They are located in the toe of the Goat Hill Gulch debris fan downgradient from the subsidence area that provides a sink for waste-rock leachates that come from both Goat Hill Gulch and Capulin Canyon. Waste waters from mining activities are effectively diverted underground (to the underground mines) by this subsidence area. Water from these wells should be unaffected by mining activities, and evidence to support this claim comes from four lines of evidence. First, sampling and analysis for more than 100 anthropogenic organic compounds (including solvents, petroleum products, phenols) were made in these ground waters, and no detectable concentrations were found (Molycorp, Inc., written commun., 2004). Second, nitrate concentrations were detected but at low concentrations (less than1 mg/L). Third, the concentrations of major and trace solutes closely resemble those in ground water from areas of similar pH but known not to be disturbed by mining activities. Introduction of a substantial amount of contaminants into the lower Goat Hill Gulch debris fan would have changed the chemistry of the ground water in some obvious manner. Fourth, if anthropogenic activities have caused the introduction of enough fluid or contaminants to change the groundwater chemistry, it would have to have been an obvious or intentional spill in this gulch that should have been acknowledged in the record and known to regulatory agencies. Such an event has not happened according to inquiries made to both Molycorp and regulatory agencies. Hence, it seemed reasonable to compare the pre-mining concentrations in table 10 with results from wells MMW–42A and MMW–44A. Water from these wells was not sampled or analyzed by the USGS, but a QA/QC report (McCleskey and others, 2004) demonstrated that comparisons of USGS results with those from Molycorp were of high quality. The comparison is given in table 11.

A few noteworthy differences appear in this comparison. Iron, manganese, and dissolved-solids concentrations are substantially lower in waters from wells MMW–42A and MMW–44A, and aluminum and copper concentrations are higher in these waters. Other constituent concentrations are remarkably close to the estimated concentrations. The reason that iron and manganese concentrations are lower and copper concentrations are higher has to do with the difference in redox properties between waters from SC–1A and those from MMW–42A and MMW–44A. Waters from SC–1A are reduced (dissolved oxygen concentrations are near detection and usually less than 0.5 mg/L), and waters from MMW–42A and MMW–44A are oxidized (dissolved oxygen concentrations range from 1.4 to 4 mg/L). Oxidation will remove iron and manganese from solution and not remove copper from solution. Reduction will remove copper from solution. Hence, concentrations of

redox-sensitive species in Straight Creek ground waters cannot be used to estimate pre-mining concentrations in Goat Hill Gulch ground waters. Iron concentrations can be estimated by assuming full oxidation and precipitation as hydrous ferric oxide in the pH range given (3–4). The ground water closest in overall composition would be that from well SC–3A, which has a pH of about 3.3, dissolved iron predominantly as ferric iron, and sulfate concentrations of about 1,600 mg/L. Median iron and manganese concentrations in SC–3A are 0.5 and 15 mg/L, respectively. These values provide a lower bound to the measured values from MMW–42A and MMW–44A. Concentrations of copper in SC–3A are about 0.8 mg/L, but some of the copper has been removed by reduction so that this value should also be a lower bound. Water from SC–3A has dissolved-solids concentrations of about 2,300 mg/L, closer to those of MMW–42A and MMW–44A than those of the estimated pre-mining concentration. These comparisons indicate that some adjustments are needed for the values of pre-mining ground-water quality constituents of the Goat Hill Gulch debris fan.

The final estimated values of ground-water quality constituents and properties for the Goat Hill Gulch debris fan were based on the preliminary values in table 11 with the following adjustments. Solute concentrations from ground waters of MMW–42A are more dilute than those from MMW–44A and are likely to have mixed with some Red River alluvial ground water because of the location of this well. Therefore, ground-water concentrations from MMW–44A were used as an upper limit. The pH range was left unchanged because it accurately represents the range that occurs naturally for ground waters in the Red River Valley of this water composition. The final estimated values are listed in table 12.

Table 12. Estimated final values for water-quality constituents of concern for alluvial ground waters in Goat Hill.

[Values exceeding ground-water quality standards (table 1) shown in bold; mg/L, milligrams per liter]

Water-quality constituent (Goat Hill alluvium)	Values, in mg/L (except pH)	New Mexico standard, in mg/L (except pH)
Aluminum (Al)	**350**	5.0
Beryllium (Be)	**.06**	[1].004
Cadmium (Cd)	**.1**	.01
Chromium (Cr)	**.6**	.05
Cobalt (Co)	**.5**	.05
Copper (Cu)	**6**	1.0
Fluoride (F)	**28**	1.6
Iron (Fe)	**5**	1.0
Lead (Pb)	.001	.05
Manganese (Mn)	**41**	.2
Nickel (Ni)	**1.1**	.2
Sulfate (SO_4)	**3,600**	600.0
Zinc (Zn)	10	10.0
Dissolved solids	**2,500**	1,000
pH (standard units)	**3–4**	6–9

[1]Federal standard, not New Mexico standard.

Sulphur Gulch

Sulphur Gulch, mistakenly named for the bright yellow coatings of ferrimolybdite resembling sulfur, has an erosional surface that cuts deep into the alteration of the molybdenum ore body, exposing a small portion of the intrusive body (aplite dikes and granitic stockwork). This catchment is probably least analogous to the Straight Creek alluvial system, but there may be some analogy with respect to the bedrock conditions at Straight Creek. Perhaps the most important aspect of Sulphur Gulch is the striking change in lithology from the upper part of the drainage to the lower part. At the head of the drainage, a scar is exposed containing QSP alteration and from which acid waters develop. However, at lower elevations the drainage cuts deeper into a thick section of fluorite-carbonate veining that can neutralize acid water and establish a circumneutral pH with low metal concentrations except for manganese, iron, calcium, magnesium, and strontium (Ludington and others, 2005, their fig. 6C; this report, fig. 2). Fluoride concentrations might also be elevated during neutralization, but because of the abundant amount of calcium and the consequent common-ion effect on the solubility of fluorite, concentrations of fluoride are relatively lower.

Sulphur Gulch is composed of three relatively comparable subcatchments—upper Sulphur Gulch, Blind Gulch, and Spring Gulch. The boundaries of these subcatchments are shown in figure 56. Sulphur Gulch lithology is dominated by a large scar of QSP alteration. Blind Gulch contains Tertiary granite stock, Tertiary andesite, and Proterozoic metamorphic rocks (fig. 57). Granite and andesite dominate the Blind Gulch outcrop with potassic alteration, carbonate-fluorite veining, and propylitic alteration dominating the alteration assemblages. Spring Gulch is a downdropped block of intense propylitic alteration. “AVIRIS data (Livo and Clark, 2002) maps of carbonate and epidote signals indicate that the most intense areas of propolytic alteration along the lower Red River occur in the downdropped Spring Gulch block east of the mine site... .” (Ludington and others, 2005). Hence, water draining upper Sulphur Gulch will be an acid-sulfate type similar to water draining the Straight Creek scar; water draining Blind and Spring Gulches will be a neutral-pH, carbonate-buffered type. Blind Gulch drainage mixes with upper Sulphur Gulch drainage, then that mixture mixes with drainage from Spring Gulch. If the relative proportions and compositions of these drainage waters can be estimated, then these mixtures can be simulated with a geochemical code to estimate resultant water chemistry of the drainage water that infiltrates and dominates the ground-water chemistry of the Sulphur Gulch debris fan.

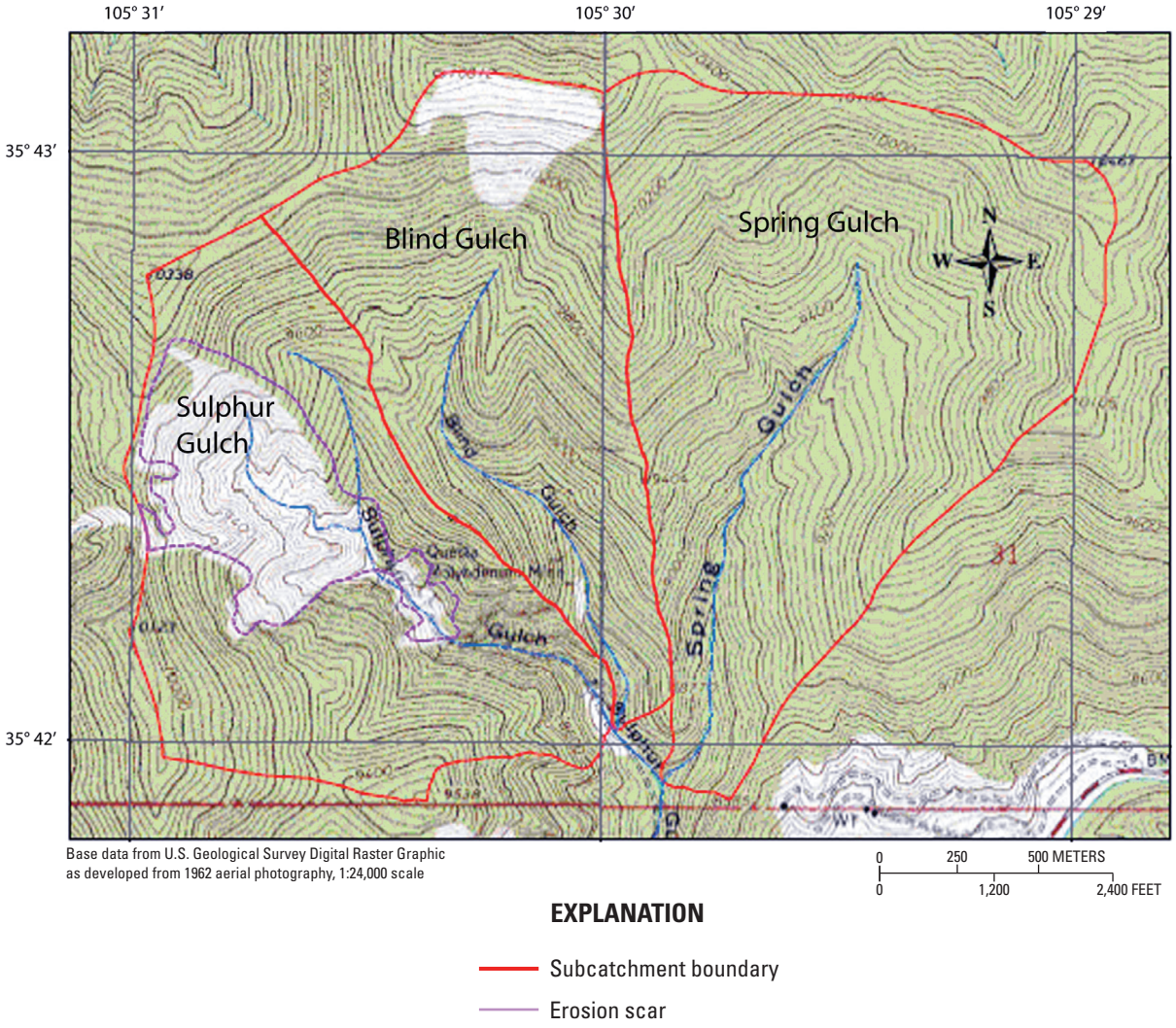

Figure 56. Topographic map of the three subcatchments that constitute Sulphur Gulch—upper Sulfur Gulch, Blind Gulch, and Spring Gulch.

The proportion of water discharge, or yield, from upper Sulphur, Blind, and Spring Gulches has been estimated as 35 percent, 25 percent, and 40 percent, respectively. These proportions were determined by using estimates of precipitation and evapotranspiration (Naus and others, 2006). The water compositions from each catchment were estimated as follows. Upper Sulphur Gulch drainage-water composition is assumed to be nearly identical to Straight Creek drainage-water composition. Waters from Blind and Spring Gulches are represented by a water issuing from the propylitic zone in the area west of Little Hansen (Verplanck and others, 2006). These water compositions, listed in table 13, proportions of mixing, and appropriate mineral solubility controls were used as input to the PHREEQCi code (Parkhurst and Appelo, 1999) using the same thermodynamic data listed in table 1–1 of Appendix 1. Saturation indices were checked to see if supersaturation occurred with respect to amorphous aluminum hydroxide and ferrihydrite, $Fe(OH)_3$. These are the most soluble forms for aluminum and iron minerals and the most likely ones to precipitate upon mixing under oxidizing conditions. After mixing, the water enters the alluvial aquifer of the debris fan, and it is assumed that the iron is reduced. The aluminum concentration that results from using amorphous aluminum hydroxide as the precipitating phase (22.8 mg/L) seems high relative to the trend of aluminum with pH shown in figure 29C. Consequently, a range of reasonable aluminous mineral phases was substituted for amorphous aluminum hydroxide to determine the effect of different solubility-product constants (K_{sp}) on the aluminum concentration. The results, listed in table 14, also affect the pH and iron concentrations. The water that is most analogous to this simulated mixture is the La Bobita ground water. Two samples with the closest pH values (4.45 and 4.54) from La Bobita were used as additional constraints for aluminum and iron concentrations

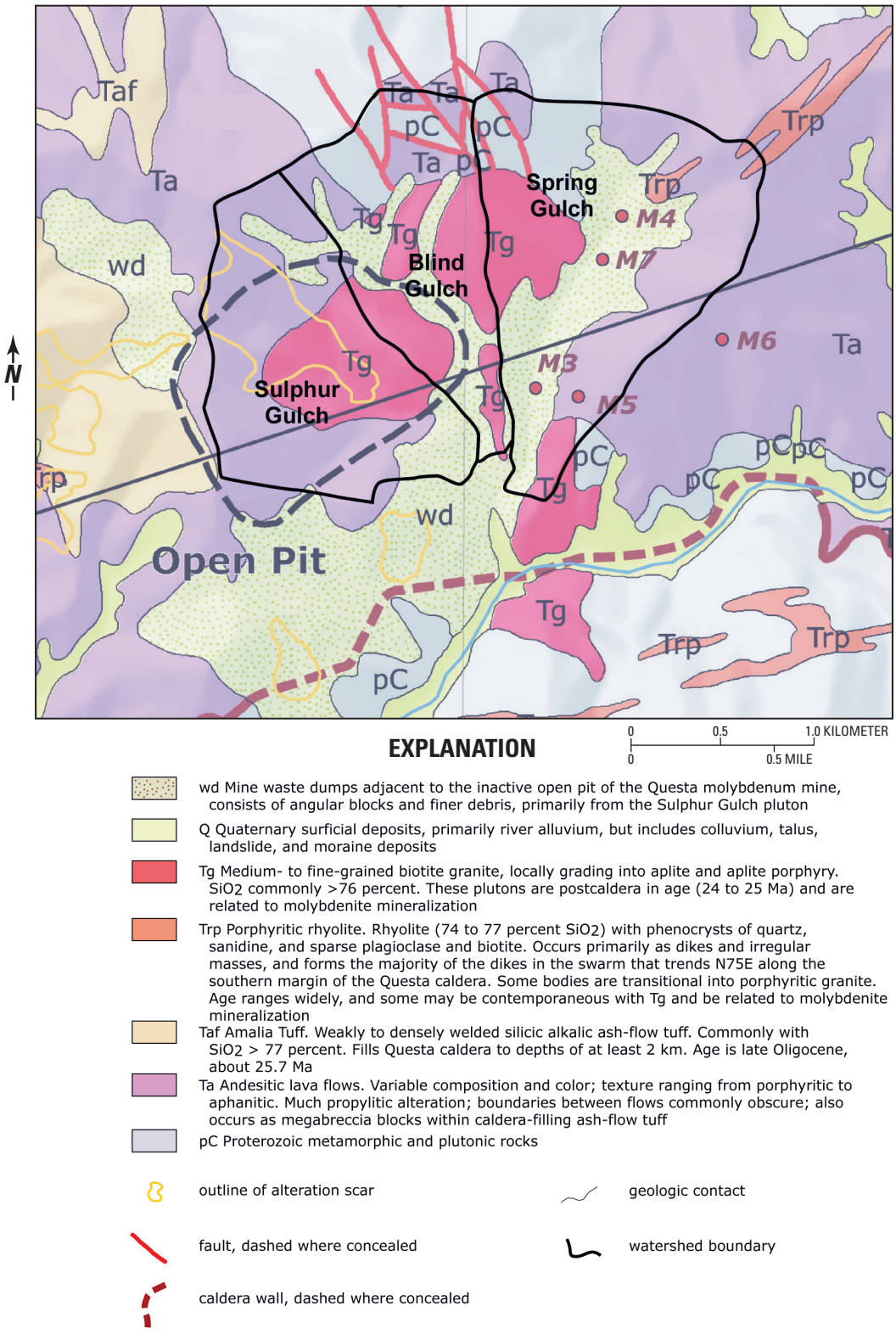

Figure 57. Geologic map of the three subcatchments that constitute Sulphur Gulch—upper Sulfur Gulch, Blind Gulch, and Spring Gulch.

Table 13. Compositions of water used for the reactive mixing calculations.

[Mixture composition is derived from two-step serial mixing calculations using PHREEQC, with mixing proportions indicated in column headings; specific conductance and dissolved-solids values were calculated using WATEQ4F; values of zero used for mixing calculations for concentrations less than method detection limit; °C, degrees Celsius; µS/cm, microsiemens per centimeter; ppm, parts per million; Eh, redox potential; V, volts; mg/L, milligrams per liter; <, less than; --, not calculated]

Catchment Analog	Upper Sulphur Gulch Straight Creek	Blind and Spring Gulches West of Little Hansen Spring	Straight Creek : West of Little Hansen mixture
Proportion initial mixture			**0.53 : 0.47**
Proportion final mixture			**0.57 : 0.43**
Temperature, °C	7.7	9.5	8.96
pH	3.0	7.71	5.45
Specific conductance, µS/cm	3,776	1,080	1,898
Total dissolved solids, ppm	2,810	886	1,327
Eh, V	.780	.449	.443
	Constituent, mg/L		
Calcium	349	176	229
Magnesium	113	39.1	61.5
Sodium	8.1	22.6	18.2
Potassium	.75	2.38	1.89
Sulfate (SO_4)	[1]2,070	412	913
Alkalinity as HCO_3	<1	213	31.6
Fluoride	7.70	2.00	3.73
Silica	74.2	19.1	35.8
Aluminum	91.5	<.002	22.7
Iron (total)	65.0	<.002	.16
Iron (II)	.50	<.002	.15
Manganese	20.8	<.001	6.30
Copper	1.87	<.0005	.57
Nickel	.727	<.002	.21
Zinc	7.63	<.004	2.31
Cadmium	.039	<.0005	.012
Lead	.012	<.0001	.004
Chromium	.040	<.0005	.012
Cobalt	--	--	--
Beryllium	.078	<.001	.025

[1]Initial SO_4 concentration of 2,030 mg/L adjusted to charge balance the solution.

Table 14. pH, aluminum, and iron concentrations calculated by assuming different aluminous minerals precipitate upon mixing in the Sulphur Gulch catchment.

[Log K_{sp}, logarithm of the solubility-product constant; mg/L, milligrams per liter; T, total; a, amorphous; μc, microcrystalline; c, crystalline]

Phase	Log Ksp	pH	Al, in mg/L	Fe(T), in mg/L
$Al(OH)_3$(a)	10.8	5.45	22.8	0.16
Gibbsite (μc)	9.35	4.95	20.4	.18
Gibbsite (c)	8.11	4.52	19.5	.24
Kaolinite	7.435	4.18	18.8	.43
Basaluminite (a)	26.3	4.68	18.2	.20
Basaluminite (c)	22.7	4.33	17.4	.31
Alunite	–1.4	5.68	23.8	.16

Table 15. Water-quality constituents of concern for lower Sulphur Gulch drainage and debris fan.

[Values exceeding ground-water quality standards (table 1) shown in bold; mg/L, milligrams per liter]

Water-quality constituent (Sulphur Gulch alluvial ground water)	Range, in mg/L (except pH)
Aluminum (Al)	**12–23**
Beryllium (Be)	**0.03**
Cadmium (Cd)	0.01
Chromium (Cr)	0.01
Cobalt (Co)	**0.09**
Copper (Cu)	0.6
Fluoride (F)	**3.7**
Iron (Fe)	0.01–0.4
Lead (Pb)	0.004
Manganese (Mn)	**6.3**
Nickel (Ni)	0.2
Sulfate (SO_4)	**913**
Zinc (Zn)	2.3
Dissolved solids	**1,327**
pH (standard units)	**4.2–5.7**

and set the lower bound. Trace elements such as Co, Ni, Cr, Zn, and Cd were treated conservatively and simply diluted in the appropriate proportions. Beryllium was the only element that was treated differently from the others. Beryllium was assumed to be present in a higher concentration in the original upper Sulphur Gulch drainage water than in the Straight Creek drainage water because of the closer proximity of Sulphur Gulch to beryllium-enriched alteration of the Questa ore body. The original concentration before mixing was assumed to be equal to the highest concentration found in the USGS study for unmined areas, that from well CC–2A (0.078 mg/L). It was then mixed conservatively to obtain the final concentration.

The final mixed composition in table 13, assumed to be similar to the type of water that entered the Sulphur Gulch debris fan, was used to provide the concentrations for constituents of concern listed in table 15. All values were rounded off to the nearest two digits except when the concentration was less than 1 mg/L, and then they were rounded off to the nearest digit.

Sugar Shack Catchments

The area of the Sugar Shack waste-rock piles facing the Red River (areas marked 1, 2, and 3 in fig. 51; areas marked 8, 9, and 10 on plate 1) contain natural scars buried under waste rock. Before mining, the only aquifer of note would be the relatively impermeable bedrock. With waste-rock piles in place, they now have the potential to form overlying unconsolidated aquifers, although the greater portion of them are unsaturated (Molycorp, oral and written commun., 2002–2005). The question is often posed as to how much of the mobilized contaminants from this area originate from natural scars and how much from waste-rock leachates. It must be noted again that the aim of this USGS study was to determine what were the pre-mining ground-water quality concentrations, not to distinguish between what is being released currently from natural scars and what is being released currently from waste-rock piles where the two are intermixed in the same small catchment. Some of our results may be helpful in reaching those conclusions, but they are not the goal of this study.

These three catchments are not the same geologically. The two on the sides (1 and 3 in fig. 51; 8 and 10 on plate 1; now designated “outside catchments”) have scars that are nearly the size of that in Straight Creek, but the total catchment area is much less. The catchment in the middle has a larger area than the other two and has no scar mapped except for rather small areas of scar overlap from the other catchments that could be within the errors of mapping accuracy. The middle catchment is also more deeply incised than the other catchments, which suggests it may be a “healed scar.” The term “healed scar” is meant to designate an area where a scar previously existed that no longer exists because something has changed to allow vegetation to develop and the erosion rate has slowed. The east forks of Straight Creek and Hottentot Creek may be examples of “healed scars.” Geologically, a healed scar is an area where the erosion has incised the QSP-altered bedrock enough that the rock now exposed to weathering has a decreased pyrite content. The weathering and erosion may have removed enough rock to get below the main zone of QSP alteration, or it may be simply a QSP zone of lower pyrite content. In either situation, the acid production has either stopped or decreased sufficiently to allow vegetation to grow.

The two outside catchments can be assumed to drain water of similar chemistry to Straight Creek. Based on the median values from table 5, the water-quality constituents of concern are listed for these catchments in table 16.

Table 16. Water-quality constituents of concern for two Sugar Shack catchments (8 and 10 on plate 1).

[Values exceeding ground-water quality standards (table 1) shown in bold; mg/L, milligrams per liter]

Water-quality constituent (Sugar Shack outside catchments)	Values, in mg/L (except pH)
Aluminum (Al)	**92**
Beryllium (Be)	**.03**
Cadmium (Cd)	**.04**
Chromium (Cr)	.04
Cobalt (Co)	**.3**
Copper (Cu)	**2**
Fluoride (F)	**8**
Iron (Fe)	**65**
Lead (Pb)	.01
Manganese (Mn)	**21**
Nickel (Ni)	**.7**
Sulfate (SO_4)	**2,030**
Zinc (Zn)	8
Dissolved solids	**2,800**
pH (standard units)	**3.0**

Table 17. Water-quality constituents of concern for middle Sugar Shack catchment (area 9 on plate 1).

[Values exceeding ground-water quality standards (table 1) shown in bold; mg/L, milligrams per liter; <, less than]

Water-quality constituent (Sugar Shack catchments)	Values, in mg/L (except pH)	Source
Aluminum (Al)	33–72	Table 1–2 Appendix 1
Beryllium (Be)	**0.02–0.07**	Table 1–2 Appendix 1
Cadmium (Cd)	<0.001–**0.02**	Table 1–2 Appendix 1
Chromium (Cr)	< 0.005–0.02	Table 1–2 Appendix 1
Cobalt (Co)	**0.07–0.25**	Table 1–2 Appendix 1
Copper (Cu)	0.4–**1.4**	Based on Straight Creek surface-water correlation; Nordstrom and others (2005)
Fluoride (F)	1.4–**68**	Table 1–2 Appendix 1
Iron (Fe)	**6–50**	Based on two Straight Creek samples of 525 and 1510 mg SO_4/L
Lead (Pb)	<0.0007	Table 1–2 Appendix 1
Manganese (Mn)	**2–14**	Table 1–2 Appendix 1
Nickel (Ni)	0.2–**0.6**	Table 1–2 Appendix 1
Sulfate (SO_4)	500–**1,500**	See text
Zinc (Zn)	0.7–5	Table 1–2 Appendix 1
Dissolved solids	700–**2,000**	Based on two Straight Creek samples of 525 and 1,510 mg SO_4/L
pH (standard units)	**3.5**	Measurement, see text

The middle catchment is likely mineralized, but to a lesser extent than the outside catchments. An estimate of the chemistry of this water can be obtained as follows. The east fork of Straight Creek is thought to be a "healed" scar; that is, it probably contained a scar at one time, but weathering has eroded through the pyrite-rich zone and now vegetation can grow. There is rarely any drainage from the east fork of Straight Creek. On one occasion a small flow of water was found, and the pH and specific conductance were measured at 3.45 standard units and 973 µS/cm, respectively. These data can be used as an analog for the middle catchment water chemistry. The correlation between specific conductance and sulfate concentrations for Straight Creek surface and ground waters gives a sulfate concentration of 486 mg/L for the east fork of Straight Creek. Utilizing the correlation equations in table 1–2 of Appendix 1 and the estimated sulfate concentration, the concentrations of other constituents were estimated (first number of range in table 17). Consideration of yield estimates from east fork drainage would indicate that water mixing from this drainage with the scar drainage of Straight Creek to produce the ground water sampled in SC–1A would have to contain sulfate concentrations to 1,500 mg/L. Hence, the same correlations were used to derive the upper limit of concentrations of other constituents in table 17.

Bedrock Ground Water

Bedrock ground waters on the mine site can contain a large range of solute concentrations depending on the lithology and type of alteration, on whether in a predominantly recharge or predominantly discharge zone, and on depth (affects redox parameters and degree of mixing with shallow ground water or surface water). For this discussion, only bedrock in the saturated zone and lying under some debris or soil/sediment cover will be considered. Bedrock ground waters have already been considered for Capulin Canyon and will not be considered further. The bedrock ground waters under consideration here would include the area underlying Sulphur Gulch and Sugar Shack catchments. Results from the Straight Creek bedrock ground-water investigation will be considered for analogous characteristics.

Of the four wells that were completed in bedrock in the Straight Creek catchment (SC–1B, SC–2B, SC–3B, SC–5B) problems were encountered with two wells, SC–2B and SC–3B. Well SC–2B was supposed to be an alluvial well, but water was not reached until bedrock was penetrated because it was located too close to the side of the canyon. When the well was completed, about one-third of the screened interval was accessible to the air and was open to oxidation. It cannot be considered further. Well SC–3B gave water-chemistry results that appeared to have some similarities with alluvial ground water and may have been slightly affected by being in a mixing zone. Though these irregularities exist for well SC–3B, it may be representative of some types of bedrock ground waters on the mine site. A common characteristic of waters from wells SC–1B and SC–5B is that they have reached aqueous

Table 18. Water-quality constituents of concern for the range of pre-mining bedrock ground waters exclusive of those in Capulin Canyon.

[Values exceeding ground-water quality standards (table 1) shown in bold; mg/L, milligrams per liter; ≤, less than or equal to]

Water-quality constituent (bedrock ground waters)	Values, in mg/L (except pH)	Source
Aluminum (Al)	0.004–0.01	SC–1B, SC–5B
Beryllium (Be)	0.001–**0.08**	SC–1B, SC–5B, MMW–35B, CC–2A
Cadmium (Cd)	≤0.0001	SC–1B, SC–5B
Chromium (Cr)	≤0.007	SC–1B, SC–5B
Cobalt (Co)	0.02	SC–1B, SC–5B
Copper (Cu)	≤0.003	SC–1B, SC–5B
Fluoride (F)	1–**3**	SC–1B, SC–5B, MMW–35B
Iron (Fe)	0.5–**2**	SC–1B, SC–5B
Lead (Pb)	≤0.001	SC–1B, SC–5B
Manganese (Mn)	**2–6**	SC–1B, SC–5B, MMW–35B
Nickel (Ni)	0.001–0.005	SC–1B, SC–5B
Sulfate (SO_4)	**1,400–1,900**	SC–1B, SC–5B
Zinc (Zn)	≤0.005	SC–1B, SC–5B
Dissolved solids	**2,000–3,500**	SC–1B, SC–5B
pH (standard units)	6.5–7.8	SC–1B, SC–5B

saturation with respect to siderite, rhodochrosite, calcite, celestine, and gypsum. Waters from SC–5B and SC–2B also have reached saturation with respect to fluorite. Ground water from SC–3B has only reached saturation with respect to siderite, fluorite, and gypsum.

The mineralogy of the alteration zones occurring in bedrock at the mine site indicate that the mineral dissolution and saturation levels found in Straight Creek bedrock ground waters apply to the mine site. Gypsum, rhodochrosite, calcite, and fluorite saturation are often reached in bedrock ground waters on the mine site (wells MMW–34B and MMW–35B; LoVetere and others, 2004). Sufficient similarity in mineralogy and water chemistry exists to utilize the data from SC–1B and SC–5B as analogs for pre-mining bedrock ground-water concentrations on the mine site with the exception noted earlier that beryllium, manganese, and iron concentrations seem to be higher on the mine site than at the Straight Creek site. The results are listed in table 18. Caution must be applied in using these results because some bedrock ground waters may be oxidizing or may mix with alluvial ground waters of lower pH so that a large range of "bedrock" ground-water chemistry is possible. The results in table 18 are meant to represent the larger proportion of bedrock ground-water chemistry, but certainly not the full range.

Summary

In April 2001, the U.S. Geological Survey (USGS) and the New Mexico Environment Department (NMED) began a cooperative study to infer the pre-mining ground-water quality at the Molycorp molybdenum mine site in the Red River Valley of northern New Mexico. This study was prompted by discussions between Molycorp and NMED and, as described in DP1055 (Discharge Permit 1055), indicated the USGS should execute a study of natural background (pre-mining) concentrations in ground water at the mine site. This report summarizes the results of this study with the estimates of pre-mining ground-water quality.

The Red River Valley lies along a volcanic caldera boundary, is highly mineralized, and contains highly mineralized ground water. It is within this terrain that molybdenite mineralization was discovered and has provided an economic source of molybdenum for 85 years. It has been known that naturally acidic ground water occurs in this valley and may be widespread. It is an area where natural concentrations of metals are high enough to be environmentally deleterious, and this background level needs to be better defined so as to apply justifiable regulatory standards.

Most of the rock exposed to weathering both on the mine site and east of the mine site along the north flank of the Red River consists of two Tertiary volcanic flows—a rhyolitic tuff overlying an andesite. The Tertiary andesite (and the tuff to some extent) has been hydrothermally altered to varying degrees. The most intense alteration, quartz-sericite-pyrite (QSP), contains substantial pyrite and weathers quickly to form iron-rich acid-sulfate waters that hasten physical weathering. This QSP alteration forms scar areas of rapid debris flow, keeping rock outcrops denuded of vegetation. Catchments containing scars also contain acid ground waters in the debris fan that eventually are neutralized by the carbonate-buffered water in the Red River alluvial aquifer.

The exact flow path of ground water, the exact composition of reactive minerals and their surfaces encountered during ground-water flow, and the exact dissolution rate of every important reactive mineral for any specific site are not predictable quantities. Just the mineral dissolution rate alone is a complex function of surface area, surface composition, temperature, pH, and solution composition. Therefore, direct measurements of the spatial and temporal variations of water chemistry are necessary. However, once the data are obtained, a quantitative and deterministic interpretation that can be generalized for similar sites is possible. This was the approach used in this study.

The key to the determination of pre-mining ground-water quality at the mine site was to study the geological, hydrological, and geochemical processes at a proximal analog site that has not been disturbed by mining. The Straight Creek catchment was chosen for this purpose; it contains the same geologic and hydrologic features as the mine site and differs primarily in not having an erosional surface that cuts as

deep into the hydrothermally altered zones as the mine site. Twenty-seven reports detail the geological, mineralogical, hydrological, and geochemical characteristics of the analog site and other areas in the Red River Valley, including the mine site, that help to infer the physical and chemical properties of ground water at the mine site before mining took place. These 27 reports include surface mapping of mineralogy by Airborne Visible-Infrared Imaging Spectroscopy (AVIRIS); environmental geology of the Red River Valley; mineralogy and mineral chemistry to identify the source of dissolved constituents of concern; geophysical studies on depth to ground-water table and to bedrock; bedrock fractures and their potential influence on ground-water flow; lake-sediment chemistry; leaching studies of scar and waste-rock materials; compilations of historical surface-water and ground-water quality; synoptic/tracer studies with mass loadings in the Red River; temporal trends in Red River water quality; reactive-transport modeling of the Red River; hydrology and water balance for the Red River Valley; ground-water geochemistry of wells in areas unaffected by mining; and quality assurance and quality control of water analyses. Specific studies aimed at elucidating ground-water processes at the Straight Creek analog site include electrical surveys; high-resolution seismic surveys; age-dating with tritium/helium; water budget, ground-water hydrology, and geochemistry; and comparison of mineralogy and lithology to that of the mine site.

Eleven wells were installed and monitored, surface-water drainage was monitored, and two existing wells were monitored in the Straight Creek catchment. The contact between the Straight Creek debris fan and bedrock was outlined with high-resolution seismic profiles modeled tomographically. The bottom of the debris fan lies on a highly irregular surface, and ground water in the debris fan is acidic with pH values of 3–4, carrying high concentrations of dissolved sulfate and metals. In the underlying bedrock, the ground water has neutral pH, and most trace elements are in low concentration, but iron, manganese, and sulfate remain at high concentration.

The Straight Creek debris fan is fed primarily by Straight Creek surface water of low pH (2.5–3) derived from the weathering of QSP-altered bedrock with a high pyrite content (up to 10 percent). This surface water contains only oxidized iron, but after it infiltrates the fan, it becomes reduced with the removal of some copper and the addition of silica and sodium. This ground water is diluted to one-half of its original concentration from canyon seepage and from mixing with Red River alluvial ground water at the toe. Some aluminum and silica are removed in the most diluted waters (near pH 4). Most dissolved constituents in these alluvial ground waters are diluted proportionally with sulfate, as shown by significant linear correlations with sulfate. Exceptions include barium, which is limited by barite solubility, and strontium, which appears to be derived from carbonate mineral dissolution. These same linear correlations held for most elements in other catchments containing naturally acidic ground water. These trends provided a constraint on mineral weathering under acidic conditions.

Mineral solubility controls are effective in limiting the concentrations of nine constituents. These controls are manifested in two ways—by the common-ion effect, which shows up in plots of key dissolved constituents, and by plots of saturation indices. Ferric iron is limited by the solubility of a hydrous ferric-oxide phase (HFO), and ferrous iron is limited by the solubility of siderite. Manganese is limited by the solubility of rhodochrosite. Aluminum and silica are limited by the solubility of amorphous aluminum hydroxide, a hydrous aluminosilicate colloid or clay, and amorphous silica, depending on pH and concentration. Calcium is limited by the solubility of gypsum or calcite, depending on pH. Magnesium concentrations approach dolomite solubility saturation for a few waters. Fluoride is limited by the solubility of fluorite. Barium is limited by the solubility of barite. Solubility limits for calcite, siderite, rhodochrosite, and fluorite are reached at circumneutral pH values. Solubility limits for HFO are reached at pH values of 2.5 and higher. Solubility limits for aluminum are reached at pH values of 4 and higher for ground water and 5 or higher for surface water. Gypsum and barite solubilities are independent of pH.

The metal-sulfate correlation trends for acidic ground waters at Straight Creek generally agreed well with data from ground waters in other catchments unaffected by mining activities and provided a framework to delineate ranges of concentrations for each catchment on the mine site where no solubility control exists. The geochemical constraints that define solute concentrations had to be applied separately to bedrock and alluvial aquifers and, in the example of Capulin Canyon, had to be applied to different parts of the catchment because of hydrothermal alteration and mineralization that changes substantially with distance. Exceptions to the correlation trends were noted for beryllium, fluoride, and manganese because examples were found where the pH is too low (about 6.0) for any solubility control.

Sulfate loading from natural scar areas upstream from the mine site (Hottentot, Straight, and Hansen Creeks) has been thought to be a substantial source of sulfate loading into the Red River during ground-water emergence in the Columbine Park area. Using data of yields of water flow from the appropriate catchments, a water flow balance was derived for the area of the upstream scars. Estimates and measurements of sulfate concentrations for these ground waters were then combined with the water-flow balance to complete a sulfate-load balance for this limited section of the river. The results indicate that sulfate from scar drainages continues downstream in the Red River alluvium to the mine site and might account for more than 50 percent of the sulfate loading that emerges into the Red River in the Columbine Park reach if no sulfate fluxes entered the Red River alluvium from the mine site. However, increases in sulfate concentration occur in the alluvial ground water along the mine-site reach, which suggests substantial sulfate fluxes from the mine site. This investigation has not attempted to measure sulfate fluxes from the mine site nor to resolve how much of the sulfate loading is from mining activities relative to that from natural scars on the mine site. Further data are needed to determine the sources and amounts of these loads.

The results demonstrate that ground-water quality standards in the State of New Mexico can be exceeded by natural conditions in the Red River Valley. Standards are commonly exceeded by tenfold with manganese, iron, fluoride, and sulfate. Manganese can exceed the standards by as much as 250 times. The high manganese concentrations are caused by the common occurrence and high solubility of rhodochrosite and manganiferous calcite in acidic water. The high natural concentrations of other constituents were caused by the particular geological and hydrological conditions that exist in the Red River Valley. Extensive hydrothermal alteration has emplaced pyrite, sphalerite, chalcopyrite, calcite, rhodochrosite, fluorite, and illite with enriched concentrations of cobalt, nickel, cadmium, beryllium, and chromium in addition to iron, zinc, copper, sulfur, and manganese that are major components of these minerals. Cobalt and nickel are primarily found in the pyrite, cadmium in the sphalerite, beryllium in the illite, and chromium in the chlorite.

This investigation took a scientific approach to determine the sources of constituents and properties of regulatory concern (Al, Be, Cd, Co, Cr, Cu, F, Fe, Mn, Ni, Pb, SO_4, Zn, and pH) and hydrogeochemical processes affecting their transport. The objective was to infer pre-mining ground-water chemistry at an active mine site. The results have shown that the objective is achievable but greatly complicated by the small-scale heterogeneities in geology, mineralogy, and hydrology. Such heterogeneities increase the number of measurements needed, the level of detail that must be interpreted, and the uncertainties in the final estimates. The approach used including metal-solute concentration trends relative to sulfate concentrations, flux or mass-loading estimates, and the generalizations based on mineral solubility controls should be transferable to other sites where estimates of natural water/rock interactions in mineralized landscapes are required.

References Cited

Alpers, C.N., and Blowes, D.W., eds., 1994, Environmental geochemistry of sulfide oxidation: Washington, D.C., American Chemical Society Symposium Series 550, 681 p.

Alpers, C.N., and Nordstrom, D.K., 2000, Estimation of pre-mining conditions for trace metal mobility in mineralized areas, *in* Proceedings, Fifth International Conference on Acid Rock Drainage, ICARD 2000, v. 1: Littleton, Colo., Society for Mining, Metallurgy, and Exploration, p. 463–472.

Balarew, D., 1925, Löslichkeit und Korngrösse: Zeitscrift für anorganische und allgemeine Chemie, v. 145, p. 122–126.

Ball, J.W., and Nordstrom, D.K., 1991, User's manual for WATEQ4F, with revised thermodynamic data base and test cases for calculating speciation of major, trace, and redox elements in natural waters: U.S. Geological Survey Open-File Report 91–183, 189 p.

Ball, J.W., and Nordstrom, D.K., 1998, Critical evaluation and selection of standard state thermodynamic properties for chromium metal and its aqueous ions, hydrolysis species, oxides, and hydroxides: Journal of Chemical & Engineering Data, v. 43, no. 6, p. 895–918.

Ball, J.W., Runkel, R.L., and Nordstrom, D.K., 2005, Questa baseline and pre-mining ground-water quality investigation. 12. Geochemical and reactive-transport modeling based on tracer injection-synoptic sampling studies for the Red River, New Mexico, 2001–2002: U.S. Geological Survey Scientific Investigations Report 2005–5149, 68 p.

Banks, D.A., Giuliani, G., Yardley, B.W.D., and Cheilletz, A., 2000, Emerald mineralization in Colombia—fluid chemistry and the role of brine mixing: Mineralium Deposita, v. 35, p. 699–713.

Baron, Dirk, and Palmer, C.D., 1996, Solubility of jarosite at 4-35°C: Geochimica et Cosmochimica Acta, v. 60, p. 185–195.

Bates, R.L., and Jackson, J.A., eds., 1980, Glossary of geology (2d ed.): Falls Church, Va., American Geological Institute, p. 418.

Bigham, J.M., and Nordstrom, D.K., 2000, Iron and aluminum hydroxysulfates from acid sulfate waters, *in* Alpers, C.N., Jambor, J.L., and Nordstrom, D.K., eds., Reviews in mineralogy and geochemistry, v. 40, Sulfate minerals—crystallography, geochemistry, and environmental significance, Ribbe, P.H., series ed., Washington, D.C.: Washington, D.C., Mineralogical Society of America and the Geochemical Society, p. 351–403.

Blanchard, P.J., Bartolino, J.R., Naus, C.A., and Morin, R.H., 2007, Questa baseline and pre-mining ground-water quality investigation. 15. Methods and results of Phase II and III well installation and development and results of well logging, hydraulic testing, and water-level measurements in the Red River Valley, New Mexico, 2002–04: U.S. Geological Survey Scientific Investigations Report 2006-5246, 56 p.

Blowes, D.W., Ptacek, C.J., Jambor, J.L., and Weisener, C.G., 2004, The geochemistry of acid mine drainage, *in* Lollar, B.S., ed., Environmental geochemistry, v. 9, Treatise on Geochemistry, Holland, H.D., and Turekian, K.K., ex. eds.: Amsterdam, Elsevier, p. 149–204.

Blowes, D.W., Ptacek, C.J., and Jurjovec, Jasna, 2003, Mill tailings—hydrogeology and geochemistry, *in* Jambor, J.L., Blowes, D.W., and Ritchie, A.I.M., eds., Environmental aspects of mine wastes: Mineralogical Association of Canada, Short Course Series, v. 31, chap. 5, p. 95–116.

Booth, C.J., 2002, The effects of longwall coal mining on overlying aquifers, *in* Younger, P.L., and Robins, N.S., eds., Mine water hydrogeology and geochemistry: London, U.K., The Geological Society, The Geological Society Special Publication no. 198, p. 17–45.

Borland, J.P., DeWees, R.K., McCracken, R.L., Lepp, R.L., Ortiz, D., and Shaull, D.A., 1990, Water resources data, New Mexico, water year 1989: U.S. Geological Survey Water-Data Report NM–89–1, 426 p.

Bowser, C.J., and Jones, B.F., 2002, Mineralogic controls on the composition of natural waters dominated by silicate hydrolysis: American Journal of Science, v. 302, p. 582–662.

Brady, K.B.C., Smith, M.W., and Schueck, Joseph, eds., 1998, Coal mine drainage prediction and pollution prevention in Pennsylvania: Pennsylvania Department of Environmental Protection.

Brandt, Felix, Bosbach, Dirk, Krawczyk-Bärsch, Arnold, Thuro, and Bernhard, Gert, 2003, Chlorite dissolution in the acid pH-range—a combined microscopic and macroscopic approach: Geochimica et Cosmochimica Acta, v. 67, p. 1451–1461.

Bricker, O.P., Jones, B.F., and Bowser, C.J., 2004, Mass-balance approach to interpreting weathering reactions in watershed systems, *in* Drever, J.I., ed., Treatise on geochemistry, v. 5, Surface and ground water, weathering, and soils: Amsterdam, Elsevier, p. 119–132.

Briggs, P.H., Sutley, S.J., and Livo, K.E., 2003, Questa baseline and pre-mining ground-water quality investigation. 11. Geochemistry of alteration scars and waste piles: U.S. Geological Survey Open-File Report 2003–458, 17 p., *http://pubs.usgs.gov/of/2003/ofr-03-458*

Brown, J.G., and Glynn, P.D., 2003, Kinetic dissolution of carbonates and Mn oxides in acidic water—measurement of in situ field rates and reaction transport modeling: Applied Geochemistry, v. 18, p. 1225–1239.

Caine, J.S., 2003, Questa baseline and pre-mining ground-water quality investigation. 6. Preliminary brittle structural geologic data, Questa mining district, southern Sangre de Cristo Mountains: U.S. Geological Survey Open-File Report 2003–280, 31 p., *http://pubs.usgs.gov/of/2003/ofr-03-280*

Caine, J.S., 2007, Questa baseline and pre-mining ground-water quality investigation. 18. Characterization of brittle structures in the Questa caldera and speculation on their potential impacts on the bedrock ground-water flow system, Red River watershed, New Mexico: U.S. Geological Survey Professional Paper 1729, 37 p.

Carpenter, R.H., 1968, Geology and ore deposits of the Questa molybdenum mine area, Taos County, New Mexico, *in* Ridge, J.D., ed., Ore deposits of the United States, 1933–1967 (Graton-Sales volume): New York, American Institute of Mining, Metallurgical, and Petroleum Engineers, v. 2, p. 1328–1350.

Church, S.E., Fey, D.L., and Marot, M.E., 2005, Questa baseline and pre-mining ground-water quality investigation. 8. Lake-sediment geochemical record from 1960 to 2002, Eagle Rock and Fawn Lakes, Taos County, New Mexico: U.S. Geological Survey Scientific Investigations Report 2005–5006, 40 p.

Dietzel, Martin, 2000, Dissolution of silicates and the stability of polysilicic acid: Geochimica et Cosmochimica Acta, v. 64, p. 3275–3281.

Driscoll, C.T., Baker, J.P., Bisogni, J.J., and Schofield, C.L., 1984, Aluminum speciation and equilibria in dilute acidic surface waters of the Adirondack region of New York State, *in* Bricker, O.P., ed., Geological aspects of acid deposition: Boston, Butterworth Publishers, p. 55–75.

Dzomback, D.A., and Morel, F.M.M., 1990, Surface complexation modeling: New York, Wiley-Interscience, 393 p.

Emsley, John, 2001, Nature's building blocks, an A–Z guide to the elements: Oxford, UK, Oxford University Press, 539 p.

Exley, Christopher, Schneider, Celine, and Doucet, F.J., 2002, The reaction of aluminium with silicic acid in acidic solution—an important mechanism in controlling the biological availability of aluminium?: Coordination Chemistry Reviews, v. 228, p. 127–135.

Felmy, A.R., Dhanpat, Rai, and Moore, D.A., 1993, The solubility of (Ba, Sr)SO_4 precipitates—thermodynamic and reaction path analysis: Geochimica et Cosmochimica Acta, v. 57, p. 4345–4363.

Fernández-Rubio, Rafael, 1999, Mine, water, and the environment: International Mine Water Association, September 13–17, 1999, Sevilla, Spain, 834 p.

Fleischer, Michael, 1955, Minor elements in some sulfide minerals, *in* Bateman, A.M., ed., Economic geology, Fiftieth Anniversary Volume, 1905–1955, Part II: Lancaster, Pa., Lancaster Press, p. 970–1024.

Gale, V.G., and Thompson, A.J.B., 2001, Reconnaissance study of waste rock mineralogy—Questa, New Mexico, petrography, PIMA spectral analysis and Rietvold analysis: Petrascience Consultants, Inc., January 31, 2001.

Garrels, R.M., and Christ, C.L., 1965, Solutions, minerals, and equilibria: New York. Harper and Row, 450 p.

Glynn, P.D., 1991, Effect of impurities in gypsum on contaminant transport at Pinal Creek, Arizona, *in* Mallard, G.E., and Aronson, D.A., U.S. Geological Survey Toxic Substances Hydrology Program—Proceedings of the Technical Meeting, Monterey, California, March 11–15, 1991: U.S. Geological Survey Water-Resources Investigations Report 91–4034, p. 466–474.

Goleva, G.A., 1977, Hydrogeochemistry of ore elements: Nedra, Moscow, 215 p.

Hageman, P.L., and Briggs, P.H., 2000, A simple field leach for rapid screening and qualitative characterization of mine-waste material on abandoned mine lands, *in* Proceedings from the Fifth International Conference on Acid Rock Drainage, Denver, Colo., May 21–24, 2000: Society for Mining, Metallurgy and Exploration, Inc., v. II, p. 1463–1475.

Harrington, L.F., Cooper, E.N., and Vasudevan, D., 2003, Fluoride sorption and associated aluminum release in variable charge soil: Journal of Colloid and Interface Science, v. 267, p. 302–313.

Hem, J.D., 1985, Study and interpretation of the chemical characteristics of natural waters (3d ed.): U.S. Geological Survey Water-Supply Paper 2254, 264 p.

Hem, J.D., and Roberson, C.E., 1990, Aluminum hydrolysis reactions and products in mildly acidic aqueous systems, *in* Melchior, D.C., and Bassett, R.L., eds., Chemical modeling of aqueous systems II, American Chemical Society Symposium Series 416: Washington, D.C., American Chemical Society, p. 429–446.

Hina, A., and Nancollas, G.H., 2000, Precipitation and dissolution of alkaline earth sulfates—kinetics and surface energy, *in* Alpers, C.N., Jambor, J.L., and Nordstrom, D.K., eds., Sulfate minerals—crystallography, geochemistry, and environmental significance: The Mineralogical Society of America and the Geochemical Society, Reviews in Mineralogy and Geochemistry; v. 40, p. 277–301.

Icopini, G.A., Brantley, S.L., and Heaney, P.J., 2005, Kinetics of silica oligomerization and noncolloid formation as function of pH and ionic strength at 25ºC: Geochimica et Cosmochimica Acta, v. 69, p. 293–303.

Ihde, A.J., 1984, The development of modern chemistry: New York, Dover Publications, 851 p.

Iler, R.K., 1979, The chemistry of silica—solubility, poly merization, colloid and surface properties, and biochemistry: New York, Wiley-Interscience, 866 p.

Jambor, J.L., Blowes, D.W., and Ritchie, A.I.M., 2003, Environmental aspects of mine wastes: Mineralogical Association of Canada, Short Course Series, v. 31, 430 p.

Kimball, B.A., Nordstrom, D.K., Runkel, R.L., and Verplanck, P.L., 2006, Questa baseline and pre-mining ground-water quality investigation. 23. Quantification of mass loading for Red River, New Mexico: U.S. Geological Survey Scientific Investigations Report 2006–5004, 44 p.

Knight, P.J., 1990, The flora of the Sangre de Cristo Mountains, New Mexico, *in* Bauer, P.W., Lucas, S.G., Mawer, C.K., and McIntosh, W.C., eds., Tectonic development of the southern Sangre de Cristo Mountains, New Mexico: New Mexico Geological Society, 41st field conference, September 12–15, 1990, p. 94–95.

Krauskopf, K.B., 1956, Factors controlling the concentrations of thirteen rare metals in sea-water: Geochimica et Cosmochimica Acta, v. 9, p. 1–32.

Krauskopf, K.B., and Bird, D.K., 1995, Introduction to geochemistry (3d ed.): New York, McGraw-Hill, 647 p.

Lipman, P.W., 1981, Volcano-tectonic setting of tertiary ore deposits, southern Rocky Mountains: Arizona Geological Society Digest, v. 14, p. 199–213.

Livo, K.E., and Clark, R.N., 2002, Mapped minerals at Questa, New Mexico, using airborne visible-infrared imaging spectrometer (AVIRIS) data—preliminary report: U.S. Geological Survey Open-File Report 2002–0026, 13 p.

LoVetere, S.H., Nordstrom, D.K., Maest, A.S., and Naus, C.M., 2004, Questa baseline and pre-mining ground-water quality investigation. 3. Historical ground-water quality for the Red River Valley, New Mexico: U.S. Geological Survey Water-Resources Investigations Report 2003–4186, 49 p. (contains CD).

Lucius, J.E., Bisdorf, R.J., and Abraham, Jared, 2001, Results of electrical surveys near Red River, New Mexico: U.S. Geological Survey Open-File Report 2001–0331, available on Web, accessed August 21, 2007, at *http://pubs.usgs.gov/of/2001/of-1-331.html*

Ludington, S.D., Plumlee, G.S., Caine, J.S., Bove, D.J., Holloway, J.M., and Livo, K.E., 2005, Questa baseline and pre-mining ground-water quality investigation. 10. Geologic influences on ground and surface waters in the lower Red River watershed, New Mexico: U.S. Geological Survey Scientific Investigations Report 2004–5245, 45 p.

Maest, A.M., Nordstrom, D.K., and LoVetere, S.H., 2004, Questa baseline and pre-mining ground-water quality investigation. 4. Historical surface-water quality for the Red River Valley, New Mexico, 1965 to 2001: U.S. Geological Survey Scientific Investigations Report 2004–5063, 150 p.

Maki, Nobufumi, and Tanaka, Nobuyuki, 1985, Cobalt, rhodium, and iridium, *in* Bard, A.J., Parsons, Roger, and Jordan, Joseph, eds., Standard potentials in aqueous solution: New York, Marcel Dekker, Inc., p. 367–382.

Mast, M.A., Verplanck, P.L., Yager, D.B., Wright, W.G., and Bove, D.J., 2000, Natural sources of metals to surface waters in the upper Animas River watershed, Colorado, *in* Proceedings, Fifth International Conference on Acid Rock Drainage, ICARD 2000, v. 1: Littleton, Colo., Society for Mining, Metallurgy, and Exploration, p. 513–522.

McAda, D.P., and Naus, C.A., in press, Questa baseline and pre-mining ground-water quality investigation. 22. Groundwater budget for the Straight Creek drainage basin, Red River Valley, New Mexico, *with a section on* Sulphur Gulch water budget, by K.R. Vincent: U.S. Geological Survey Scientific Investigations Report 2007–5149.

McCleskey, R.B., Nordstrom, D.K., and Naus, C.A., 2004, Questa baseline and pre-mining ground-water quality investigation. 16. Quality assurance and quality control for water analyses: U.S. Geological Survey Open-File Report 2004–1341, 105 p.

McCleskey, R.B., Nordstrom, D.K., Verplanck, P.L., Steiger, J.I., and Kimball, B.A., 2003, Questa baseline and pre-mining ground-water quality investigation. 2. Low-flow (2001) and snowmelt (2002) synoptic/tracer water chemistry for the Red River, New Mexico: U.S. Geological Survey Open-File Report 2003–148, 166 p.

Melancon, S.M.S., Blakely, L.S., and Janik, J.J., 1982, Site specific water quality assessment—Red River, New Mexico: U.S. Environmental Protection Agency Report 600/x–82–025.

Meyer, J.W., and Leonardson, R.W., 1990, Tectonic, hydrothermal and geomorphic controls on alteration scar formation near Questa, New Mexico: New Mexico Geological Society Guidebook, v. 41, p. 417–422.

Meyer, J.W., and Leonardson, R.W., 1997, Geology of the Questa mining district—volcanic, plutonic and hydrothermal history: Socorro, New Mexico, Bureau of Mines and Mineral Resources Bulletin, Open File Report 431, 187 p.

Molling, P.A., 1989, Applications of the reaction progress variables to the hydrothermal alteration associated with the deposition of the Questa molybdenum deposit, New Mexico: Baltimore, Johns Hopkins University, unpublished Ph. D. dissertation, 229 p.

National Academy of Sciences, NAS, 1977, Drinking water and health: Washington, D.C., National Academy of Sciences Press, p. 308.

Naus, C.A., McAda, D.P., and Myers, N.C., 2006, Questa baseline and pre-mining ground-water quality investigation. 21. Hydrology and water balance of the Red River Valley, New Mexico 1930–2004: U.S. Geological Survey Scientific Investigations Report 2006–5040, 37 p.

Naus, C.A., McCleskey, R.B., Nordstrom, D.K., Donohoe, L.C., Hunt, A.G., Paillet, F.L., Morin, R.H., and Verplanck, P.L., 2005, Questa baseline and pre-mining ground-water quality investigation. 5. Well installation, water-level data, and surface- and ground-water geochemistry in the Straight Creek drainage basin, Red River Valley, New Mexico, 2001–03: U.S. Geological Survey Scientific Investigations Report 2005–5088, 228 p.

Nordstrom, D.K., 1982, The effect of sulfate on aluminum concentrations in natural waters—some stability relations in the system Al_2O_3–SO_3–H_2O at 298 K: Geochimica et Cosmochimica Acta, v. 46, p. 681–692.

Nordstrom, D.K., 1999, Some fundamentals of aqueous geochemistry, *in* Plumlee, G.S., and Logsdon, M.J., eds., Environmental geochemistry of mineral deposits, Reviews in economic geology, Part A—Processes, techniques, and health issues, v. 6A: Littleton, Colo., Society of Economic Geologists, Inc., p. 117–123.

Nordstrom, D.K., 2000, Advances in the hydrogeochemistry and microbiology of acid mine waters: International Geology Review, v. 42, 499–515.

Nordstrom, D.K., 2004, Modeling low-temperature geochemical processes, *in* Drever, J.I., ed., Treatise on geochemistry, v. 5, Surface and ground water, weathering, and soils: Amsterdam, Elsevier, p. 37–72.

Nordstrom, D.K., 2005, A river on the edge—Water quality in the Red River and the USGS background study, *in* Price, L.G., Bland, Douglas, McLemore, V.T., and Barker, J.M., eds., Mining in New Mexico—the environment, water, economics, and sustainable development: Decision-Makers Field Conference 2005, Taos region, New Mexico Bureau of Geology and Mineral Resources, Socorro, N. Mex., p. 64–67.

Nordstrom, D.K, 2006, Investigation 25—Summary Report Summary of results and baseline and pre-mining ground water geochemistry, Red River Valley, Taos County, New Mexico, 2001–2005:U.S. Geological Survey Professional Paper 1728.

Nordstrom, D.K., and Archer, D.G., 2003, Arsenic thermodynamic data and environmental geochemistry, *in* Welch, A.H., and Stollenwerk, K.G., eds., Arsenic in ground water: Boston, Kluwer Publishers, p. 1–26.

Nordstrom, D.K., and Ball, J.W., 1986, The geochemical behavior of aluminum in acidified surface waters: Science, v. 232, p. 54–56.

Nordstrom, D.K., and May, H.M., 1996, Aqueous equilibrium data for mononuclear aluminum species, *in* Sposito, Garrison, ed., The environmental chemistry of aluminum (2d ed.): Boca Raton, Fla., CRC Lewis Publishers, chap. 2, p. 39–80.

Nordstrom, D.K., McCleskey, R.B., Hunt, A.G., and Naus, C.A., 2005, Questa baseline and pre-mining ground-water quality investigation. 14. Interpretation of ground-water geochemistry for wells other than the Straight Creek catchment, Red River Valley, Taos County, New Mexico, 2002–2003: U.S. Geological Survey Scientific Investigations Report 2005–5050, 84 p.

Nordstrom, D.K., and Munoz, J.L., 1994, Geochemical thermodynamics (2d ed.): Boston, Blackwell Scientific Publications, 493 p.

Nordstrom, D.K., Plummer, L.N., Langmuir, D., Busenberg, E., May, H.M., Jones, B.F., and Parkhurst, D.L., 1990, Revised chemical equilibrium data for water-mineral reactions and their limitations, chap. 31 in Chemical modeling, *in* Bassett, R.L., and Melchior, D., eds., Aqueous systems II.: American Chemical Society Symposium Series 416, p. 398–413.

Nordstrom, D.K., Wright, W.G., Mast, M.A., Bove, D.L., and Rye, R.O., 2007, Aqueous-sulfate stable isotopes—a study of mining-affected and natural acidic drainage, *in* Church, S.E., and von Guerard, Paul, eds., Abandoned mine lands: U.S. Geological Survey Professional Paper 1651, chap. E8.

Oze, Christopher, Fendorf, Scott, Bird, D.K., and Coleman, R.G., 2004, Chromium geochemistry in serpentinized ultramafic rocks and serpentine soils from the Franciscan complex of California: American Journal of Science, v. 304, p. 67–101.

Parkhurst, D.L., 1987, Chemical analyses of water samples from the Picher Mining area, northeastern Oklahoma and southeast Kansas: U.S. Geological Survey Open-File Report 87–453, 43 p.

Parkhurst, D.L., 1995, User's guide to PHREEQC—a computer program for speciation, reaction-path, advective transport, and inverse geochemical calculations: U.S. Geological Survey Water-Resources Investigations Report 95–4227, 143 p.

Parkhurst, D.L., 1997, Geochemical mole-balancing modeling with uncertain data: Water Resources Research, v. 33, p. 1957–1970.

Parkhurst, D.L., and Appelo, C.A.J., 1999, User's guide to PHREEQC (Version 2)—a computer program for speciation, batch-reaction, one-dimensional transport, and inverse geochemical calculations: U.S. Geological Survey Water-Resources Investigations Report 99–4259, 312 p.

Parkhurst, D.L., Plummer, L.N., and Thorstenson, D.C., 1982, BALANCE—a computer program for calculating mass transfer for geochemical reactions in ground water: U.S. Geological Survey Water-Resources Investigations Report 82–14, 29 p.

Pickering, W.F., 1979, Copper retention by soil/sediment components, *in* Nriagu, J.O., ed., Copper in the environment, part 1, Ecological cycling: New York, Wiley-Interscience, p. 217–253.

Playton, S.J., Davis, R.E., and McClaflin, R.G., 1980, Chemical quality of water in abandoned zinc mines in northeastern Oklahoma and southeastern Kansas: Oklahoma Geological Survey Circular 82.

Plumlee, G.S., and Logsdon, M.J., eds., 1999, Environmental geochemistry of mineral deposits—reviews in economic geology, part A—Processes, techniques, and health issues, v. 6A: Littleton, Colo., Society of Economic Geologists, Inc., 371 p.

Plumlee, G.S., Lowers, H.A., Ludington, S.D., Koening, A.E., and Briggs, P.H., 2005, Questa baseline and pre-mining ground-water quality investigation. 13. Mineral microscopy and chemistry of mined and unmined porphyry molybdenum mineralization along the Red River, New Mexico—implications for ground- and surface-water quality: U.S. Geological Survey Scientific Investigations Report 2005–1442, 95 p.

Plumlee, G.S., Ludington, S., Vincent, K.R., Verplanck, P.L., Caine, J.S., and Livo, K.E., in press, Questa baseline and pre-mining ground-water quality investigation. 7. A photographic record of chemical weathering, erosional processes, and potential debris-flow hazards in scar areas developed on hydrothermally altered rocks: U.S. Geological Survey Open-File Report 2006–1205.

Plummer, L.N., Busby, J.F., Lee, R.W., and Hanshaw, B.B., 1990, Geochemical modeling of the Madison aquifer in parts of Montana, Wyoming, and South Dakota: Water Resources Research, v. 26, p. 1981–2014.

Plummer, L.N., Parkhurst, D.L., and Thorstenson, D.C., 1983, Development of reaction models for groundwater systems: Geochimica et Cosmochimica Acta, v. 47, p. 665–685.

Posey, H.H., Renkin, M.L., and Woodling, John, 2000, Natural acid drainage in the upper Alamosa River of Colorado, *in* Proceedings, Fifth International Conference on Acid Rock Drainage, ICARD 2000, v. 1: Littleton, Colo., Society for Mining, Metallurgy, and Exploration, p. 485–498.

Powers, M.H., and Burton, B.L., 2004, Questa baseline and pre-mining ground-water quality investigation. 1. Depth to bedrock determinations using shallow seismic data acquired in the Straight Creek drainage near Red River, New Mexico: U.S. Geological Survey Open-File Report 2004–1236, 18 p.

Powers, M.H., and Burton, B.L., 2007, Questa baseline and pre-mining ground-water quality investigation. 24. Seismic refraction tomography for volume analysis of saturated alluvium in the Straight Creek drainage and its confluence with Red River, Taos County, New Mexico: U.S. Geological Survey Scientific Investigations Report 2006–5166, 19 p.

Rehrig, W.A., 1969, Fracturing and its effects on molybdenum mineralization at Questa, New Mexico: Tucson, University of Arizona, Ph.D. dissertation, 194 p.

Robertson Geoconsultants, Inc., RGC, 2000a, Interim background characterization study, Questa mine, New Mexico: Report 052008/6, June 2000, 33 p. (text only).

Robertson Geoconsultants, Inc., RGC, 2000b, Interim mine site characterization study, Questa mine, New Mexico: Report: 052008/10, November 2000.

Robertson Geoconsultants, Inc., RGC, 2001a, Background study data report, Questa mine, New Mexico: Report 052008/12, January 2001.

Robertson Geoconsultants, Inc., RGC, 2001b, Interim geochemical load balance for Red River basin near Questa mine, New Mexico: Report 052008/18, November 2001, 38 p. (text only).

Runkel, R.L., 1998, One-dimensional transport with inflow and storage (OTIS)—a solute transport model for streams and rivers: U.S. Geological Survey Water-Resources Investigations Report 98–4018, accessed at *http://co.water.usgs.gov/otis/*.

Runkel, R.L., and Kimball, B.A., 2002, Evaluating remedial alternatives for an acid mine drainage stream—application of a reactive transport model: Environmental Science and Technology, v. 36, p. 1093–1101.

Runnells, D.D., Shepard, T.A., and Angino, E.E., 1992, Metals in water—determining natural background concentrations in mineralized areas: Environmental Science and Technology, v. 26, p. 2316–2322.

Schilling, J.H., 1956, Geology of the Questa molybdenum mine area, Taos County, New Mexico: Socorro, State Bureau of Mines and Mineral Resources, New Mexico Institute of Mining and Technology Bulletin 51, 87 p.

Seal, R.R. II, 2003, Stable isotope geochemistry of mine waters and related solids, *in* Jambor, J.L., Blowes, D.L., and Ritchie, A.I.M., eds., Environmental aspects of mine wastes: Mineralogical Association of Canada Short Course Series, v. 31, p. 303–334.

Seal, R.R. II, Alpers, C.N., and Rye, R.O., 2000, Stable isotope systematics of sulfate minerals, *in* Alpers, C.N., Jambor, J.L., and Nordstrom, D.K., eds., Sulfate minerals—crystallography, geochemistry, and environmental significance: Reviews in Mineralogy and Geochemistry, v. 40, p. 541–602.

Shaw, Shannon, Wels, Christoph, Robertson, Andrew, Fortin, Sebastien, and Walker, Bruce, 2003, Background characterization study of naturally occurring acid rock drainage in the Sangre de Cristo Mountains, Taos County, New Mexico, *in* 6th International Conference on Acid Rock Drainage, April 2003, Cairns, Australia: p. 605–616.

Smith, K.S., Hageman, P.L., Briggs, P.H., Sutley, S.J., McCleskey, R.B., Livo, K.E., Verplanck, P.L., Adams, M.G., and Gemery-Hill, P.A., 2007, Questa baseline and pre-mining ground-water quality investigation. 19. Leaching characteristics of composited materials from mine waste-rock piles and naturally altered areas near Questa, New Mexico: U.S. Geological Survey Scientific Investigations Report 2006–5165, 49 p.

Smolka, L.R., and Tague, D.F., 1989, Intensive water quality survey of the middle Red River, Taos County, New Mexico, September 12–October 25, 1988: Santa Fe, New Mexico Health and Environment Department, Surveillance and Standards Section, Surface Water Quality Bureau, May, 87 p.

South Pass Resources, Inc., 1995, Supplemental report—discussion of the geology, hydrology, and water quality of the mine area, Molycorp facility, Taos County, New Mexico: Scottsdale, Ariz., February 15, 1995, 15 p.

Steffen, Robertson & Kirsten, 1995, Questa molybdenum mine geochemical assessment: Lakewood, Colo., SRK Project no. 09206, April 13, 1995, 44 p.

Tagirov, B., Schott, Jacque, and Harrichoury, J.C., 2002, Experimental study of aluminum-fluoride complexation in near-neutral and alkaline solutions to 300°C: Chemical Geology, v. 184, p. 301–310.

Toran, Laura, 1987, Sulfate contamination in groundwater from a carbonate-hosted mine: Journal of Contaminant Hydrology, v. 2, p. 1–29.

U.S. Geological Survey, 2004, Daily streamflow for the Nation, U.S. Geological Survey 08265000 Red River near Questa, New Mexico: Information available on Web, accessed 2005 at *http://nwis.waterdata.usgs.gov/usa/nwis/discharge*

Vail Engineering, Inc., 1989, A geochemical investigation of the origin of aluminum hydroxide precipitation in the Red River, Taos County, New Mexico: Consultants' report for Molycorp, Inc., June 1989, 43 p.

Vail Engineering, Inc., 1993, Interim study of the acidic drainage to the middle Red River, Taos County, New Mexico: Report to Molycorp, Inc., July 9, 1993.

Vail Engineering, Inc., 2000, Analysis of acid rock drainage in the middle reach of the Red River, Taos County, New Mexico: Interim report, July 4, 2000.

Vartanyan, G.S., ed., 1988, The impact of mining on the environment: Moscow, Proceedings of an International Workshop, June 18–25, 1986, UNEP, UNESCO, GKNT, 490 p.

Verplanck, P.L., Nordstrom, D.K., and McCleskey, R.B., 2006, Questa baseline and pre-mining ground-water quality investigation. 20. Water chemistry trends of the Red River, Taos County, New Mexico, with data from selected seeps, tributaries, and snow, 2000–2004: U.S. Geological Survey Scientific Investigations Report 2006–5028, 139 p.

Veselý, J., Norton, S.A., Skivan, P., Majer, V., Krám, P., Navrátil, T., and Kaste, J.M., 2002, Environmental chemistry of beryllium, *in* Grew, E.S., ed., Beryllium—mineralogy, petrology, and geochemistry, Reviews in mineralogy and geochemistry, v. 50: Washington, D.C., Mineralogical Society of America, p. 291–317.

Vincent, K.R., in press, Questa baseline and pre-mining ground-water quality investigation. 17. Geomorphology of the Red River Valley, Taos County, New Mexico, and influence on ground-water flow in the shallow alluvial aquifer: U.S. Geological Survey Scientific Investigations Report 2006–5156.

Western Regional Climate Center, 2003, Historical climate information, New Mexico climate summaries, Red River, New Mexico (297323): Information available on Web, accessed July 17, 2003, at *http://www.wrcc.dri.edu/*

Wood, S.A., 1991, Speciation of Be and solubility of bertrandite/phenalite minerals in hydrothermal solutions, *in* Pagel, Leroy, ed., Source transport and deposition of metals: Rotterdam, A.A. Balkema, p.147–150.

Wood, S.A., 1992, Theoretical prediction of speciation and solubility of beryllium in hydrothermal solution to 300ºC at saturated vapour pressure—application to bertrandite/phenakite deposits: Ore Geology Reviews, v. 7, p. 249–278.

Yager, D.B., Mast, M.A., Verplanck, P.L., Bove, D.J., Wright, W.G., and Hageman, P.L., 2000, Natural versus mining-related water quality degradation to tributaries draining Mount Moly, Silverton, Colorado, *in* Proceedings, Fifth International Conference on Acid Rock Drainage, ICARD 2000, v. 1: Littleton, Colo., Society for Mining, Metallurgy, and Exploration, p. 535–547.

Younger, P.L., Banwart, S.A., and Hedin, R.S., 2002, Mine water—hydrology, pollution, remediation: Dordrecht, Netherlands, Kluwer Academic Publishers, 442 p.

Younger, P.L., and Robins, N.S., eds., 2002, Mine water hydrogeology and geochemistry: London, Geological Society Special Publication no. 198, 396 p.

Zhu, M.-X., Xie, Mei, and Jiang, Xin, 2006, Interaction of fluoride with hydroxyaluminum-montmorillonite complexes and implications for fluoride-contaminated acidic soils: Applied Geochemistry, v. 21, p. 675–683.

Appendix 1

Table 1–1. Thermodynamic data used by WATEQ4F for modeling aqueous speciation and mineral solubility.

[References are: 1, Ball and Nordstrom (1991); 2, Nordstrom and others (1990); 3, Nordstrom and May (1996); 4, Baron and Palmer (1996); ΔH, enthalpy of reaction, in kilocalories per mole; K, equilibrium constant for the reaction]

Aqueous species	Reaction	ΔH	Log K	Reference
OH^-	$H_2O \leftrightarrows H^+ + OH^-$	13.362	–14.00	2
$MgOH^+$	$Mg^{2+} + H_2O \leftrightarrows MgOH^+ + H^+$	15.952	–11.44	2
MgF^+	$Mg^{2+} + F^- \leftrightarrows MgF^+$	3.2	1.82	2
$MgCO_3^\circ$	$Mg^{2+} + CO_3^{2-} \leftrightarrows MgCO_3^\circ$ $Log\ K_{MgCO_3^\circ} = 0.991 + 0.00667T$	2.713	2.98	2
$MgHCO_3^+$	$Mg^{2+} + HCO_3^- \leftrightarrows MgHCO_3^+$ $Log\ K_{MgHCO_3^+} = –59.215 + 2537.455/T + 2\ 0.92298 Log_{10}(T)$	.79	1.07	2
$MgSO_4^\circ$	$Mg^{2+} + SO_4^{2-} \leftrightarrows MgSO_4^\circ$	4.55	2.37	2
$CaOH^+$	$Ca^{2+} + H_2O \leftrightarrows CaOH^+ + H^+$	0	–12.78	2
$CaHCO_3^+$	$Ca^{2+} + HCO_3^- \leftrightarrows CaHCO_3^+$ $Log\ K_{CaHCO_3^+} = 1209.12 + 0.31294T – 34765.05/T – 478.782 Log_{10}(T)$	2.69	1.106	2
$CaCO_3^\circ$	$Ca^{2+} + CO_3^{2-} \leftrightarrows CaCO_3^\circ$ $Log\ K_{CaCO_3^\circ} = –1228.732 – 0.299444T + 35512.75/T + 485.818 Log_{10}(T)$	3.545	3.224	2
$CaSO_4^\circ$	$Ca^{2+} + SO_4^{2-} \leftrightarrows CaSO_4^\circ$	1.65	2.3	2
CaF^+	$Ca^{2+} + F^- \leftrightarrows CaF^+$	4.12	.94	2
$NaCO_3^-$	$Na^+ + CO_3^{2-} \leftrightarrows NaCO_3^-$	8.91	1.27	2
$NaHCO_3^\circ$	$Na^+ + HCO_3^- \leftrightarrows NaHCO_3^\circ$	0	–.25	2
$NaSO_4^-$	$Na^+ + SO_4^{2-} \leftrightarrows NaSO_4^-$	1.12	.7	2
NaF°	$Na^+ + F^- \leftrightarrows NaF^\circ$	0	–.24	2
KSO_4^-	$K^+ + SO_4^{2-} \leftrightarrows KSO_4^-$	2.25	.85	2
$AlOH^{2+}$	$Al^{3+} + H_2O \leftrightarrows AlOH^{2+} + H^+$ $Log\ K_{AlOH^{2+}} = 4.771 –2899.05/T$	13.24	–5	3
$Al(OH)_2^+$	$Al^{3+} + 2H_2O \leftrightarrows Al(OH)_2^+ + 2H^+$ $Log\ K_{Al(OH)_2^+} = 88.5 – 9391.6/T – 27.121 Log_{10}(T)$	26.9	–10.1	3
$Al(OH)_3^\circ$	$Al^{3+} + 3H_2O \leftrightarrows Al(OH)_3^\circ + 3H^+$	42.16	–16.8	3
$Al(OH)_4^-$	$Al^{3+} + 4H_2O \leftrightarrows Al(OH)_4^- + 4H^+$ $Log\ K_{Al(OH)_4^-} = 40.875 –10908.4/T – 11.041 Log_{10}(T)$	43.38	–22.99	3
AlF^{2+}	$Al^{3+} + F^- \leftrightarrows AlF^{2+}$	1.06	7.0	3
AlF_2^+	$Al^{3+} + 2F^- \leftrightarrows AlF_2^+$	1.98	12.7	3
AlF_3°	$Al^{3+} + 3F^- \leftrightarrows AlF_3^\circ$	2.16	16.8	3
AlF_4^-	$Al^{3+} + 4F^- \leftrightarrows AlF_4^-$	2.2	19.4	3
$AlSO_4^+$	$Al^{3+} + SO_4^{2-} \leftrightarrows AlSO_4^+$	2.29	3.5	3
$Al(SO_4)_2^-$	$Al^{3+} + 2SO_4^{2-} \leftrightarrows Al(SO_4)_2^-$	3.11	5.0	3
$FeOH^+$	$Fe^{2+} + H_2O \leftrightarrows FeOH^+ + H^+$	13.2	–9.5	2
$Fe(OH)_3^-$	$Fe^{2+} + 3H_2O \leftrightarrows Fe(OH)_3^- + 3H^+$	30.3	–31	1
$FeHCO_3^+$	$Fe^{2+} + HCO_3^- \leftrightarrows FeHCO_3^+$	0	2.0	2

Table 1–1. Thermodynamic data used by WATEQ4F for modeling aqueous speciation and mineral solubility.—Continued

[References are: 1, Ball and Nordstrom (1991); 2, Nordstrom and others (1990); 3, Nordstrom and May (1996); 4, Baron and Palmer (1996); ΔH, enthalpy of reaction, in kilocalories per mole; K, equilibrium constant for the reaction]

Aqueous species	Reaction	ΔH	Log K	Reference
$FeSO_4^\circ$	$Fe^{2+} + SO_4^{2-} \leftrightarrows FeSO_4^\circ$	3.23	2.25	1
$Fe(OH)_2^\circ$	$Fe^{2+} + 2H_2O \leftrightarrows Fe(OH)_2^\circ + 2H^+$	28.6	–20.5	2
$FeOH^{2+}$	$Fe^{3+} + H_2O \leftrightarrows FeOH^{2+} + H^+$	10.4	–2.19	2
$FeSO_4^+$	$Fe^{3+} + SO_4^{2-} \leftrightarrows FeSO_4^+$	3.91	4.04	2
$FeCl^{2+}$	$Fe^{3+} + Cl^- \leftrightarrows FeCl^{2+}$	5.6	1.48	2
$FeCl_2^+$	$Fe^{3+} + 2Cl^- \leftrightarrows FeCl_2^+$	0	2.13	2
$FeCl_3^\circ$	$Fe^{3+} + 3Cl^- \leftrightarrows FeCl_3^\circ$	0	1.13	2
$Fe(OH)_2^+$	$Fe^{3+} + 2H_2O \leftrightarrows Fe(OH)_2^+ + 2H^+$	17.1	–5.67	2
$Fe(OH)_3^\circ$	$Fe^{3+} + 3H_2O \leftrightarrows Fe(OH)_3^\circ + 3H^+$	24.8	–12.56	2
$Fe(OH)_4^-$	$Fe^{3+} + 4H_2O \leftrightarrows Fe(OH)_4^- + 4H^+$	31.9	–21.6	2
FeF^{2+}	$Fe^{3+} + F^- \leftrightarrows FeF^{2+}$	2.7	6.2	2
FeF_2^+	$Fe^{3+} + 2F^- \leftrightarrows FeF_2^+$	4.8	10.8	2
FeF_3°	$Fe^{3+} + 3F^- \leftrightarrows FeF_3^\circ$	5.4	14	2
$Fe(SO_4)_2^-$	$Fe^{3+} + 2SO_4^{2-} \leftrightarrows Fe(SO_4)_2^-$	4.6	5.38	2
$Fe_2(OH)_2^{4+}$	$2Fe^{3+} + 2H_2O \leftrightarrows Fe_2(OH)_2^{4+} + 2H^+$	13.5	–2.95	2
$Fe_3(OH)_4^{5+}$	$3Fe^{3+} + 4H_2O \leftrightarrows Fe_3(OH)_4^{5+} + 4H^+$	14.3	–6.3	2
$H_3SiO_4^-$	$H_4SiO_4^\circ \leftrightarrows H_3SiO_4^- + H^+$ $Log\ K_{H_3SiO_4^-} = -302.3724 - .050698T + 15669.69/T - 1119669/T^2 + 08.18466Log_{10}(T)$	6.12	–9.83	2
$H_2SiO_4^{2-}$	$H_4SiO_4^\circ \leftrightarrows H_2SiO_4^{2-} + 2H^+$ $Log\ K_{H_2SiO_4^{2-}} = -294.0184 - 0.07265T + 11204.49/T - 1119669/T^2 + 108.18466Log_{10}(T)$	17.6	–23	2
SiF_6^-	$H_4SiO_4^\circ + 4H^+ + 6F^- \leftrightarrows SiF_6^{2-} + 4H_2O$	–16.26	30.18	1
$SrOH^+$	$Sr^{2+} + H_2O \leftrightarrows SrOH^+ + H^+$		–13.29	2
$SrHCO_3^+$	$Sr^{2+} + HCO_3^- \leftrightarrows SrHCO_3^+ Log\ K_{SrHCO3} + = -3.248 + 0.01486T$	6.05	1.18	2
$SrCO_3^\circ$	$Sr^{2+} + CO_3^{2-} \leftrightarrows SrCO_3^\circ$ $Log\ K_{SrCO3^\circ} = -1.019 + 0.012826T$	5.22	2.81	2
$SrSO_4^\circ$	$Sr^{2+} + SO_4^{2-} \leftrightarrows SrSO_4^\circ$	2.08	2.29	2
$BaOH^+$	$Ba^{2+} + H_2O \leftrightarrows BaOH^+ + H^+$		–13.47	2
$BaHCO_3^+$	$Ba^{2+} + HCO_3^- \leftrightarrows BaHCO_3^+$ $Log\ K_{BaHCO_3^+} = -3.0938 + 0.013669T$	5.56	.982	2
$BaCO_3^\circ$	$Ba^{2+} + CO_3^{2-} \leftrightarrows BaCO_3^\circ$ $Log\ K_{BaCO3^\circ} = 0.113 + 0.008721T$	3.55	2.71	2
$BaSO_4^\circ$	$Ba^{2+} + SO_4^{2-} \leftrightarrows BaSO_4^\circ$	2.08	2.29	2
$MnCl^+$	$Mn^{2+} + Cl^- \leftrightarrows MnCl^+$	0	.61	2
$MnCl_2^\circ$	$Mn^{2+} + 2Cl^- \leftrightarrows MnCl_2^\circ$	0	.25	2
$MnCl_3^-$	$Mn^{2+} + 3Cl^- \leftrightarrows MnCl_3^-$	0	–.31	2
$MnOH^+$	$Mn^{2+} + H_2O \leftrightarrows MnOH^+ + H^+$	14.4	–10.59	2
$Mn(OH)_3^-$	$Mn^{2+} + 3H_2O \leftrightarrows Mn(OH)_3^- + 3H^+$	0	–34.8	1

Table 1–1. Thermodynamic data used by WATEQ4F for modeling aqueous speciation and mineral solubility.—Continued

[References are: 1, Ball and Nordstrom (1991); 2, Nordstrom and others (1990); 3, Nordstrom and May (1996); 4, Baron and Palmer (1996); ΔH, enthalpy of reaction, in kilocalories per mole; K, equilibrium constant for the reaction]

Aqueous species	Reaction	ΔH	Log K	Reference
MnO_4^-	$Mn^{2+} + 4H_2O \leftrightarrows MnO_4^- + 8H^+ 5e^-$	176.62	–127.824	1
MnO_4^{2-}	$Mn^{2+} + 4H_2O \leftrightarrows MnO_4^{2-} + 8H^+ + 4e^-$	150.02	–118.44	1
MnF^+	$Mn^{2+} + F^- \leftrightarrows MnF^+$	0	.84	2
$MnSO_4^\circ$	$Mn^{2+} + SO_4^{2-} \leftrightarrows MnSO_4^\circ$	3.37	2.25	2
$MnHCO_3^+$	$Mn^{2+} + HCO_3^- \leftrightarrows MnHCO_3^+$	0	1.95	2
$CuCl_2^-$	$Cu^+ + 2Cl^- \leftrightarrows CuCl_2^-$	1.23	8.22	1
$CuCl_3^{2-}$	$Cu^+ + 3Cl^- \leftrightarrows CuCl_3^{2-}$	1.91	8.42	1
$CuCO_3^\circ$	$Cu^{2+} + CO_3^{2-} \leftrightarrows CuCO_3^\circ$	0	6.73	1
$Cu(CO_3)_2^{2-}$	$Cu^{2+} + 2CO_3^{2-} \leftrightarrows Cu(CO_3)_2^{2-}$	0	9.83	1
$CuCl^+$	$Cu^{2+} + Cl^- \leftrightarrows CuCl^+$	8.65	.43	1
$CuCl_2^\circ$	$Cu^{2+} + 2Cl^- \leftrightarrows CuCl_2^\circ$	10.56	.16	1
$CuCl_3^-$	$Cu^{2+} + 3Cl^- \leftrightarrows CuCl_3^-$	13.69	–2.29	1
$CuCl_4^{2-}$	$Cu^{2+} + 4Cl^- \leftrightarrows CuCl_4^{2-}$	17.78	–4.59	1
CuF^+	$Cu^{2+} + F^- \leftrightarrows CuF^+$	1.62	1.26	1
$CuOH^+$	$Cu^{2+} + H_2O \leftrightarrows CuOH^+ + H^+$	0	–8	1
$Cu(OH)_2^\circ$	$Cu^{2+} + 2H_2O \leftrightarrows Cu(OH)_2^\circ + 2H^+$	0	–13.68	1
$Cu(OH)_3^-$	$Cu^{2+} + 3H_2O \leftrightarrows Cu(OH)_3^- + 3H^+$	0	–26.9	1
$Cu(OH)_4^{2-}$	$Cu^{2+} + 4H_2O \leftrightarrows Cu(OH)_4^{2-} + 4H^+$	0	–39.6	1
$Cu_2(OH)_2^{2+}$	$2Cu^{2+} + 2H_2O \leftrightarrows Cu_2(OH)_2^{2+} + 2H^+$ $Log\ K_{Cu2(OH)22+} = 2.497 - 3833/T$	17.539	–10.359	1
$CuSO_4^\circ$	$Cu^{2+} + SO_4^{2-} \leftrightarrows CuSO_4^\circ$	1.22	2.31	1
$CuHCO_3^+$	$Cu^{2+} + HCO_3^- \leftrightarrows CuHCO_3^+$	0	2.7	1
$ZnCl^+$	$Zn^{2+} + Cl^- \leftrightarrows ZnCl^+$	7.79	.43	1
$ZnCl_2^\circ$	$Zn^{2+} + 2Cl^- \leftrightarrows ZnCl_2^\circ$	8.5	.45	1
$ZnCl_3^-$	$Zn^{2+} + 3Cl^- \leftrightarrows ZnCl_3^-$	9.56	.5	1
$ZnCl_4^{2-}$	$Zn^{2+} + 4Cl^- \leftrightarrows ZnCl_4^{2-}$	10.96	.2	1
ZnF^+	$Zn^{2+} + F^- \leftrightarrows ZnF^+$	2.22	1.15	1
$ZnOH^+$	$Zn^{2+} + H_2O \leftrightarrows ZnOH^+ + H^+$	13.4	–8.96	1
$Zn(OH)_2^\circ$	$Zn^{2+} + 2H_2O \leftrightarrows Zn(OH)_2^\circ + 2H^+$	0	–16. 9	1
$Zn(OH)_3^-$	$Zn^{2+} + 3H_2O \leftrightarrows Zn(OH)_3^- + 3H^+$	0	–28.4	1
$Zn(OH)_4^{2-}$	$Zn^{2+} + 4H_2O \leftrightarrows Zn(OH)_4^{2-} + 4H^+$	0	–41.2	1
$ZnOHCl^\circ$	$Zn^{2+} + H_2O + Cl^- \leftrightarrows ZnOHCl^\circ + H^+$	0	–7.48	1
$ZnSO_4^\circ$	$Zn^{2+} + SO_4^{2-} \leftrightarrows ZnSO_4^\circ$	1.36	2.37	1
$Zn(SO_4)_2^{2-}$	$Zn^{2+} + 2SO_4^{2-} \leftrightarrows Zn(SO_4)_2^{2-}$	0	3.28	1
$ZnHCO_3^+$	$Zn^{2+} + HCO_3^- \leftrightarrows ZnHCO_3^+$	0	2.1	1
$ZnCO_3^\circ$	$Zn^{2+} + CO_3^{2-} \leftrightarrows ZnCO_3^\circ$	0	5.3	1
$Zn(CO_3)_2^{2-}$	$Zn^{2+} + 2CO_3^{2-} \leftrightarrows Zn(CO_3)_2^{2-}$	0	9.63	1

Table 1–1. Thermodynamic data used by WATEQ4F for modeling aqueous speciation and mineral solubility.—Continued

[References are: 1, Ball and Nordstrom (1991); 2, Nordstrom and others (1990); 3, Nordstrom and May (1996); 4, Baron and Palmer (1996); ΔH, enthalpy of reaction, in kilocalories per mole; K, equilibrium constant for the reaction]

Aqueous species	Reaction	ΔH	Log K	Reference
HCO_3^-	$H^+ + CO_3^{2-} \leftrightarrows HCO_3^-$ $Log\ K_{HCO_3^-} = 107.8871 + 0.03252849T - 5151.79/T + 563713.9T^2 - 38.92561Log_{10}(T)$	–3.561	10.329	2
$H_2CO_3°$	$H^+ + HCO_3^- \leftrightarrows H_2CO_3°$ $Log\ K_{H_2CO_3°} = 356.3094 + 0.06091964T - 21834.37/T + 1684915T^2 - 126.8339Log_{10}(T)$	–2.177	6.352	2
HSO_4^-	$H^+ + SO_4^{2-} \leftrightarrows HSO_4^-$ $Log\ K_{HSO_4^-} = -56.889 + 0.006473T + 2307.9/T + 19.8858Log_{10}(T)$	3.85	1.988	2
HF°	$H^+ + F^- \leftrightarrows HF°$ $Log\ K_{HF°} = -2.033 + 0.012645T + 429.01/T$	3.18	3.18	2
HF_2^-	$H^+ + 2F^- \leftrightarrows HF_2^-$	4.55	3.76	2
$H_2F_2°$	$2H^+ + 2F^- \leftrightarrows H_2F_2°$	0	6.768	1
Mineral phase	**Reaction**	**ΔH**	**Log K**	**Reference**
K–Jarosite	$KFe_3(SO_4)_2(OH)_6 + 6H^+ \leftrightarrows K^+ + 3Fe^{3+} + 2SO_4^{2-} + 6H_2O$	–45.0	–11.0	4
Ferrihydrite	$Fe(OH)_3 + 3H^+ \leftrightarrows Fe^{3+} + 3H_2O$	0	4.891	2
Siderite (c)	$FeCO_3 \leftrightarrows Fe^{2+} + CO_3^{2-}$	–2.48	–10.89	2
Siderite (d)	$FeCO_3 \leftrightarrows Fe^{2+} + CO_3^{2-}$	0	–10.45	2
Rhodochrosite	$MnCO_3 \leftrightarrows Mn^{2+} + CO_3^{2-}$	–1.43	–11.13	2
$Al(OH)_{3(a)}$	$Al(OH)_3 + 3H^+ \leftrightarrows Al^{3+} + 3H_2O$	–26.5	10.8	2
Gibbsite (c)	$Al(OH)_3 + 3H^+ \leftrightarrows Al^{3+} + 3H_2O$	–24.5	9.35	2
Gibbsite (c)	$Al(OH)_3 + 3H^+ \leftrightarrows Al^{3+} + 3H_2O$	–22.8	8.11	2
K–Alunite	$KAl_3(SO_4)_2(OH)_6 + 6H^+ \leftrightarrows K^+ + 3Al^{3+} + 2SO_4^{2-} + 6H_2O$	–50.25	–1.4	2
$SiO_{2(a)}$	$SiO_2 + 2H_2O \leftrightarrows H_4SiO_4°$ $Log\ K_{Amorphous\ Silica} = -0.26 - 731/T$	3.34	–2.71	2
Chalcedony	$SiO_2 + 2H_2O \leftrightarrows H_4SiO_4°$ $Log\ K_{Chalcedony} = -0.09 - 1032/T$	4.72	–3.55	2
Quartz	$SiO_2 + 2H_2O \leftrightarrows H_4SiO_4°$ $Log\ K_{Quartz} = 0.41 - 1309/T$	5.99	–3.98	2
Fluorite	$CaF_2 \leftrightarrows Ca^{2+} + F^-$ $Log\ K_{Fluorite} = 66.348 - 4298.2/T - 2571Log(T)$	4.69	–10.6	2
Calcite	$CaCO_3 \leftrightarrows Ca^{2+} + CO_3^{2-}$ $Log\ K_{Calcite} = -171.9065 - .077993T + 2839.319/T + 71.595Log(T)$	–2.297	–8.48	2
Gypsum	$CaSO_4 \cdot 2H_2O \leftrightarrows Ca^{2+} + SO_4^{2-} + 2H_2O$ $Log\ K_{Gypsum} = 68.2401 - 3221.51/T - 25.0627Log(T)$	–.109	–4.58	2
Dolomite	$CaMg(CO_3)_2 \leftrightarrows Ca^{2+} + Mg^{2+} + 2CO_3^{2-}$	–9.436	–17.09	2
Strontianite	$SrCO_3 \leftrightarrows Sr^{2+} + CO_3^{2-}$ $Log\ K_{Strontianite} = 155.0305 - 7239.594/T - 56.58638Log(T)$	–.40	–9.271	2
Celestite	$SrSO_4 \leftrightarrows Sr^{2+} + SO_4^{2-}$ $Log\ K_{Celestite} = 14805.9622 - 2.4660924T + 756968.533/T - 40553604/T^2 + 5436.3588Log(T)$	–1.037	–6.63	2
Barite	$BaSO_4 \leftrightarrows Ba^{2+} + SO_4^{2-}$ $Log\ K_{Barite} = 136.035 - 7640.41/T - 48.595Log(T)$	6.35	–9.97	2

Table 1–2. List of analytic equations for linear best fits of correlated data in the form of y=mx + b.

[R^2 is the correlation coefficient]

y–axis parameter	x–axis parameter	equation	R^2	Data used for linear regression
aluminum	sulfate	y = 0.0385x + 14.5	0.93	Straight Creek, SC1A, SC3A, SC6A, SC5A
beryllium	fluoride	y = 0.0026x – 0.0013	0.85	SC1A, SC3A, SC6A, SC5A, AWWT1, SC7A
beryllium	lithium	y = 0.1058x – 0.0005	0.87	SC1A, SC3A, SC6A, SC5A, AWWT1, SC7A
beryllium	sulfate	y = 0.00005x – 0.0046	0.84	SC1A, SC3A, SC6A, SC5A
cadmium	sulfate	y = 0.00002x – 0.0103	0.96	Straight Creek, SC1A, SC3A, SC6A, SC5A, AWWT1, SC7A, SC8A
cadmium	zinc	y = 0.0056x – 0.0031	0.92	Straight Creek, SC1A, SC3A, SC6A, SC5A, AWWT1, SC7A, SC8A
calcium	sulfate	y = 0.17x + 14.2	0.95	Straight Creek, SC1A, SC3A, SC6A, SC5A, AWWT1, SC7A, SC8A
chromium	sulfate	y = 0.00002x – 0.0107	0.75	Straight Creek, SC1A, SC3A, SC6A, SC5A, SC7A, SC8A
chromium	nickel	y = 0.0558x – 0.0063	0.76	Straight Creek, SC1A, SC3A, SC6A, SC5A, SC7A, SC8A
cobalt	nickel	y = 0.444x – 0.0058	0.98	Straight Creek, SC1A, SC6A, SC5A, AWWT1, SC7A, SC8A
copper	sulfate	y = 0.0006x – 0.288	0.82	SC1A, SC3A, SC6A, SC5A
copper	zinc	y = 0.151x – 0.136	0.84	SC1A, SC3A, SC6A, SC5A
fluoride	sulfate	y = 0.0049x – 0.970	0.85	SC1A, SC3A, SC6A, SC5A
fluoride	calcium	y = 0.0244x – 0.260	0.87	SC1A, SC3A, SC6A, SC5A
lithium	sulfate	y = 0.0001x – 0.041	0.84	SC1A, SC3A, SC6A, SC5A
magnesium	sulfate	y = 0.0049x – 0.970	0.95	SC1A, SC3A, SC6A, SC5A
magnesium	calcium	y = 0.272x + 14.3	0.95	SC1A, SC3A, SC6A, SC5A
manganese	sulfate	y = 0.0111x – 3.06	0.97	Straight Creek, SC1A, SC3A, SC6A, SC5A, AWWT1, SC7A, SC8A
nickel	sulfate	y = 0.0004x – 0.0289	0.95	Straight Creek, SC1A, SC3A, SC6A, SC5A
silica	sulfate	y = 0.0158x + 63.8	0.75	SC1A, SC3A, SC6A, SC5A
specific conductance	sulfate	y = 1.46x + 179	0.97	Straight Creek, SC1A, SC3A, SC5A, AWWT1, SC7A, SC8A
specific conductance	sulfate	y = 1.20x + 391	0.97	Red River
zinc	sulfate	y = 0.0041x – 1.28	0.96	Straight Creek, SC1A, SC3A, SC6A, SC5A, AWWT1, SC7A, SC8A
zinc	manganese	y = 0.371x – 0.140	0.99	Straight Creek, SC1A, SC3A, SC6A, SC5A, AWWT1, SC7A, SC8A

Appendix 2. Mathematical derivation of curves for mixing lines shown in figures 8 and 9.

The derivation for the mixing lines shown in figures 8 and 9 is based on three important assumptions:

1. Constituents are soluble and conservative (do not react on mixing).
2. There are only two dominant end–member compositions (1 and 2) to produce the mixture (3).
3. The end–member compositions are sufficiently different to discern mixing.

From conservation of mass:

$$M_1 + M_2 = M_3, \text{ where M = mass and } M_3 = \text{mass of mixture}$$

Because M= CQ, where C = concentration and Q = discharge

$$C_1Q_1 + C_2Q_2 = C_3Q_3$$

and

$$Q_1 + Q_2 = Q_3$$

or

$$Q_1/Q_3 + Q_2/Q_3 = 1$$

and

$$x + (1–x) = 1$$

so that

$$C_1x + C_2(1–x) = C_3$$

or

$$C_2 + C_1x – C_2x = C_3$$

In terms of element ratios:

$$(C_1/C_4)x + (C_2/C_4)(1–x) = C_3/C_4$$

For figures 8 and 9, the proportion, x, is directly related to the sulfate concentration, C_4, and the element ratio, C_3/C_4 changes as a function of x, the mixing proportion. The ratios C_1/C_4 and C_2/C_4 are constant for the particular time of sampling because they are the conservative end–members.

Publishing support provided by:
Denver and Rolla Publishing Service Centers

For more information concerning this publication, contact:

U.S. Geological Survey
Branch of Regional Research, Central Region
Lakewood, CO 80225–0046
(303) 236–5021
http://water.usgs.gov/nrp/proj.bib/nordstrom.html